BERICHTE
aus dem MARUM und dem Fachbereich Geowissenschaften der Universität Bremen

No. 291

Sahling, H., Bergès, B., Boelmann, J., Dimmler, W., Geprägs, P., Glockzin, M., Kaboth, S., Nowald, N., Pape, T., Römer, M., d. Santos Ferreira, C., Schroedter, L., Tomczyk, M.

R/V HEINCKE CRUISE REPORT HE-387.
Gas emissions at the Svalbard continental margin.
Longyearbyen – Bremerhaven, 20 August – 16 September 2012.

Berichte, MARUM Zentrum für Marine Umweltwissenschaften, Fachbereich Geowissenschaften, Universität Bremen, No. 291, 170 pages, Bremen 2012

ISSN 0931-0800

The "Berichte aus dem MARUM und dem Fachbereich Geowissenschaften" are produced at irregular intervals by the Department of Geosciences, Bremen University and by MARUM – Center for Marine Environmental Sciences. They serve for the publication of cruise, project and technical reports.

Reports can be ordered from:

Monika Bachur

MARUM – Zentrum für Marine Umweltwissenschaften

Universität Bremen

Postfach 330 440

D 28334 BREMEN

Phone: (49) 421 218-65516

Fax: (49) 421 218-65515

e-mail: MBachur@uni-bremen.de

Reports can also be downloaded from:

http://nbn-resolving.de/urn:nbn:de:gbv:46-MARUM9

Citation:
Sahling, H. and cruise participants
R/V Heincke Cruise Report HE-387. Gas emissions at the Svalbard continental margin. Longyearbyen – Bremerhaven, 20 August – 16 September 2012.
Berichte, MARUM – Zentrum für Marine Umweltwissenschaften, Fachbereich Geowissenschaften, Universität Bremen, No. 291, 170 pages. Bremen, 2012. ISSN 0931-0800.

ISSN 0931-0800

R/V HEINCKE
Cruise Report HE-387

Gas emissions at the Svalbard continental margin

HE-387
Longyearbyen - Bremerhaven
20 August – 16 September, 2012

Cruise sponsored by: Deutsche Forschungsgemeinschaft (DFG)
Bundesministerium für Bildung und Forschung (BMBF)

Edited by
Heiko Sahling and Greta Ohling
With contributions of cruise participants

The cruise was performed by
MARUM Center for Marine Environmental Sciences

marum

Universität Bremen

R/V HEINCKE Cruise Report HE-387

Table of Contents

Preface

Gas emissions from the continental margin west of Spitzbergen were the scientific mission of the cruise on R/V HEINCKE He-387. These gas emissions were described by Westbrook et al. (2009) and occur at water depths around 380 m. The author's hypothesis that gas bubble emission might originate from dissociating gas hydrate due to a 1°C temperature increase of the water masses at that respective depth in the last 30 years. The finding by Westbrook et al. (2009) has stimulated intensive research efforts in that area with the first publications being just published about the subsurface settings using seismic data (Rajan et al. 2012, Sarkar et al. 2012). Other jet unpublished studies concentrated on the fate of the emitted methane in the water column.

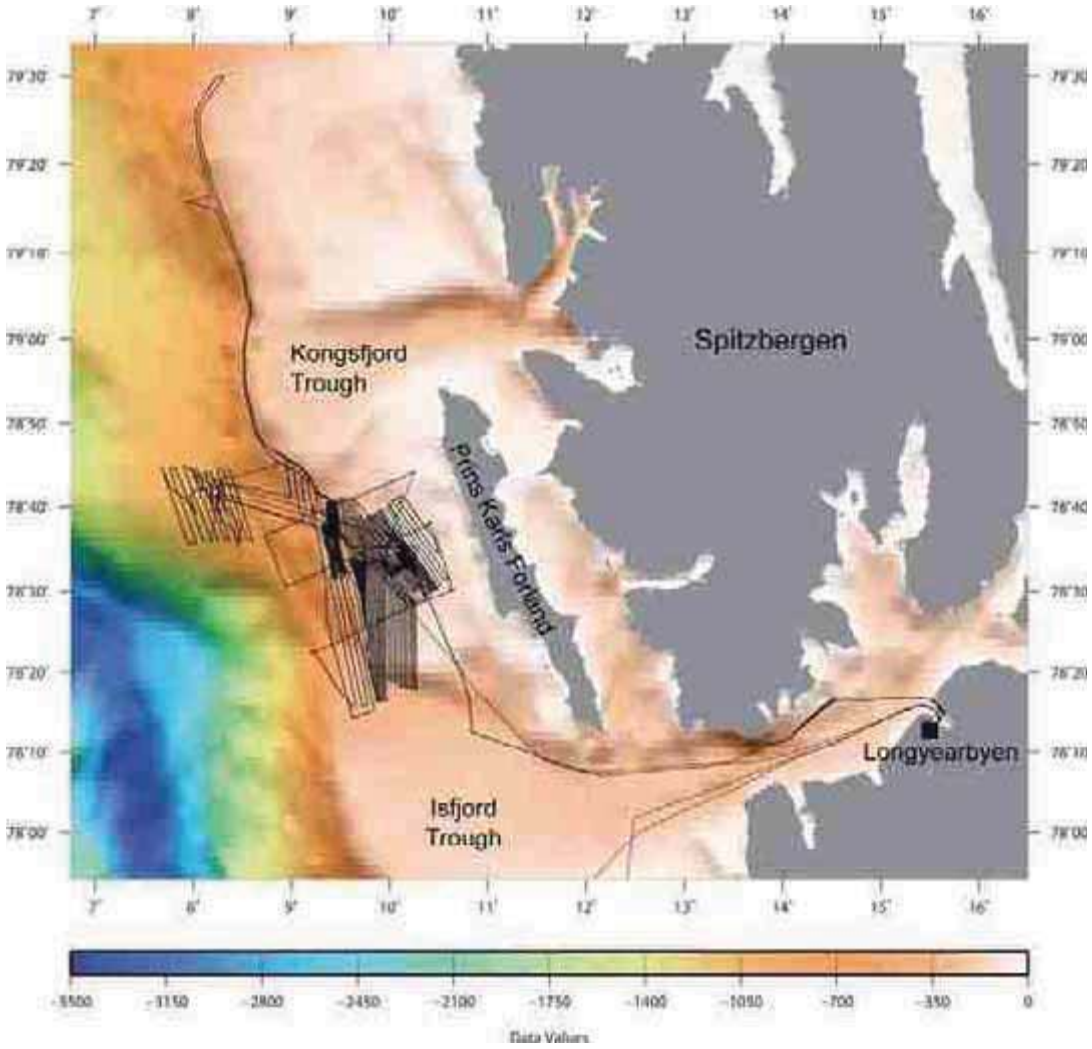

Fig. I: Cruise track of R/V HEINCKE cruise He-387 west of Spitzbergen. The cruise started 20 Aug 2012 in Longyearbyen, with a port call 9 Sept 2012 in Longyearbyen to exchange personal and ended 16 Sept 2012 in Bremerhaven.

In the research areas Geosphere-Biosphere Interaction at MARUM (GB 4 and 5) one overarching topic is to study the relevance of natural gas emissions at hydrocarbon seeps on the biogeochemistry of the oceans. We therefore applied for ship time on R/V HEINCKE and received a MARUM incentive funds grant to carry out the expedition He-387 that took place 19 Aug to 16

Sept 2012. Since R/V HEINCKE is equipped with state-of-the-art hydroacoustic equipment, it can significantly contribute to the ongoing research efforts at the west Svalbard continental margin.

The major objectives were, to use hydroacoustic techniques in order to map the distribution of gas bubble emissions and to relate these to seafloor morphology. Using the remotely operated vehicle (ROV) Cherokee, we intended to map and quantify bubble streams at the seafloor in order to estimate the flux of methane into the ocean. Most participating scientists are affiliated with MARUM but we have invited additional experts from other institutions to comprehensively study the topic.

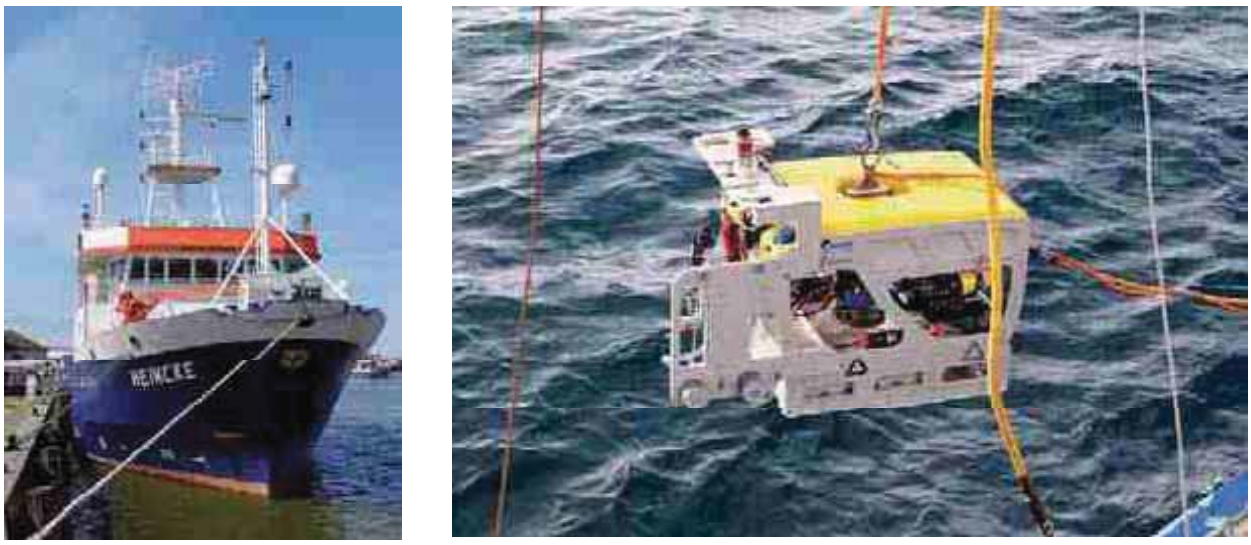

Fig. II: Research vessel HEINCKE at the pier in Bremerhaven (left). Launching of ROV Cherokee during R/V HEINCKE Cruise HE-387 (right).

Fig. III: Group of scientists and technicians on HE-387.

Personel aboard R/V HEINCKE

Table I: Scientific crew.

Name	Working group	Affiliation	Travel time
Heiko Sahling	Chief Scientist	MARUM	20/8 – 16/9/2012
Thomas Pape	Gas Geochemistry	MARUM	20/8 – 09/9/2012
Patrizia Geprägs	Gas Geochemistry	MARUM	20/8 – 09/9/2012
Michael Glockzin	Methane in sea surface	IOW	20/8 – 09/9/2012
Jan Boelmann	Optical bubble quantification	HS Bremerhaven	20/8 – 09/9/2012
Nicolas Nowald	ROV Pilot	MARUM	20/8 – 09/9/2012
Werner Dimmler	ROV Co-Pilot	FIELAX	20/8 – 09/9/2012
Christian d. Santos Ferreira	Mapping	MARUM	20/8 – 09/9/2012
Leah Schroedter	Research Assistance	MARUM	20/8 – 09/9/2012
Miriam Römer	Hydroaocustics	MARUM	20/8 – 09/9/2012
Michal Tomczyk	Hydroacoustics	MARUM	20/8 – 16/9/2012
Benoît Bergès	Hydroacoustics	UoS	20/8 – 16/9/2012
Stefanie Kaboth	Sediment Sampling	AWI	09/9 – 16/9/2012

Participating Institutions

MARUM	Zentrum für marine Umweltwissenschaften, University of Bremen, Leobener Str. 28334 Bremen, Germany
IOW	Institut für Ostseeforschung, Warnemünde, Chemical Oceanography, Seestr. 15, 18119 Warnemünde, Germany
HS Bremerhaven	Hochschule Bremerhaven, Labor für Maritime Technologien, An der Karlstadt 8, 27568 Bremerhaven, Germany
FIELAX	Gesellschaft für wissenschaftliche Datenverarbeitung mbH, Schleusenstr. 14, 27568 Bremerhaven, Germany
UoS	University of Southampton, University Road, Southampton SO17 1BJ, United Kingdom
AWI	Alfred-Wegener-Institut für Polar- und Meeresforschung, Am Handelshafen, 27515 Bremerhaven, Germany

Table II: Crew members onboard (from left to right).

Name	Work onboard
Robert Voss	Master
Remo Franke	1. Officer
Hero Nannen	2. Officer
Jürgen Szymanski	Chief Engineer
Abu Hackman	Electrician
Ronald Klafack	Cook
Stefan Fischer	Bosum
Dirk Gätjen	AB
Andreas Gulich	SM
Günter Lewin	SM
Roman Boxler	AB
Andre Constapel	SM

Shipping operator: Briese Schiffahrts GmbH & Co. KG, Hafenstrasse 12, 26789 Leer, Germany

1. Introduction and Geological Background
(H. Sahling)

1.1 Introduction

Gas hydrates have long been discussed as dynamic methane reservoirs in marine sediments highly susceptible to climatic changes in the geological past. In a recent publication, however, evidences are presented for gas hydrate dissociation at present (Westbrook et al., 2009). The authors found vigorous gas bubble emissions at the upper continental slope west of Svalbard at water depths around 360 to 400 m. They attribute the release of methane to hydrate dissociation due to an observed 1°C temperature increase of the bottom water during the last 30 years. The released methane enters the hydrosphere and, eventually, the atmosphere where it could contribute as greenhouse gas to accelerate global warming.

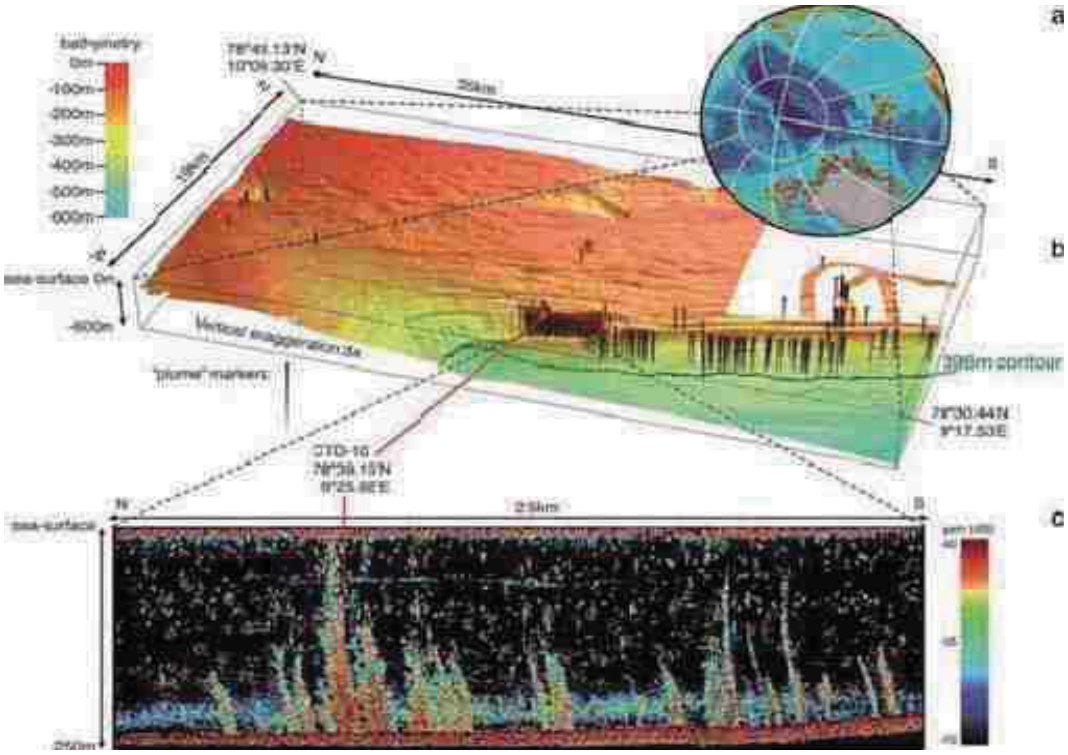

Fig. 1.1: (a) The working area and (b) gas emissions at the continental margin west of Svalbard. (c) Gas emissions were recorded as flares or plumes with the EK60 echosounder (from Westbrook et al. 2009).

Westbrook et al. (2009) estimated the amount of methane that can be released from dissociating gas hydrate for the entire continental margin of the Svalbard archipelago. By assuming that similar processes as observed in a spatially limited area could potentially occur all along the continental margin, they estimated the enormous amount of 20 Tg methane (Tg = 10^{12}g) to be released every year.

It should be noticed, however, that Westbrook et al. (2009) also proposed an alternative explanation for the observed emission of gas bubbles. Gas may be trapped below hydrate deposits as indicated by the pronounced bottom simulating reflector (BSR). As a consequence, the gas is only released above the upper limit of the gas hydrate stability zone (GHSZ) at ~400 m.

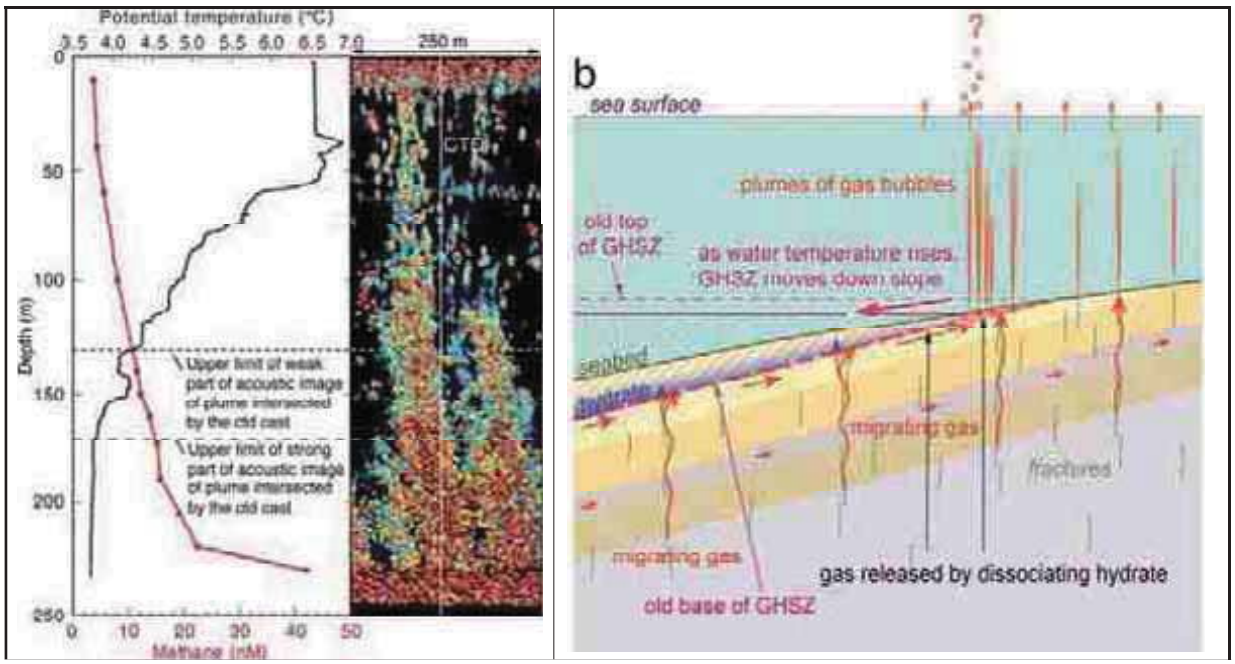

Fig. 1.2: (Left) Methane concentration and temperature profile at a CTD station intersecting a bubble plume. Methane concentration increases consistently downwards and shows a strong increase in the lowermost 40 m of the water column, which corresponds to the depth of greatest reflections in the echosounder. (Right) A schematic sketch illustrating the deepening of the upper limit of the gas hydrate stability zone (GHSZ) and the release of gas (from Westbrook et al. 2009).

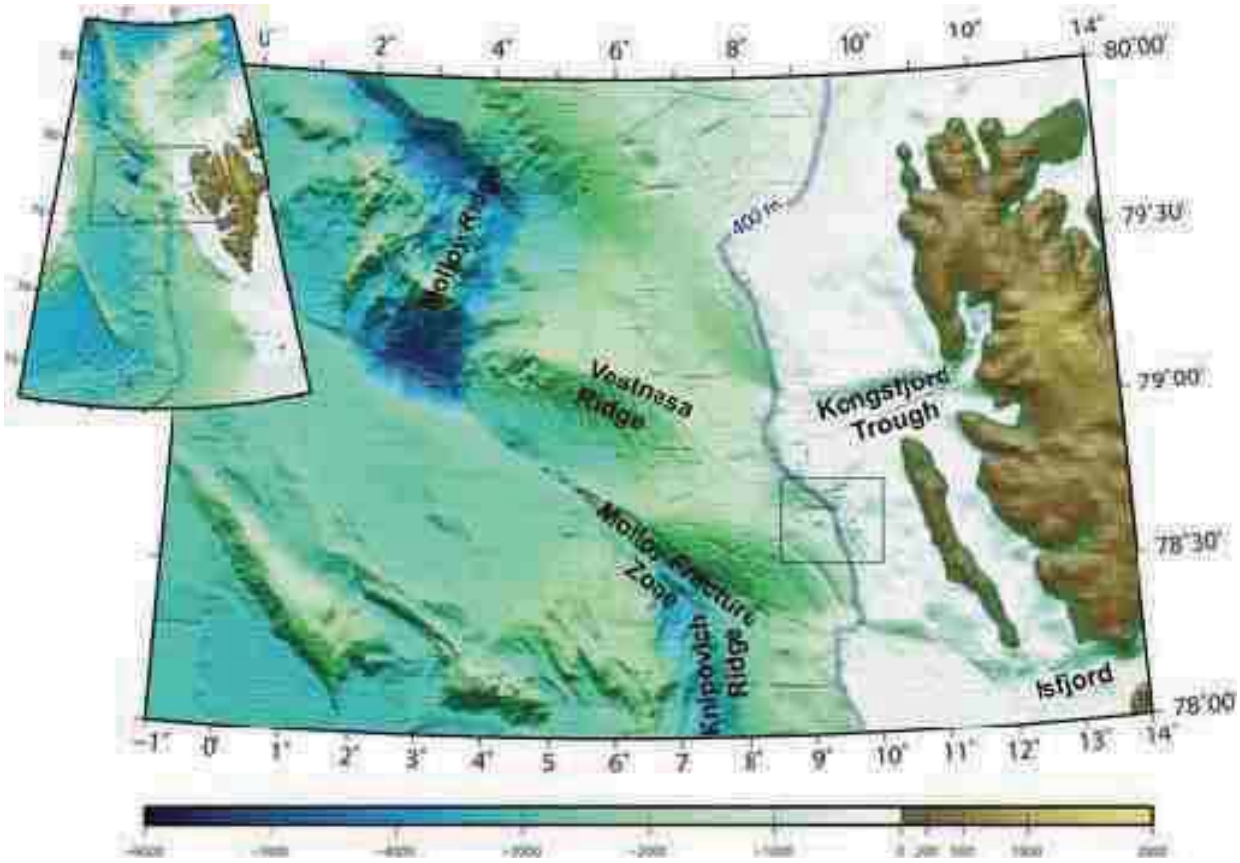

Fig. 1.3: Bathymetric map showing major structural elements west of Spitzbergen.

1.2 Geological Setting

The Norwegian-Svalbard continental margin is a highly dynamic area showing abundant evidence of fluid migration in the sediments, submarine mass wasting, normal faulting, hydrocarbon accumulation, sediment fan development, and gas hydrate occurrence (Vogt et al. 1999, Vanneste et al. 2005, Hustoft et al. 2009). The major structural elements are shown in Fig. 1.3. The Knopovich Ridge is a slowly and obliquely spreading northernmost extension of the Mid-Atlantic Ridge system, abutting the West-Svalbard margin in the Fram Strait (Thiede and Myhre, 1996). A series of transform faults like the Molloy Fracture Zone and short spreading centres, e.g. Molloy Ridge, ultimately connect the Knipovich Ridge with the Gakkel Ridge. Deposited sediments on the western Svalbard margin are either glacigenic debris flows in trough-mouth fans beyond the shelf break or turbiditic, glaciomarine and hemipelagic sediments, in parts reworked by contour currents (Vorren et al. 1998).

1.3 Objectives

The main objective of the cruise is to quantify the amount of methane that is released as gas bubbles from the seafloor. Our approach combines hydroacoustic mapping of gas emissions using ship-based echosounder (multibeam EM 710, fish finder EK 60) with ROV-based studies. The ROV is equipped with a horizontally-looking sonar allowing to map individual gas bubble streams at the seafloor. The volume flux of methane is then estimated by quantifying the flux of individual bubble streams using three different methods, direct measurement with a bubble catcher as well as visually using the ROV video system and acoustically by using the horizontally-looking sonar.

A further objective of the cruise is to use the ship-based echosounder for mapping the distribution of gas emission over wider areas of the shelf and continental slope. Combining this flare mapping with the multibeam mapping of the bathymetry may allow better understanding of the geological control on bubble emissions.

As the source of the gas that is emitted at the seafloor has not been studied so far, another objective is to collect gas at the seafloor with the pressure-tight gas bubble sampler for further analyses of the gas composition and isotope signature. The gas composition has an influence on the hydrate stability and, thus, the determination of the gases will help calculate more precisely the upper limit of the gas hydrate stability zone.

In order to study the fate of methane and to answer the question if methane enters the atmosphere, three different techniques are combined. Firstly, ship-based echosounder allow to track how high gas bubble plumes rise in the water column. Secondly, measuring of dissolved methane extracted from hydrocasts by the vacuum extraction method should give insights at what depths in the water the methane mainly dissolves. Finally, the concentration at the sea surface is continuously measured by the equilibrator technique throughout the cruise.

2. Cruise Narrative

(H. Sahling)

After exactly six days of transit from Bremerhaven R/V HEINCKE arrived Sunday, 19 Aug 2012, in Longyearbyen, Spitzbergen. We embarked on **Monday, 20 Aug 2012**, in the morning at about 08:00 local time. This is the beginning of the cruise HE–387. The day is spent setting up the equipment. Meanwhile the ship sailed up and down the Isfjord opposite of the Adventfjord. There was no space on the pier and strong winds from NW with gales up to 7 Bft did not allow anchoring. In the night the ship slowly moved out of the Isfjord.

On **Tuesday, 21 Aug 2012**, the open sea was reached. Strong NW winds slowed the ship's speed down to 4-5 knots so that at 14:00 UTC (UTC = local time - 2 hours) the research area was reached and the scientific programme started with a ***Sound Velocity Probe Station 01*** (***SVP 01***) needed for the following ***Hydroacoustic Survey (HS 02)***. This survey consisted of the transit to known gas emissions located at about 80 m water depth. This area is in the following referred to as Gas Flares at 80 m. The gas emissions where found during the British James Clarke Ross cruise 253 in 2011 lead by Prof. Ian Wright from NOC, Southampton. Benoît Bergès and Michal Tomczyk took part in that cruise and conducted the hydroacoustic gas flare mapping and are also participants of this present cruise. Objective of HS 02 is the mapping of gas emissions with the fish finding sonar EK 60 as well as with the water column data recorded by swath echosounder EM 710. In order to map the distribution of flares in detail, two sets of surveys were conducted with survey lines running NW-SE due to the prevailing strong NW winds and a line spacing of about 80 m to allow sufficient coverage. One reason for choosing the Gas Flares at 80 m as first area to focus on was the fact that R/V MARIA S. MERIAN (Chief Scientist Prof. Christian Berndt) sailed in the research area at the same time conducting research at the Gas Flares at 380 m.

On **Wednesday, 22 Aug 2012**, the second survey set of HS 02 was abandoned in order to conduct at 12:30 UTC ***SVP 03*** followed by several survey lines ***HS 04*** for multibeam EM 710 calibration. The calibrations allow deriving correction factors for pitch, roll, heave etc. influencing the multibeam, which should lead to increasing data quality. The calibration became possible due to improving weather with NW wind around 4 Bft. A CTD probe with Niskin bottle rosette ***CTD 05*** was deployed in the area of gas emissions at 80 m in order to unravel the physical structure of the water column and to measure the methane concentration based on the vacuum gas extraction method. In the night the abandoned HS 02 profile was continued as station ***HS 06***. This survey was extended by several lines with the intention to survey larger areas of the shelf for evidence of gas emissions.

On **Thursday, 23 Aug 2012**, the weather was excellent with NW winds around 3, sun and clear sky and wonderful sight of the mountain range of Spitzbergen. The remotely operated vehicle Cherokee ***ROV Dive 01 Stat. 07*** was deployed at 09:00 UTC at the flares at 80 m. The dive site was chosen after analysing EK 60 and EM 710 records revealing the existence of an intensive flare cluster composed of many weak flares as well as several strong flares that could be traced all the way through the water column to the sea surface. After some time learning how to visualize gas emissions with the horizontally-looking scanning sonar Imaginex, the tool was

efficiently used in order to detect and also quantify gas emissions. Gas samples were obtained; later analyses revealed that the gas is dominantly composed of methane of probably microbial origin. Video sequences and photos were taken for the analyses of gas bubble sizes and volume flux estimates. While being close to the intensive gas emission site with the ship, the system to measure methane concentration close to the sea surface by the equilibration technique (called equilibrator in the following) detected the highest values measured so far during the cruise, indicating that some of the methane released at the seafloor is transported to the sea surface indeed. At the gas emission site visually inspected by ROV, gravity corer ***GC 08*** was deployed and a handful gravel as well as a living sea urchin and a clam recovered. The coarse grained material at the seafloor does not allow any penetration of the corer. About two hours were spent for the high-resolution mapping of two flare clusters, one surveyed by ROV before and one additional one, by crossing it with the ship from different directions several times during ***HS 09***. Due to a non-stationary ship, ***CTD 10*** at the flare cluster was taken outside of the bubble plume. In the night the long overview profiles of HS 06 were continued as ***HS 11*** amended by several lines extending the survey area to a considerable large box.

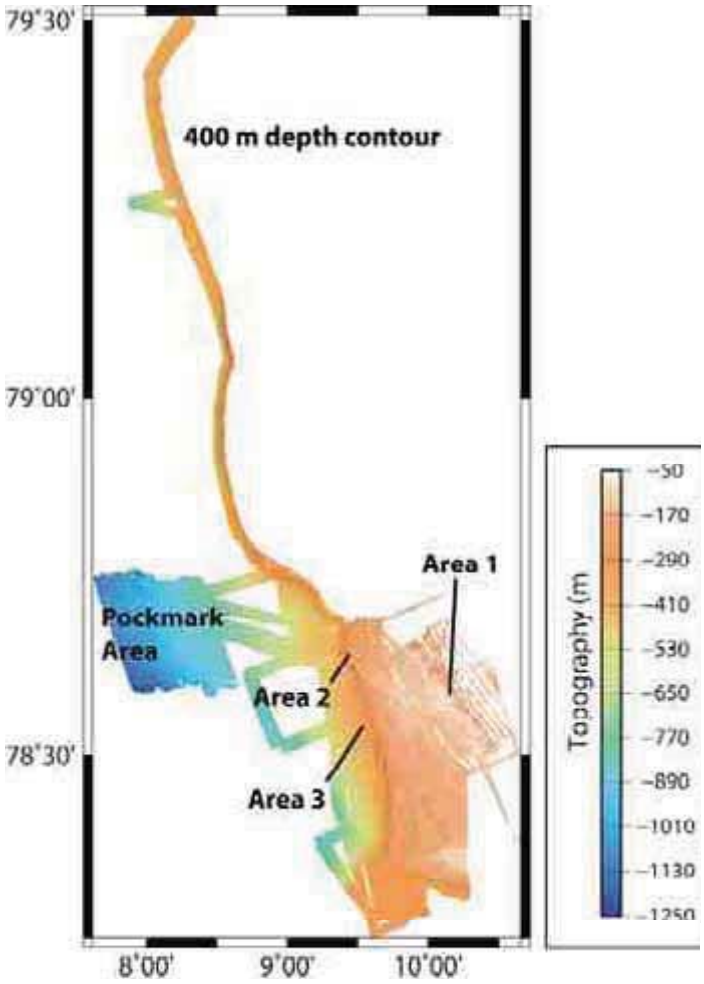

Fig. 2.1: Overview of bathymetry acquired during the Cruise HE-387 and names of significant areas in which the research concentrated.

Friday, 24 Aug 2012, was a sunny, calm day ideal for deploying the ***ROV Dive 02 Stat. 12*** again. Target area was the intensive flare cluster at 80 m depth. The dive concentrated on the

mapping of individual gas emissions by sonar Imaginex by transecting with the ROV in a systematic way through the area of interest. With this, we should be able to unravel how many bubble streams sum up to a flare as seen in ship-based echosounder. By quantifying the flux of gas at a representative number of streams it should further be possible to quantify the flux of the entire area. The dive continued with the use of a specially designed imaging plate in order to take good videos of bubble streams for automated optical analyses. It turned out that visuals of the bubbles close to the claw of the ROV arm and against the dark background of the water column are as good or even better than the imaging plate, which has the drawback of limiting additional sampling with the manipulator. For that reason, the imaging plate will not be used any further.

After the ROV dive, an experiment to learn about the extent of surface methane plumes was conducted. The weather conditions appeared ideal, as it was a calm day with no apparent surface currents, as stated by the navigators on the bridge. In order to allow the equilibrator to measure the methane concentration close to the sea surface, the ship was kept stationary until a stable methane value was achieved followed by a small transect of less than a cable length over the plume. This approach worked very well, although it was time consuming. However, the experiment had to stop as soon as the wind speed from southerly directions increased, as suddenly the entire pattern of elevated methane concentration over the bubble plume was over and water with low concentration replaced the water at site. The experiment (***HS 13***) was accompanied by ***CTD 14***, both stations together were part of the experiment. The second half of the night ***HS 015*** was conducted to finalize the overview mapping of the bubble plumes at the shelf.

Saturday, 25 Aug 2012, the ROV was equipped with a hydrophone in order to listen to the sound that bubbles make when being emitted at the seafloor. This technique of passive acoustics has been developed in the working group of Prof. Tim Leighton at the University of Southampton. The technique is planned to be used by Benoît Bergès during ***ROV Dive 03 Stat. 16*** at the flares at 80 m water depth. At the same spots the bubble streams were quantified with the active sonar Imaginex, all sources of noise on the ROV were turned off in order to run the hydrophone with as low background noise as possible. However, it turned out after the dive that the background noise was too high to use the data. The intention of ***HS 17-1*** was to fill in a gap in the bathymetric data and ***HS017-2*** to systematically map flares at the 280 m depth site. As strong winds with gales up to 10 Bft from E were forecasted, the intention of ***HS 18*** was to look for gas emissions further north along the upper slope at approx. 400 m water depth, as the weather forecast for that area was much better. Therefore we went north for about two hours.

However, as the weather was still good enough, on **Sunday, 26 August 2012**, survey ***HS 19*** was conducted along profiles given by Jens Greinert to us at the 380 m flare locations. He and his colleagues have conducted this survey in several years, so the data can serve as time study documenting potential change in the position or intensity of the flares. Four of the eight profiles were acquired before the wind speed increased such that we went north with a small roundabout at known pockmarks at 900 m water depth. Seismic data show a pipe or chimney structure and it is said that gas hydrates have been recovered by British colleagues at that site before. ***HS 20*** revealed that the pockmarks are filled with sediments of low backscatter, probably fine grained material that was deposited in the depressions. The low backscatter patches show up as very

distinct features in the multibeam backscatter map. However, no evidence of gas emissions were found at that site, so ***HS 21*** brought us to the north. The navigators steered the ship such that we followed the 400 m depth contour on the way north and the 360 m depth contour on the way back. No evidence for gas emission was observed; neither in the EM 710 nor in EK60. We reached the northernmost point of our cruise at about 79°30'N at about midnight. While further north strong winds blew, we had calm seas, blue sky and a moving view on the mid-night sun probably for the last time. In our main working area the sun already disappears below the horizon and it is getting darker in the night from day to day.

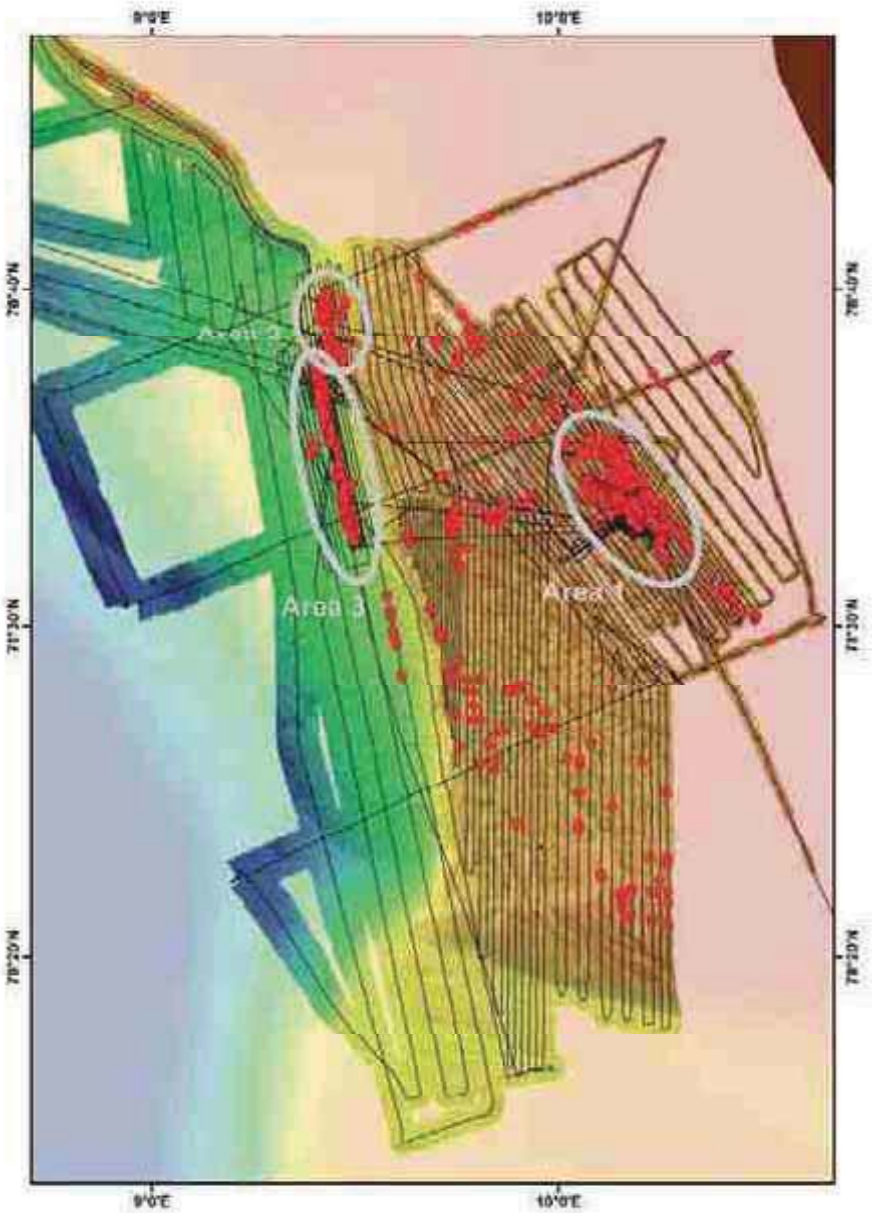

Fig. 2.2: Cruise track of HE–387 with flare positions as picked from EK 60 echosounder records. Gas bubble emissions cluster in three areas termed Area 1, 2, and 3.

Monday, 27 August 2012, the station work started with ***SVP 22*** in order to obtain a recent sound velocity profile for the GAPS system. ***ROV Dive 04 Stat. 23*** was conducted at the 280 m Flare Sites. The main intention was to sample gas by Gas Bubble Catcher, the analyses later revealed that the emitted gas is methane of microbial origin. Furthermore, the dive was used to locate and quantify individual bubble streams. The ***CTD 24*** was taken at one of the streams

characterized before during ROV dives and revealed increased methane concentrations close to the seafloor, which is consistent with our view that most of the methane from the bubbles is already lost by diffusion from the bubble to the surrounding sea water close to the seafloor. In the night, the missing profiles of HS 019 were finalised as station number ***HS 25*** augmented by about 8 profiles in the area.

Tuesday, 28 August 2012, started with the bad news that the sonar Imaginex on the ROV was not working anymore. After trying to fix the problem without success, another sonar (Tritech) was mounted and the ROV deployed, but due to loose cables it had to be recovered after a few minutes in the water. Finally, ***ROV Dive 05 Stat. 26*** started at about 13:00 LT to study the gas emissions at the 280 m flare site. A newly designed and constructed bubble catcher worked very well and the bubble streams causing three different flares in the ship-based echosounders could be mapped and quantified. In order to use EK 60 also for quantification of bubble plumes, the three sites were crossed after the dive with the ship from two different directions during ***HS 27***. The night was spent with EM 710 mapping of bathymetry and qualitatively to look for flares (HS 027) at the shelf with closely spaced lines. It turned out that the line spacing is too close.

Wednesday, 29 August 2012, started with ***CTD 28*** at a 380 m flare position. Afterwards, it was planned to conduct a ROV dive but the deck unit computer of the Tritech sonar did not work. Therefore, a short ***HS 29*** survey for flare mapping with EM 710 was conducted along profiles that run across slope perpendicular to those already acquired ones. After a two hour transit three gravity corer ***GC 30-1***, ***GC 30-2,*** and ***GC 30-3*** were taken at and close to the low backscatter patches at the pockmarks in 900 m. Handling of the gravity corer on HEINCKE is somehow challenging as the wire of the fishing winch is used and redirected through several blocks to the side frame. But as the weather was calm the three gravity corers could safely be deployed and recovered. The sediments contained fine-grained material with some drop stones. The corers were not opened therefore no sediment description is available. However, the preliminary interpretation is, that the normal sediments are fine-grained with frequently occurring drop stones causing the regular medium backscatter of the area. The low backscatter is caused by fine-grained material without dropstones that deposited in the depressions or south of some small-scale elevations, which is lee of a presumably southward flowing bottom current. The night the larger area was mapped by EM 710 during ***HS 31-1*** in connection to ***SVP 31-2***.

Thursday, 30 August 2012 commenced at 06:00 LT with ***CTD 32*** at the pockmark site in 900 m water depth measuring very cold water temperatures close to the seafloor. Our preliminary interpretation was that this cold temperatures result from southward flowing water from the Arctic basin. After a short transit ***ROV Dive 6 Stat. 33*** at flares at 380 m water depth in the northern segment took place. Instead of the Sonar Imaginex the Tritech was used, but we found out during the dive that the sonar position within the vehicle is causing a very limited view with shadow zones making a systematic bubble stream survey difficult. Furthermore, we found large fish (coalfish) that traverse vertically through the sonar beam also causing a strong echo that is very intensive and round-shaped while that of bubbles is usually somehow linear. Bubble streams were found at only one of the flare locations picked by EM 710 and these emissions were transient. This is probably the result of bubbles accumulating within cavities inside the

seafloor which are periodically released. One such cavity was found and documented. It was formed by rocks that closely resemble authigenic methane-related carbonates. The cavity was broken. No bubble streams were observed. But small patches of whitish mats (probably sulphide oxidizing bacteria) were observed around holes in the roof of the cavity suggesting sulphide-rich conditions. In addition, fields covered by several meters by pogonophoran tube worms with some bacterial mats were observed in soft sediments. Probably detritus attached to the tubes gave them a thick appearance in the video. The tubes were grabbed with the ROV manipulator. On deck, the detritus was washed away and very thin tubes of less than 1 mm were recovered. These are certainly anobturate siboglinids (a.k.a. pogonophora sensu strictu). Gas collected at the sites is clearly methane of microbial origin. However, some variation in the gas composition was observed. The ROV dive had to be abandoned in the early afternoon due to increasing wind speeds. Bathymetric mapping of the outer shelf was conducted in the night during ***HS 34***. In the evening, the mid-of-the-cruise-party (Bergfest) was celebrated.

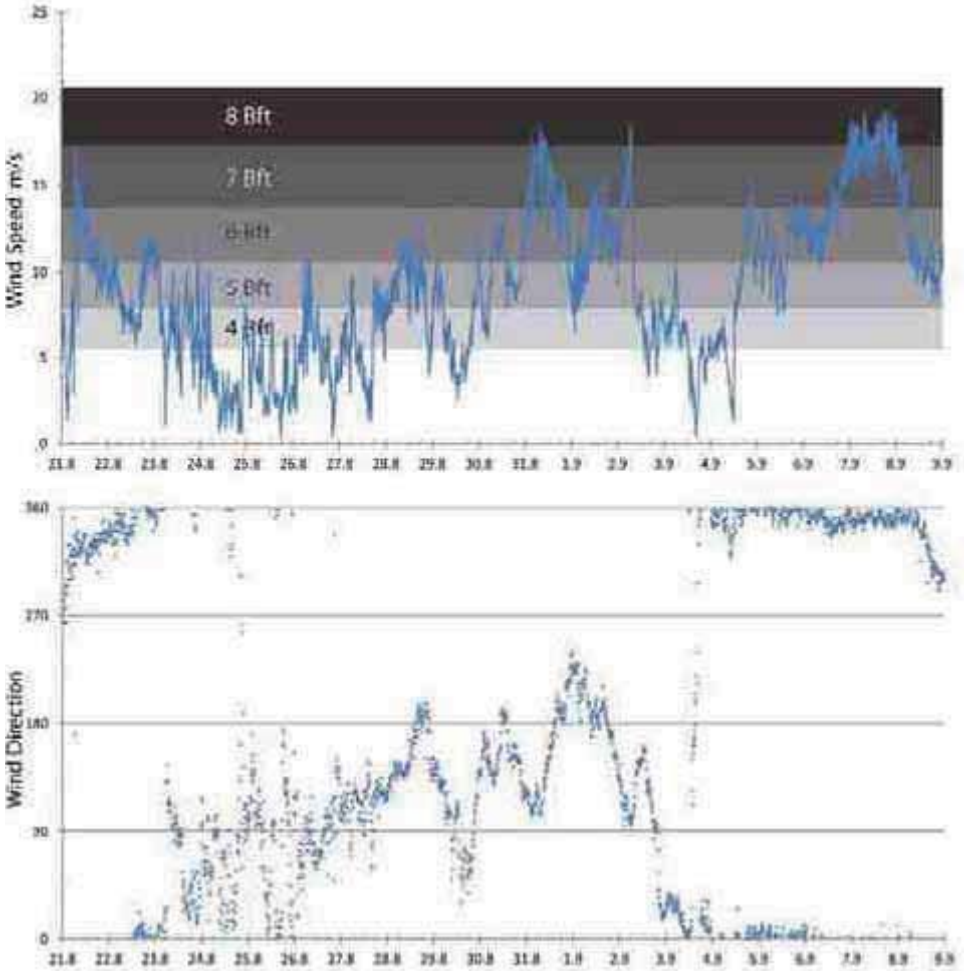

Fig. 2.3: Wind speed and wind direction during cruise HE-387. Plotted are the 10 min values recorded by the ship's meteorological station.

Friday, 31 August 2012, was a windy day. Too windy for any station work with SE winds up to 9 Bft in gales. Therefore the day and the following night were spent with hydroacoustic surveys. The intention of ***HS 35-1*** was to repeat the four profiles running along the upper slope at the flares at 380 m in order to study their temporal variation. However, due to the winds, only those lines running with the wind resulted in acceptable hydroacoustic data quality, therefore, we run

two lines a second time with the wind from S to N. Afterwards, a small transect crossing the deepest flares so far at 440 m and more shallow was conducted. They were found and appeared to be, thus, relatively stable but their appearance clearly identified them as weak bubble emissions. In the night the bathymetric survey of the outer shelf was continued during ***HS 35-2***.

Saturday, 1 September 2012, was too windy for a ROV but just good enough for a 24-hour campaign of measuring surface methane concentration along three transects running roughly W-E in combination with a total of 9 CTDs (***CTD 36-1 to CTD 44 and HS 36-2 to 43-2***). The intention of the campaign was to study the background levels of methane in the different water systems running along the Spitzbergen west coast as well as to investigate whether the gas emissions charge the water with methane to a detectable level. In summary, we found no methane anomaly at the sea surface that could be related to methane gas bubble emissions.

Sunday, 2 September 2012. The ship sails very slowly against the strong winds from S in order to run the survey ***HS 45*** at the slope south of Area 3 to look for gas emissions that have not been discovered in the area so far. Only one of the planned 4 profiles was accomplished because of decreasing wind speeds, we could deploy in the early afternoon the ***ROV Dive 7 Stat. 46*** at the flares in Area 3. Again we are confronted with the fact that the bubble streams escape sporadically, which makes it very difficult to map and quantify the streams. In the night the profiles of HS 45 as well as additional lines at the northern shelf were accomplished as ***HS 47***.

Monday, 3 September 2012, the weather was good to start ***ROV Dive 8 Stat. 48*** at flares in Area 3 in the morning. During the dive physical markers were placed by manned submersible Jago as well as weights of a lander system were encountered. During the dive it became apparent that the gas emissions are bound to morphological lows while streams were absent at morphological highs. The highs are characterized by gravel and pebbles and generally lack of soft sediments whereas at least some sediments occur in the depressions. In addition, carbonate crusts were observed at the bubble emissions and fields with pogonophoran tube worms and bacterial mats. Transit to Area 1 and using EK 60 to check whether gas emissions are still active at the ~90 m site (***HS 49***). At relatively smooth seas a mooring ***Moor 50*** was deployed for listening with the hydrophone S1M1 to the sound of bubbles when being emitted at the seafloor. Positioning was guided by GAPS beacon also mounted on the mooring and worked well. The mooring was placed only a few meters away from a set of at least three bubble streams (WP 1 of ROV Dive 3). In the night the flares at 380 m in Area 3 were again surveyed (***HS 51***) with EM 710 set to only 35°/35° fan opening and settings optimized for flare imaging.

Tuesday, 4 September 2012, the mooring was picked up again (***Stat. 52***). Unfortunately, the sound made by the bubbles is smaller than the ambient background noise, as first analyses by Benoît Bergès revealed. At flares in 90 m water depth in Area 1 ***ROV Dive 9 Stat. 53*** focused on the mapping of a bubble stream cluster identified by EK 60. In the area hundreds of bubble streams occur, which makes it again difficult to quantify them. However, we tried this by accidentally taking sonar scans within the cluster that should later help to extrapolate the flux of individual streams to the total area. After the dive, the area was again crossed with the ship in order to acquire EK 60 records from the bubble cluster (***HS 54***). As the highest methane

concentrations during the entire cruise were measured in surface waters while the ship was on station during the ROV dive just above a strong flare, a spontaneous program to study the extent of the methane plume was conducted (flare hunting II ***HS 55-1***). We found that the extent of the methane plume is very limited and constrained to a few tens of meters above the gas emission in horizontal distance. ***CTD 55-2*** was taken in the gas bubble plume. In the night ***HS 56*** accomplished additional data for bathymetry and the distribution of flares in Area 1 and on the northern shelf.

Wednesday, 5 September 2012, the waves were too high to deploy the ROV safely. Although the wind was not so strong (N 5-6) considerable waves developed in the open sea surrounding us. Therefore the time was used to transit to the pockmark area located at depth of about 800 to 1200 m in order to look for any evidence of methane seeping activity at the morphological depressions (***HS 57-1*** and ***HS 57-2***). In summary, acoustic turbidity signatures were found in the subsurface of some pockmarks with SES 2000. But the nature of this signature could not be studied; the waves were too high to deploy a gravity corer for some conclusive insight.

The survey continued into **Thursday, 6 September 2012**. Because of still strong winds we continued surveying ***HS 58*** in order to map with EM 710 a small-scale slump north of Area 2. In the night we started to map the southern sector of the shelf ***HS 59*** to look for additional flares as well as to fill gaps in the bathymetry.

Friday, 7 September 2012, the wind increased to N 8. Due to the high waves we only sailed in N-S direction and mapped further the southern shelf (HS 59).

Saturday, 8 September 2012, decreasing wind speeds allowed us to deploy ***CTD 60*** that was intended to study whether the elevated methane concentrations close to the seafloor measured in CTD 42 and 43 at the southern CTD/surface methane transect is stable and characteristic for the area, which could be confirmed. While filling a gap in the bathymetric data (***HS 61***) we sailed to a position in Area 2, where Susan Mau had asked to take water samples at a site with gas emission. Three CTDs were required to fulfil the request (***CTD 62-1 to 62-3***). In the evening, a fourth time four lines transecting the flares in Area 3 along the slope were conducted (***HS 63)***. At about 23:15 local time we finished the work in our main working area and steamed to Longyearbyen.

Sunday, 9 September 2012, 08:15 to 12:00 local time at the pier in **Longyearbyen.** Most of the scientists left at 12:00 the vessel to fly back to Germany. Michal, Benoît and Heiko stayed for the transit. In addition, Stefanie joined the transit in order to take from 18:00 to 22:00 UTC three ***MUC 64-1 to 64-3*** at about 1300 m water depth on the way south. About 11 cores were good enough to place them into the fridge at 0 °C in order to maintain benthic foraminifera alive. The experiments carried out by Jutta Wollenburg at AWI investigate the impact of varying pH on the condition and geochemical signature of the benthic foraminifera. With these stations the scientific program of He-387 ended.

Monday, 10 September 2012 to **Sunday, 16 September 2012** transit to Bremerhaven.

3. Methods

3.1 Hydroacoustics

3.1.1 Multibeam Mapping
(Christian dos Santos Ferreira)

Multibeam surveys were conducted using the echosounder KONGSBERG MARITIME (formerly SIMRAD) available at R/V HEINCKE. The system is an EM710, 1-by-2-degree broadband multi beam echosounder system (MBES) operating between 70 kHz and 100 kHz band. It has 200 beams and its maximum water depth limit is at 1500-2000 meters according to the manufacturer. However, its best performance is obtained only from 1000 meters to shallower waters.

During the fast post-processing made on board (plotting, quick cleaning and gridding) the multibeam data was analyzed using the latest MB System 5 (release 1983, August 2012) (Caress and Chayes, 2001). This version was released aiming better support to EM710 backscatter and sidescan maps and was quite important for this cruise.

3.1.2 Mapping of Gas Emissions with EM710
(Miriam Römer)

Additionally to seafloor mapping, the multibeam Kongsberg EM710 allows to record water column features. Gas emissions become visible as flares, similar to flare observations with the single beam echosounder EK60. The advantage of flare mapping with EM710 is the three dimensional view as an entire volume is mapped with the fan and not only flares exactly below the vessel are recorded. Positioning the sources of flares is therefore a lot more precise.

During HE-387 the water column data was not implemented in the *.all files produced by SIS but saved individually as *.wcd files. Both is possible but files become very large when saved together and quick bathymetry processing is a lot easier and faster if the water column information is already stored in a separate file.

For visualization the software package IVS Fledermaus was used which enables a three dimensional view of the data. In a first step, the FM Midwater tool is needed to open the *.wcd sonar file and convert it to a *.gwc file, which can be displayed in the software. Afterwards the entire three dimensional fan can be exported as an *.sd file and opened with Fledermaus, where it can be replayed in 3D for instance together with the underlying bathymetry (Fig. 3.1.1). When scrolling through the fan view, source locations of appearing flares can be picked directly with the geo-picking tool (Fig. 3.1.2). As a last step, the positions have been exported as a table to be displayed in GIS maps for further planning.

It is also possible to extract only the anomalies within the fans that make up the flares. For this, the clippings have to be set in FM Midwater in the way that more or less only the flares are still visible and as export option ‘export ASCII’ has to be chosen. The text file has to be opened as ungridded data within the DMagic tool of the Fledermaus package and converted to a *.pfm file, which again can be imported into the 3D Fledermaus. The single points can now still be edited and flares cleaned manually.

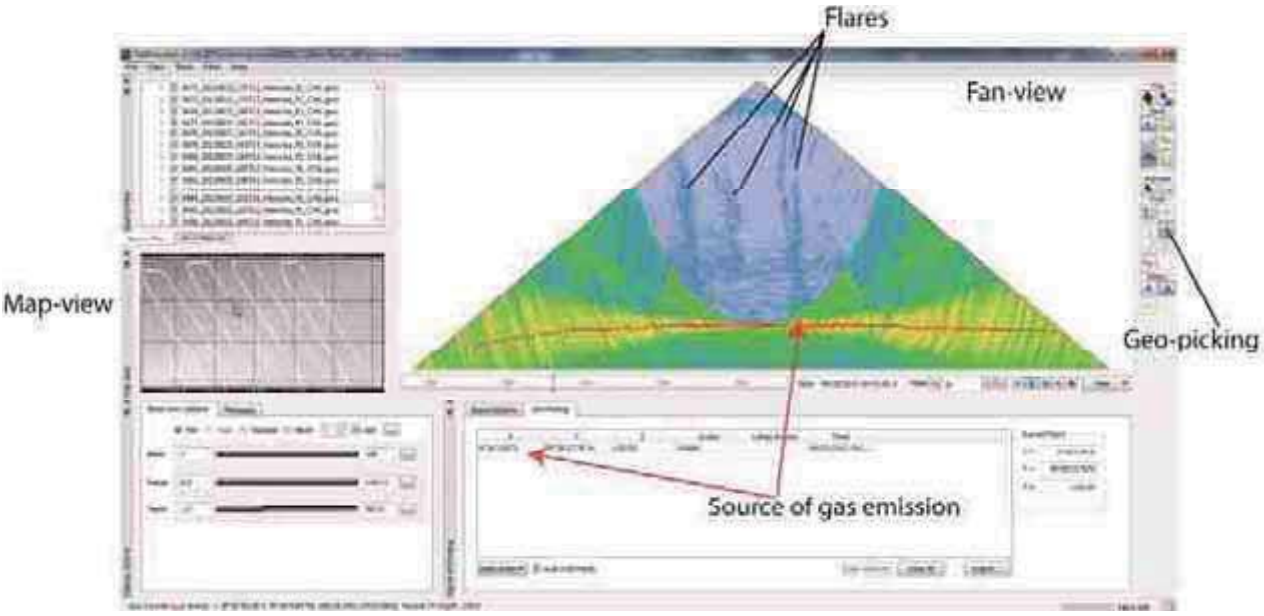

Fig. 3.1.1: FM Midwater tool to display the fan in 2D and convert the sonar files into *sd files which can be opened with IVS 3D Fledermaus.

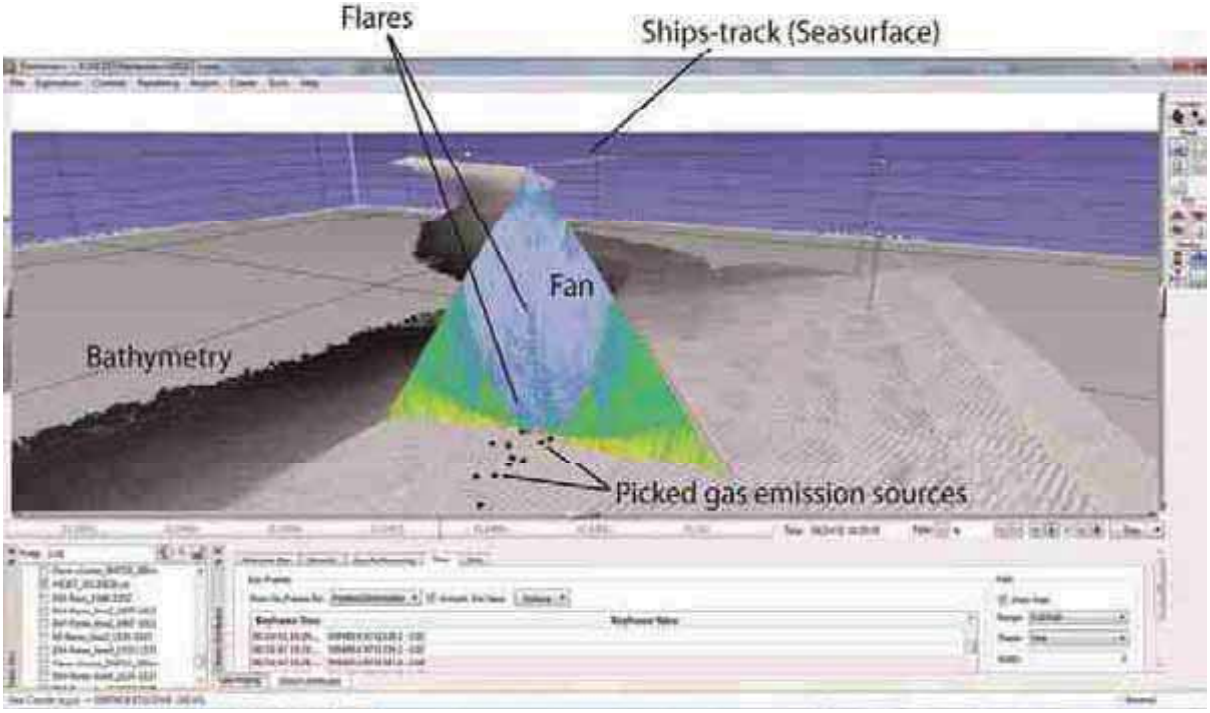

Fig. 3.1.2: Replaying fan in the 3D view of Fledermaus together with the achieved bathymetry.

3.1.3 Mapping of Gas Emissions with EK60
(Benoît Bergès)

The EK60 system is a single beam scientific echosounder, giving measures of echo strengths of targets within the insonified volume of the beam. The data were visualized using the ER60 software (Fig. 3.1.3). With this echosounder, the footprint was approximately 12% of the water depth and four frequencies were available: 38 kHz, 70 kHz, 120 kHz and 200 kHz.

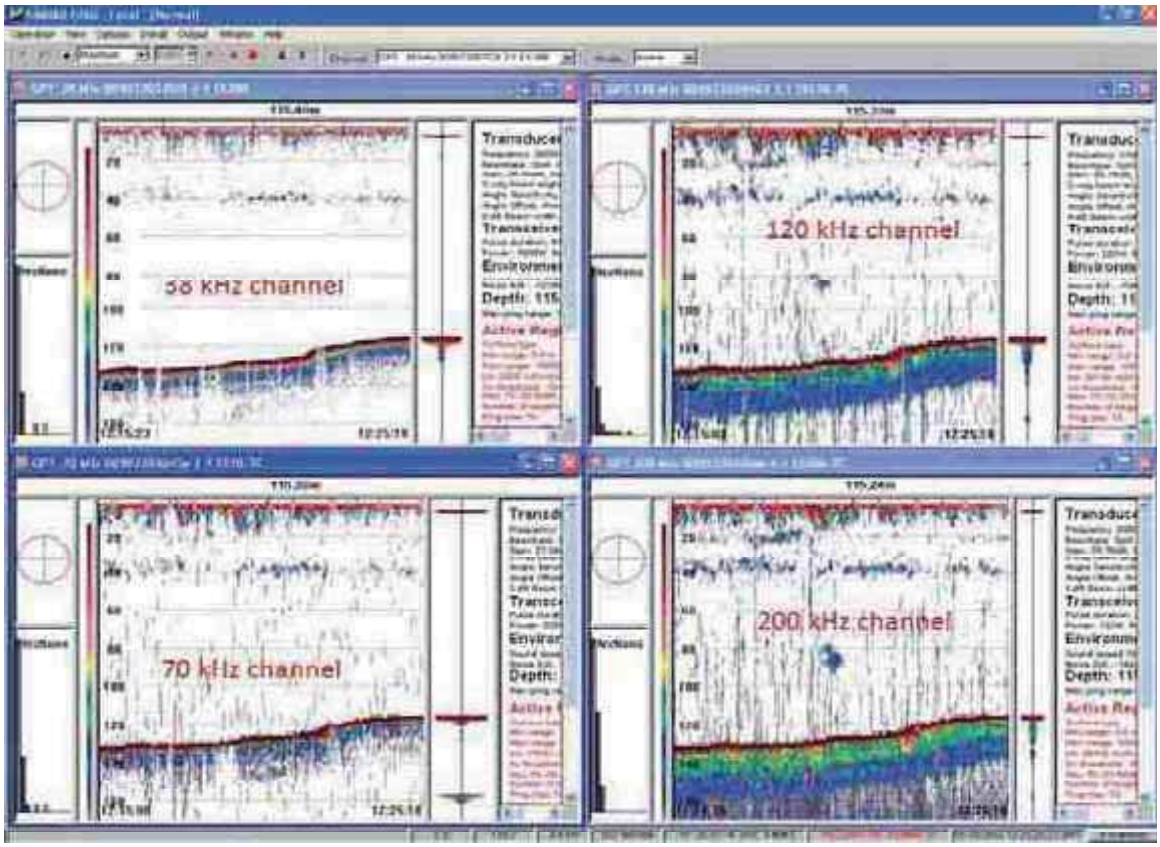

Fig 3.1.3: Overview of the ER60 interface showing the four channels that were available (Sv levels).

The overall performances of the echosounder were very good during the cruise, being very stable over time and producing an interesting data set. Only some noise issue was experienced during rough weather conditions (Fig. 3.1.4). In addition, because of transmission losses, every channel could not perform the same at any depth. Channels that were available without significant amount of noise over the different areas that were studied are the following:

Area 1 (~90m): 38 kHz; 70 kHz; 120 kHz; 200 kHz
Area 2 (~240m): 38 kHz; 70 kHz
Area 3 (~380m): 38 kHz; 70 kHz
Area 4 (~900m): 38 kHz

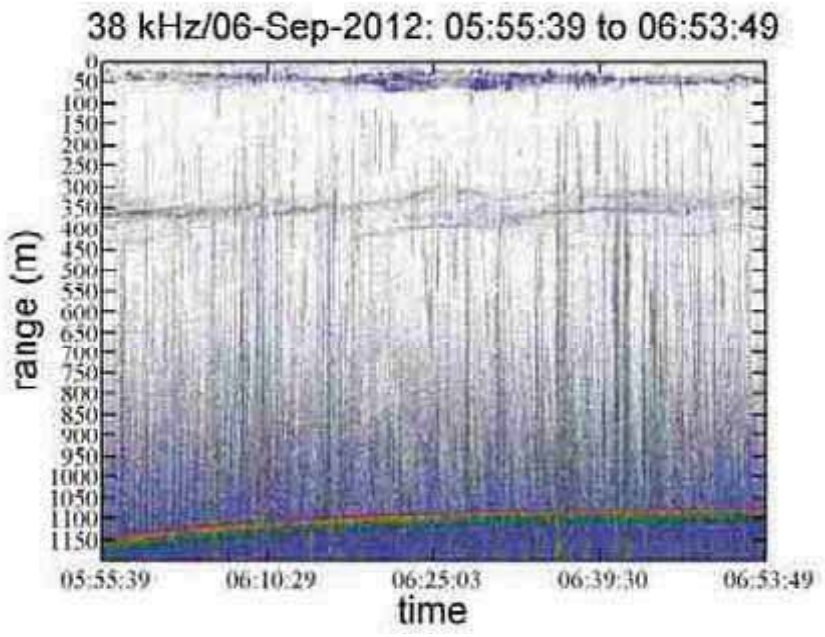

Fig. 3.1.4: Echogram from 06 September 2012 between 05:55:39 and 06:53:49. At that time, the weather was very rough and because of the waves, the data are very noisy.

Data were stored within the *.raw format and processed afterwards using the readEKRaw EK/ES60 ME/MS70 MATLAB toolkit designed and shared by Rick Towler. This MATLAB package was used to convert the power levels from the *.raw files into Sv levels and to plot echograms. The quantity Sv corresponds to the volume backscattering per unit volume. It represents the backscattering strength within a unit volume and is expressed in dB re 1 m^{-1}. This quantity is often used when individual targets are very small in the sampled volume, having different echoes combining to give a certain signal level.

EK60 flare mapping. From the readEKRaw MATLAB package, a toolkit for mapping flares was designed. This consists of an interface where the user is reading each echogram and is asked to pick manually the flares that appear. For each echogram, the procedure consisted on:

- Investigating the echogram
- Setting up the echogram to the correct depth
- Specifying the number of flares that are observed
- Picking each flares manually using the graphical interface

For each flare that is picked up, calculations are performed and the following values are stored in an excel file:

- Id of the flare following the format: DayMonthNumbering
- Time of appearance of the flare (based on the mid-point of the selected area)
- Longitude of the flare (based on the mid-point of the selected area)
- Latitude of the flare (based on the mid-point of the selected area)
- The strength of the flare (sum of all Sv level within the area)
- The strength of the flare per unit area
- The area of the flare
- The height of the flare

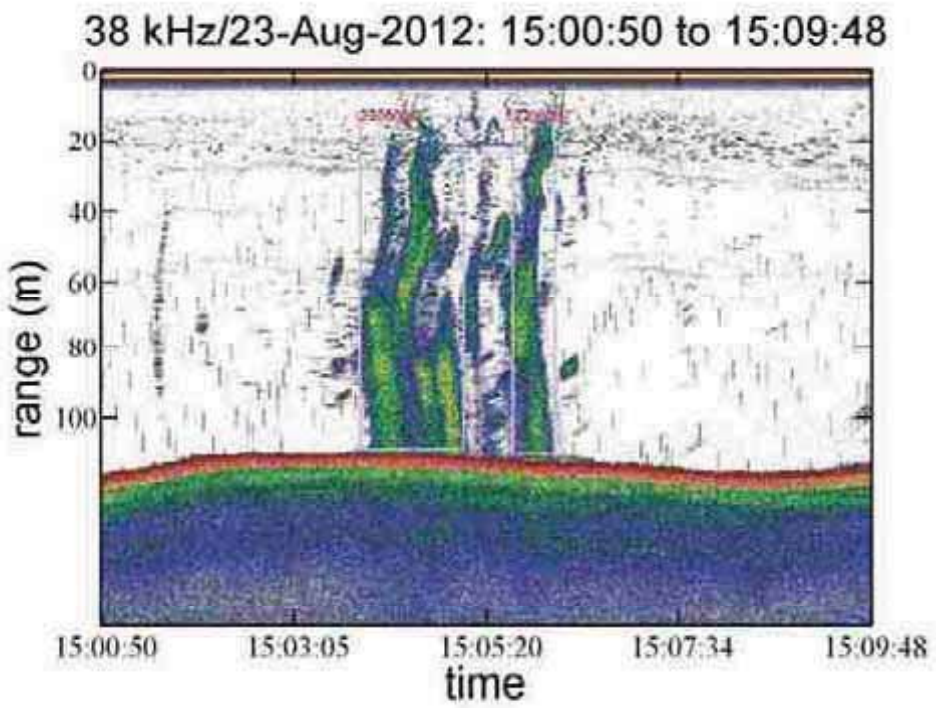

Fig. 3.1.5: Echogram from the 23 August 2012 between 15:00:50 and 15:09:48. This shows an echogram where two flares (2308096 and 2308097) were picked up manually for mapping.

EK60 for bubble flux quantification. It is planned to use the EK60 data that were collected during this cruise in order to perform some quantification. As the EK60 echosounder is calibrated using a standard procedure, it gives absolute measures, it makes it very interesting for a purpose of estimating gas volumes. This could be done by performing an inversion on the Sv levels that were observed from bubble plumes at different frequencies. Such inversion technique has been used for zooplankton estimation and classification and some good results have been obtained (Lebourges-Dhaussy, 1996; Simmonds and MacLennan, 2005). Applied to bubble size distribution estimates, this technique has been applied to surface bubbles that are created under breaking waves (Vagle and Farmer, 1992). While such a technique gives good results, the model used is applied only on small bubbles that are resonant to the frequencies used for the study (ka << 1). In the case of methane seepages, bubbles that are produced are much bigger and are not likely to be resonant at the frequencies used by the EK60. It is then necessary to adapt the method by using a more appropriate model for backscattering strength. The accuracy of the technique could be investigated by comparing flow rates measured during ROV dives and estimates from the EK60. This would allow having order of magnitude estimates for gas releases from the acoustic surveys (large scale estimate).

Depending on the frequency, a gas bubble is responding differently to an acoustic field. Different echo levels are then experienced depending of the frequency that is used. This is a well-known dependency and for single target this is described by the scattering cross section σ_s. The difference of echo level at different frequencies is then directly related to the density of bubbles of different sizes. At a frequency f_i, the backscattering volume expressed as inverse meter (m^{-1}) is related to the bubble distribution as followed:

$$s_v^{f_i} = \int_0^{+\infty} \sigma_s(f_i, R_0) n(R_0) dR_0$$

with $n(R_0)$ the bubble size distribution expressed in number of bubbles per cubic meters. This equation defines a Fredholm integral of the first kind that can be discretized. The determination of $n(R_0)$ consists on solving the following inverse problem expressed in matrix form:

$$n = \sigma_e^{-1} S_v$$

The performance of the inversion relies on the accuracy of the model used for σ_e. The few numbers of frequencies also limit the accuracy of the bubble size distribution calculation and then volume estimates. Different models have to be studied together with algorithms allowing computing under-determined inverse problems.

3.1.4 Sediment Echosounder SES2000
(Miriam Römer)

The narrow-beam parametric subbottom profiler SES-2000 Medium is a product of Innomar and was used during few surveys on HEINCKE Cruise HE-387 in order to obtain subbottom information and visualize sub-seafloor structures. The power of the sensor unit has to be switched on first by the captain and afterwards the SESWIN operation system can be started from the PC at the bridge. The system settings were set as suggested by FIELAX and best results were obtained using the transmission frequency of 8 kHz with the additional setting given in Table 3.1.1.

Table 3.1.1: Settings for subbottom acquisition with SESWIN used during HE-387.

Transmit	LF-Frequency LF-Pulses	8kHz 3
Range		50 m (sometimes 100 m)
Process	Stacking Smoothing Soft TVG Normalized gain Median-Filter	2 2 0.3 Yes yes
Gain	LF HF	~50-60 ~60-70
Depth	Detection Sensitivity: LF HF Detection offset from depth Bottom averaging	 40% 40% 0% 5
Threshold	LF Mode LF Min Level LF SRange HF Mode HF Min Level HF SRange	Log 6-9 5 Log 6-9 5

Two different types of files are stored: *.ses files and *.raw files (has to be explicitly checked on in the system settings!). After acquiring the data, the *.ses files can be opened with the post-processing software ISE 2.9.2 available on board. Some cleaning of the data was performed and it is possible to export the result as *.sd file, which can be opened in IVS 3D Fledermaus together with for instance bathymetry data and flare positions to gain a better overview.

3.1.5 Motion Sensor and Lever Arms
(Christian dos Santos Ferreira)

A central device for running ship-based echosounders such as EK 60, EM 710 or SES 2000 is the motion sensor at HEINCKE IXSEA PHINS. This motion sensor provides basic data on the movement of the ship that is needed to obtain meaningful data from the echosounder. For a perfect setup, the level arms between motion sensor, transducers, and GPS are needed as well. The experience from other ships is, that imperfect performance of the motion sensor or imprecise lever arms can reduce the quality of the data significantly.

One problem that we were confronted with during our cruise is wobbling to be seen in the multibeam data EM 710. In order to rule out any problems inherent to the multibeam system, a calibration was performed at the beginning of the cruise. However, even after the calibration the problems with the wobbling persisted. Furthermore, the level arm settings have been double-checked based on the available documentation. It can largely been ruled out that this is the source of error. Therefore, we suggest two sources of error that we can not fix during the cruise and that we will report to those responsible for maintenance of the system. One possible source could be a technical problem with the motion sensor, either with the hardware or the software. We noticed that the firmware version of the motion sensor is quite old and that an update might be considered. A further possible source of error could be that the survey alignment (the distances/angles between GPS, motion sensor, and EM710 transducers) done at 2009. It should be carefully considered to check if these alignments are correct.

Another problem identified with the EM710 was the rate which this sensor is receiving motion data from the PHINS. The PHINS can deliver data up to 100Hz, but the system is set to deliver data at 10Hz (since 2009). Since R/V HEINCKE is often working at shallow areas (~20-25 meters water depth), the ping rate of the EM710 can easily reach a frequency of 25 Hz, which using this installation setting means that more than 50% of the multibeam data has no motion data available, and therefore must be interpolated. Since we worked at depths >50 m we set the motion data rate to 20 Hz. However, currently the serial port speed set cannot hold a higher rate, and therefore we advise that this problem should be addressed in the future with the intention to increase the data to at least 50 Hz.

During our cruise we figured out that in the data of SES2000 and EK60 wobbling was also an issue since both systems were incorrectly set. Both systems require that their offsets (distance from the motion sensor to their transducers) are correctly inserted into the PHINS, which is later recalculating the motion at the positions from these two systems, and sending this information to them. For the EK60 there was no offset inserted (and applied) and the SES2000 had the offset inserted but not applied. In order to apply the offset we set “IO settings => Output data => Out C => Lever arm” to “Secondary lever arm”. We note that these erroneous settings have been used since 2009. During our cruise we inserted one distance offset for both systems (EK 60 and SES 2000) into the PHINS as the transducers are very close to each other. However, this is not the optimal solution as there is a difference indeed. But as the wobbling decreased significantly, we used these settings. For the future, it would be good to split the output although we are aware of the shortage of output channels, as all of the PHINS are in use already.

3.1.6 Sound Velocity Probe (SVP)

(Miriam Römer)

The MIDAS SVP (Fig. 3.1.6) is fitted with Valeport's digital time off light sound velocity sensor, a fast response PRT temperature sensor, and a high accuracy temperature compensated piezo-resistive 0.01% pressure transducer.

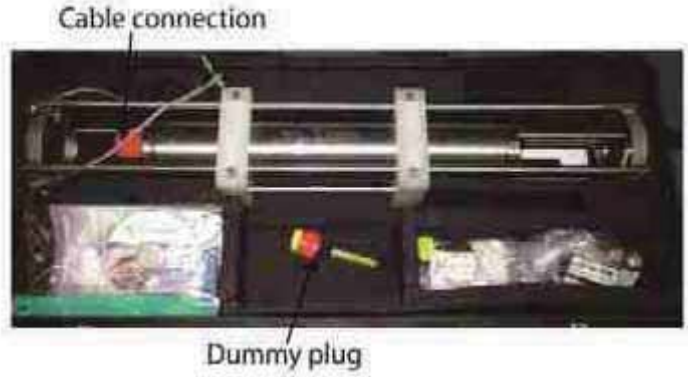

Fig. 3.1.6: Image of the sound velocity probe on R/V HEINCKE.

The sound velocity range is between 1375 and 1900 m/s with a resolution of 0.001 m/s and an accuracy of ±0.02m/s. The instrument operates autonomously, with setup and data extraction performed by direct communication with PC before and after deployment. It can also operate in real time, but during HE-387 it was always operated autonomously. The system is supplied with DataLog Express Windows based PC software, for instrument setup, data extraction and display. DataLog Express is license free.

Deployment steps:

1. Connect probe to PC (with a serial port) and with power supply
2. Open the progam DataLog Express
3. Connect with probe
4. Check the settings (select OFFLINE operation mode)
5. Start with RUN
6. Disconnect cable between probe and PC and adopt dummy plug to the probe
7. Connect probe to winch and bring it into water
8. With a speed of ~0.5 m/s down to ~10 m above seafloor and with full speed (~2 m/s) back on board
9. Clean the probe with fresh water and dry it
10. Disconnect the dummy plug and connect the probe with the PC
11. Save the file with the program DataLog Express to the PC (*.000 file)
12. Disconnect the probe and store it in the box

After deployment, the sound velocity profile has to be implemented in the multibeam SIS:

1. Open the SVP Editor from the SIS menu (Tools/Custom/SVP Editor): Expand the view by dragging the boundaries of the window
2. Open the SVP file (File/Open in editor): Browse for the SVP input file and press Open. The Raw file editor opens
3. Select the delimiter from the drop down list
4. Press Split to apply the delimiter. A new window will appear
5. Delete the header and mark the columns not needed. Position the mouse in the first data row to mark that column
6. Press Delete selected columns to remove the marked columns
7. Move the columns by position the mouse pointer on the column header row and drag the column to right position
8. Press OK when selected columns are in right place
9. Back in the Raw file editor remove all header rows by marking them and press Delete
10. Select Save as - the file extension is automatically set to *.asvp

Now the sound velocity profile can be loaded into SIS and checked for errors:

1. Open the SVP Editor from the SIS menu (Tools/Custom/SVP Editor): Expand the view by dragging the boundaries of the window
2. Open the *.asvp (File/Open) menu:
3. Check the observations for double entries or upward depths by choosing Tools/Check profile
4. Observations that are suggested removed are highlighted
5. Press Delete row to delete highlighted entries
6. Repeat until the profile is acceptable
7. Save the file from the File/Save as menu. It is recommended to use a filename that identifies date and time.
8. Select Runtime parameters/Sound speed: Use the browse button to open the correct *.asvp file
9. Press Use Sound Speed Profile to apply the selected sound speed profile

3. 2. Water Characterization and Sampling

3.2.1. Thermosalinograph

(Heiko Sahling)

In order to continuously measure temperature and salinity just below the sea surface a thermosalinograph of the company Seabird is installed (SBE 21). The tool is equipped with an external temperature probe (SBE 38) measuring the temperature directly at the water inlet. All measurements as well as the derived parameters (e.g. sound velocity) are stored in the DSHIP data base.

3.2.2. Physico-Chemical Investigations of the Water Column

(Thomas Pape, Patrizia Geprägs)

Hydrocasts were carried out using the ship-based Sea-Bird Electronics, Inc. SBE911plus (Sea-Bird Electronics) CTD, which comprised of two conductivity (SBE 4c) and temperature (SBE3 plus) sensors each and one pressure sensor. The system was additionally equipped with a dissolved oxygen (DO) sensor (SBE 43), a fluorometer (WET Labs, Eco FL) and a transmissometer (WET Labs, C-Star). The CTD sensors were calibrated at SBE in October 2010 (P) and June 2011 (C + T), respectively. The DO sensor used at the beginning of the cruise did not work sound and was replaced after CTD station 5 (GeoB16828). Reliable DO data was collected since CTD station 6 (GeoB16832).

The underwater unit was attached to a SBE 32 carousel water sampler with 11x4 L water sampling bottles (OceanTest Inc.), which were closed at selected depths during the upcast. The CTD/rosette system was lowered with 0.5 m s^{-1} in the upper to intermediate water column and 0.2 m s^{-1} in bottom waters, whereas heaving in-between the bottle firing procedure was conducted with 0.3 to 0.5 m s^{-1}.

Position control by ship tracking showed that the vessel moved less than 15 m into each direction during hydrocasts in the 80m seep area.

3.2.3 Methane and Carbon Dioxide Concentrations in Surface Waters
(Michael Glockzin)

The analytical setup consists of a methane carbon dioxide-Analyzer (MCA, Los Gatos Research) joined to an established custom-built equilibrator setup (Fig. 3.2.1). The analyzer uses off-axis integrated cavity output spectroscopy (ICOS) and combines a highly specific infrared band laser with a set of strongly reflective mirrors to obtain an effective laser path length of several kilometers. This allows detecting methane and carbon dioxide in the equilibrated gas phase with high precision (less than 0.1%) and frequency (Gülzow et al. 2011). The seawater for the analysis was taken continuously from the crane-and-seawater pump setup available in the wet lab of R/V HEINCKE (pump installed at 2.80 m water depth). The system was checked by standard gas measurements (2ppm CH_4 and 380 ppm CO_2) occasionally. To estimate air-sea flux, measurements of the methane and carbon dioxide concentration of the ambient air were conducted at different dates and locations during the cruise, with the tubing outlet installed on the starboard side above the bridge of R/V HEINCKE. Measurements for methane and carbon dioxide together with all related parameters (e.g. temperatures and flow rates of seawater and air in equilibrator etc.) were taken at a 5s interval together with the ships position (via NMEA string) and all parameters were recorded continuously by laptop. For the calculation of in-situ concentrations of CH_4 and CO_2, hydrographic and meteorological data were taken from the DSHIP system (inlet at 3.30 m water depth).

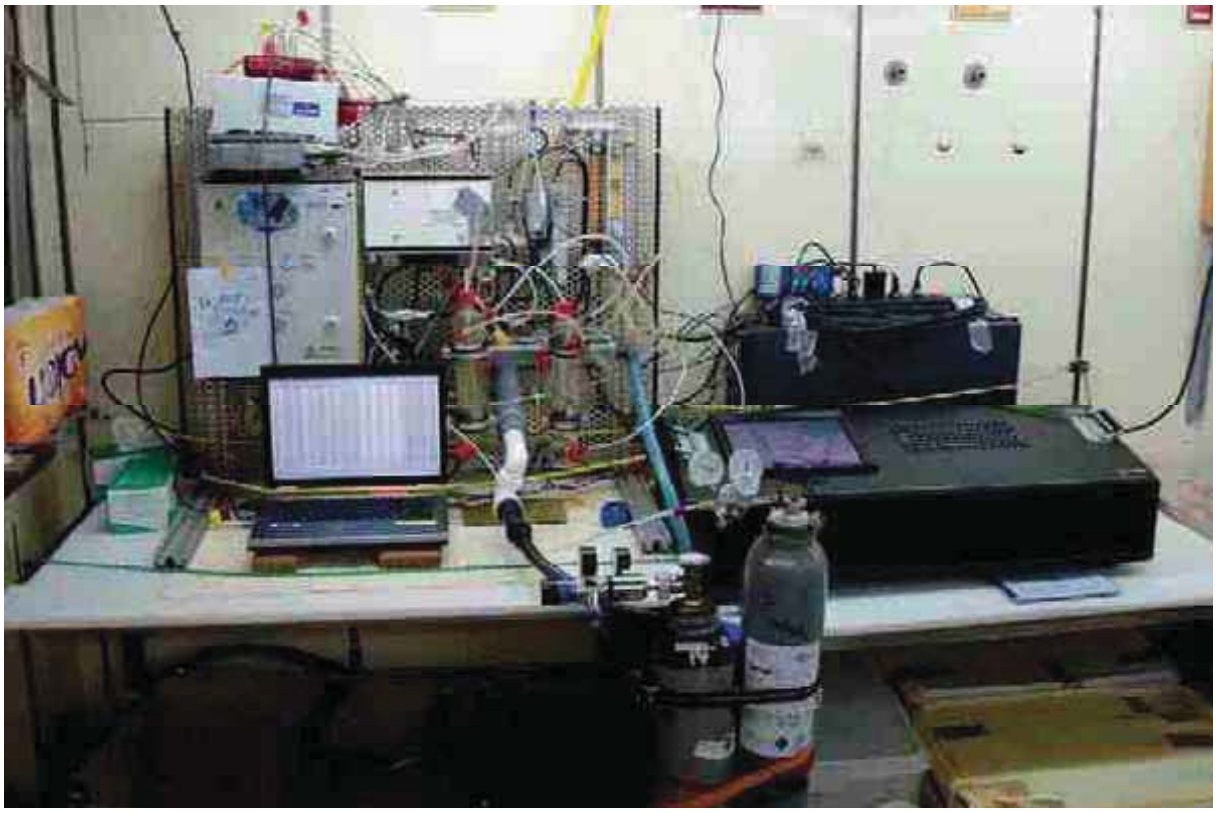

Fig. 3.2.1: Image of the set-up for continuous methane and carbon dioxide measurements on board R/V HEINCKE Cruise HE-387.

3.3 Seafloor Sampling

3.3.1 Sediment Sampling by Gravity Corer
(Thomas Pape)

For sampling of surface sediments four gravity corer stations (GeoB16808, 16830-1, -2, -3) were performed during HE-387. The gravity corer equipped with a 3 m- or 5 m- core cutting barrel and a weight of approx. 1.2 tons. Plastic tubes were used as liners. The GC was lowered with a rope velocity of 1.0 m s^{-1} down to about 50 m above ground and hold for about three minutes to mute oscillation. The GC was penetrated into the sediment with 1.0 m s^{-1}. Because the rope tension was not documented for the winch running the GC, direct control of the penetration procedure was not given and the rope was lowered until the rope length exceeded the water depth by more than 20 meters. Heaving of cores was done with a rope speed of 1.0 m s^{-1} as well. After recovery on deck, the liners were cut into 1 m-segments, capped and transferred into the cooling room (4°C).

3.3.2 Pore Water Extraction
(Thomas Pape)

For a first insight into fluid origin and near-surface migration in the 900 m pockmark area, pore waters were extracted from gravity core GeoB16830-3 using the Rhizon technique (Dickens et al., 2007; Seeberg-Elverfeldt et al., 2005). The pore water samples were taken along the 4.24 m long core in 50 cm-intervals. The volume of pore water collected was transferred with medical syringes headspace-free into 10 mL-glass bottles and sealed with screw caps equipped with PTFE inlays. The glass bottles are stored in the darkness at 4°C until analysis in the home lab. In total,

3.3.3 Multicorer
(Heiko Sahling)

A conventional multicorer was used to recover sediments from the seafloor. The multicorer was provided by the AWI. It was only operated on the way back from Longyearbyen to Bremerhaven in order to collect benthic foraminifera to be carried living to the AWI.

3.4 MARUM-CHEROKEE ROV Operations

3.4.1 System Description
(Nico Nowald, Werner Dimmler)

The MARUM-Cherokee ROV is a 1000 m depth rated, mid-size inspection class ROV, manufactured by Sub-Atlantic, Aberdeen. It was adapted and improved for scientific use and is operated by MARUM since 2001. The ROV was deployed on 25 expeditions from national and international vessels with a total of 148 dives up to now. The system requires a crew of two, pilot and co-pilot, as well as two persons to operate the winch. During R/V HEINCKE Cruise HE-387, the vehicle was deployed in order to locate, to quantify and to sample gas emitting from the seafloor in the working area west off Svalbard, Norway. The ROV system consists of three major components: the vehicle, the winch and a topside control unit.

Vehicle: Vehicle dimensions are 130 x 90 x 90 cm (L x B x H) and total weight in air is 450 kg. The ROV requires a 380VAC input into the isolation-transformer which is part of the system and which provides 220V for the vehicle´s low power devices (cameras, PCB´s, Pan & Tilt Unit, etc) and 440V for thrusters and light. Power consumption during operation is around 12 kW. As standard navigational instruments, the Cherokee is equipped with a compass, an altimeter and a depth sensor. The vehicle is electrically propelled by 4 axial thrusters and three 230 VAC dimmable LEDs, provides a total light power of 1500 W. For scientific observation, three cameras are installed on the ROV. The main camera is a Tritech Typhoon PAL device with zoom capabilities, mounted to a Pan & Tilt unit. One static, fixed focus DSPL Multisea Cam is overlooking the area directly in front of the ROV. Still images with a 5 Megapixel resolution can be acquired with a Kongsberg OE-14, that is also mounted to the vehicle´s Pan & Tilt unit. A bracket attached to the still camera, carries a pair of lasers for size measurement of objects on the ocean bottom (distance 11.3 cm). The vehicle is equipped with a forward looking Tritech Seaking dual frequency sonar (325/675 kHz) for obstacle detection. Maximum scanning range is 300 m. The hydroacoustical realtime data are processed and displayed by a dedicated PC, located in the topside control unit. To collect objects from the seafloor and to carry out experiments, a Hydro-Lek HLK-EH-5 manipulator with five DOF is mounted on the starboard side of the vehicle. The manipulator is non-proportional and powered and controlled by a combined hydraulical pump that includes a 6 station valve pack. The operating pressure of the manipulator is 110 bar and the device has a lifting capacity of 25 kg. In order to store objects or to install scientific tools, the ROV is equipped with a toolbox that can be opened and closed hydraulically. The toolbox is mounted under the mainframe of the vehicle. Two serial links are available to connect external, scientific sensors. For navigation during operation, the Cherokee used the USBL positioning system GAPS, that is installed on the R/V HEINCKE. One acoustic beacon was placed on the ROV and was powered by the vehicle´s on-board power supply. A second beacon was mounted to the depressor, which is also part of the system. The depressor consists of a small steel frame (50 x 50 x 50 cm) with a 24V/38Ah DSPL battery, which powers the beacon. With some additional lead, its weight is around 100 kg. It is attached to the supply cable on a cable grip 50 m behind the vehicle. The depressor´s weight pulls the cable straight during operation, taking away some of the drag on the cable. This allows the ROV to maneuver freely within an operation radius of 50 m.

Fig.3.4.1: Cherokee prior to deployment: in the hangar to the left, the winch and to the right of the ROV, the depressor.

Winch and supply cable: The spooling winch is an MPD, Aberdeen custom design winch with level wind and a Focal 180 fibre optic rotary joint, carrying approximately 920 m supply cable. Overall weight of the winch, including the cable, is 1.8 t. It requires a 380VAC input and power consumption is 3.5 kW. The supply cable, manufactured by JDR, NL has an aramid inlay for protection purposes and diameter of the cable is 27 mm. The cable contains 20 conductors providing electrical power and the analogue telemetry channels for the sonar and vehicle controls. The cable also includes four Multimode 62.5 um fibres that are used for 4 x PAL video and 4 x RS232 serial channels.

Topside Control Unit (TCU): The TCU consists of three cases, that are placed in the ship´s laboratory from which the vehicle is remotely operated. Two cases are equipped with several monitors for the Pilot and Co-Pilot. The monitors display the video signals from the vehicle´s cameras, navigational information of ship and ROV, as well as the sonar software. The third case is a 19" rack that contains the major components to operate the vehicle, such as the main power switches, 3 PCs, several PCBs for power supply, video overlays, vehicle control and the video/data telemetry.

The system was mobilized on Monday, 13 May 2012, in Bremerhaven and a first successful test was already done in the port. The winch was placed in the hangar and the TCU, as well as the transformer, were placed in the vessels dry lab. The block was attached to the small A-frame on the starboard side on the vessel, from which the vehicle was launched and recovered.

Fig. 3.4.2: The TCU in the drylab: to the left, the two cases with the monitors and to the right the 19" rack. The remote controls for the vehicle and manipulator are seen in front of the monitors.

In order to navigate and to coordinate ship and ROV, the Cherokee uses the POSIVIEW software. POSIVIEW receives the GAPS data telegram, that includes ship and ROV position via UDP stream, as well as the compass information from one of the ROV´s serial links. The software allows to calibrate a navigation map that is used as a base for mission planning and navigation during operation. Ship, ROV and depressor position, their heading and tracks are displayed on the map. Markers can be placed on the map, in order to relocate places of interest during a later dive. A clone of the Pilots POSIVIEW screen was transmitted to the bridge via a VLC connection, which helped the R/V HEINCKE navigators to position the ship according to the ongoing mission.

3.4.2 USBL Positioning System GAPS

(Nico Nowald, Heiko Sahling)

GAPS is a portable USBL (Ultra Short Baseline) positioning system with integrated Inertial Navigation System and GPS. The system was developed by IXSEA, France. Given accuracy is

0.2 % of the distance to go. The system consists of three components: the antenna that bears four hydrophones and a transducer, the beacon and a deck unit with a PC that does the processing. The antenna transmits an interrogation signal to the beacon that replies with an acoustic ping. The four hydrophones receive the reply at different times, which allows the processing unit to calculate the position of the beacon relative to the ship. With aid of an additional GPS input, the absolute position of the beacon can be determined. Four interrogation frequencies can be chosen, ranging between 19.5 kHz and 21 kHz.

Two beacons (serials #346 & #347) are available on the R/V HEINCKE for use. Beacon #347 has a remote transducer head that allows a more flexible installation on a vehicle and was placed on the ROV. Beacon #346 was mounted to the depressor. The serial data output from the GAPS deck unit was fed into a terminal server, which distributed the GAPS PTSAG data telegramm into the TCU network architecture via UDP. The GAPS PC in the CTD lab, could be remotely configured from the Co-Pilots seat in the dry lab via a VLC connection.

The general performance of the GAPS system was satisfying. However, there have been issues with clearly wrong positioning of the vehicle when the ship came to close to an intensive gas emission site. This could generally be avoided. In addition, at the first dives the interrogation time was quite long with several seconds. That has been changed later in order to receive more frequently the position of the vehicle.

3.4.3 Scientific Payload

(Nico Nowald, Thomas Pape, Miriam Römer, Heiko Sahling)

Marker. The marker deployed during the cruise were a simple construction consisting of a brick with a 10 mm borehole in the middle and a polypropylene plate (PP) with a length of 100 x 100 mm (Fig. 3.4.3). Both parts were connected to each other with a Dyneema rope. The length of a Marker was 300 mm and weight approximately 2 kg. Each plate carried a different number from 1 to 10 and a total of 10 Markers were prepared for the campaign.

Niskin bottle. The ROV is equipped with a 1l, Hydro-Bios Kiel, water bottle that is installed in the toolbox on the starboard side of the vehicle. The bottle is triggered by pulling on a releaser rope using the manipulator. It can be easily removed from the toolbox by removing one screw. The bottle is a permanent installation on the vehicle.

Bubble Catcher. A custom made bubble catcher was used to quantify the amount of emitted gas.

Gas Bubble Sampler. Bubble forming vent gas was collected with a modified version of the in situ pressure Gas Bubble Sampler (GBS, Pape et al., 2010) adapted to the capacities of the ROV Cherokee. Briefly, the GBS consists of a pressure-tight steel cylinder, a pressure needle valve on top, and a pressure ball valve at the lower end which is connected to an inverted gas collector funnel via a plastic hose (Fig. 3.4.3).

Before the ROV dive, both valves are closed on deck preserving atmospheric pressure inside the GBS. In order to sample vent gas injected into the water column, gas bubbles were collected in the funnel only a few centimeters above the seafloor. By opening the ball valve with the ROV manipulator, the funnel content was sucked into the pressure chamber as a consequence of the

pressure difference. Subsequently, the lower valve was closed preserving the sample under in situ pressure. Because the ROV Cherokee is equipped with a single manipulator arm only, the GBS was directly mounted to its frame. During the sampling procedure the manipulator was used to hold the gas collector funnel directly above the orifices and to handle the ball valve.

Fig. 3.4.3: ROV Cherokee scientific payload: (upper left) bubble catcher (2nd version), (upper right) Niskin bottle manufactured by Hydro-Bios, (middle) gas bubble catcher, (lower left) marker, (lower right) CTD mounted at the back of the vehicle.

CTD. A small CTD probe has been fixed at the back of the ROV during the dives in order to characterize the water column during ascent to the seafloor and rise again to the sea surface of the ROV. The resulting profiles are used to complete the CTD casts with the rosette (see Chapter 4.7). Additionally, the temperature profiles when surveying close to the seafloor may show differences or anomalies when passing seepage areas as anomalies could result from fluids escaping from the seafloor which often have slightly higher temperatures.

The CTD is made by 'Sea & Sun Technology' and communication with the probe is enabled with the corresponding software package SST's Standard Data Acquisition. Before deployment, the probe has to be configured: the time of acquisition (the entire time planned for ROV dive) and the interval (1 second) has to be set and sent to the probe. After deployment the probe is connected again to the PC and the program opens for data read out. A raw data file (*.SRD) is created by the program that can be transformed using the command "ASCII Wandlung" and a *.TOB file is created which can be opened with usual editors or Microsoft excel for further editing or profile illustration. The following data are recorded: Battery [Volt], Date and Time, Conductivity [mS/cm], Pressure [dbar], Depth [m], Temperature [°C], Density [kg/m3], Salinity [ppt], Sound velocity [m/s].

3.5 Visual Bubble Quantification

(Jan Boelmann)

There were two methods used for visual quantification of bubble fluxes which delivers results for comparison with other quantification methods like sonar and hydro acoustic measurements. At first there is the manual quantification which is used for a fast and good estimation.

Manual quantification. For both methods the video from the bubble stream must be separated into single frames to measure the bubble sizes. A second pre-step is the scale factor which is used to estimate the size. Therefore scaling aids like a scaling plate with known grids or known distances at the equipment from the ROV like screws or other mechanical parts. These parts were hold into the bubble stream to get the scale factor for each zoom position of the camera. Fig. 3.5.1 shows the scaling plate and the manipulator jaw for scaling.

Due to the low shutter speed of the camera the bubbles were blurred during the recording of each frame. This causes that the bubbles look like needles or long ellipsoids which can be used to measure the rising speed. With a frame rate of 25 frames per second the shutter is longer open than it takes for a single frame which means that the bubble major diameter is equal to the velocity and the minor diameter corresponds to the bubble diameter. Fig. 3.5.2 shows the minor and major axis of a bubble.

To calculate the vertical rinsing speed of a bubble the velocity must be multiplied by the sinus of the angle. The flux of a bubble stream given in mL per minute can be calculated by the minor diameter over time.

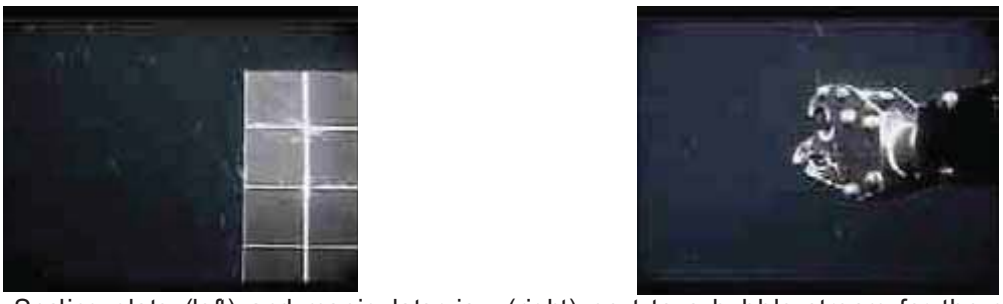

Fig. 3.5.1: Scaling plate (left) and manipulator jaw (right) next to a bubble stream for the purpose of scaling.

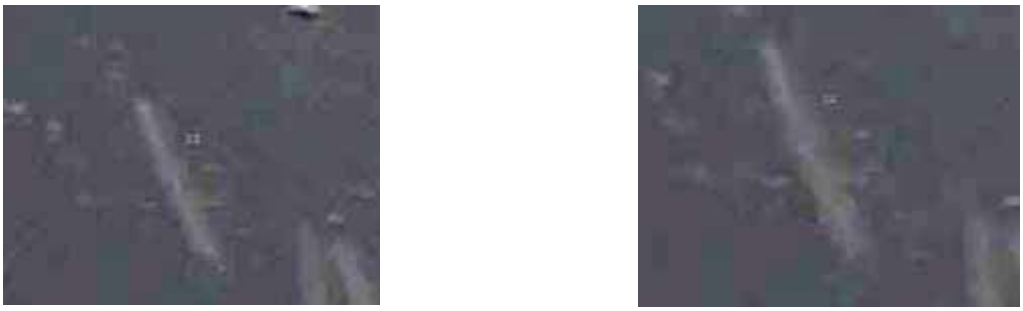

Fig. 3.5.2: Major and minor axis measurement.

Fig. 3.5.3: Examples illustrating the automated quantification method: (upper) original frame with a bubble stream, (middle) result of the image processing, (lower) detected bubbles overlaying the original frame.

Automated quantification. Based on the same frames the automated quantification uses image processing tool to detect the bubbles in each frame. Therefore thresh-holding and edge detection algorithms will be used to get the bubble information needed. The Fig. 3.5.3 shows an original frame with a bubble stream as well as the results of the image processing and the detected bubble over the original frame. Objects that don't fit to criteria's like size, shape or movements into

different directions will be sorted out by a following tracking algorithm. For example the two particles on the right hand site on the picture.

3.6 Active Acoustics – Sonar IMAGINEX
(Michal Tomczyk)

Hydroacoustic methods are candidates to be the most sensitive and reliable way to remotely determine bubble fluxes over a large area. This chapter presents the method for quantification of gas bubble emissions from the seafloor using forward-looking sonar.

The Imagenex 881a device is a digital multifrequency imaging sonar. As exemplified by the schematic presented in Fig. 3.6.1, it is a rotating system that is aimed to scan bubble plumes in order to obtain their echo levels at different frequencies. The emission frequencies range from 280 kHz to 1.1 MHz in 5 kHz steps. The sonar head contains a processing unit that gives relative echo levels as outputs. In order to obtain absolute backscattering volumes (as is needed to quantify the gas flux), the digital output of the system was calibrated at each frequency. The vertical opening angle is depending on frequencies: 40° at 310 kHz, 20° at 675 kHz and 10° at 1 MHz. The horizontal beam angle is also dependent on frequencies: 4° at 310 kHz, 1.8° at 675 kHz and 0.9° at 1 MHz. The transmitted pulse length was 40 µsec. The absorption was set depending on emitted signal frequencies, increasing with higher frequencies. The selected horizontal range for quantification was 2 meters with 500 sampling points along a beam. A higher range >10 meters was set for the purpose of gas bubble plumes mapping, with 250 sampling points along a beam. The data from the sonar scans (sound intensities proportional to acoustic wave pressure, range, pulse duration etc.) are stored as binary files with a format specific for the Imagenex sonar (the extension of these files is .81a). In order to quantify gas bubble streams emanating from the seafloor, the sonar was mounted on ROV Cherokee (Fig. 3.6.2). Processing of the data was conducted using Matlab.

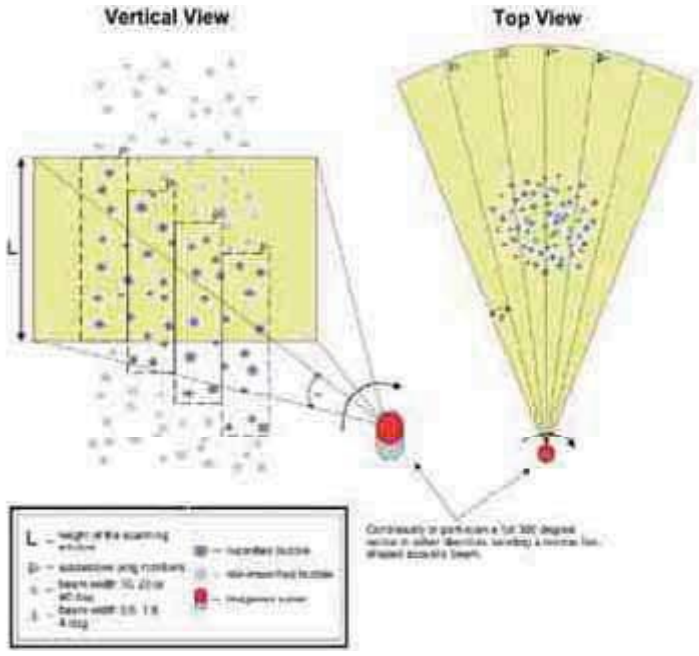

Fig. 3.6.1: The sketch shows the operation procedure for forward-looking sonar. The Imagenex 881a sonar-head has a rotating system providing the capability to obtain a full 360 degree sector scanning. The sonar measures the scatter intensities from objects by sending a narrow fan-shaped acoustic beam.

Fig. 3.6 2: The picture shows the front of ROV Cherokee with the Imagenex sonar on the top.

The Imagenex 881A sonar was used for flux quantifications by scanning a specific sector with bubbles rising from a seep when the ROV is stationary. For each sonar scan, the raw scattering intensities within a range bin centered at range r were converted to the volume scattering strength M_v (m^{-1}) by means of the standard sonar equation (Clay and Medwin, 1977):

$$10\log_{10}(M_v) = 10\log_{10}\left(\int_L A^2 dr\right) + K + 40\log_{10}(r) + 2\alpha r - 10\log(U),$$

where A is the digital scattering amplitude integrated over a pulse length (L), K is the calibration factor for the Imagenex transducer defined by calibration procedure with tungsten-carbide sphere in a water tank, a is the acoustic absorption through the water at the transmit frequency (dB m^{-1}), and U is the insonified volume:

$$U = \left(\frac{\Phi}{3}\right)\left[\left(r+\frac{L}{4}\right)^3 - \left(r-\frac{L}{4}\right)^3\right],$$

F is the ideal beam pattern (solid angle).
In order to correlate the backscatter intensity and the corresponding gas flux a model from Nikolovska et al. (2008) was used which is based on integration of backscatter intensities, denoted with M_1. These backscatter intensities derived from gas bubbles are calculated through the relation:

$$M_1(n,r) = \frac{\int_{n=1}^{n=n}\int_L M_n(n,r)r^2 dndr}{\int_L r^2 dr},$$

where n is the ping number, r is the distance along the pulse length L, and Mn is the scatter intensity at the point n and r. This integration takes into account the backscattering intensity of one inhomogeneity relative to its position in the sound beam and its position relative to the neighboring inhomogenities.

Finally, by assuming a buoyant gas-liquid mixture (i.e., the buoyant force B is given by the relation: $B = Q*\varrho*\Delta\rho / \rho_{mixture}$, where Q is the gas flux, ϱ gravitational acceleration, $\Delta\rho$ is the density difference between liquid medium and gas, and $\rho_{mixture}$ is the density of the mixture).

The second method for quantification is based on acoustic inversion (Leighton and White, 2011) which should provide bubble size distribution data from the backscatter of the active sonar. Provided the sonar covers an appropriately wide range of frequencies, this can be done if the absolute intensity of the signal emitted by the sonar is known, and the absolute intensity of the echo from the cloud (if the absolute levels are not known, but the ratio is, then an estimate can still be made) by consideration of the acoustic scattering cross-section of the bubbles in the cloud). This method can be conducted when the absolute calibration of the active sonar will be finished.

3.7 Passive Acoustics – Hydrophone SM2M

(Benoît Bergès)

Data acquisition was performed using the Song Meter SM2M Ultrasonic autonomous submersible marine recorder (Fig. 3.7.1). This is a unit designed for short or long term deployments in fresh or salt water to depths of up to 150 m. It contains a processing unit that allows the user to set up flexible scheduling for the recordings. Batteries are D cells batteries (up to 32): 1.5 V alkaline, 1.2 NiMH, 3 V (or 3.3 V) lithium batteries. Data are stored on SDHC or SDXC cards (up to 4).

Fig. 3.7.1: Picture of the SM2M unit that was used for collecting passive acoustic data of bubble streams.

Model. From data collected by the hydrophone, signal processing can be applied in order to reduce the noise level and have clearer signal from the bubbles. The power spectral density $\Sigma(\omega)$ of the signal can be expressed as:

$$\Sigma(\omega) = \int_0^{+\infty} D(R_0)|X_1(\omega, R_0)|^2 dR_0,$$

with $|X_1(\omega, R_0)|^2$ denoting the squared magnitude of the Fourier transform of the response of a single bubble of radius R_0 (Leighton and White, 2011). The quantity $D(R_0)$ is the bubble-emission size distribution as a function of R_0, defined such that

$$\int_{R_1}^{R_2} D(R_0) dR_0$$

represents the number of bubbles generated per second with a radius in the range (R_1, R_2).

This problem can be solved numerically as the equation defines a Fredholm integral of the first kind that can be discretized. The determination of the bubble distributions consists on solving the inverse problem expressed in matrix form as:

$$D = X_b^{-1} S$$

The number of radius bins is chosen to be equal to the number of frequency bins in order to build a square problem. However, the problem remains ill-posed which means that the inevitable measurement errors in $S(\omega)$ are magnified. Tikhonov regularisation is applied in order to achieve a positive and stable solution for $D(R_0)$. Assuming spherical bubbles, the flow rate is calculated as follows:

$$F_g = \frac{4\pi}{3} \int_{R_1}^{R_2} D(R_0) R_0^3 dR_0$$

This gives the final results for flow rates that can be compared with other measures (i.e. bubble video counting, bubble catching, Imaginex sonar quantification).

3.8 Gas Analyses

(Thomas Pape, Patrizia Geprägs)

Vent gas. After recovery of the ROV Cherokee on deck, a pressure sensor was connected to the GBS pressure chamber via its upper valve to continuously monitor the internal pressure. The gas contained in the GBS was released incrementally via an assembly of gas-tight valves and valve-activated ports for gas sub-sampling. Gas quantification was carried out using a 'gas catcher', which consists of two inverted plastic cylinders. Repeatedly, after release of a certain gas aliquot, gas sub-samples were taken and transferred into glass serum vials for onboard analysis of molecular compositions and long-term storage.

Gas dissolved in the water column. Water samples from selected water depths were taken during the upcasts of sixteen hydrocasts with the CTD/rosette system (11 x 4 L water sampling bottles). In addition, bottom water from several decimeters above the seafloor was taken during seven ROV dives with a 1 L sampling bottle mounted to the ROV rack. Immediately upon recovery on deck between 600 and 800 mL of the water samples were transferred into pre-evacuated 1 L gas tight glass bottles. The dissolved gas was prepared from the water samples by high-grade vacuum extraction (Fig. 3.8.1) (Lammers & Suess, 1994; Rehder et al., 1999; Schmitt et al., 1991) within a few hours of collection. The released gas was taken with gas-tight syringes via a septum of the extraction system and transferred into 20 ml serum glass vials pre-filled with saturated NaCl solution for on-board analysis and long-term storage.

Fig. 3.8.1: Installation of the gas high-grade vacuum extraction system on board the R/V HEINCKE.

Onboard analysis of molecular gas compositions and concentrations of methane. The gas samples were analyzed onboard for their molecular compositions and methane concentrations with a two-channel 6890N (Agilent Technologies) gas chromatograph (GC); (Pape et al., 2010). Light hydrocarbons (C_1 to C_6) were separated, detected, and quantified with a capillary column connected to a Flame Ionization Detector, while permanent gases (O_2, N_2, CO_2) as well as C_1 and C_2 hydrocarbons were determined using a stainless steel column packed with mole sieve and coupled to a Thermal Conductivity Detector. Calibrations and performance checks of the analytical system were conducted regularly using commercial pure gas standards and gas mixtures. The coefficient of variation determined for the analytical procedure was lower than 2%.

Hydrate phase boundaries. Gas hydrate phase boundaries were calculated using the HWHYD U.K. software (Masoudi & Tohidi, 2005) loaded with molecular compositions of vent gas collected at three seeps located at about 380 mbsl and water salinities at the respective depth.

4. Results & Discussion

4.1 Overview and Summary of Hydroacoustic Surveys

(Miriam Römer, Heiko Sahling)

In total, over 50 hydroacoustic surveys were conducted during HE-387 with a total length of nearly 2000 nautical miles. Most of the surveys were performed with the purpose of bathymetric mapping together with searching for flares (hydroacoustic anomalies caused by gas bubbles in the water column). Therefore, almost the entire time of the cruise the multibeam Kongsberg EM710 and also the single beam echosounder EK60 were acquiring data. Additionally to the bathymetric data the EM710 records were used to acquire backscatter information to characterize the seafloor. Several surveys were focused on detailed flare mapping using the water column data of the multibeam echosounder. These surveys were conducted with a very close line spacing as flares are only visible in the inner part of the multibeam swath. The subbottom profiler SES2000 (Innomar) transmitted and recorded only during few surveys. As the transmission causes noise signals in the other echosounder records (of EM710 and EK60), the SES2000 was not running the entire cruise, especially as the subbottom data were not in focus. Only in particular areas the subbottom information was of interest, for long transects along the margin from the shallow shelf to the deep basin and in Area 4, as numerous pockmarks accompanied with low backscatter anomalies were observed in that area and we hoped to find gas indications in the shallow sediments using the subbottom profiler. A survey list is presented in Appendix 2. In the following, we give an overview and summary of the areas of focus during the cruise (Figs. 4.1.1 to 4.1.4).

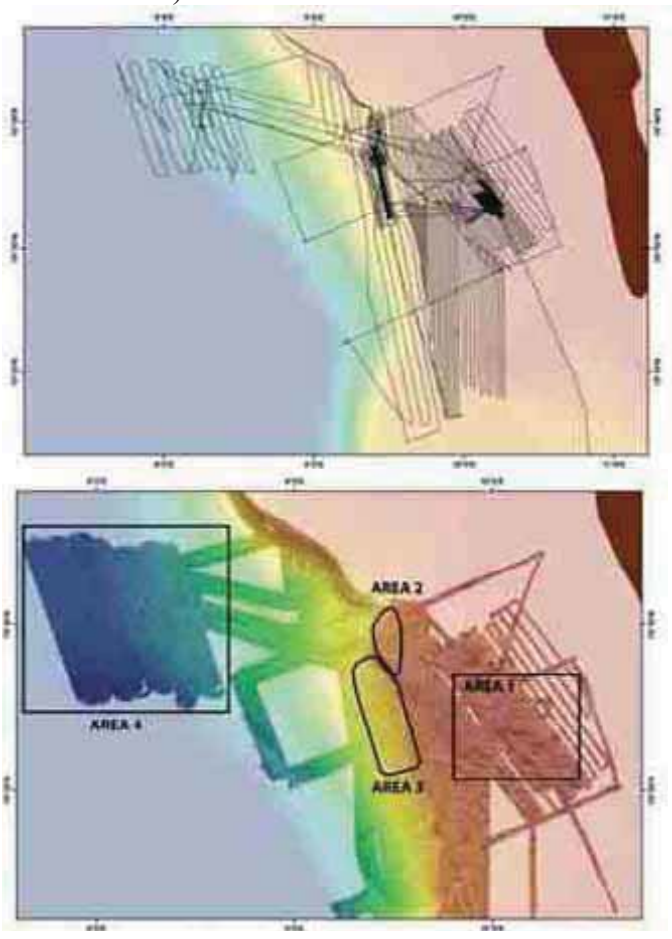

Fig. 4.1.1: (Top) Track line of Cruise HE-387. (Bottom) Bathymetry with indication of the main areas of research during Cruise HE-387. Please note that the survey along the 400 m depth contour towards the north as well as part of the areas mapped in the south are missing. In addition, more bathymetry data have been compiling during the cruise that are not shown here. The research concentrated on the four areas: Area 1 ('flares at 80 m') on the shelf, Area 2 ('flares at 280 m') as well as Area 3 ('flares at 380 m') on the upper slope and Area 4 ('Pockmark-Area') at water depth between 800 and 1200 m.

Area 1

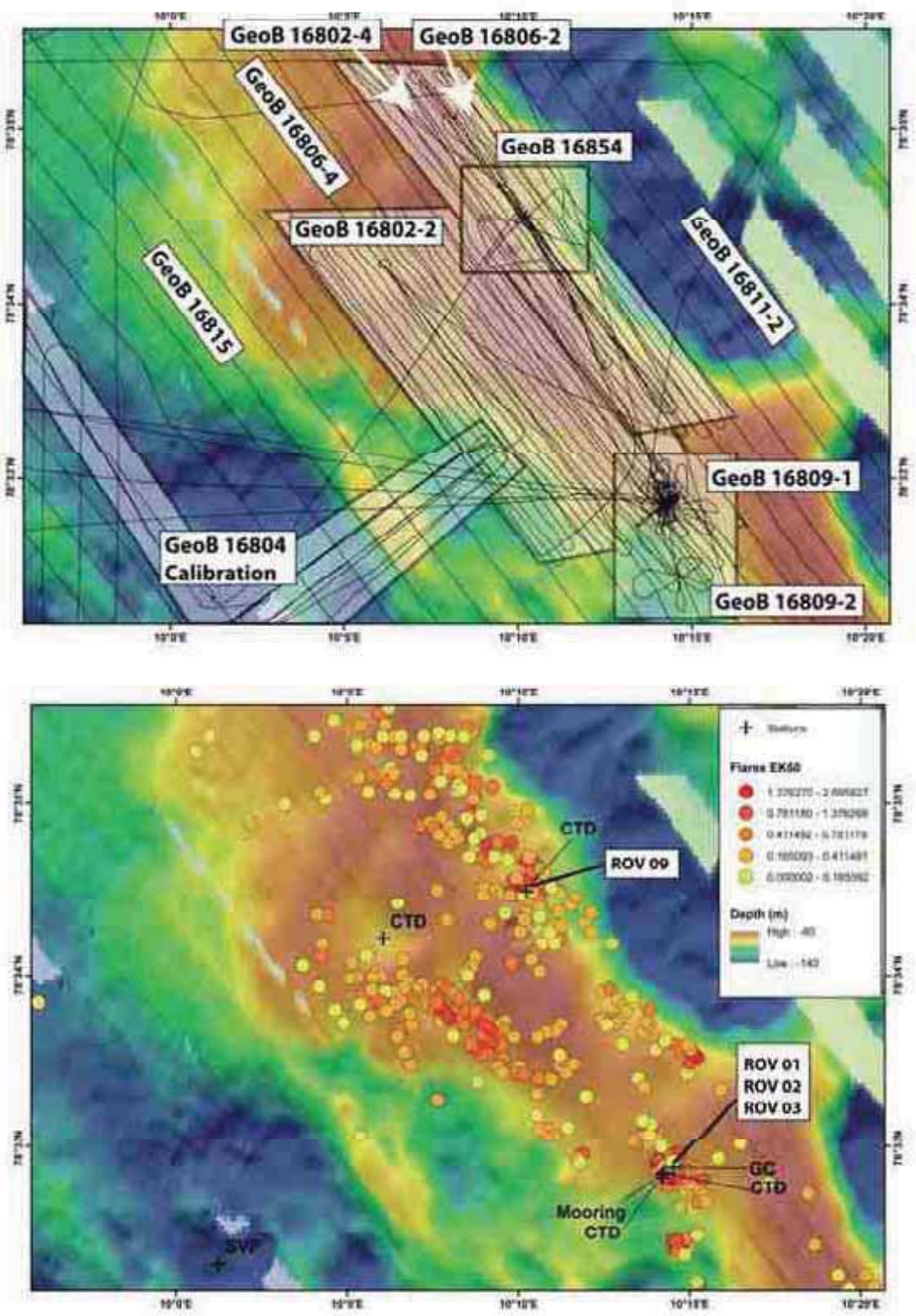

Fig. 4.1.2: Area 1 was initially termed '80-m flare area' and is located on the shelf at about 80-90 m water depth. Basically surveys with three different motivations have been carried out in this area (upper panel): (1) closely-spaced lines for EM 710 flare mapping and bathymetry data, (2) overview lines to map the larger area with bathymetry and look for flares in EK 60 and (3) EK 60 surveys for crossing individual gas emissions. (lower panel) Bathymetry and flares as picked from EK 60 records. The color-coding of the flares correspond to the backscatter strength of the flares (red = strong, yellow = weak; chapter 4.4). The figure illustrates that the flares are bound to the edges of a morphological high.

Area 2 and Area 3

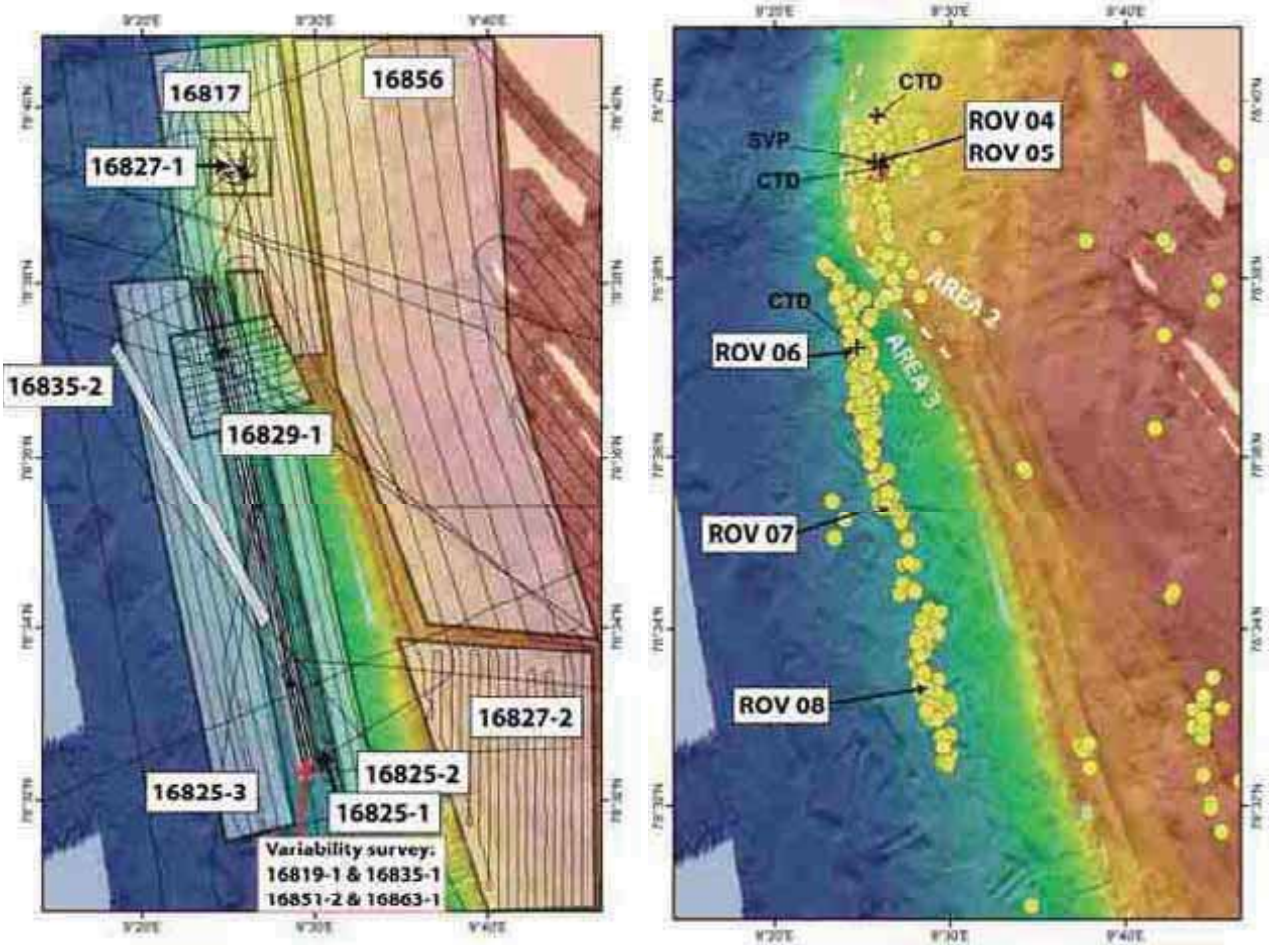

Fig. 4.1.3: (left) Hydroacoustic surveys and (right) flares and stations in the Area 2 and 3.
Area 2 is located at the outer shelf close to the shelf break and was initially called the '280-m flare site'. Its water depth is actually 240 m. Shown are EK 60 flare locations but we also mapped the flares in Area 2 with EM 710. Two dives could clearly show that the flares are caused by cluster of bubble streams. We were able to systematically map these bubble streams with the ROV horizontally-looking sonar and quantified individual bubble streams subsequently.
Area 3 is located at the upper slope approximately around 380 m water depths ('380-m flare site'). These flares are those described by Westbrook et al. (2009) as potentially occurring due to hydrate destabilization. EK 60 flare locations are shown but four surveys along a set of four closely-spaced survey lines have been conducted in order to map flares with EM 710 and to study their temporal variability. In addition, wider spaced surveys intended to look for additional flares up- and down-slope of the main flare area at 380 m but only very limited evidence was found. The deepest flare found was in about 440 m water depth. Three ROV dives were carried out in Area 3 revealing that the bubble streams are transient. This makes mapping and quantification of the streams challenging.

Area 4

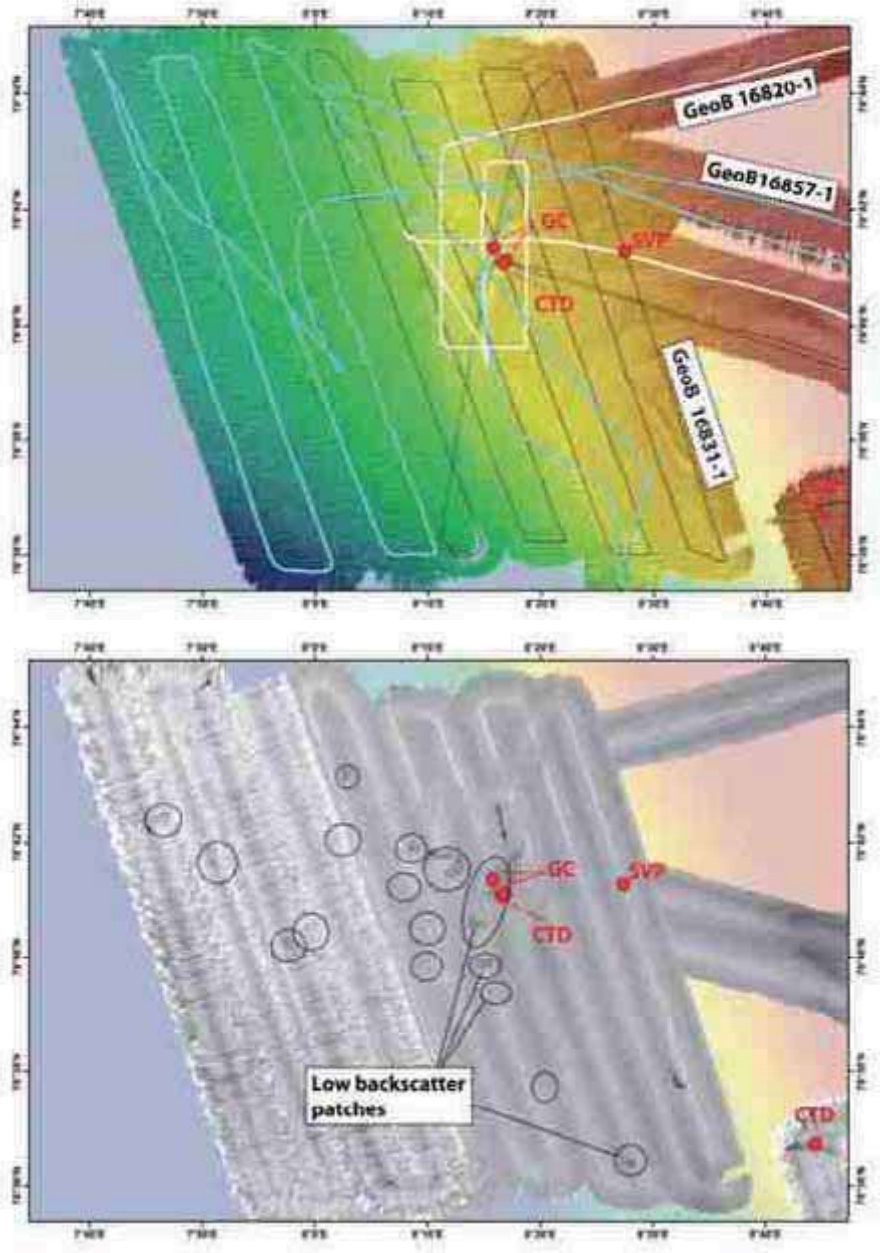

Fig. 4.1.4: (Top) Bathymetry and track line and (Bottom) backscatter map of **Area 4**. The area is characterized by circular depressions, commonly termed pockmarks. According to personal communication with Christian Berndt, these pockmarks are connected to acoustic chimneys in seismic data and that British colleagues have recovered hydrates at one of the sites. We acquired bathymetric data from the area with much better data in the eastern sector compared to the western one acquired during strong winds and high wave conditions. The influence of the sea state on the data is especially well visible in the backscatter data derived from the multibeam system. The pockmarks show low backscatter (dark), which we interpret as being caused by the deposition of fine-grained material whereas the surrounding sediments with intermediate backscatter contain dropstones in fine-grained sediments. This hypothesis is supported by the three gravity corer taken at one pockmark inside and outside of the low backscatter. The cores did not bring an indication for hydrocarbon seepage. A survey to cross several of the pockmarks was conducted but no evidence for the release of bubbles was found in EK 60 data. SES 2000 sediment echosounder shows acoustic turbidity connected to several of the pockmarks. Unfortunately, the strong wind and waves did not allow any further gravity corer deployment to further investigate the nature of the pockmarks.

4.2 Multibeam Mapping (EM 710)

(Christian dos Santos Ferreira, Heiko Sahling)

At the beginning of the cruise, the multibeam echosounder system (MBES) was calibrated by crossing a flat area at the shelf in different directions following a procedure recommended by the system manufacturer. The wobbling in the data, as described as problem in the method section persisted throughout the journey.

Most surveys were carried out for the purpose of flare mapping as well as acquiring bathymetry at the same time. Furthermore, the intention was often to cover large areas rather than to perfectly map the areas for high quality data. As a result, maps with extensive coverage were acquired (Figs. 4.2.1 and 4.2.2).

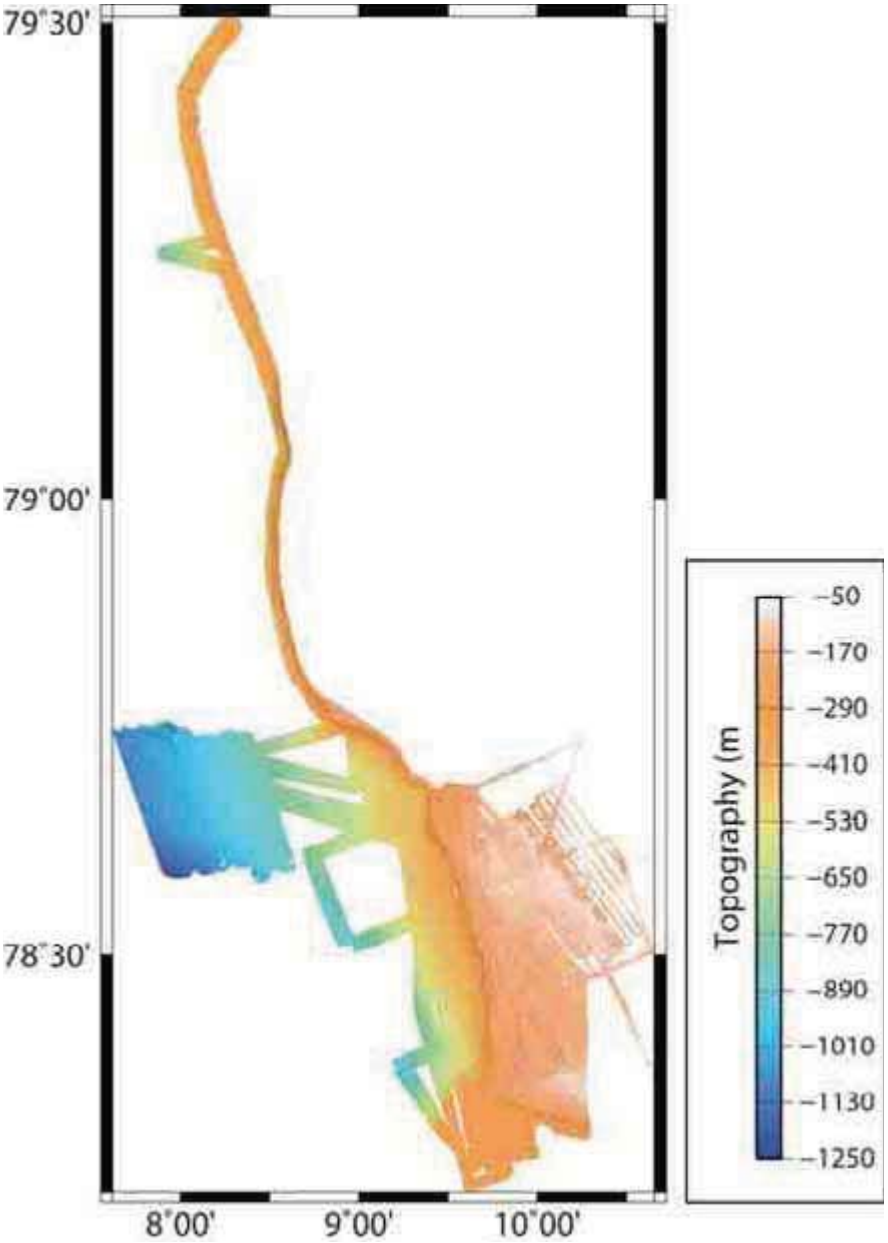

Fig. 4.2.1: Overview about the multibeam data acquired during HE-387. The long survey towards the north followed the 400 (northward) and 360 m (southward) depth contours to look for evidence of gas emission in the EM 710 data. However, no evidence was found indicating that the geological setting of the area with flares is particular.

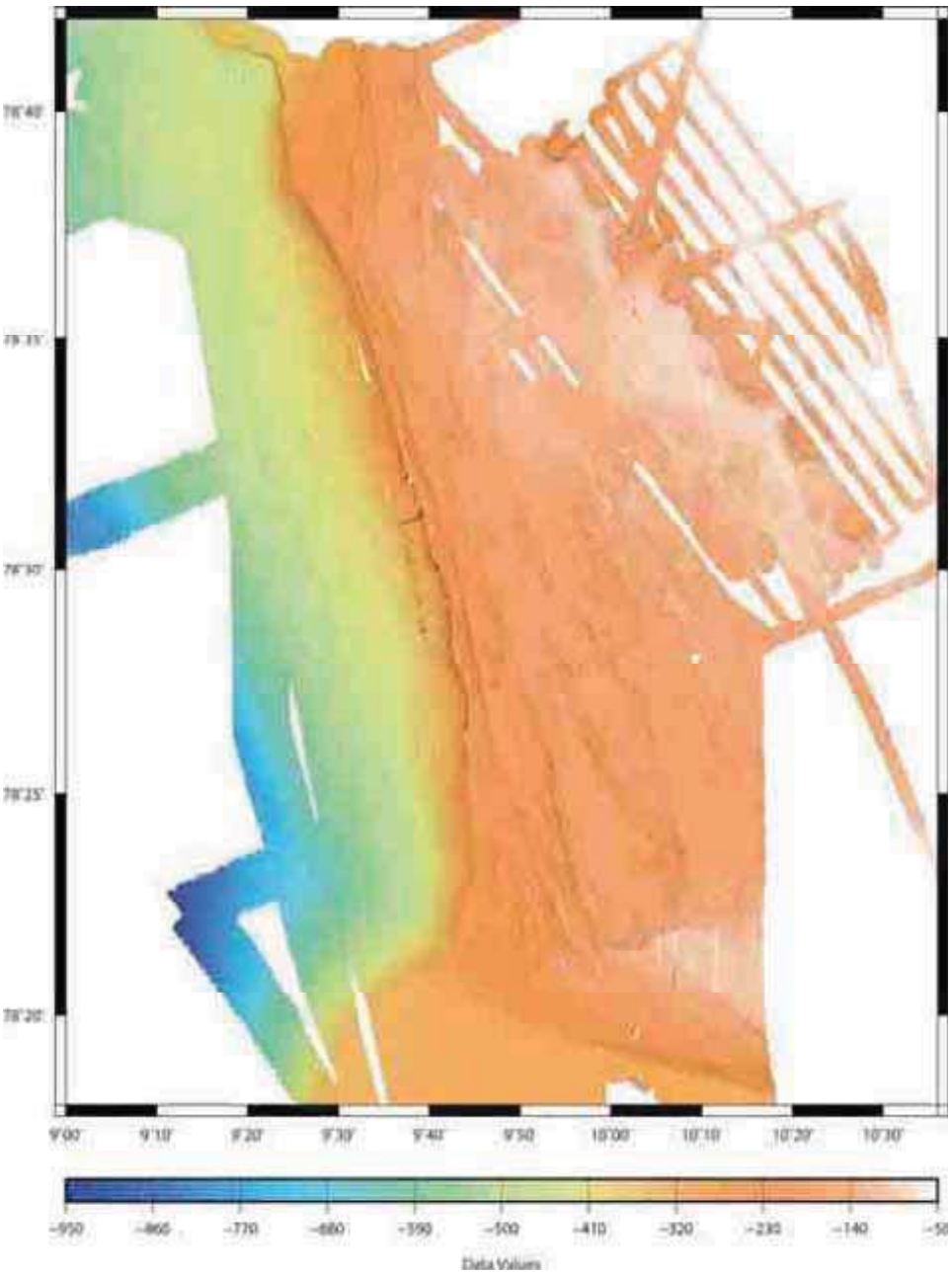

Fig. 4.2.2: The main working area where gas emissions were found including Area 1, 2, and 3. The bathymetric map shows very well the morphology of the shelf.

4.3 Sediment Echosounder (SES 2000)

(Miram Römer, Heiko Sahling)

The seafloor at the shelf and the upper slope was extremely difficult to image using the sediment echosounder SES 2000. Only one reflection caused by the sea bottom could be seen in these settings, no internal structures were seen below. We interpret this as a result of a hard bottom composed of glacigenic material, basically rocks in the size range gravel to pebbles as observed by ROV Cherokee at the seafloor. For that reason, the SES 2000 was only turned on for overview profiles crossing from the shelf to the mid-slope, as illustrated in Fig. 4.3.1. Layered sequences of sediments occur at the depth of ~1000 m and decrease in thickness upslope.

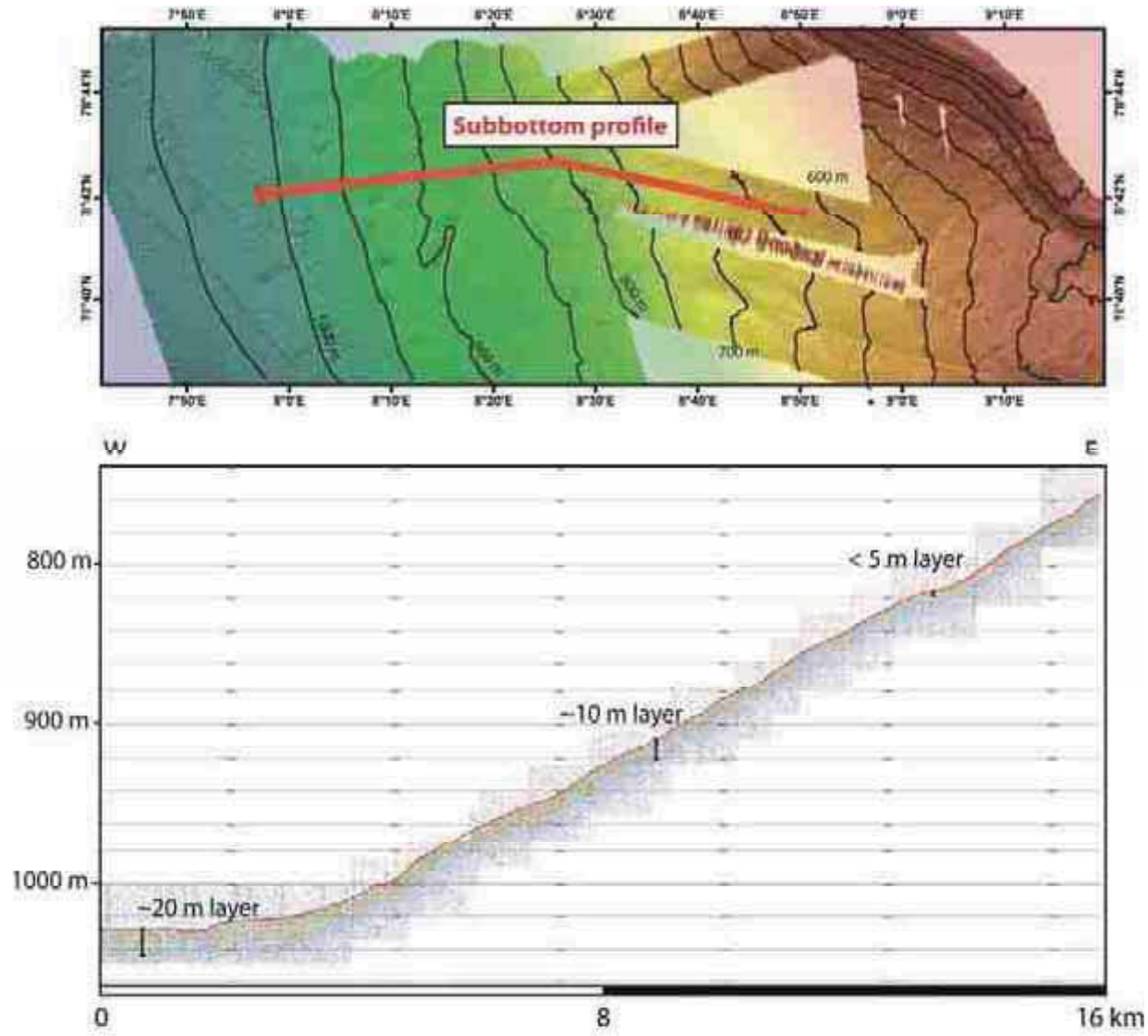

Fig. 4.3.1: A sub-bottom SES 2000 profile across the margin, the location of the profile (upper panel) and its representation (lower panel). A higher penetration depth goes along with increasing sediment thickness downslope.

In addition, the SES 2000 was used to characterize pockmarks in Area 4. For that purpose, a track was selected in order to cross as many pockmarks as possible with the ship (Fig. 4.3.2). Several of the pockmarks are characterized by acoustic turbidity: the layering of sediments is interrupted immediately below the central parts of the pockmark. We have questioned if this pattern is comparable with blanking due to gas as we know it from other systems operating at similar frequencies such as Parasound but did not come to a final conclusion. It might be that the acoustic turbidity is comparable to blanking due to gas in other systems but that the noise lever of the echosounder SES 2000 causes the turbidity. We would have liked to study the nature of the acoustic signature using gravity corer but this was not possible until the end of the cruise due to strong wind and waves.

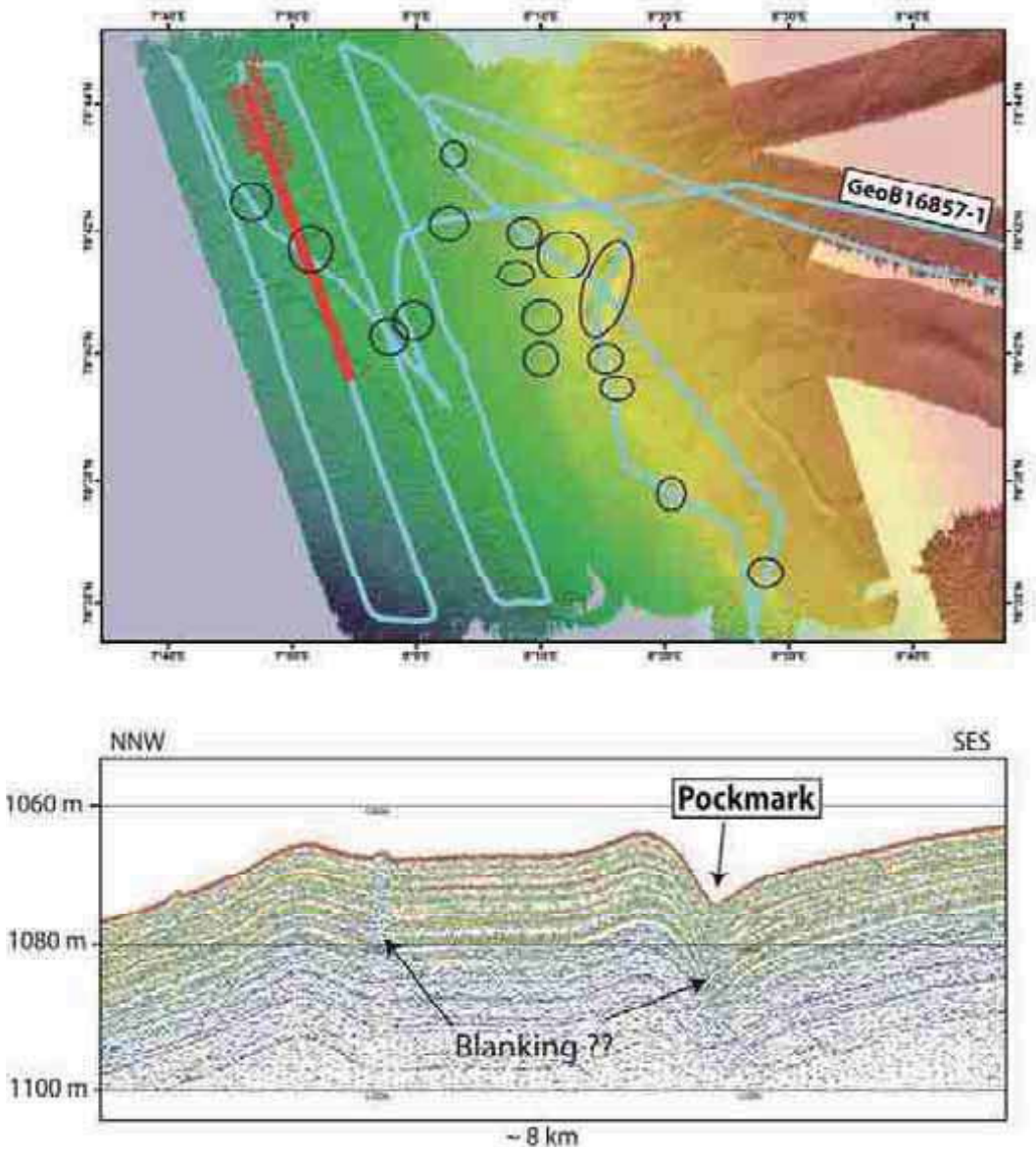

Fig. 4.3.2: (Upper panel) Pockmarks in Area 4 (encircled), the ship track and the location of the SES 2000 profile shown in the lower panel. Acoustic turbidity occurs below the central parts of pockmarks as well as one positive feature.

4.4 Mapping of Gas Emissions with EK 60

(Benoît Bergès, Miram Römer, Heiko Sahling)

All EK 60 recordings were analyzed and the reflections caused by bubbles were picked (Appendix 5). The distribution of flares is shown in Fig. 4.4.1. It shows that flares occur throughout the shelf. Flares cluster in at least three areas, the three areas studied during this cruise (Area 1, 2, and 3) as well as in a forth area, a morphological high in the southern part of the shelf. But flare intensity was generally low outside the key areas 1 to 3.

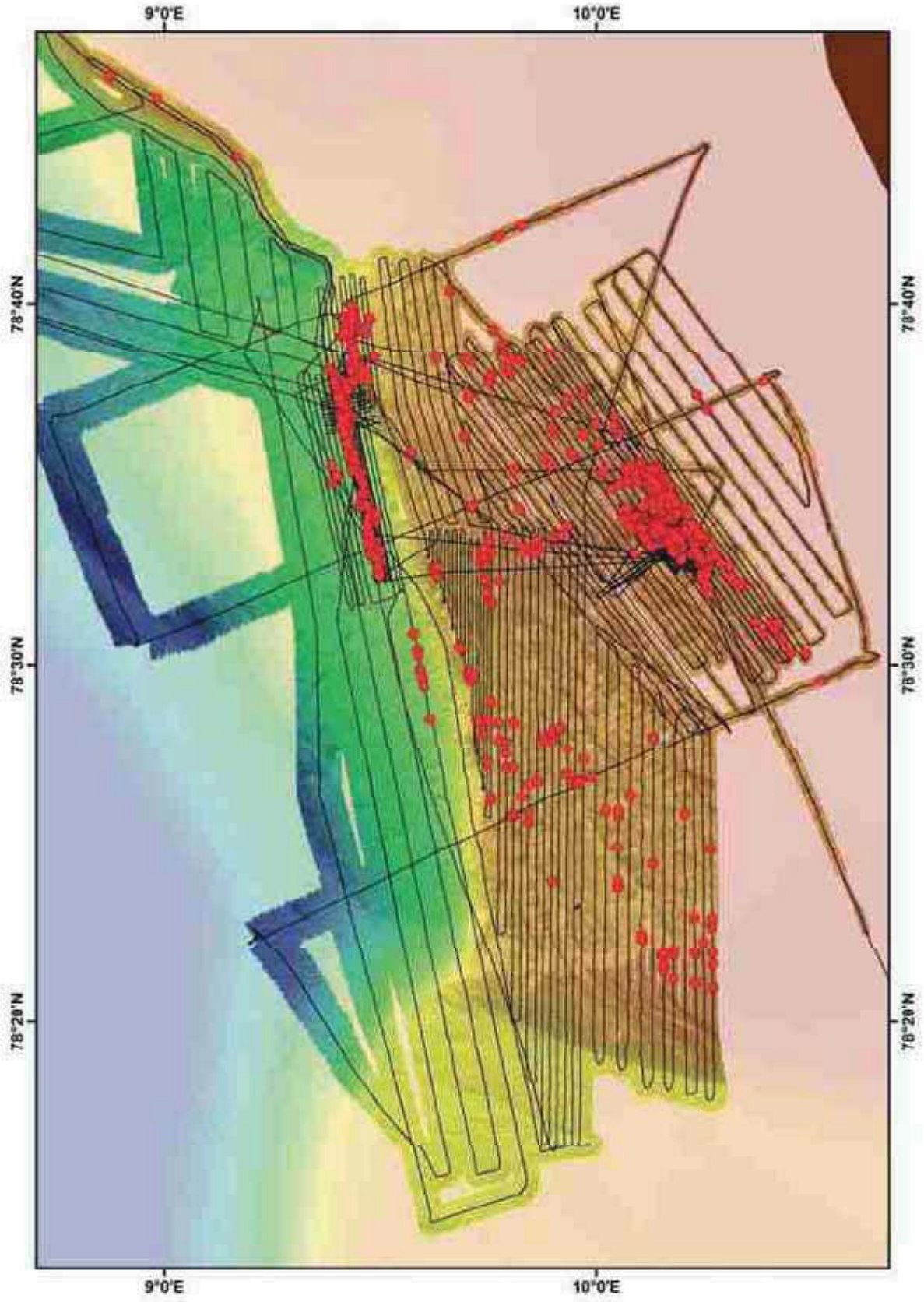

Fig. 4.4.1: Distribution of flares along the ship track obtained during the Cruise HE-387. A list of coordinates and flare characteristics is given in the Appendix 6.

4.5 Mapping of Gas Emissions with EM710

(Miriam Römer)

Due to the fact that extraction of flares from EM 710 is a time consuming procedure, it has only been conducted in selected areas. For the purpose of mapping flares before the ROV dives in the Area 2, bubble stream origins have been picked (Fig. 4.5.1). Directly after the dive, a small survey crossing the dive area several times from different directions (for EK60 mapping) was performed allowing to directly comparing the dive results with those from the survey. It reveals that three flares in that area were not detected again, whereas two new ones show up, illustrating the variability of flare locations. On the other hand it shows that some flares were stable where gas emission clusters have been found on the seafloor.

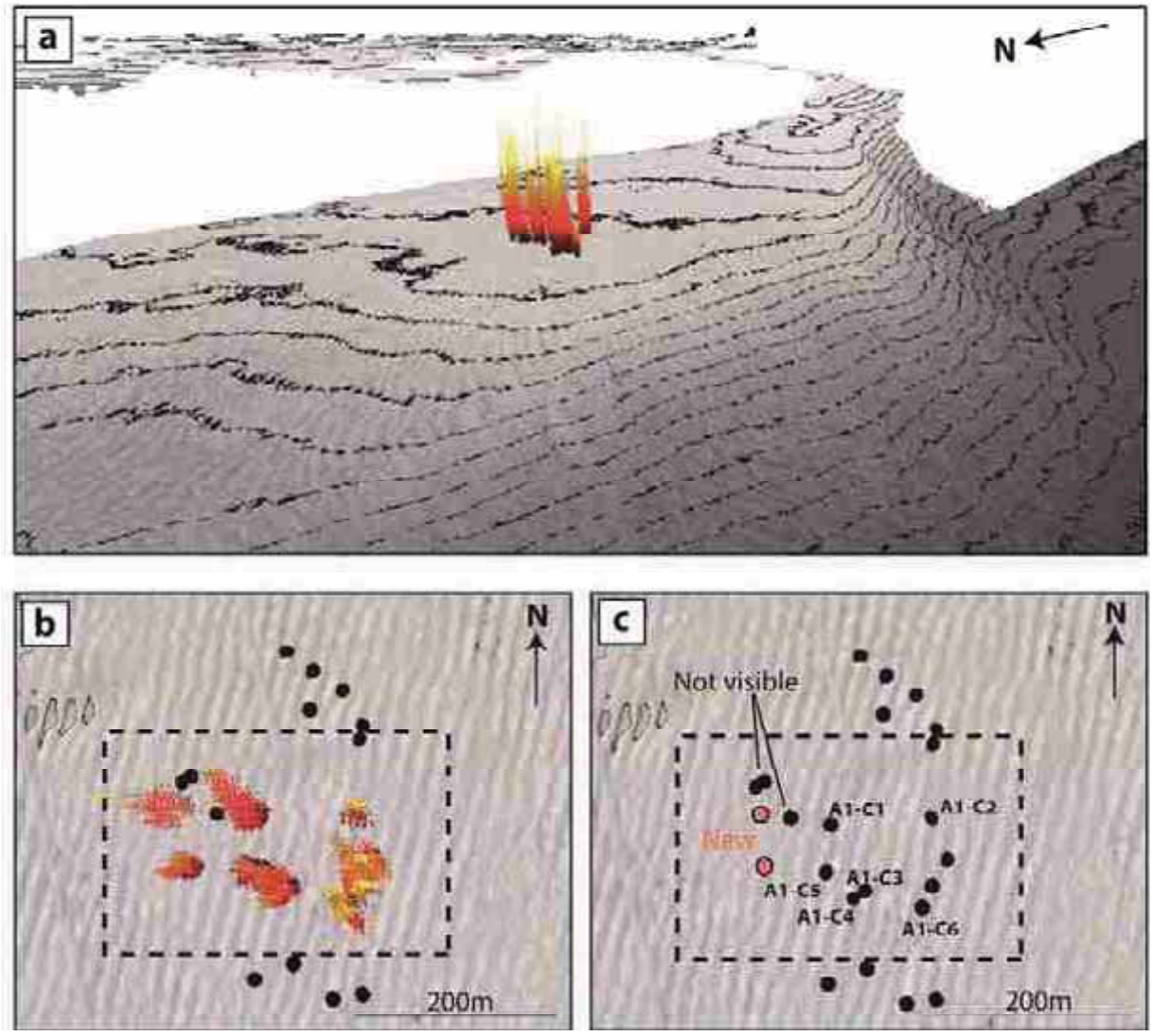

Fig. 4.5.1: (a) Extracted flares visualized in 3D Fledermaus in the Area 2. (b) The black dots represent flare locations picked prior to the ROV dives. The clouds of red and yellow points show the flares extracted from the survey after the ROV dives. This illustrates that there is a high temporal variability in the activity of bubbling. (c) Results of the ROV dives. Black dots with numbers represent those bubble stream clusters that were found with the ROV. There is generally a very good correlation between flares picked in EM 710 and those seen at the seafloor. However, two new flares emerged (marked new) after the dive.

4.6 Sound Velocity Probe (SVP) Profiles
(Miram Römer)

Four SVP deployments were performed during HE-387 (Fig. 4.6.1) in order to implement the resulting sound velocity profiles in the SIS and GAPS systems and enhance the data quality of the bathymetric information as well as the sub-positioning, respectively. All deployments were performed without any technical problems. The first SVP (GeoB16801) was deployed already when entering the working area in about 100 m water depth and the second (GeoB16803) only one day later in about 150 m water depth before starting extensive bathymetric surveys in Area 1. The third deployment (GeoB16822) was few days later in Area 2 in about 240 m water depth and the fourth and last SVP (GeoB16831-2) was the deepest deployment in Area 4 in about 840 m water depth.

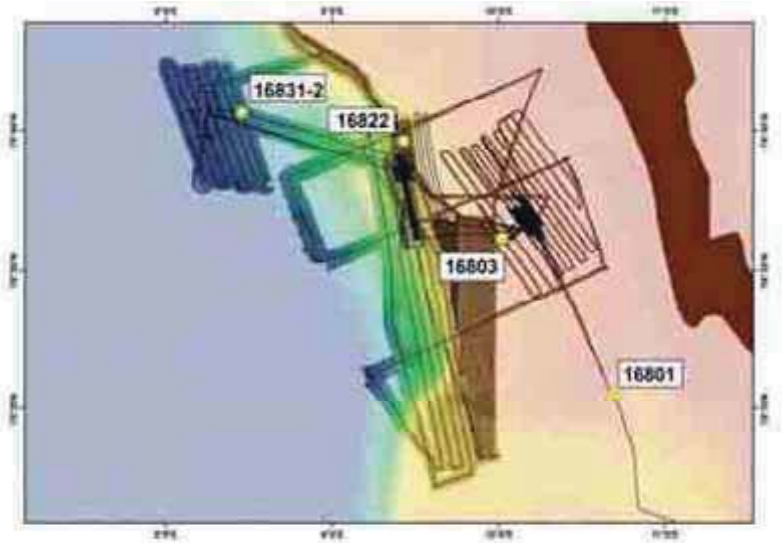

Fig. 4.6.1: Locations of SVP deployments during HE-387.

A plot of the four profiles is given in Fig. 4.6.2 and shows that the first two profiles (from the shallow shelf Area 1) differ considerably from the last two profiles achieved more westwards in higher water depth (Areas 2 and 4).

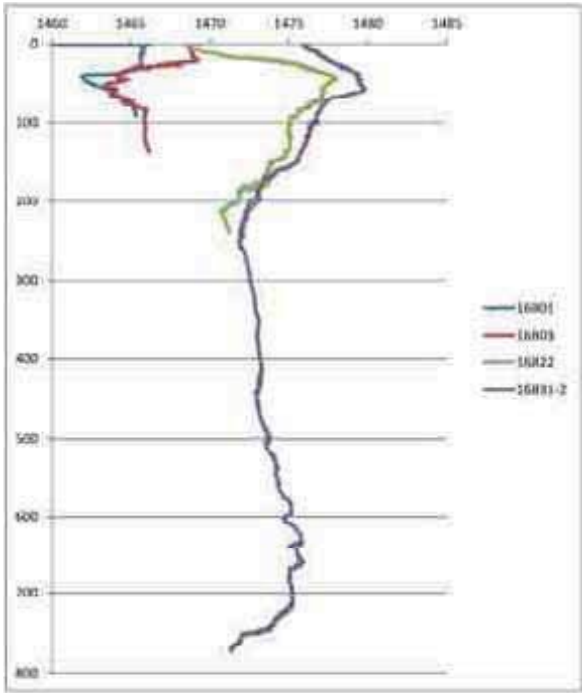

Fig. 4.6.2: Plot of all four sound velocity profiles.

4.7 Physico-Chemical Investigations of the Water Column
(Thomas Pape, Patrizia Geprägs)

4.7.1 General Hydrographic Situation in the Study Region

The oceanography of the region west of Spitsbergen comprising the working area of Cruise HE-387 is dominated by two currents, both originating from S-SE and generally flowing to the N (Fig. 4.7.1).

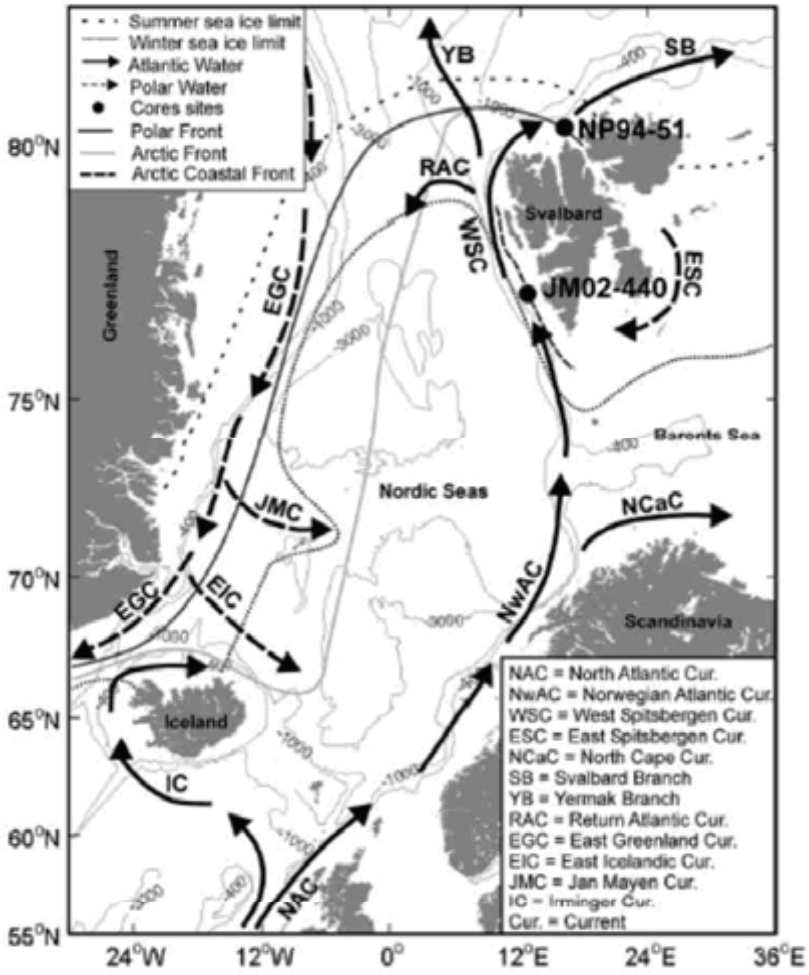

Fig. 4.7.1: Major surface water currents affecting the water masses on the shelf and slope off West-Spitsbergen (Slubowska-Woźniak et al., 2007).

The Coastal Current (CC) is sourced from the East Spitsbergen Current (ESC) and runs close to the western coast of Spitsbergen. The ESC originates from the area east of Spitsbergen, surrounds the southern tip of the peninsula and transports relatively cold and low saline water into the working area. Distant to the coastline, waters masses are being transported by the West Spitsbergen Current (WSC) along the Spitsbergen shelf break and slope. The WSC is an extension of the North Atlantic Current which transports relatively warm and saline waters into the region.

During Cruise HE-387 temperature and salinity (T and S) data from twenty CTD/rosette (CTD/ro) stations and from eight dives with the remotely operated vehicle (ROV) 'Cherokee' (for position see Fig. 4.7.2) allowed for an assignment of water masses at individual sites in the working area.

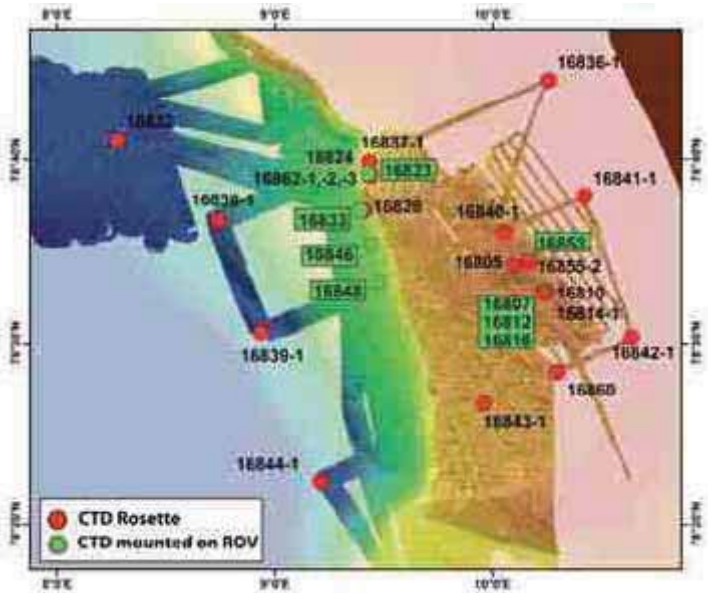

Fig. 4.7.2: Positions of CTD/ro deployments with station code (GeoB#).

The spatial distributions of the WSC and the CC as interpreted on the basis of interpolated W-E transects for T and S from four hydrocasts are illustrated in Figs. 4.7.3a and b as examples.

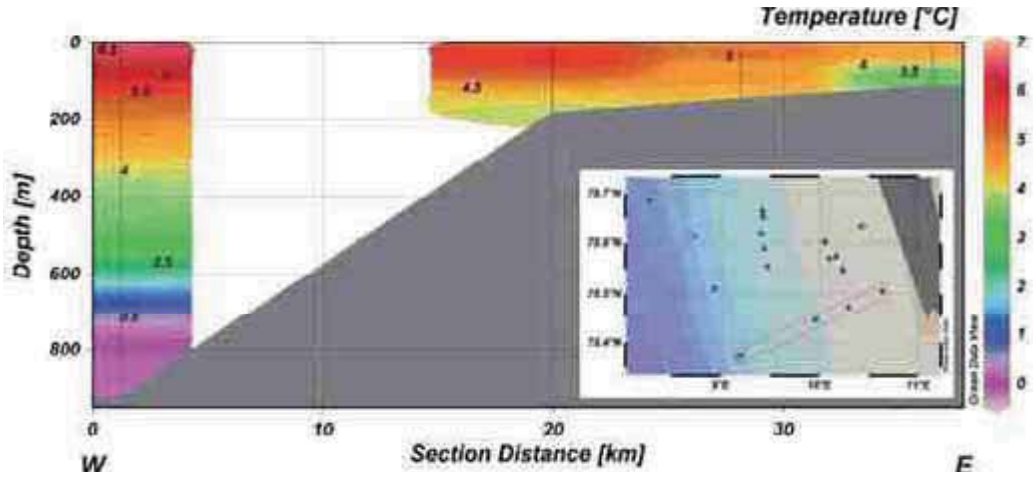

Fig. 4.7.3a: W-E profile of water column temperature distributions during HE-387.

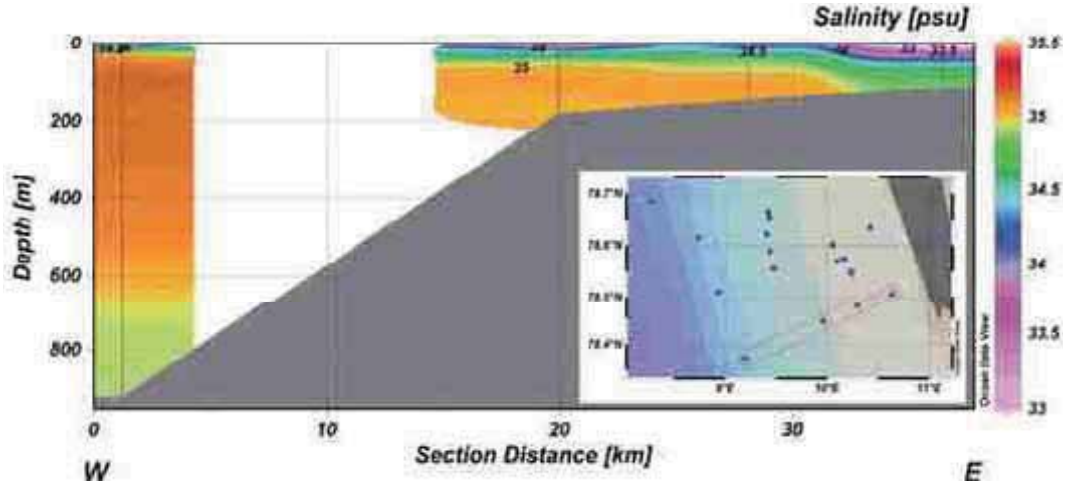

Fig. 4.7.3b: W-E profile of water column salinity distributions during HE-387.

During HE-387 near-surface water temperatures on the western Spitsbergen shelf were generally less than 4.6°C throughout the water column and approached 3.9°C close to the seafloor. Salinities ranged between 33.6 and 34.2 psu in surface waters and reached 34.9 psu in bottom waters (approx. 80 mbsl). Considering literature data this water mass was attributed to the CC.

In contrast, considerably higher water temperatures and salinities were found at stations on the slope remote from the coast. For instance, between 6.2 and 6.6°C measured in shallow waters suggested the inflow of water masses from southern regions. These waters showed comparably high and homogenous salinities between 34.6 and 35.1 psu and were related to the WSC. A distinct water mass several tens of meters in vertical thickness and characterized by relatively low salinities (~34 psu) but temperatures similar to those measured in water masses attributed to the WSC became apparent on top of the WSC.

With regard to these water column physico-chemical characteristics most of the CTD/ro stations could be related to the two currents prevailing in the working area during the time of investigation (Fig. 4.7.4).

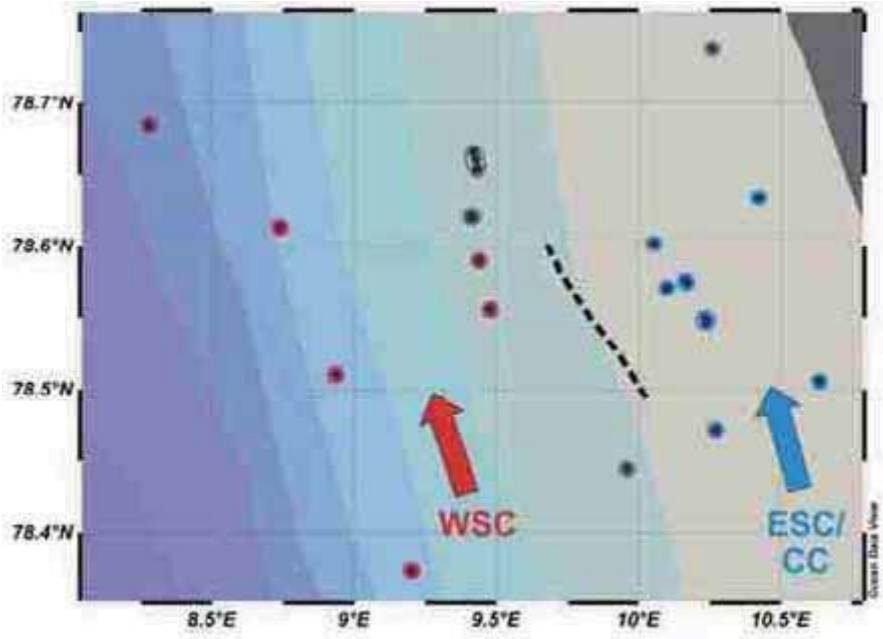

Fig. 4.7.4: Map indicating positions of all CTD/ro stations conducted during HE-387 and assignment of the prevailing water mass to the West Spitsbergen Current (WSC, red open circles) and the Coastal Current (CC)/East Spitsbergen Current (ESC; blue open circles). Grey outline = not assigned.

4.7.2 Specific Hydrographic Characteristics in the Study Region

Physico-Chemical Water Column Characteristics in Non-Seep-Areas

The water column above the four westernmost stations (GeoB 16838-1, 16839-1, 16844-1, 16832) performed during HE-387 was considered to be less affected by seepage activity. Two major water masses prevailing in that area could be assigned on the basis of T and S (Fig. 4.7.5a). The uppermost water mass (up to 85 meters in thickness) was generally characterized by temperatures between 6.2 and 6.9°C and salinities exceeding 35.0 psu. With increasing depth T and S decreased from about 6°C and 35.1 psu at about 50 mbsl to less than 0°C and 35.0 psu in waters deeper than approx. 700 mbsl (Figs. 4.7.5a and b).

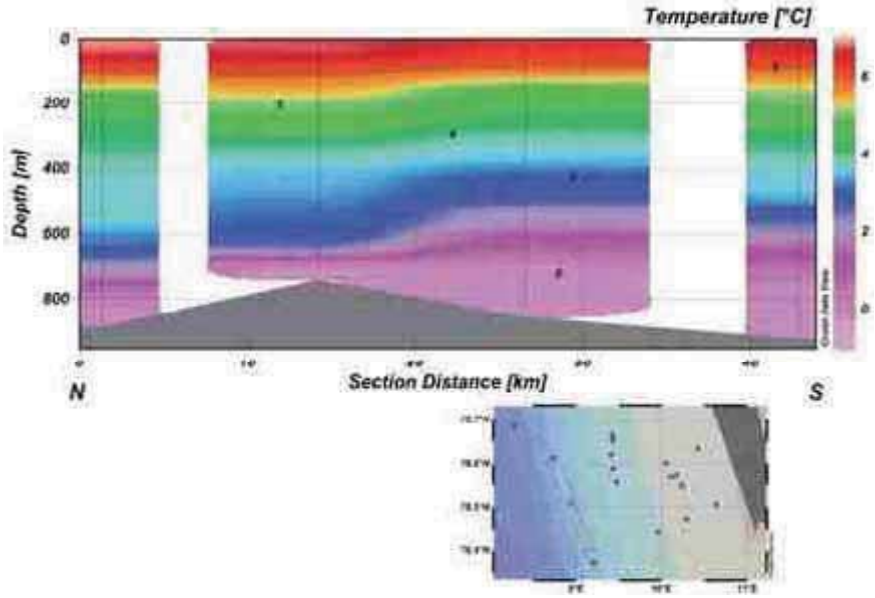

Fig. 4.7.5a: NW-SE profile of water column temperature distributions at the westernmost CTD stations during HE-387.

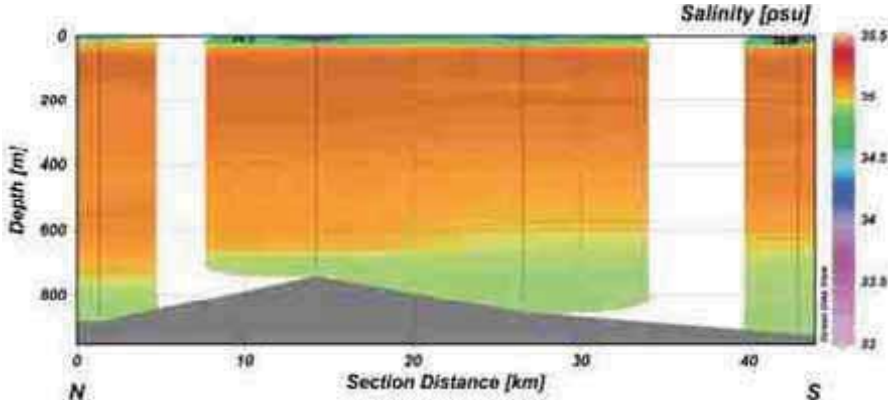

Fig. 4.7.5b: NW-SE profile of water column salinity distributions at the westernmost CTD stations during HE-387 (for profile see Fig. 4.7.5a).

The presence of the two major water masses at the deep-water stations conducted during HE-387 is illustrated in the S-T diagram (Fig. 4.7.5c).

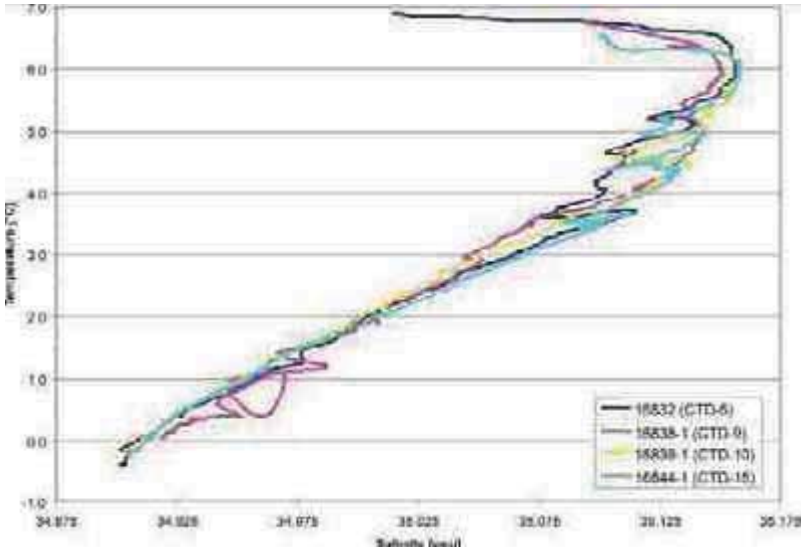

Fig. 4.7.5c: Salinity-temperature plot for the four westernmost hydrocasts during HE-387.

Negative temperatures were present at water depths exceeding 722 to 814 mbsl and minimum temperatures of –0.4°C were measured at about 878 mbsl at station GeoB16832 ('Pockmark Area') in the northwestern edge of the study area. With respect to its vertical extent, an inflow of the water body from S to N is assumed. This assumption supports the assignment of this water mass to Norwegian Sea deep waters proposed by Damm *et al.* (2005) and might conflict the interpretation as Lower Arctic Intermediate Water by Ślubowska-Woldengen *et al.* (2007).

Physico-Chemical Water Column Characteristics in Individual Seep Areas

I Seep Area 1 (ca. 95 m)

Five CTD/ro stations (GeoB16805, -10, -14-1, -40-1, -55-2) and CTD recordings during four ROV dives (16807, -12, -16, -53) provided T and S data for the water column in Seep Area 1 (Figs. 4.7.6a and b).

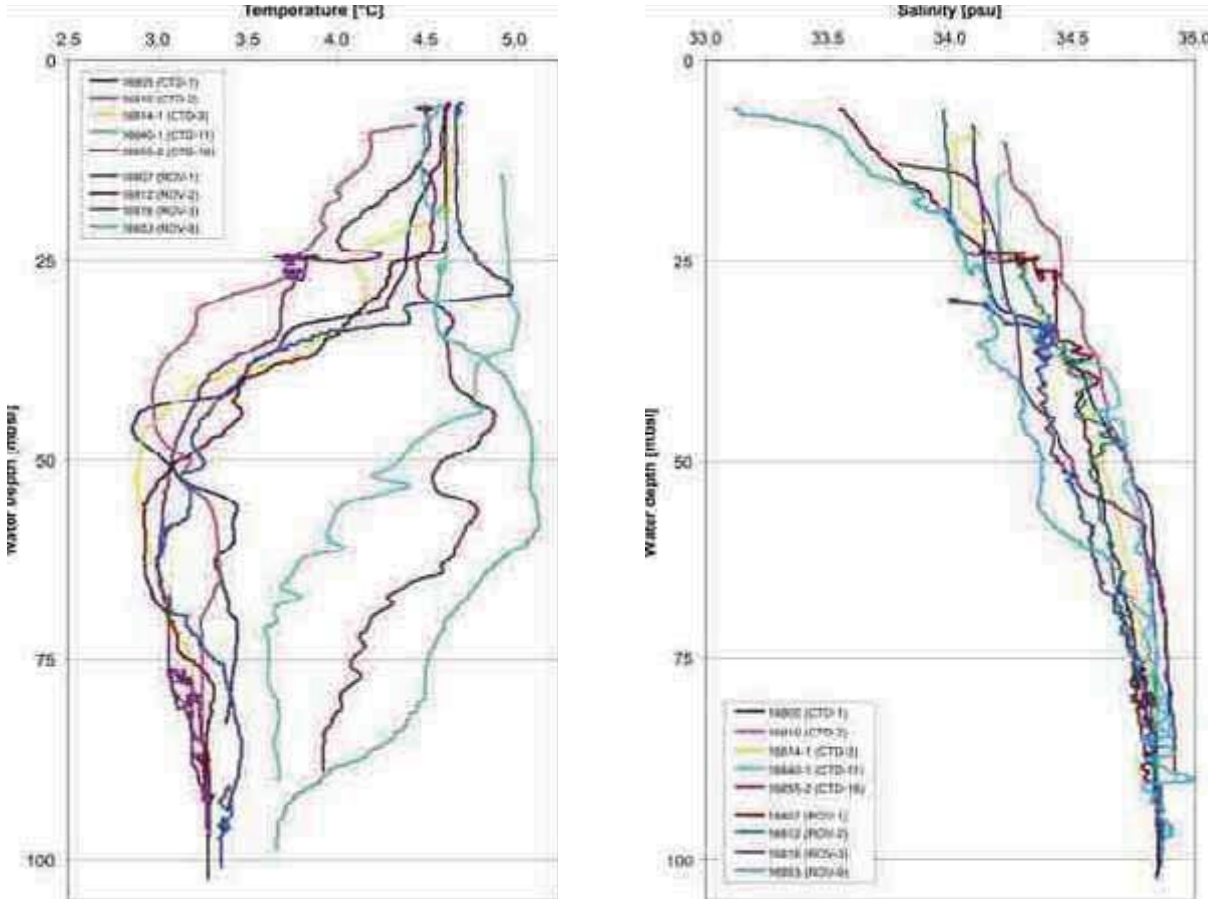

Figs. 4.7.6a and 4.7.6b: Water column T and S profiles in Seep Area 1.

Shallow water temperatures (4.2 to 4.9°C) were much lower compared to those measured for the deep-water stations. They generally decreased with depth approaching minimum temperatures of about 2.9°C at 40 to 50 mbsl for stations GeoB16805 to 16816. For those stations temperatures increased below that depth interval with depths to about 3.0 to 3.4°C at 65 mbsl and remained more or less constant (approx. 3.1 to 3.5°C) below 75 mbsl. Salinities increased with depths from 33.1 to 34.2 psu close to the surface to 34.1 to 23.8 psu in the 25 to

60 mbsl interval. Below that depth salinities increased with depths to 34.8 to 35.0 psu at about 90 mbsl.

Strong differences in particular in temperatures were observed for stations 16840, -53, and -55-2 (Fig. 4.7.6a). At these stations temperatures in waters below approx. 25 mbsl were elevated by up to ca. 1.8°C (at 50 mbsl) compared to other CTD stations carried out in that area. As shown in Figs. 4.7.6b and c equivalent differences in the composition of that water mass were only slightly visible in the salinity profiles.

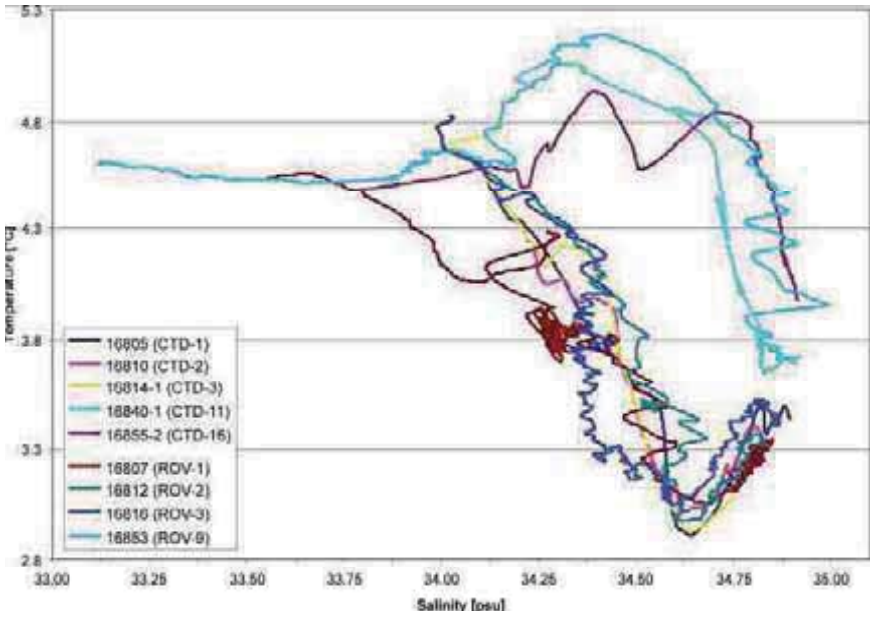

Fig. 4.7.6c: Salinity-temperature plot for CTD stations performed in Seep Area 1.

Because increases in temperature below 25 mbsl were first noticed on 01 September during station GeoB16840-1 these changes might be attributed to the inflow of a different water mass into that region. All the three stations with elevated temperatures below 25 mbsl were located close to earlier stations which showed much lower water temperatures.

The S-T diagram for all CTD data obtained from Area 1 (Fig. 4.7.6c) demonstrates the presence of three overlying water masses at a certain date with transitions situated at about 20/25 mbsl and 45/60 mbsl.

II Seep Area 2 (ca. 240 m)

Five hydrocasts (GeoB16824, -37-1, 62-1, 62-2, 62-3) and CTD data from two ROV dives (16823, -26) performed in or close to seep Area 2 revealed S and T distributions different to those recorded in Seep Area 1. Increasing temperatures (4.5 to 6.6°C) with depth from the surface to about 45 mbsl were paralleled by increases in salinity from approx. 33.1 to 35.2 psu (Figs. 4.7.7a and b). Between approx. 45 and 85 mbsl temperature decreased to 5.8 to 6.2°C at 85 mbsl, whereas salinity scattered between 34.8 and 35.2 psu. A conspicuous temperature drop towards 4.3°C at minimum at 94 mbsl found only for the first two CTD/ro stations (GeoB16824, -37-1) marked the top of a ca. 50 m thick water mass characterized by relatively low temperature (3.7°C at minimum) and salinity (34.9 psu at minimum). For all other stations, temperature decreased more or less gradually with depth and temperatures less than 4.7°C were generally

observed below 200 mbsl. Salinity remained relatively constant from 150 mbsl to maximum depth (265 mbsl) at 35.0 to 35.2 psu.

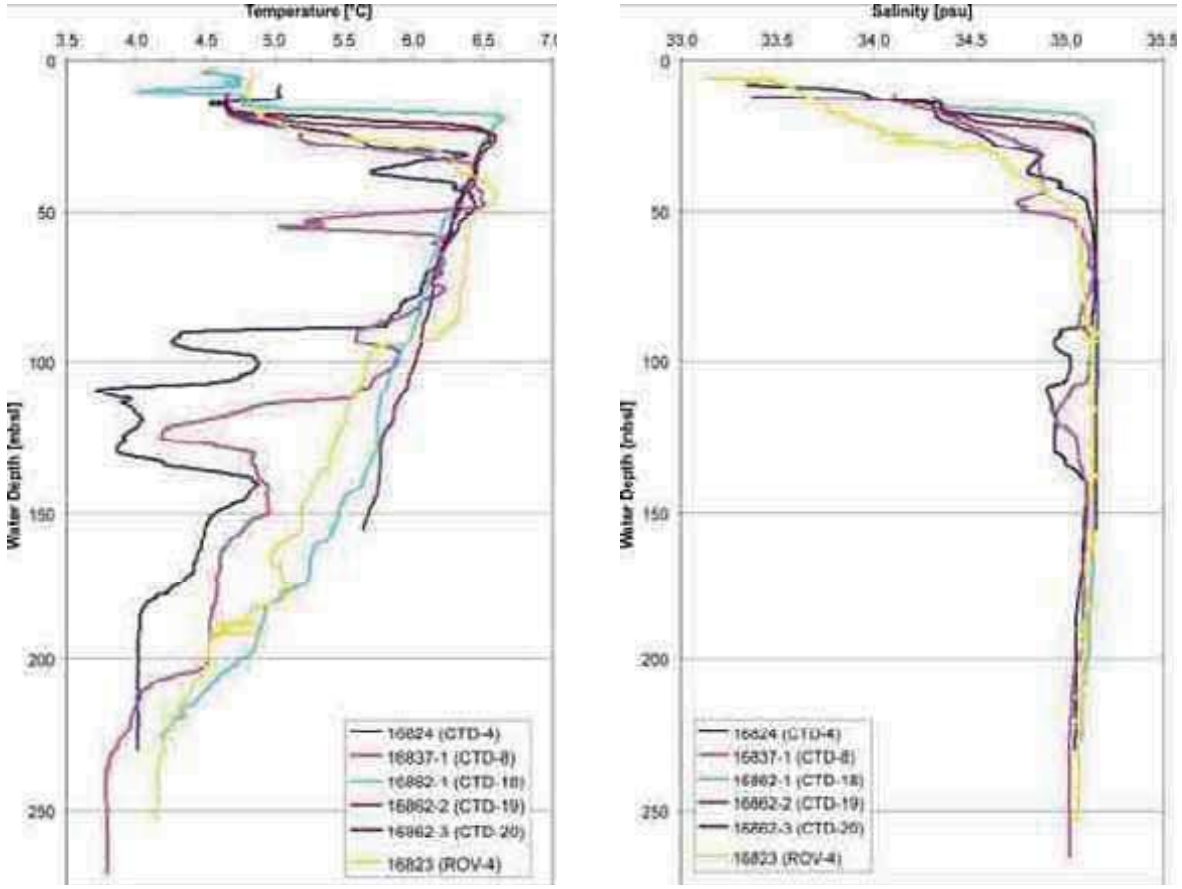

Figs. 4.7.7a and b: Water column T and S profiles in Seep Area 2.

The S-T plots for all stations performed in Area 2 suggested the presence of three separate major water masses (Fig. 4.7.7c).

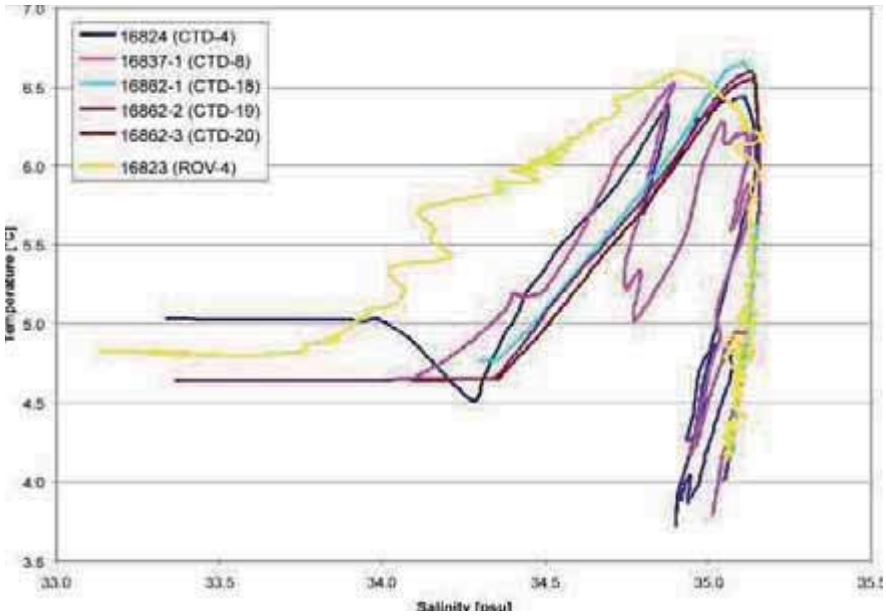

Fig. 4.7.7c: Salinity-temperature plot for CTD stations performed in Seep Area 2.

The uppermost water mass was characterized by medium temperatures and comparably low salinities, while both underlying water bodies showed higher salinities and lower and higher temperatures, respectively. With respect to similar S-T relationships, waters characterized by salinities around 35 psu might be attributed to the WSC.

III Seep Area 3 (ca. 380 m)

T and S data in Area 3 were available from a single CTD/ro station (GeoB16828) and three ROV dives (GeoB16833, -46, -48; Figs. 4.7.8a and b).

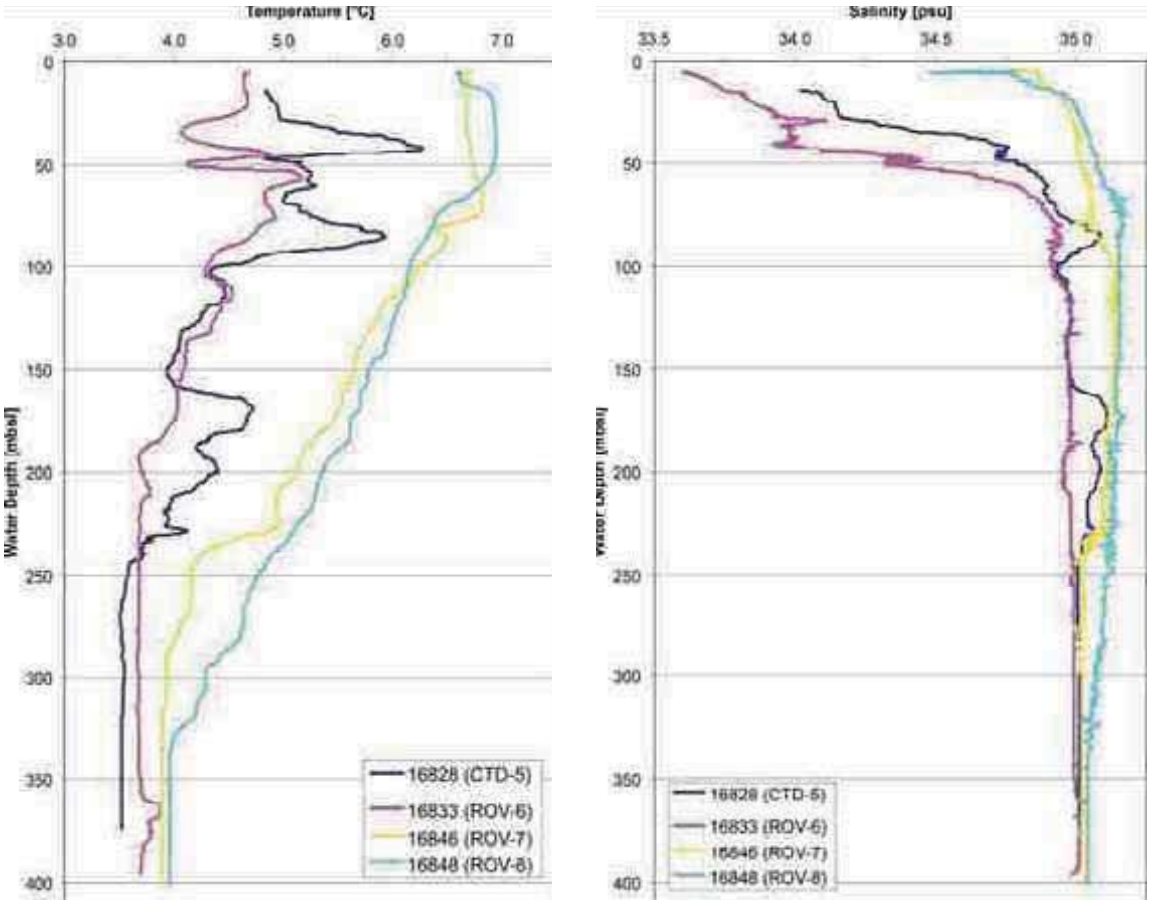

Figs. 4.7.8a and b: Water column T and S profiles in Area 3.

For the first two stations (GeoB16828, -33) temperature scattered considerably between 3.8 and 6.2°C from the surface to about 220/230 mbsl with a general decreasing trend. For stations GeoB 16846 and 16848, temperatures were more stable and decreased from about 7°C at the surface to less than 4.5°C at about 300 mbsl. Below about 320 mbsl temperatures at all stations were nearly constant between 3.8 and 4.1°C. Compared to temperature data, salinity profiles were much more stable throughout the water column. Salinity increased from as low as 33.5 psu close to the surface to about 34.8 to 35.2 psu at about 60 mbsl. Below that depth temperatures decreased or increased slightly and approached ca. 35 psu below about 320 mbsl.

The strong variations in T and S for certain water masses in Seep Area 3 are illustrated in the S-T diagram (Fig. 4.7.8c).

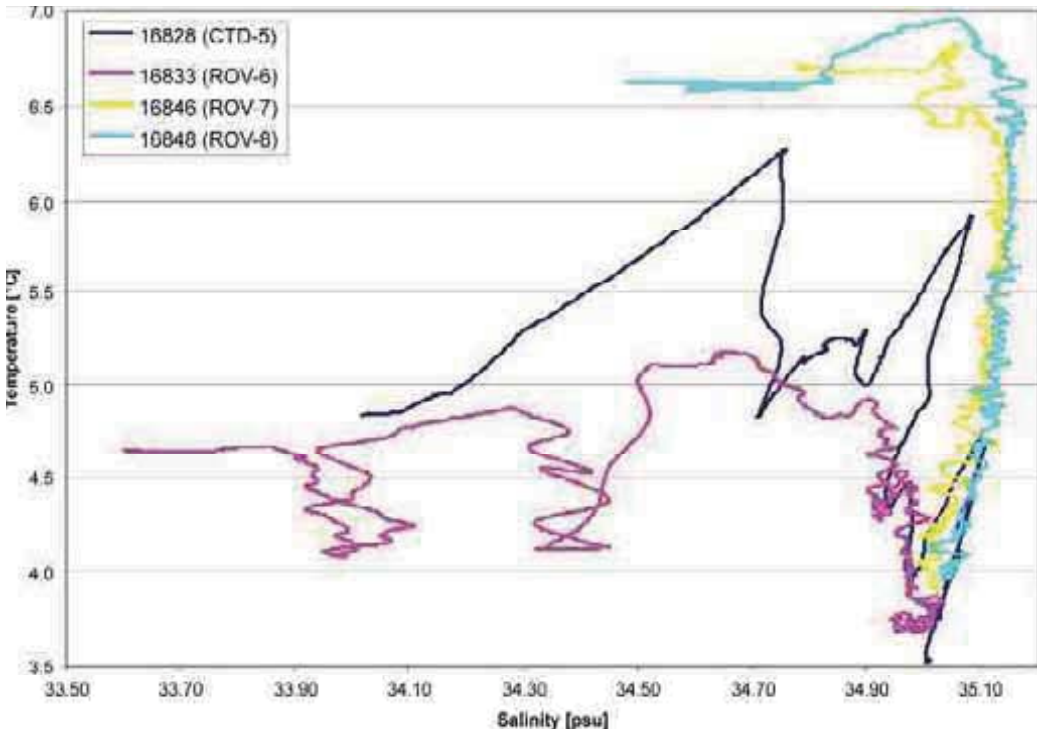

Fig. 4.7.8c. Salinity-temperature plot for CTD stations performed in Area 3.

Like for the temporal evolution of S and T in Seep Areas 1 and 2 considerably higher temperatures (approx. 0.4°C in 350 mbsl) for (a) distinct water mass(es) were observed for stations conducted after 01 September in Seep Area 3 (i.e. GeoB16846, -48). However, in contrast to the observed changes in Seep Areas 1 and 2, the increase in temperature coincided with a significant increase in salinity in the top 300 meters (Figs. 4.7.8b and c). In addition, S-T diagrams for stations 16846 and -48 resembled those obtained for the four westernmost stations remote from the Spitsbergen coast. This suggests that the proportion of relatively warm and saline water transported by the WSC increased in Seep Area 3 after 01 September as well.

4.8 ROV MARUM-CHEROKEE

(Nicolas Nowald, Werner Dimmler, Heiko Sahling)

Dive summary. During operation in the water, a constant current coming from the south was observed in all three working areas. Fortunately, the currents were rather weak, so they only had a minor influence on the behavior of the depressor and the vehicle. Dependent of the prevailing weather conditions, a proper station keeping of the ship was difficult to maintain, due to the limited navigational possibilities of the vessel. During some dives, the ROV was pulled away from its actual position so some gas quantification needed to be repeated.

On 28 August 2012, the communication to the Imagenex sonar failed prior to Dive 5. The problem could not be located and/or fixed, so the sonar was removed from the vehicle. Instead, the Tritech sonar was activated for the search of bubble streams. During the pre-dive check to Dive 6, 29 August 2012, the sonar PC crashed. A spare sonar PC was improvised on the same day, so the sonar was available again for the next dive. In order to have full, undisturbed 360° sweeps with the sonar, the sonar head was removed from its position in the foam block and was mounted on the porch with a bracket, that was constructed by the ships chief engineer.

During R/V HEINCKE Cruise HE-387, the ROV was deployed on 9 occasions in water depths between 88 m and 392 m. The vehicle spent 50 ½ h on the seafloor for the scientific examination, quantification and sampling of emitting gas off Svalbard. During the bottom time, videos and minifilm framegrabs from the two main cameras were recorded, resulting in more than 100 hours of video footage. Basic statistics are shown in Table 4.8.1 and a summary is given in Table 4.8.2 and Fig. 4.8.0.

Table 4.8.1: Dive statistics of the Cherokee ROV during R/V HEINCKE Cruise HE-387.

Dive	Bottom Time (h)	Gas Bubble Sampler	Niskin Bottles	Manipulator samples (rocks, etc.)	Gas Bubble Catcher	Still Images	Marker deployed	Marker #
1	5	2	1	4	0	31	1	#2
2	10	0	1	0	0	18	0	
3	7	0	1	0	4	84	0	
4	6	2	1	0	0	68	2	#4, #1
5	4	0	0	0	5	72	0	
6	6	2	1	3	0	61	2	#5, #3
7	3	0	1	0	4	33	0	
8	5,5	1	1	0	0	61	1	#6
9	5	0	1	0	6	26	0	
TOTAL	50,5	7	8	7	19	44	6	

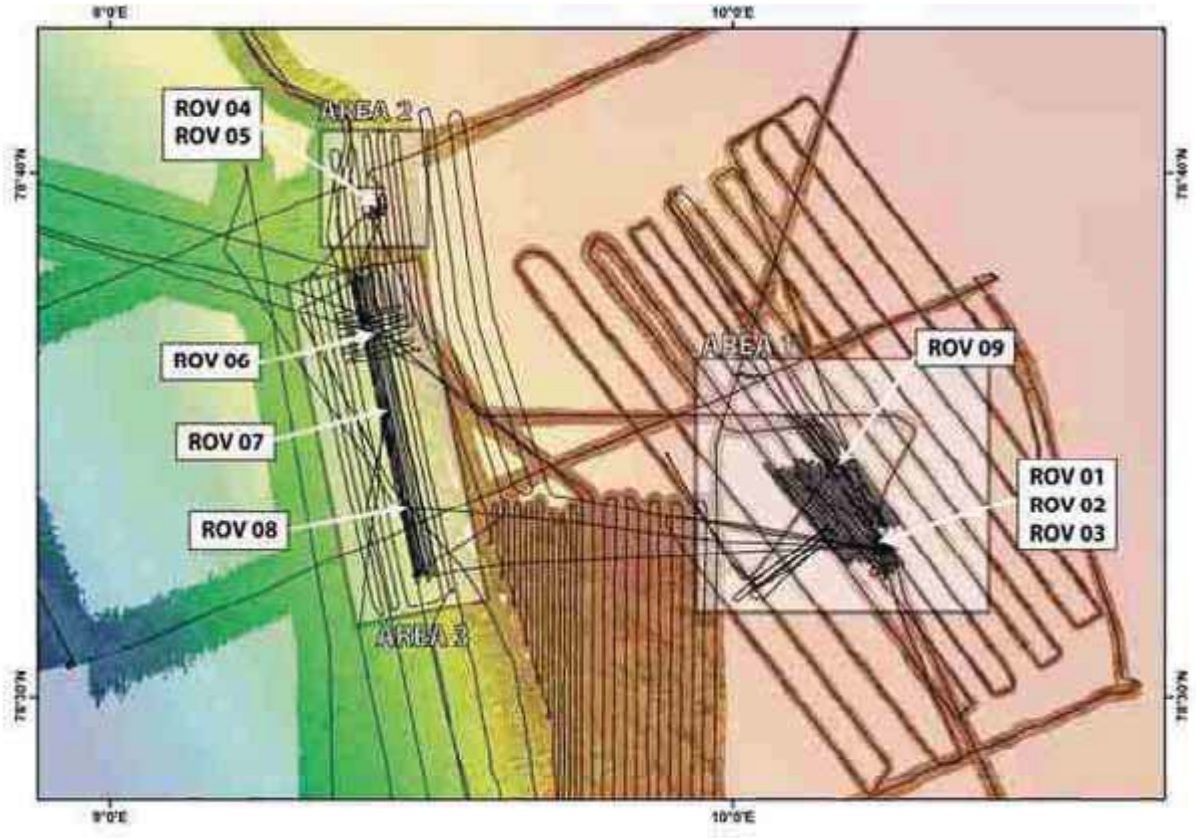

Fig. 4.8.0: ROV Cherokee dive locations during HE-387.

Table 4.8.2: Summary of ROV Cherokee dives during cruise HE–387.

ROV Dive Station No. GeoB No.	Area Date	Tools	Summary
Dive 1 Stat. 07 GeoB 16807	Area 1 23 Aug 2012	Imagenex 2 GBS Niskin bottle Marker 2	Gaining experience with sonar Imagenex, location of gas emission, sonar scans for flux quantification, deployed Marker 2, videos for bubble quantification, 2 gas samples, Niskin bottle at gas emission, rock and clamshells sampled
Dive 2 Stat. 12 GeoB 16812	Area 1 24 Aug 2012	Imagenex bubble imaging plate CTD	Gas emission mapped along three transects with Imagenex, using bubble imaging plate revealed that it is better without it
Dive 3 Stat. 16 GeoB 16816	Area 1 25 Aug 2012	Imagenex Bubble catcher 1.0 Niskin bottle Hydrophone SM2M	Quantification of bubble streams with different methods, using hydrophone
Dive 4 Stat. 23 GeoB 16823	Area 2 27 Aug 2012	Imagenex 2 GBS 3 Marker Niskin bottle CTD	2 cluster with gas emission were found and quantified, Marker 1 & 4 deployed, both GBS filled, rock samples

Dive 5 Stat. 26 GeoB 16826	Area 2 28 Aug 2012	Tritech in foam Bubble catcher 2.0 CTD	Quantification of bubble streams with different methods, using hydrophone
Dive 6 Stat. 33 GeoB 16833	Area 3 30 Aug 2012	Tritech on top 2 GBS Niskin bottle CTD	Quantification of bubble streams, Marker 3 & 5 deployed, GBS filled, sample of pogonophora and rock
Dive 7 Stat. 46 GeoB 16846	Area 3 02 Sept 2012	Tritech on top Bubble catcher 2.0 Niskin bottle CTD	Three clusters with unstable bubble emissions. Occurrence of carbonates, pogonophora and bacterial mats, quantification of bubble streams
Dive 8 Stat. 48 GeoB 16848	Area 3 03 Sept 2012	Tritech on top 2 GBS Marker Niskin bottle CTD	Mapping bubble streams by transecting along 8 lines the area. Bubble streams are transient. Marker 8 deployed, 1 GBS sample taken, Niskin closed
Dive 9 Stat. 53 GeoB 16853	Area 1 04 Sept 2012	Tritech on top Bubble catcher 2.0 Niskin bottle CTD	Defining the lateral extent of cluster C5, taking sonar scans within the cluster, Quantifying using bubble catcher and optical method

4.8.1 Cherokee Dive 01, Ship station #07, GeoB 16807

Area: **Area 1 ('80-m flare site')**
Water depth: 88 - 98 m
Date: Thursday 23 August 2012
Start down 07:20
At bottom 07:44
From bottom 12:14
On deck 12:28
Bottom time ca. 4.5 hours
Location ROV goes down: **78°32.966' N 10°14.25' E**

Responsible scientist: Miriam Römer
Protocol:
08:30 – 10:30 Heiko Sahling
10:30 – 11:45 Benoît Bergès
11:45 – End Jan Boelmann

Instruments/tools: 2 GBS
3 Marker (1, 2, 3)
Niskin bottle
CTD
Sonar

Waypoints:
Area with numerous gas flares between:

WP 1:	78°32.966'N	10°14.071'E
WP 2:	78°32.837'N	10°14.596'E
WP 3:	78°32.810'N	10°14.372'E
WP 4:	78°32.884'N	10°14.077'E

Samples and measurements:

GeoB	Instrument	Time	Position	Depth / m	Comment
16807-1	Marker 2	10:05	78.547318 10.23745 78°32.8391'N 10°14.247'E	94	Very close to bubble streams A1-C1-S1 and S2
16807-2	GBS 1	10:19	78.547314 10.23754 78°32.8388'N 10°14.2524'E	94	Sampling one of the streams A1-C1-S1 or S2
16807-3	GBS 2	10:35	78.547325 10.23745 78°32.8395'N 10°14.247'E	94	Sampling the other stream A1-C1-S1 or S2
16807-4	Niskin	11:05	78.547326 10.237436 78°32.8396'N 10°14.2462'E	94	Water sampling close to bubble streams A1-C1-S1 and S2

Key results:
Gas emissions were found with the sonar and afterwards visually at the seafloor. A group of flares was documented for sonar-based quantification and one for visually based quantification. Two bubble streams were sampled for gas analysis and a water sample has been taken.

Technical description:
The general performance of the ROV was very good. Imagenex sonar mounted on top of vehicle.

Dive description:
The ROV was stopped during diving down in about 10 m above the seafloor and the water column was scanned with the horizontally looking sonar in order to find gas bubbles hydroacoustically. During the first half an hour no gas emission could be identified while the ROV flew southward in direction to the most prominent cluster of flares localised with EM710 prior to the dive (Fig. 4.8.1). In the centre of this cluster small points of high backscatter were interpreted as gas bubble streams (A1-C1) and confirmed when diving to the seafloor and observed visually. The ROV was positioned in front of two gas bubble streams (A1-C1-S1 and A1-C1-S2) ~20 cm distant to each other. About 4-9 bubble streams could be observed with the sonar in only 1-2 m distance in front of the ROV. The sonar scan has been recorded and will be used to quantify the gas flux. The two bubble streams documented with the video equipment of the ROV escaped from the seafloor at the rim of a small (~20 cm in diameter) microbial mat (Fig. 4.8.2). Marker 2 was positioned close to the two bubble streams.

The seafloor in this area is flat and covered by numerous stones and blocks as well as shells of bivalves. Few organisms as sea urchins, shrimps and soft corals could be identified. One of the two gas bubble streams (A1-C1-S2) was documented for about half an hour with different settings and zoom factors together with the arm of the ROV in order to use the video material to visually quantify the amount of gas escaping through this stream. After this detailed documentation with sonar and video, two gas bubble samplers (GBS 1 and GBS 2) were deployed to sample gas of both gas bubble streams. Both deployments have been successful and the sampled gas will be analysed for its composition on board. During the documentation and sampling more than 30 pictures were taken. The Niskin sampler was taken.

Following the observation at the seafloor, the ROV was moved up to about 6 and later 10 m above the seafloor to gain an overview about further bubble streams in the surrounding with the sonar and also to learn about the best setting of the sonar to detect gas bubble streams for the next dives. For instance, the range in 6 – 10 m height above the seafloor should not exceed 10 m as gas bubble streams appear in this sonar as very small anomalies and become invisible using larger ranges. A short transect scanning the water column with the sonar has been performed eastwards in 5 m steps (Fig. 4.8.1).

At the end of the dive we took few samples (stones and a bivalve shell) from the seafloor.

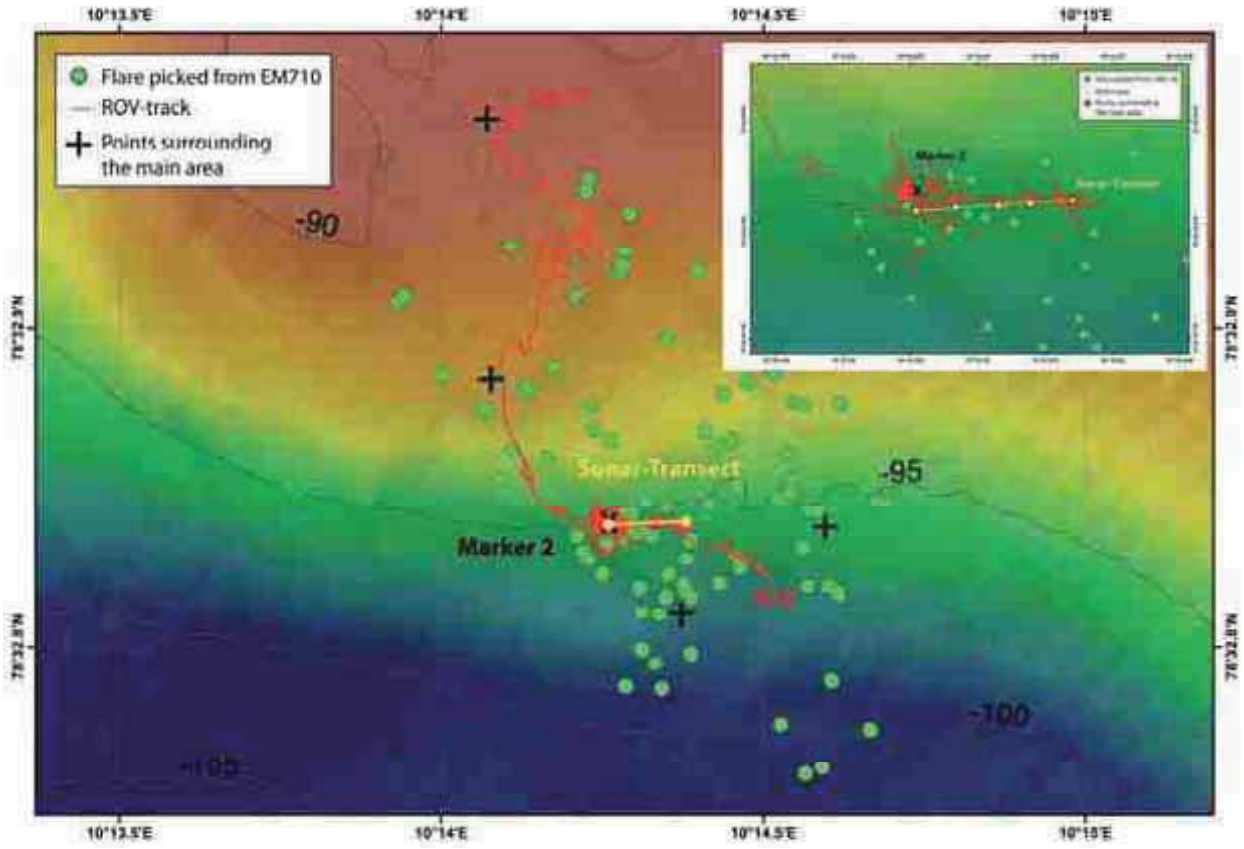

Fig. 4.8.1: Map of the area studied during ROV Cherokee Dive 01 (GeoB 16807) in Area 1.

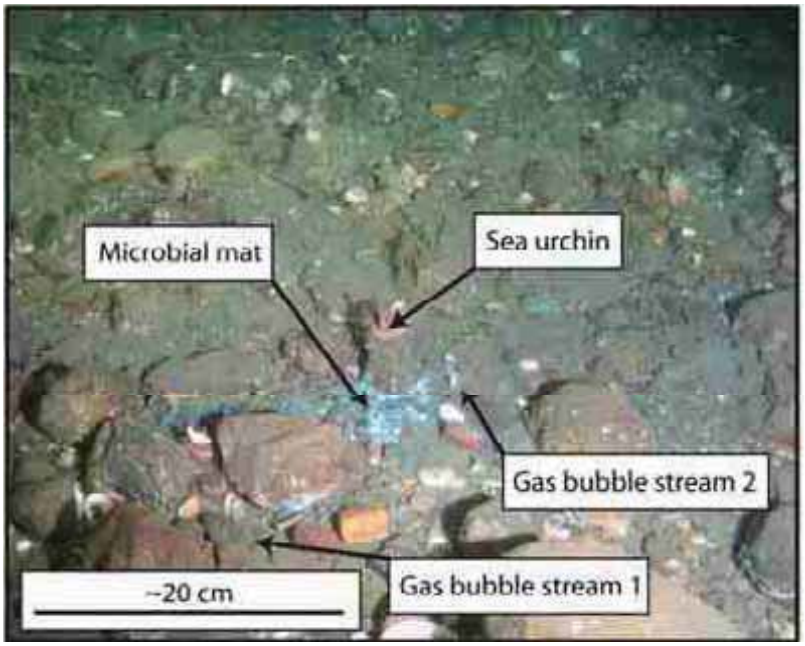

Fig. 4.8.2: Image of the seafloor in ~90 m water depth covered with stones, gravel and shells. In the centre a microbial mat is visible with the two gas bubble streams at the rim (A1-C1-S1 and A1-C1-S2), which have been documented for quantification during Cherokee Dive 01.

4.8.2 Cherokee Dive 02, Ship station #12, GeoB 16812

Area: **Area 1 ('80m flare area')**
Water depth: 95 m
Date: Friday 24 August 2012
Start down 06:04
At bottom 06:30
From bottom 15:50
On deck 16:07
Bottom time ca. 10 hours
Location ROV goes down: **78°32'957 N 10°14'224 E**

Responsible scientist: Michal Tomczyk
Protocol:
06:30 – End Jan Boelmann

Instruments/tools: Bubble imaging plate
CTD
Imagenex Sonar

Waypoints: Same as for dive 01

Samples and measurements:

GeoB	Instrument	Time	Position	Depth / m	Comment
16812-1	Niskin bottle	15:48	78.548107 10.241961 78°32.8864'N 10°14.5177'E	93	Close to A1-C4-S4 and S5

Key results:
Gas emissions mapped along three transacts. 8 bubble plumes were documented for sonar based quantification and for visually based quantification.

Technical description:
There were some problems with the ROV Cherokee. Some vital part of video record was lost. The ROV system was restarted few times. Problems with GAPS: recurrence rate large leading to a time delay. For example, the ROV did not move anymore but the GAPS position showed movement. Furthermore, the GAPS positions contained several outliers that were removed by deleting in the post-processing procedure.

Dive description:
The entire dive took almost 10 hours. At the beginning 360 degrees sonar scan was performed for a better overview, with the purpose to find gas emission sites. The objectives were flare mapping and gas emission quantification at 90 meters depth site. Three transacts with sonar Imagenex were performed: The first transact from NW to SE with 20 meters interval. The range of scanning sonar was set to 10 meters. Another two transacts from NE to SW with 10 meters interval. Nearly 240 gas bubble plumes were mapped along these transacts. Most of the flares

were correlated to the position of flares mapped with EM710. 10 bubble plumes (Area1-C2 -S1, -S2, -S3 and Area1-C4 –S1, -S2, -S3, -S4, -S5, -S6) were quantified using active acoustics, and some of them were video recorded for visually based quantification. A bubble imaging plate was used for the purpose of visual quantification. Nevertheless, it did not work out due to reflection from this plate.

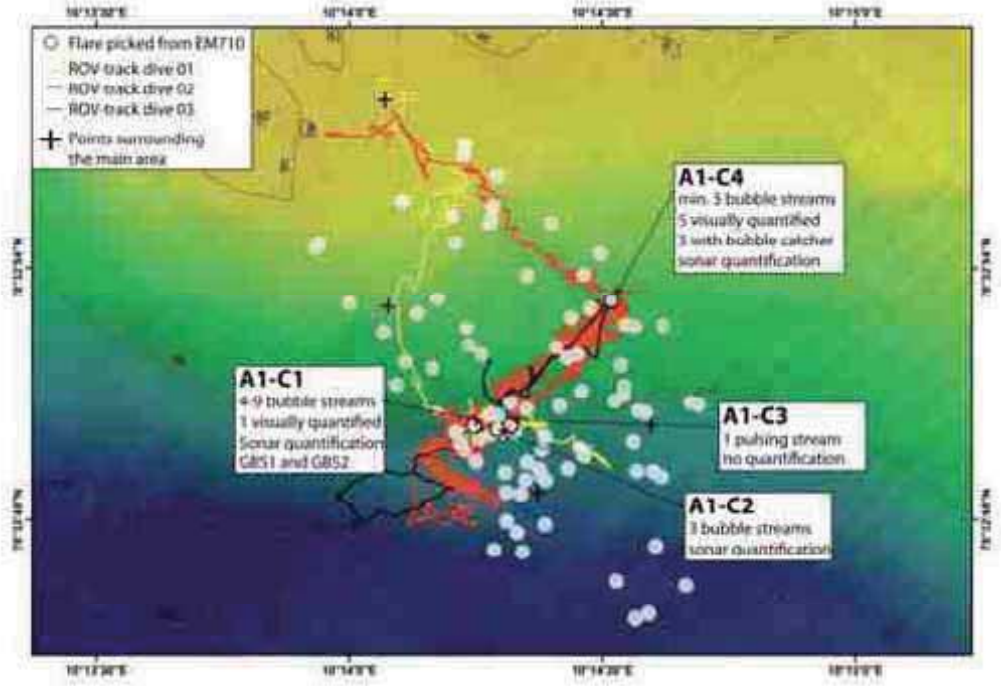

Fig. 4.8.3: Map of the dive area. Cluster A1-C2 with was documented first (sonar and visual quantification). The second part of dive took place in A1-C4 cluster where several gas bubble plumes were quantified.

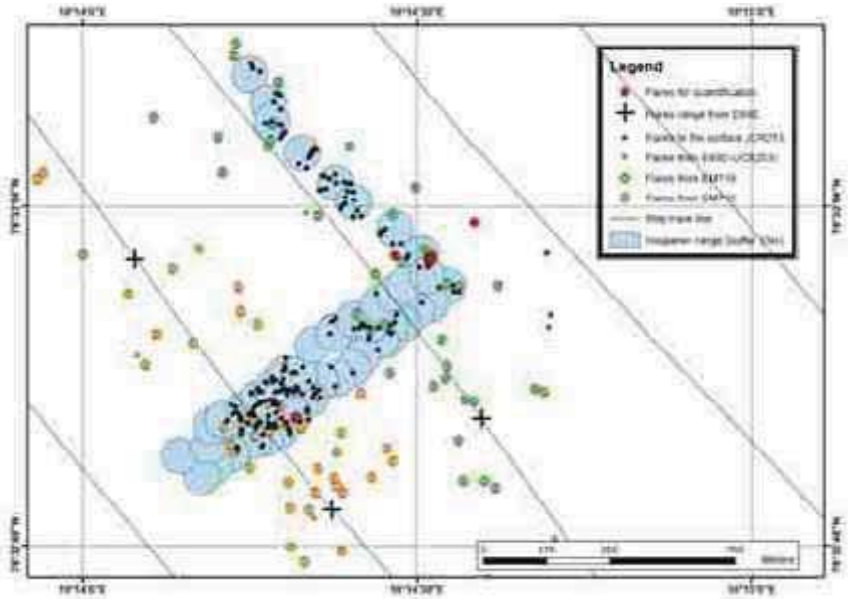

Fig. 4.8.4: Map of the dive area. Blue circle shows a location of ROV during scanning with sonar (range 10 meters). Black dots represent bubble streams mapped by Imagenex.

4.8.3 Cherokee Dive 03, Ship station #16, GeoB 16816

Area: **Area 1 ('80 m flare area')**
Water depth: 94-97 m
Date: Saturday 24 August 2012
Start down 06:03
At bottom 06:19
From bottom 12:50
On deck 13:04
Bottom time ca. 7 hours
Location ROV goes down: **78°32.89' N 10°14.09' E**
Location ROV picked up: **78°32.80' N 10°14.01' E**

Responsible scientist: Benoît Bergès
Protocol:
08:30 – 11:45 Heiko Sahling
11:45 – End Benoît Bergès

Instruments/tools: Niskin bottle
Imagenex (sonar)
SM2M (hydrophone)
Bubble catcher

Waypoints:
Selected sites for gas emission quantification:

WP 1:	78.548082N	10.241962E
WP 2:	78.547278N	10.237640E

Samples and measurements:

GeoB	Instrument	Time	Latitude	Longitude	Depth	WP
16816-1	Bubble catcher	06:55	78.548099	10.242006	92.7	1
	Imagenex	07:16	78.548091	10.241974	92.6	1
16816-2	Hydrophone	07:56	78.548104	10.241984	92.8	1
	Video	08:07	78.548093	10.242017	92.7	1
16816-3	Bubble catcher	08:53	78.548083	10.241996	92.6	1
	Video	09:00	78.548081	10.241960	92.1	1
	Video	10:11	78.548069	10.242083	91.9	1
16816-4	Bubble catcher	10:25	78.548094	10.242012	92.3	1
16816-5	Hydrophone	10:48	78.548080	10.241995	91.6	1
16816-6	Hydrophone	11:06	78.548074	10.241984	92.0	2
16816-7	Bubble catcher	11:46	78.547284	10.237641	94.3	2
	Imagenex	12:15	78.547285	10.237625	94.8	2
16816-8	Hydrophone	12:26	78.547288	10.237647	94.5	2
16816-9	Hydrophone	12:40	78.546813	10.233003	96.7	3
16816-10	Niskin bottle	12:45	78.546819	10.233001	97.2	3

Key results:
During this dive, effort was given to provide gas quantification for different bubble streams using: active acoustics, passive acoustics, video footage, bubble catcher. The aim is to produce independent gas flow rate estimates that could be compared. During this 7 hours operation, 4

bubble streams were quantified around waypoints WP1 and WP2. In addition, background noise recording and water sampling were performed.

Technical description:
ROV: good deployment
Niskin bottle: good deployment
Imagenex (SONAR): good deployment
SM2M (hydrophone): good deployment (Fig. 4.8.6)
Bubble catcher: some problems encountered to keep the device steady for a long period because of ship movement disturbing the ROV. The reset of the bubble catcher is hard to process because of the buoyancy of the gas in the device (Fig. 4.8.9).

Dive description:
The ROV was deployed around 06:00 UTC and the survey started at the location of bubble streams marked in the navigation software Posiview as streams 4 and 7&8 that were mapped during Dive 02 (WP 1). During the transit to this area, pictures were taken, providing some visual observation of the seafloor. At WP 1, the Imagenex system was turned on in order to provide an overview of the flares. Three streams were observed (labelled as stream 1, 2 and 3 in Fig. 4.8.8). Each of those three streams are investigated individually and data quantifications were collected using the Imagenex system, the bubble catcher device and video camera together with the bubble catcher as a scale frame (Fig. 4.8.9).

In addition to those measurements, the ROV was kept at its most silent level in order to reduce the noise level for hydrophone acquisition (5 mins). Then, the ROV was moved further away from the site (2.2 m and 3.5 m away) and kept silent for additional passive acoustic recording (5 mins).

After the survey of the three streams, it was decided to study more streams and WP 2 was investigated. This area is known to present a strong bubble stream activity from Dive 02. Using the Imagenex system, a sonar map of the zone was drawn and two flares were detected. The same systematic survey conducted on the flares at WP 1 was performed in order to achieve more gas quantifications.

As summarized in chapter “bubble stream analyses”, the cluster was later signified as A1-C4b. Seven bubble streams were quantified by different methods (S1 to S7).

Once the operations finished at WP 2, the ROV transited to WP 3 to deploy the Niskin bottle for water sampling. WP 3 was chosen because it does not present any bubble activity (as opposed to the water sampling performed during Dive 01). Before recovering the ROV, noisy equipment were turned off in order to acquire background noise. The result of the hydrophone recordings are presented in Chapter 4.12.

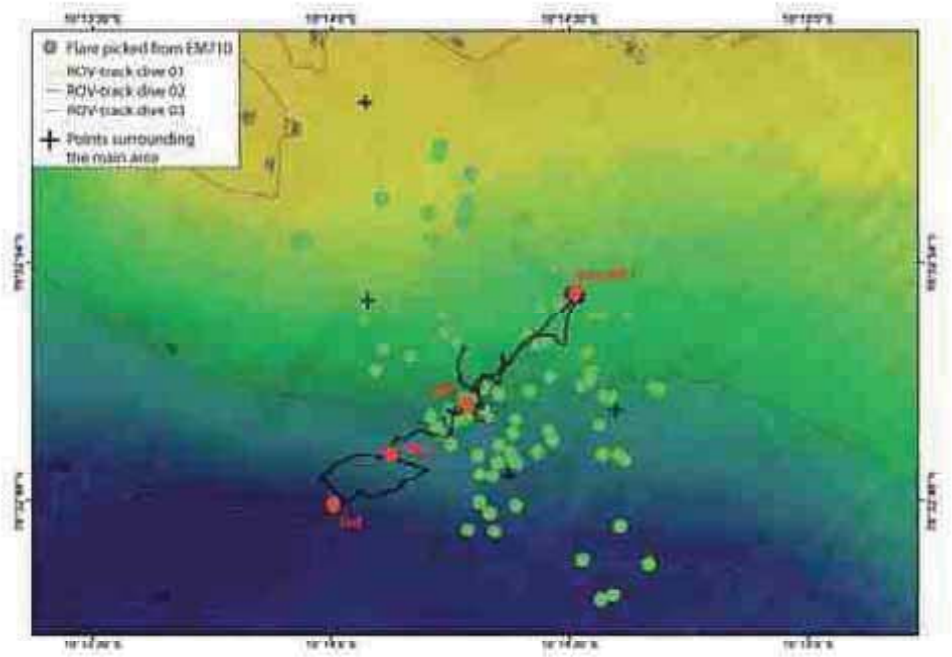

Fig. 4.8.5: Map of the area with waypoints, start point and end point.

Fig. 4.8.6: Hydrophone set up on the ROV.

Fig. 4.8.7: Image of the seafloor at the ROV deployment position (78°32.89' N 10°14.52' E, ~93m depth).

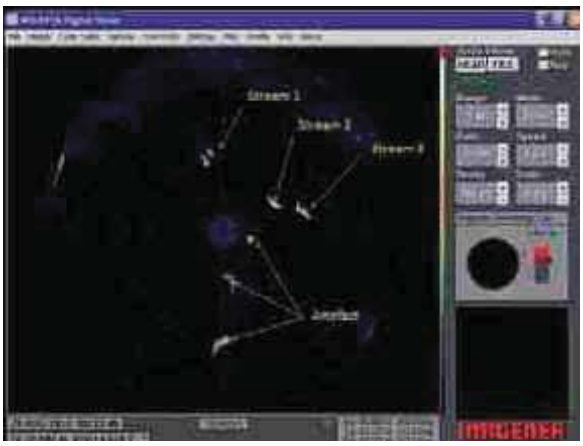

Fig. 4.8.8: Sonar overview of WP 1.

Fig. 4.8.9: Image illustrating the process used for obtaining a scaling for gas quantification using the video camera.

4.8.4 Cherokee Dive 04, Ship station #23, GeoB 16823

Area:	**Area 2 ('280 m flare area')**
Water depth:	245 m
Date:	Monday 27 August 2012
Start down	08:08
At bottom	08:27
From bottom	14:36
On deck	14:55
Bottom time	ca. 6 hours
Location ROV goes down:	**78°39'237 N 09°25'800 E**

Responsible scientist:	Miriam Römer
Protocol:	
08:30 – 10:30	Michal Tomczyck
10:30 – End	Benoît Bergès

Instruments/tools:	2 GBS
	3 Marker (1,3,4)
	Niskin bottle
	CTD
	Sonar Imagenex
Waypoints:	Dive planning based on EM 710 flare mapping.

Samples and measurements:

GeoB	Instrument	Time	Position	Depth / m	Comment
16823-1	Marker 1	08:40	78.654223 9.429338 78°39.2534'N 9°25.7603'E	241	Close to bubble streams at A2-C1
16823-2	GBS 1	09:44	78.654236 9.429257 78°39.2542'N 9°25.7554'E	242	Filled at A2-C1
16823-3	Rock sample	10:49	78.654254 9.429238 78°39.2552'N 9°25.7543'E	241	Sample of rock, maybe authigenic carbonate
15823-4	Marker 4	11:27	78.654207 9.434064 78°39.2524'N 9°26.0438'E	241	Close to bubble streams at A2-C2
16823-5	GBS 2	12:45	78.654196 9.434012 78°39.2518'N 9°26.0407'E	240	Filled at A2-C2-S3
16823-6	Rock sample	13:03	78.65419 9.434071 78°39.2514'N 9°26.0443'E	240	Maybe authigenic carbonates
16823-7	Niskin bottle	14:04	78.654181 9.433985 78°39.1086'N 9°26.0391'E	240	Filled within A2-C2

Key results:

Two clusters of gas emissions were found with the sonar and visually at the seafloor. Both were documented for sonar based quantification and for visually based quantification. At each cluster gas has been sampled with the GBS and a water sample has been taken at the end of the dive in the second cluster.

Technical description:

The general performance of the ROV was very good. During the dive a communication problem with the Imagenex sonar appeared and the ROV has been restarted. The problem could be fixed and sonar could be used also for the rest of the dive.

Dive description:

When reaching the seafloor the ROV was located already close to a flare location mapped with EM710 and the ROV needed only few minutes to reach the area where gas emissions were expected (Fig. 4.8.10). A cluster of bubble streams (A2-C2) has been detected at the south-western part of the area with the horizontally looking sonar and immediately also visually with the cameras mounted on the ROV. About 15 single anomalies were visible in the sonar (probably representing each a single gas bubble stream) within a radius of less than 2 m. They could be identified and correlated visually. As a first impression, the bubble streams seem to have different bubble sizes and rising speeds. Marker 1 was set close to the bubble streams. Sonar records were taken in order to quantify the bubble streams and afterwards also video records of single bubble streams (A2-C1-S1, 2, 4). A gas sample has been taken with GBS1. Close to the

cluster of bubble streams (~2 m) cracks in the seafloor within carbonate crusts were found and a rock sample was taken (Fig.4.8.11d). Finally the area was surveyed in all directions to ensure, the cluster has been entirely detected, which produces the flare visible in EM710 and indeed no other gas emissions have been detected in the surrounding ~20 m.

In the second part of the dive the ROV flew eastwards to another area where a flare in EM710 indicated a source of gas emissions and a cluster of bubble streams have been found at the expected location (Fig. 4.8.10). Marker 4 was positioned very close to a group of bubble streams that have been recorded both with sonar and video (A2-C2-S1, 2, but 3 is missing, 4, 5 and 6, 7) for quantification. The area is characterized by large blocks of probably authigenic carbonates and gas seems to accumulate below some of them. Gas bubble streams escaping from the rims of those blocks show pulsing bubble escape and seem to be characterized by larger bubbles. GBS2 was filled with gas escaping from A2-C2-S6 and 7 (which have only a few cm distance to each other). The sonar scanning showed few more bubble streams in the surrounding few meters and a part have been again scanned for quantification. And a strong but pulsing gas stream escaping from a rim of a huge carbonate block was recorded for visual quantification (A2-C2-S8, Fig. 4.8.11g). A piece of carbonate was taken (Fig. 4.8.11h). To verify if the cluster is the only one in this area, the surrounding was mapped by sonar. In this case, additional bubble streams could be identified (by sonar and visually) northeast of cluster A2-C2; unfortunately there was not enough time to map in more detail if there is a new cluster or if the bubble streams form a larger cluster connected to A2-C2.

At the end of the dive the ROV flew to the north-western located small depression in order to document different seafloor characteristics. Indeed, in the steeper part a lot finer sediment cover and a dense coverage of smaller cm-scale pebbles highly settled by sponges and ascidia in the deepest part of the depression (Fig. 4.8.11j) could be observed.

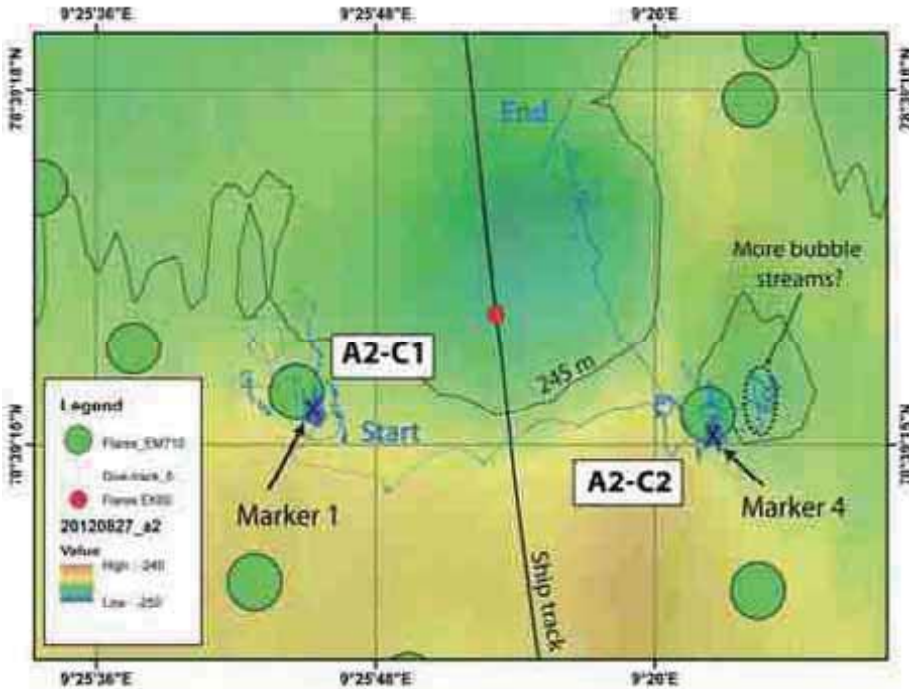

Fig. 4.8.10: Map of the dive area. Cluster A2-C1 with Marker 1 was documented first. GBS 1 and a carbonate sample were taken. The second part of the dive was performed at A2-C2 where Marker 4 was set. GBS 2 and a carbonate sample and a water sample with the Niskin bottle were taken at this site.

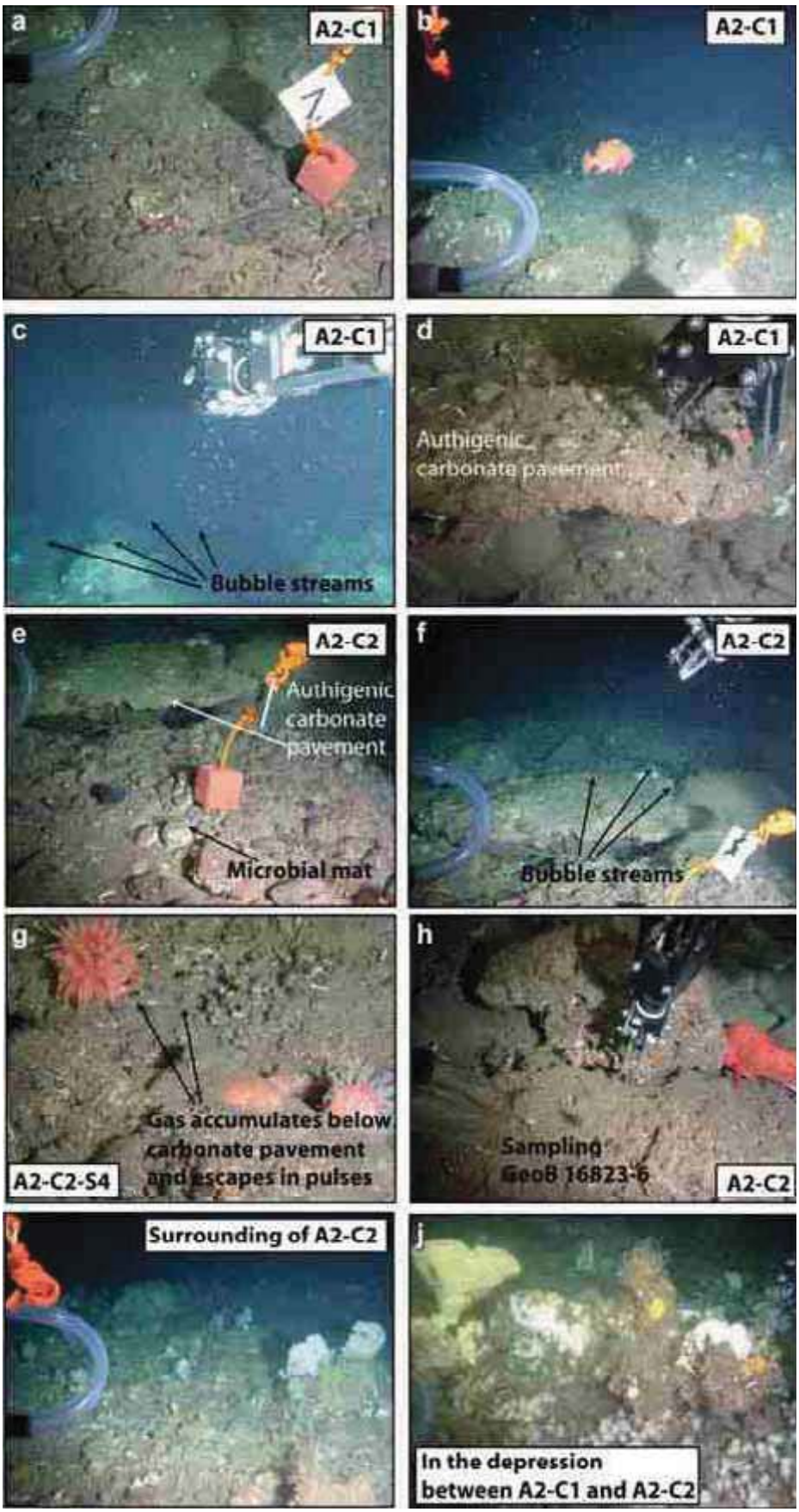

Fig. 4.8.11: Images of the seafloor in ~245 m water depth. a to d at A2-C1, f-h at A2-C2 and i-j during the final survey into the depression.

4.8.5 Cherokee Dive 05, Ship station #26, GeoB 16826

Area: **Area 2 (280 m flare area)**
Water depth: 238-240m
Date: Tuesday 28 August 2012
Start down 09:50
At bottom 10:30
From bottom 14:43
On deck 14:56
Bottom time ca. 5 hours

Location ROV goes down: **78°39.242' N 09°25.993' E**
Location ROV picked up: **78°39.227' N 09°26.247' E**

Responsible scientist: Benoît Bergès
Protocol:
08:30 – End Heiko Sahling

Instruments/tools: ROV SONAR (Tritech)
Bubble catcher v2
Video camera

Points of Interest:

WP 1	78°39.215'N	9°25.829'E	A2-C3	1 stream
WP 2	78°39.216'N	9°25.786'E	A2-C4	1 stream
WP 3	78°39.224'N	9°25.738'E	A2-C5	No stream, potentially transient ones
WP 4	78°39.202'N	9°25.997'E	A2-C6	5 streams, potentially 6

Samples and measurements:

GeoB	Instrument	Time	Latitude	Longitude	Depth	WP	Comments
16826-1	Bubble catcher	11:43	78.653601	9.430568	241.5	1	C3-S1
	Video	11:50	78.653611	9.430521	241.5	1	C3-S1
16826-2	Bubble catcher	12:32	78.653602	9.429771	241.1	2	C4-S1
	Video	12:49	78.653603	9.429752	241	2	C4-S1
16826-3	Bubble catcher	14:03	78.653346	9.433252	241	4	C6-S1
16826-4	Bubble catcher	14:07	78.653358	9.433191	241.5	4	C6-S2
16826-5	Bubble catcher	14:10	78.653362	9.433287	241.4	4	C6-S3
16826-6	Bubbler catcher	14:27	78.653350	9.433280	241.6	4	C6-S4
16826-7	Bubbler catcher	14:37	78.653368	9.433126	239.3	4	C6-S5

Key results:
During this dive, bubble streams mapping and quantification using video camera and a new version of the bubble catcher were performed. Four areas were investigated, corresponding to

bubble flares detected using the EM710 multibeam echosounder. On those sites, referenced as A2-C3 (WP 1), A2-C4 (WP 2), A2-C5 (WP 3) and C2-C6 (WP 4), many streams were discovered using the sonar head mounted on the ROV (Tritech) and by visual observation.

Technical description:
SONAR: the Imagenex system stopped functioning when turned on the morning of the 28th. In order to carry on with the dive, it was decided to use the sonar head that is regularly mounted on the ROV (Tritech) for bubble streams mapping. The position of the Tritech sonar is within the vehicle and, thus, it can only look forward. In addition, shadow zones exist casued by, probably, the plate holding the GBS. After further investigation on the evening of the 28th, it was confirmed that the Imagenex system is not functioning.
Bubbler catcher: good deployment of the new version. This system gives some more ease to empty the gas and the reading of the amount of gas (Fig. 4.8.13).
ROV: forced to bring back ROV on deck at the beginning of the survey because of cabling problems (bad set up).

Dive description:
Due to investigations on the failure of the Imagenex system early in the morning, the dive was delayed by nearly four hours. It was finally decided to make use of the ROV mounted sonar head (Tritech) for bubble streams mapping.

The ROV was put into water at 09:50 UTC but brought back on deck at 10:09 UTC due to cabling problems. The system was deployed again at 10:22 UTC and the scientific program started around 10:30 UTC.

Prior to bubble streams hunting, care was given to find fine tuning of the sonar system (Tritech). Fig. 4.8.14-1 gives an overview of the features that appeared when no bubble streams were around the ROV. It can be observed that the region near the centre was found to be very noisy and an artefact appears as a line at ~5 m range, however, this last feature occurred at all range settings. An optimum setting for the ROV to have coverage of ~5-6 m is about 3 m above the seafloor.

After getting used to the new system, survey was conducted firstly at the A2-C3 area (WP 1). Several scans provided information on location of bubble emissions (Fig. 4.8.14-2) and a regular stream labelled as A2-C3-S1 was localized. In addition, on some scans, a transient stream seemed to appear but no visual evidences of this irregular feature were discovered. The ROV was driven next to A2-C3-S1 (Fig. 4.8.14-3) and quantifications were conducted using the new bubble catcher and the video camera.

Secondly, A2-C4 area was investigated (WP 2). Only one stream was discovered and labelled as A2-C4-S1 (Fig. 4.8.1-4). The ROV has been positioned next to this stream and quantification was made using the bubble catcher (table 4.8.3) and the video camera.

Then, the ROV headed to A2-C5 in order to proceed to another systematic bubble stream mapping. No streams were found on the way from A2-C4 to A2-C5. Sonar scans of A2-C5 could not provide robust information of bubble emissions. Some bubble stream like features appeared on the sonar images but no longer than the time for the sonar to cover one scanning sector. No streams were labelled in this area but there might be transient bubble emissions.

The last survey was conducted to the A2-C6 area. No streams were spotted with the sonar during the transit. A2-C6 was found to have several bubble streams (Fig. 4.8.14-6). Five streams were labelled from A2-C6-S1 to A2-C6-S5 during the survey. Bubble streams A2-C6-S1, A2-C6-S2 and A2-C6-S3 were first discovered, followed by A2-C6-S4 and A2-C6-S5. Those last two were not spotted firstly because they were found to have transient emission of bubbles during the survey. At the very end of the survey, a sixth stream, believed to be transient might have been spotted. For each streams apart from the sixth one, quantifications were performed using the bubble catcher device.

The survey ended after the quantification of A2-C6-S5. The ROV was recovered afterwards at 14:43 UTC.

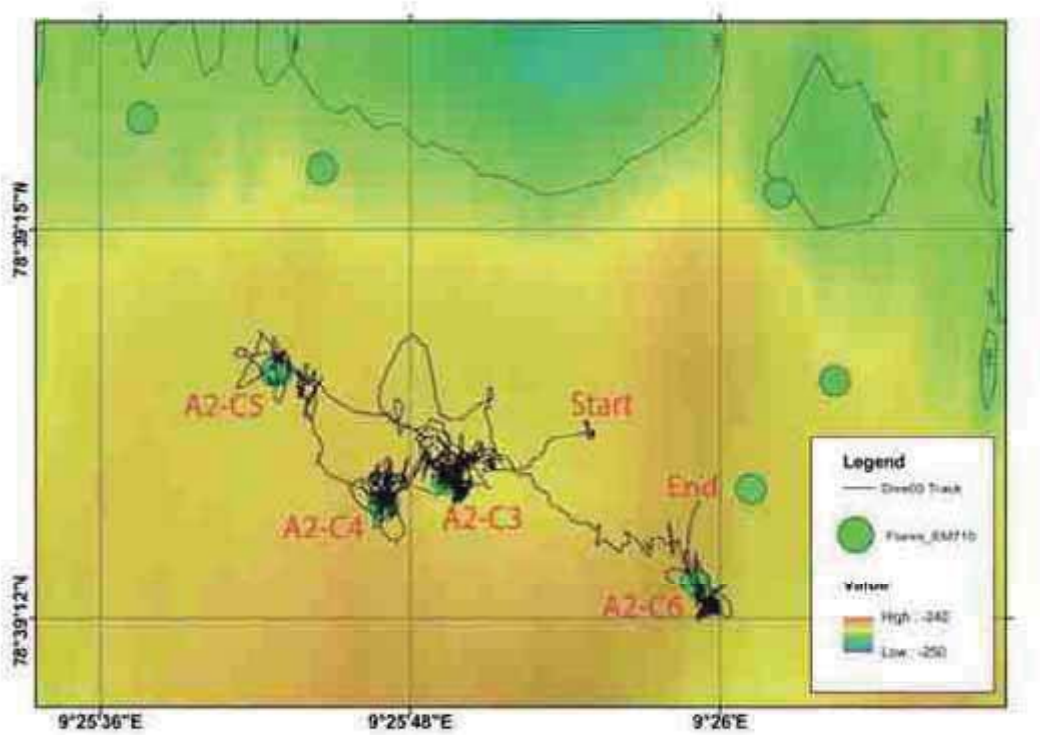

Fig. 4.8.12: Dive 05 track and bubble stream clusters encountered during the dive.

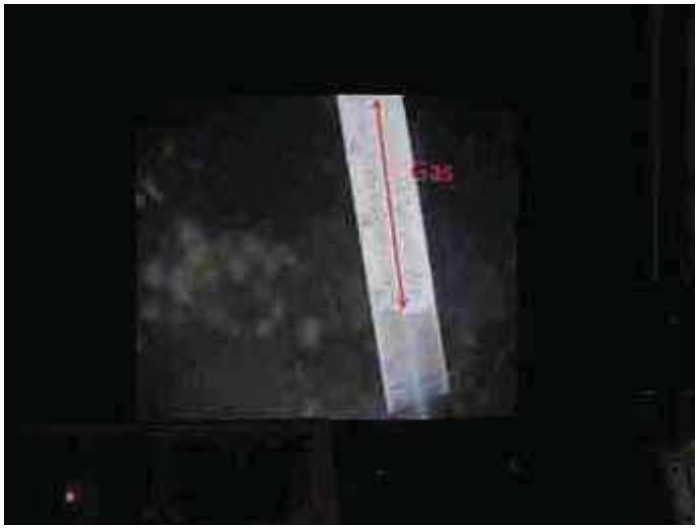

Fig. 4.8.13 Quantification process using bubble catcher version 2.

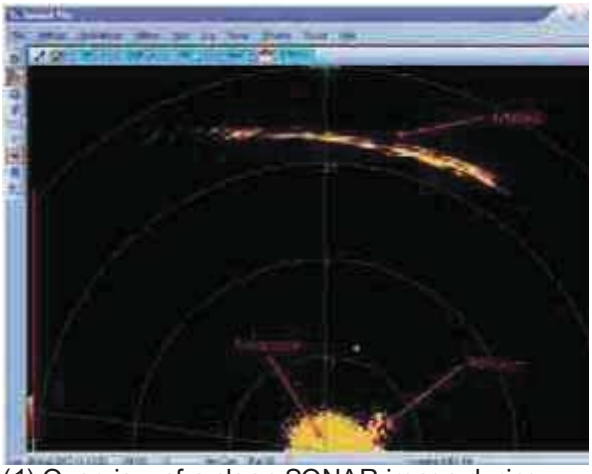

(1) Overview of a clean SONAR image during dive 5

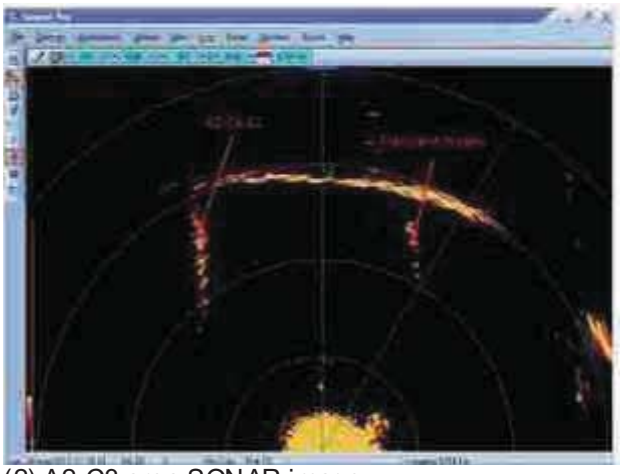

(2) A2-C3 area SONAR image

(3) Picture of A2-C3-S1

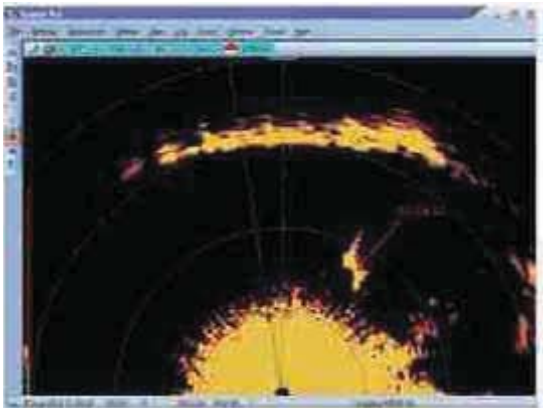

(4) SONAR image of A2-C4-S1

(5) Picture of A2-C4-S1

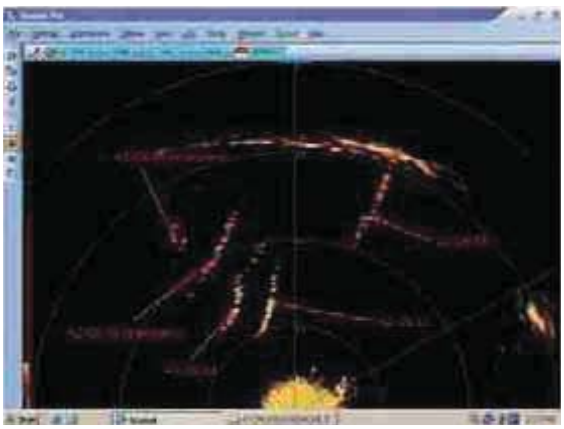

(6) SONAR image of A2-C6

Fig. 4.8.14: Overview over sonar scans and seafloor images at the bubble streams.

1) Picture of A2-C6-S1

2) Picture of A2-C6-S2

3) Picture of A2-C6-S3

4) Picture of A2-C6-S4

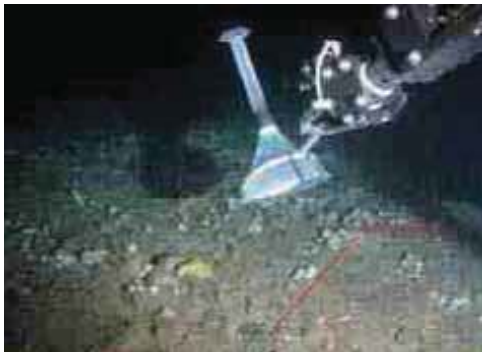

5) Picture of A2-C6-S5

Fig 4.8.15: Bubble catcher deployments at bubble streams.

Table 4.8.3: Results of the bubble catcher measurements.

Stream	UTC time	Volume (mL)	Time period (s)	Flow rate (mL/s)
A2-C3-S1	11:43:41	30	-	
quantification 1	11:44:01	40	20	0.5
	11:44:23	50	22	0.455
A2-C3-S1	11:47:39	10	-	
quantification 2	11:48:02	20	23	0.435
	11:48:24	30	22	0.455
	11:48:45	40	21	0.476
A2-C4-S1	12:37:52	10	-	
	12:40:16	20	144	0.069
	12:42:48	30	152	0.0658
	12:45:32	40	164	0.0610
	12:47:49	50	137	0.0730
A2-C6-S1	14:04:57	10	-	
	14:05:18	20	21	0.476
	14:05:45	30	27	0.3704
	14:06:11	40	26	0.385
	14:06:34	50	23	0.435
A2-C6-S2	14:07:48	10	-	
	14:08:19	20	31	0.323
	14:08:50	30	31	0.323
	14:09:22	40	32	0.313
	14:09:52	50	30	0.333
A2-C6-S3	14:13:26	10	-	
	14:15:20	20	114	0.088
	14:16:50	30	90	0.111
	14:18:27	40	97	0.103
	14:19:59	50	92	0.109
A2-C6-S4	14:29:18	10	-	
	14:30:46	20	88	0.114
	14:31:49	30	63	0.159
	14:33:02	40	73	0.137
A2-C6-S5	14:40:34	10	-	
	14:41:05	20	31	0.323
	14:41:36	30	31	0.323
	14:42:28	40	52	0.192
	14:43:01	50	33	0.303

4.8.6 Cherokee Dive 06, Ship station #33, GeoB 16833

Area: **Area 3 (380 m flare area)**
Water depth: 383 m
Date: Thursday 30 August 2012
Start down 06:57
At bottom 07:14
From bottom 12:30
On deck 13:00
Bottom time ca. 5 hours
Location ROV goes down: **78°37'247 N 09°24'591 E**

Responsible scientist: Jan Boelmann
Protocol:
08:30 – 11:30 Miriam Römer
11:30 – End Heiko Sahling

Instruments/tools: 2 GBS
3 Marker (5, 3, 6)
Niskin bottle
CTD
Sonar (Tritech) mounted on top of vehicle

Waypoints: Dive planning was based on EK 60 and EM 710 flare positions

Samples and measurements:

GeoB	Instrument	Time	Position	Depth / m	Comment
16833-1	Marker 5	07:36	78.620337 9.410981	381	Close to bubble streams at A3-C1-S1
16833-2	GBS 1	07:59	78.620308 9.410987	382	Filled at A3-C1-S1
16833-3	GBS 2	09:40	78.620172 9.409495	384	Filled at A3-C3-S1
16833-4	Marker 3	09:56	78.620155 9.40942	384	Close to bubble streams at A3-C3-S1
16833-5	Claw sample	11:03	78.619445 9.406541	387	Pogonophora
16833-6	Claw sample	11:23	78.619486 9.406807	386	Rock sample, maybe authigenic carbonates
16833-7	Niskin bottle	12:23	78.62015 9.409384	384	Filled within A3-C3-S1

Key results:
Several groups of flares from the ship multibeam echosounder systems (EM710) were surveyed during this dive to improve pick up method for flares. At two clusters (C1 and C3) periodically pulsing gas emissions were found within the Tritech sonar. Two streams were exemplarily documented for optical quantification. GBS were taken at both sites and a water sample has been taken at C3-S1 close to the releasing point just before the recovery of the ROV. At both clusters microbial mats and carbonates were found.

Technical description:
The general performance of the ROV was very good.

Dive description:
After reaching the seafloor the survey started with cluster one A3-C1 in the centre of the mapped area. Microbial mats were found along the edges of the cluster which consists mainly of carbonates. At the entry into cluster a single gas stream (A3-C1-S1) was found in the sonar and was also visible in cameras. The Marker #5 was placed next to the releasing point. Also video recordings have been done for optical quantification (see Fig. 4.8.18). For the on board gas quantification the gas bubble sampler 1 was taken as well as several pictures. During the sampling a second periodically pulsing weak stream was visible in the camera. After the GBS the releasing source was filmed with the two laser dots for special quantifications.

At the on-going survey there were more periodically pulsing streams found.

To quantify the size of the cluster and to see if there were differences in the surroundings the ROV flew a systematically survey around that area. Outside the cluster were no microbial mats and no carbonates found so that the cluster builds up a hard structured border. For a rough estimation the ROV was positioned in the centre of the cluster to do a 360° sonar scan. This showed between three and ten single periodically pulsing streams.

To continue the dive the ROV flew to the cluster C2 and C3 for closer observations. The seafloor did not show the same clear structures as in cluster C1. There were only a few microbial mats and carbonates. During the survey over the clusters the ROV forced some streams with large bubbles due to the pressure differences but all of them stopped after a few seconds.

For further observations and possible streams the ROV flew to the Possible Flare Position (PFP) 1 with visual contact to the seafloor. During the survey around that area were no microbial mats or carbonates found.

Due to this the ROV flew back to cluster C3 for visual quantification of the Stream A3-C3-S1. After the video recordings the marker #3 was placed and the GBS 2 was filled up. This was followed with a transit to the PFP 2 again with visible seafloor. During the transit and at the PFP 2 was nothing interesting found. Only a group of fishes followed the ROV which causes visible reflections in the sonar. To complete the survey of the mapped area the ROV flew to the PFP 3.

In direction S/SE was a large microbial mat together with tube worms visible (see C4 in map for position and figures attached). For closer analysis a sample of the tube worms were taken by the ROV and confirmed the occurrence of pogonophora (Siboglinidae, Anobturata). For a size estimation of the extent of bacterial mats/pogonophora the area was surveyed systematically.

The survey over the PFP 3 and PFP 4 showed nothing of interest, no microbial mats or carbonates so that the ROV continued the dive to the cluster C3 again where a water sample with the Niskin bottle was taken close to the release source of the stream C3-S1. Due to the weather the scientific program stopped here and the recovery of the ROV started.

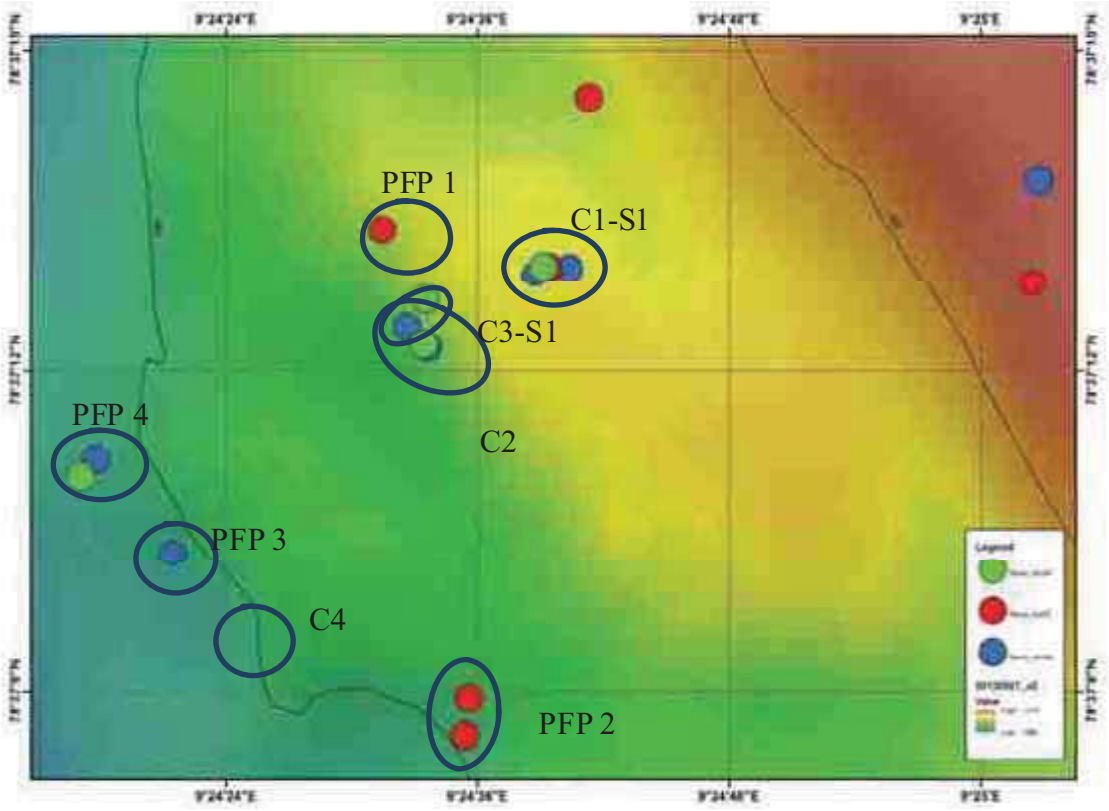

Fig. 4.8.16: Map of the dive area. Cluster A3-C1 with Marker 5 was documented first. GBS 1 was taken. The second part of the dive was performed at A3-C3 where Marker 3 was set. GBS 2 and a water sample with the Niskin bottle were taken at this site. A microbial sample was taken at the Poro field. The clusters C2/C4/C5/C6 and C7 showed no significant proof for steady streams.

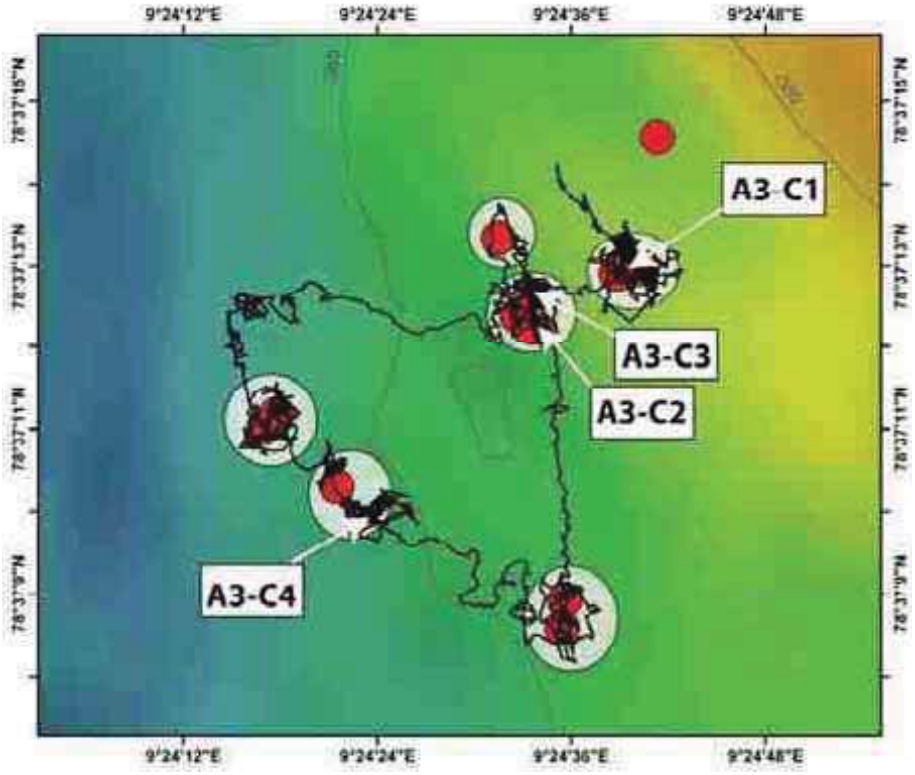

Fig. 4.8.17 Map of the dive area with the ROV path. Started in the upper North/East going to centre with a following flew to the South and flew over the western area back to centre.

Fig 4.8.18: Seafloor images taken by ROV showing microbial mats, carbonates at stream positions, marker released, GBS, and bubble recording.

4.8.7 Cherokee Dive 07, Ship station #46, GeoB 16846

Area:	**Area 3 (380 m flare area)**
Water depth:	384-388 m
Date:	Sunday 02 September 2012
Start down	12:10
At bottom	12:29
From bottom	15:16
On deck	15:45
Bottom time	ca. 3 hours

Location ROV goes down: **78°35'387 N 09°26'586 E**

Responsible scientist: Miriam Römer
Protocol:
12:00 – End Heiko Sahling

Instruments/tools: Bubble catcher (BC)
Niskin bottle
CTD
Sonar (Tritech) monted on top of vehicle

Samples and measurements:
Sonar recording (screenshot bitmaps and continued recording). Numerous photos were taken.

GeoB	Instrument	Time	Position	Depth	Comment
16846-1	Bubble catcher	13:30	78.589671 9.443781	385	A3-C5-S1
16846-2	Bubble catcher	13:38	78.589658 9.443724	385	A3-C5-S2
16846-3	Bubble catcher	13:40	78.589666 9.443778	385	A3-C5-S3
15846-4	Bubble catcher	13:46	78.589661 9.443764	385	A3-C5-S4
16846-5	Bubble catcher	14:03	78.589696 9.443397	385	A3-C6-S1
16846-6	Bubble catcher	14:17	78.589687 9.443407	385	A3-C6-S2
16846-7	Niskin bottle	15:14	78.589669 9.447185	384	Filled within A3-C7

Key results:
Three clusters with numerous but unstable gas bubble streams were found at the seafloor. Additional areas characterized by authigenic carbonates and microbial mats but lacking gas bubble emissions have been detected. Four bubble streams at A3-C5 and two at A3-C6 were quantified using the bubble catcher.

Technical description:
The general performance of the ROV was very good.

Dive description:

After reaching the seafloor, the ROV moved relatively fast and direct to the position, where the strongest flare in the hydroacoustics have been observed (red cross in Fig. 4.8.19). On the way another possible flare position (PFP) 1 was passed but no seep indication has been observed. Nevertheless, no search for the emission site was performed. The ROV passed over the cross of the centre of the strongest flare location and the first anomalies in the sonar became visible only few meters southeast of it. The area was scanned using the sonar resulting in the detection of a second cluster few meters westwards. Both clusters were documented with numerous sonar screenshots in order to quantify the amount of bubble streams and their variability. A3-C5 (the eastern cluster) and A3-C6 (the western cluster) are composed each of about 6-8 bubble streams, which show high variability. First the ROV went down closer to the seafloor at A3-C5 and the bubble streams were documented visually. The seafloor is covered by carbonates that are broken in large blocks and big cracks separate them. The bubble streams escape both, from areas above the carbonate crust and out of the cracks (Figs. 4.8.20). Especially the streams coming out of the cracks are highly variable in activity and show a pulsing character, as the gas is probably accumulated below the carbonates and released in pulses. Four streams were quantified using the bubble catcher (BC) and flux rates are between ~6 and ~40 ml/min for each bubble stream (Table 4.8.4).

The same documentation has been performed for A3-C6. The area look quite similar to A3-C5 and the bubble streams are as well very unstable and pulsing. Two streams could be quantified with the BC, the first releases bubbles in single pulses and only 3 ml/min was measured, whereas the second was measured for over a minute and released in that time very continuously about 30 ml/min.

The ROV searched in the surrounding area of the two clusters if more seep areas can be identified. Westwards of the clusters were indeed some carbonates visible but without gas bubble streams indicating transient activity of the seeps. Moving westwards to the PFP 3 we again found carbonates and microbial mats at the seafloor but lacking any gas bubble streams although this area was surveyed intensely. Finally moving to PFP 4, we found another seep site (A3-C7) with carbonates and microbial mats at the seafloor (Fig. 4.8.20) and also 3-4 sporadically active bubble streams. At the end of the dive a water sample was taken close to the bubble streams at A3-C7.

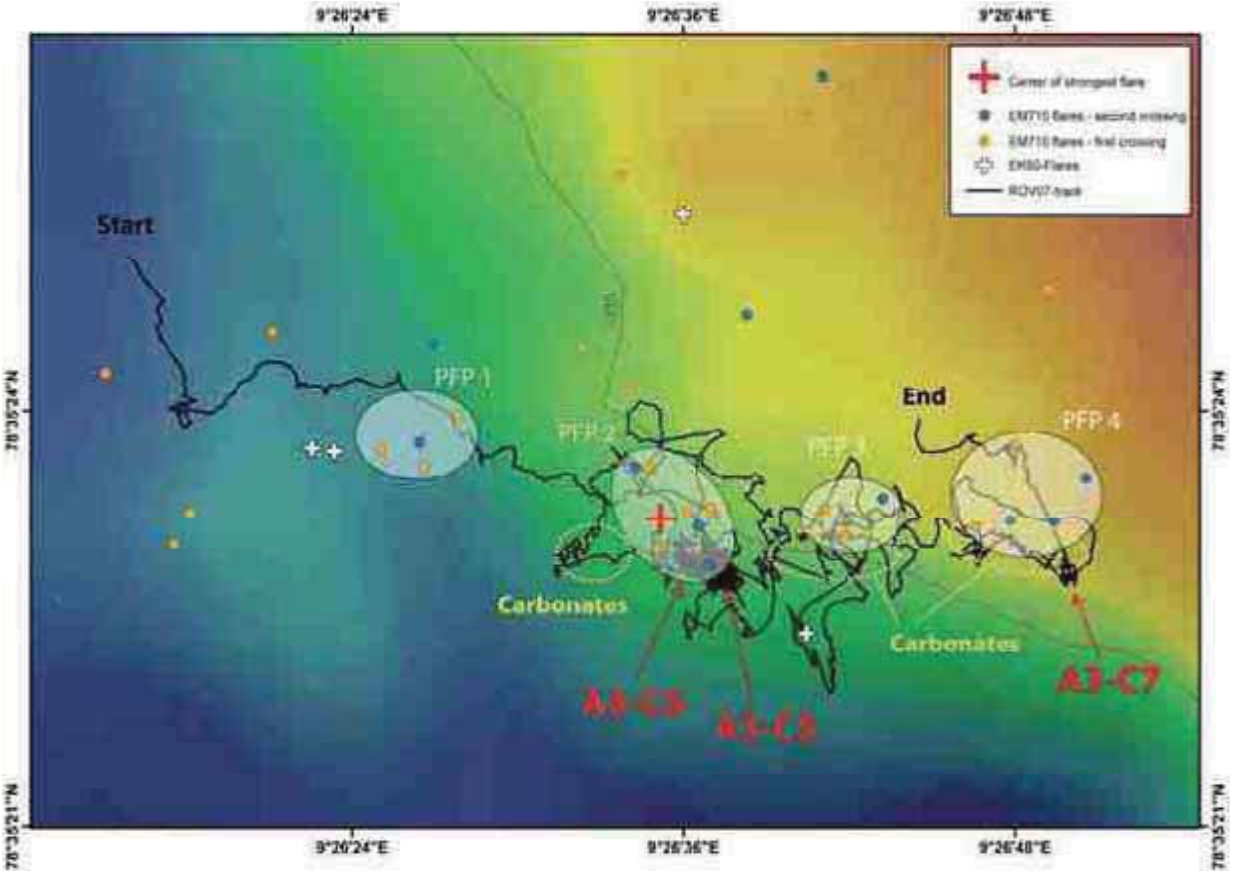

Fig. 4.8.19: Map of the area of ROV Cherokee Dive 07 (GeoB 16846). In total, four possible flare positions (PFP) were passed in order to find the gas emissions at the seafloor. PFP 1 was only marginally and fast passed, therefore we lack detailed information in that area. At PFP 2 we found two clusters with gas emissions, and at PFP 4 also one cluster. At PFP 3 seep indications in form of carbonate crusts at the seafloor have been found, but no gas emission was detected indicating inactivity during the dive time.

Table 4.8.4: Measurements with the BC to quantify single bubble streams during Dive 07 of cluster A3-C5 and A3-C6.

Bubble stream	Time	Volume (ml)	Flux (ml/min)
A3-C5-S1	13:30:18	10	
	13:31:54	20	6.25
	13:33:29	30	6.32
A3-C5-S2	13:38:20	20	
	13:38:40	30	30
	13:39:05	40	24
	13:39:20	50	40
A3-C5-S3	13:40:19	10	
	13:40:35	20	37.5
A3-C5-S4	13:45:54	10	
	13:46:06	20	50
	13:46:25	30	31.6
A3-C5-S1	14:03:03	10	
	14:06:23	20	3
A3-C5-S2	14:17:18	10	
	14:17:36	20	33.3
	14:17:55	30	31.6
	14:18:14	40	31.6
	14:18:33	50	31.6

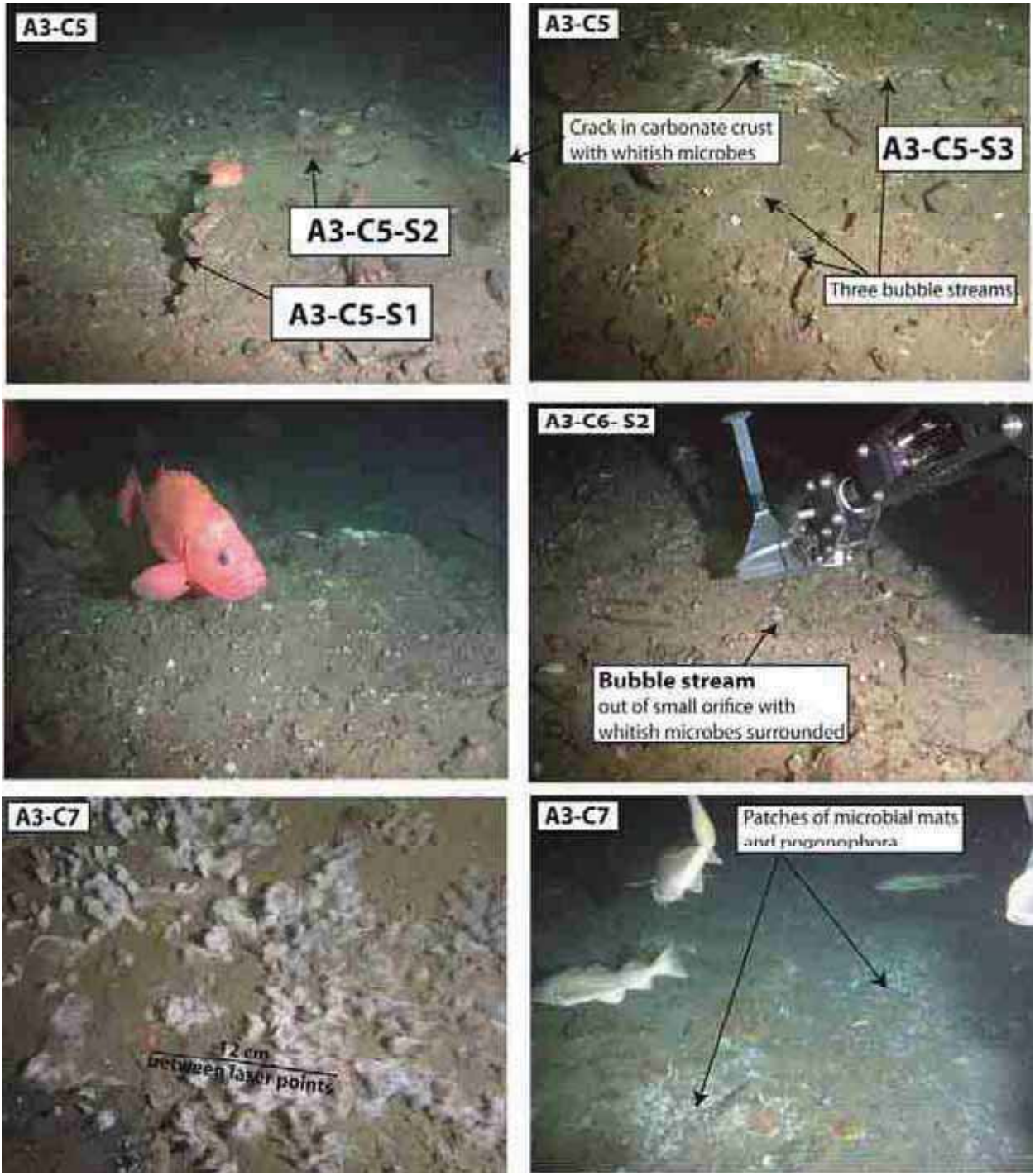

Fig. 4.8.20: Seafloor pictures taken during ROV Cherokee Dive 07 (GeoB16846).

4.8.8 Cherokee Dive 08, Ship station #48, GeoB 16848

Area: **Area 3 (380-m flare area)**
Water depth: 382-392m
Date: Sunday 2 September 2012
Start down 09:50
At bottom 10:30
From bottom 14:43
On deck 14:56
Bottom time ca. 5 hours
Location ROV goes down: **78°33.352' N 09°28.605' E**
Location ROV picked up: **78°33.520' N 09°28.250' E**

Responsible scientist: Benoît Bergès
Protocol:
08:30 – End Miriam Römer

Instruments/tools: ROV SONAR (Tritech)
Gas bubble sampler (GBS)
Video camera
Markers

Points of Interest:

WP 1	78°33.33'N	9°28.53'E	A3-C8	5 transient very weak streams spotted on SONAR + ~ 3 visually observed. Potential for more streams
WP 2	78°33.33'N	9°28.55'E	A3-C9	6 transient streams spotted on SONAR + ~ 2-3 visually observed. Weights of lander systems observed
WP 3	78°33.31'N	9°28.65'E	A3-C10	2-3 unstable streams from SONAR scan.
WP 4	78°33.30'N	9°28.57'E	A3-C11	5-6 unstable streams from SONAR scan + 1 visually observed
WP 5	78°33.34'N	9°28.43'E	A3-C12	No streams, only microbial mats. 2 markers (3 and 4) from Jago (MARIA S. MERIAN - Geomar cruise 2012)
WP 6	78°33.37'N	9°28.76'E	A3-C13	Bubble emission visually observed
WP 7	78°33.38'N	9°28.73'E	A3-C14	No streams, only microbial mats
WP 8	78°33.39'N	9°28.73'E	A3-C15	Bubble emission visually observed (~ 3 streams)
WP 9	78°33.43'N	9°28.63'E	A3-C16	Bubble emission visually observed

Samples and measurements:

GeoB	Instrument	Time	Latitude	Longitude	Depth	WP	comments
16848-1	Marker	07:42	78.555561	9.475157	387.1	1	Marker 8 C8
16848-2	GBS	08:06	78.555436	9.475971	386.7	2	GBS on different streams C9
	Video	09:08	78.554946	9.476559	388.9	4	C11-S1
16848-3	Niskin bottle	12:59	78.557261	9.477068	389.7	9	C16

Key results:
During this dive, care was given to survey clusters at area A3 where flares were localized using EK60 and EM710 (Fig. 4.8.21). To that purpose, the ROV was driven through parallel line with regular SONAR scans (Fig. 4.8.21 right). Bubble streams were found and observed visually. They mostly appeared to be very episodic and did not present regular venting spots, bubbles were emitted spatially at random over cluster site. Emissions of bubbles seemed to be linked to the presence of microbial mats and clusters were localized by investigating the seafloor. A video quantification was attempted on a localized bubble stream. One gas sampling was performed and a water sample was collected at the end of the dive. Several photos were taken during the dive.

Technical description:
SONAR: the SONAR head that is mounted on the ROV (Tritech) was used for localizing clusters and streams of bubbles. Some issues were encountered as area A3 presents mainly transient bubble streams. Streams that were observed on a SONAR scan were usually not observed on the following scan.
Gas bubble sampler: good deployment. Issue was encountered as bubble streams were very episodic and appearing at random.
ROV: Good performance. Pulled by the ship and because of the rough weather, the ROV drifted and the operators wrongly believed that the positioning system was malfunctioning.

Dive description:
The main goal of this dive was to assess precisely locations of clusters of bubble streams. An area was systematically surveyed using the same procedure during the dive: standing at ~3 from the seafloor, the ROV followed parallel lines (from line 1 to 8, Fig. 4.8.21) with the operators carefully observing SONAR scans (looking for bubble streams, Fig. 4.8.22 Image 1 and 2) and seafloor typography (looking for microbial mats, Fig. 4.8.22).

The scientific program started at 07:25 UTC and the ROV was sent toward the area that was later named A3-C8 (WP 1). Several SONAR scans were made of this area, spotting around 5 transient flares appearing episodically (Figs. 4.8.22 (1) and 4.8.22 (2)). The area was also visually investigated and three bubble streams could be observed on microbial mats (Fig. 4.8.22 (3)). Marker 8 was left on the seafloor at this location (Fig. 4.8.22 (4)). As it was very hard to define locations for the bubble streams, the arm of the ROV was used to investigate the "softness" of the seafloor (Fig. 4.8.22 (5)). It could not go deeper than few centimetres before encountering a hard layer.

At 07:52 UTC, the ROV headed South East toward WP 2 (A3-C9). Transient streams were observed both acoustically (5-6, Fig. 4.8.22 (6)) and visually (~2-3, Fig. 4.8.23 (1)). The ROV was landed near a group of bubble streams and gas sampling was attempted (GBS 2). The gas sample was sampled through different streams because of randomly vanishing bubble emissions. While finishing surveying the cluster, marks of a lander system by Geomar (Fig. 4.8.23 (3)). were found. Following line 1, cluster A3-C10 was found.

Then, the ROV followed line 2, finding A3-C11 where video quantification was attempted (Fig. 4.8.23 (4)) on two streams named A3-C11-S1 and A3-C11-S2. Continuing on line 2, no more clusters were located.

Further south west, line 3 and 4 were followed and cluster A3-C12 was found at the end of line 4 together with two markers from the Jago ROV (Figs. 4.8.23 (5) and (6)).

Then, the ROV transited and surveyed the area around line 5. No bubble clusters were found in this area. Line 6 started afterwards.

While proceeding to the survey of line 6, jumps in the location of the ROV were observed and it was decided to go towards Marker 8 to verify the positioning system is working properly. Marker 8 was found at its right location, confirming the position given by the system was proper. Then, line 6 was ended and lines 7 and 8 were surveyed. Cluster A3-C13, A3-C14 and A3-C15 were located at the end of line 8.

The survey of the line finished, it was then decided to go toward the north where many flare were spotted using the EK60 and the EM710. Cluster A3-C16 was found and surveyed deeply, showing transient bubble emissions. The water sample was taken from cluster.

The ROV was recovered at 13:02 UTC from cluster A3-C16.

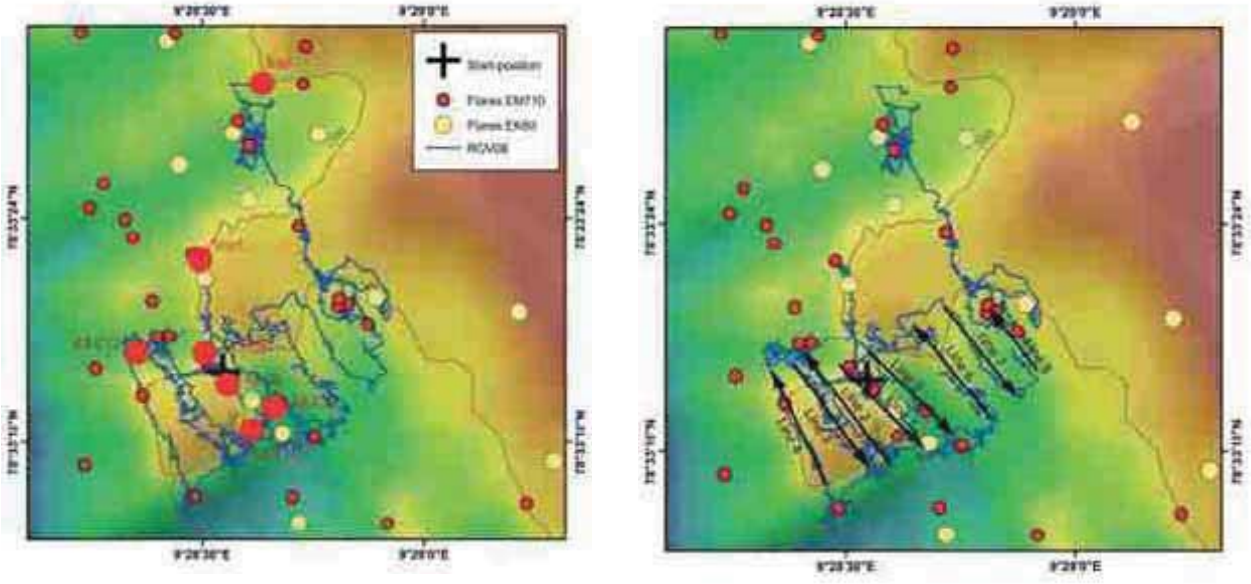

Fig. 4.8.21: (left) Map showing an overview of the dive with the ROV route and the different clusters that were localized. (right) Map showing lines that were followed by the ROV in order to proceed to a precise mapping of the area of Dive 8.

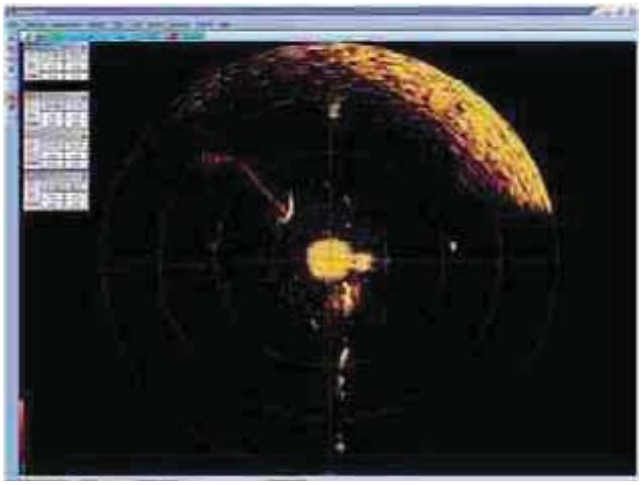

(1) SONAR image of A3-C8 showing a bubble stream appearing at port side of the ROV, 07:35:33 UTC

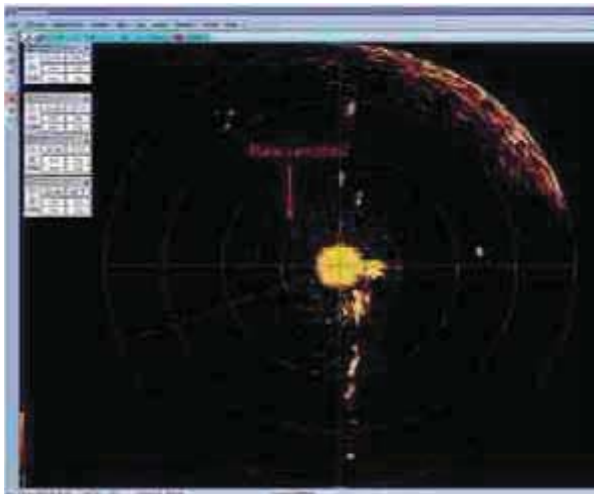

(2) SONAR image of A3-C8 showing a scan of the cluster without bubble streams that were notified, 07:35:43

(3) Picture of the seafloor of A3-C8 where bubble streams were observed

(4) Picture of the location where marker 8 was landed

(5) Picture of the ROV arm investigating the "softness" of the seafloor.

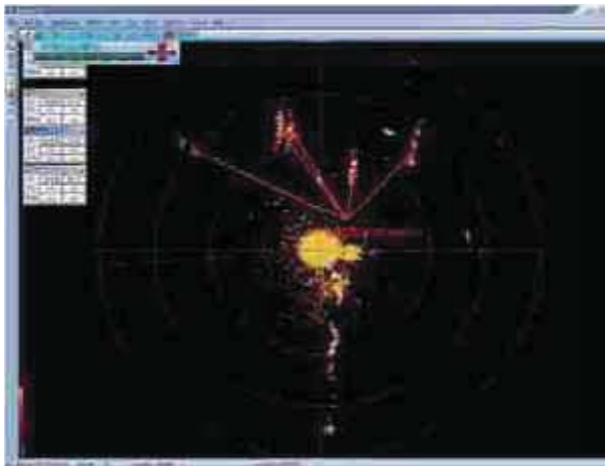

(6) SONAR image of A3-C9

Fig. 4.8.22: Seafloor images and sonar scans to describe the bubble streams.

(1) Picture of an episodic bubble stream observed at A3-C9

(2) ROV starting the gas sampling procedure from GBS 2

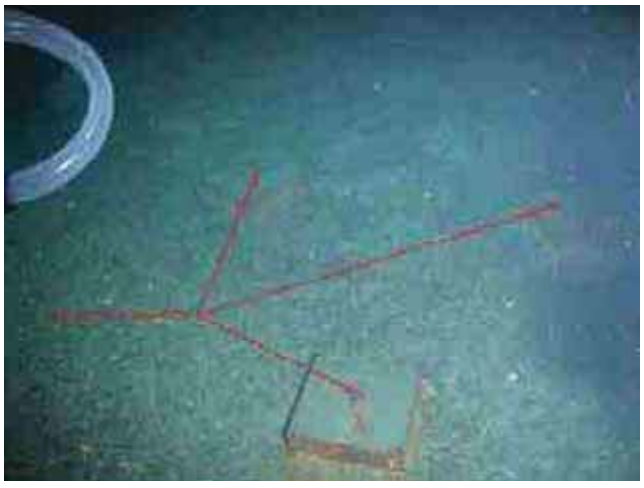

(3) Picture of the weights of a lander system (GEOMAR).

(4) Picture of A3-C11-S1 where video quantification was attempted.

(5) Picture of marker 3 and 4 from manned submersible Jago.

(6) Picture of marker 4 from manned submersible Jago.

Fig 4.8.23: Figures related to dive overview part.

4.8.9 Cherokee Dive 09, Ship station #53, GeoB 16853

Area: **Area 1 (80-m flare area)**

Water depth: 95 m
Date: Tuesday 04 September 2012
Start down: 06:50
At bottom: 06:57
From bottom: 11:58
On deck: 12:20
Bottom time: ca. 4 hours
Location ROV goes down: **78°34.450'N 10°10.040' E**

Responsible scientist: Michal Tomczyk
Protocol: Heiko Sahling

Instruments/tools: CTD
Sonar (Tritech)
Bubble catcher

Waypoints: EK60-based extent of strong flares

Samples and measurements:

GeoBr	Tool	Time	Position	Bubble stream	Description / Comment
16853-1	BC	09:50	78.574895 10.17078	A1 C5 S1	Periodic release 13.1 ml / min
16853-2	BC	09:55	78.574916 10.170812	A1C5 S2	14.0 ml / min
16853-3	BC	10:01	78.574909 10.170789	A1C5 S3	17.9 ml / min
	VQ	10:05	78.574909 10.17077	A1 C5 S3	Visual quantification
	VQ	10:18	78.574919 10.170808	A1 C5 S2	Visual quantification
16853-4	BC	10:31	78.574933 10.170848	A1 C5 S4	14.2 ml / min
16853-5	BC	10:40	78.57492 10.170842	A1 C5 S5	13.4 ml / min
16853-6	BC	10:50	78.574941 10.170897	A1 C5 S6&7	7.5 ml / min, two streams caught at the same time in funnel, both streams only cause one spot in sonar
	VQ	11.13	78.574943 10.170882	A1 C5 S8	Visual quantification, stream is steady
16853-7	BC	11:25	78.574941 10.170998	A1 C5 S8	8.1 ml / min. Stream intensity DIFFERENT from visual quantification time period before. Much less active. DO NOT USE AS INTERCALIBRATION OF METHODS.
	Sonar	11:50	78.574897 10.170967		C5 -Central
	Niskin	11:56:00	78.574917 10.170842		Closing Niskin bottle at altitude of about 2.8 m within the central strong cluster

Key results:
Defining the lateral extent of gas emission described with EK60. Mapping gas emission with the obstacle sonar Tritech. Gas bubble plumes were documented for visually based quantification. Quantification of gas flux with bubble catcher.

Technical description:
The general performance of the ROV was very good. Tritech sonar mounted on top of vehicle.

Dive description:
First of all, the walky talky that Werner lost from the ship during the deployment of the ROV was found at the seafloor again. Then, the lateral extent of gas emissions indicated from EK60 echograms was investigated using forward-looking sonar (Fig. 4.8.24). Numerous bubble streams were found forming one giant cluster that we label A1C5. This cluster consists of at least one very active central part that we call A1C5-central surrounded by numerous more dispersed bubble streams. The first action during the dive was to cross with the ROV one part (the SW sector) of the EK 60 flare location and to find out the limits of the bubble streams. At these sites we placed marker in the ROV navigation software (Posiview) labeled L1 to L7 (Table 4.8.5). For a more precise determination of these limits it is needed to go through the continuous sonar record again. Furthermore, it should be noted that we only surveyed about half of the gas emissions that are responsible for the flares in EK 60.

For a rough calculation of the area of bubble stream cluster C5, we may assume a box with a length of 60 x 60 m which results in a total area of 3600 m².

The next step was to map those flares occurring dispersed within the cluster A1 C5 using the Tritech sonar (Fig. 4.8.25 and Table 4.8.6). This survey was performed with 2 meters sonar range and a sector of 180°corresponding to 6.28 m² scanned area. The inner about 0.7 m of the sonar scan are noise from the ROV within which no bubble streams can be visualized (equivalent to 0.77 m²). As a result, about 5.5 m² of area is investigated per scan.

About 40 scans are located within bubble stream cluster C5 (corresponding to 220 m² scanned area) and a total of 74 bubble streams were counted on these. If we assume that these 40 scans are representative for the total area of 3600 m² we may roughly estimate that about 1200 bubble streams exist in cluster C5!

This is likely a maximum estimate as the cluster C5 is composed of the dispersed bubble streams in the larger area and a dense cluster of bubble streams in the center. Therefore, for a more conservative estimate we may subtract the two scans no. 26 and 27 with a total of 15 bubble streams as they were located at or close to C5-central, resulting in 59 streams in 209 m² scanned area. Extrapolating this to 3600 m² results in 1000 bubble streams in cluster C5.

The second part of the dive was to quantify gas emission with bubble catcher and get some video records for the purpose of visual quantification. This was done in the center of the cluster, where the highest intensity of gas emission was spotted. Most of observed bubble plumes were transient. Values are given in Table 4.8.7. On average, about 12 ml gas is emitted per minute per stream. Assuming that 1000 to 1200 bubble streams occur at C5 this would correspond to a flux of 12 to 14 liter / minute at 90 m water depth.

The third part of the dive was to use the sonar for scanning of the central part of the cluster with many bubble streams. The position is shown in the map; one sonar scan is shown in Fig. 4.8.26. At least 20 to 30 if not more bubble streams exist at C5-central. Also the visual appearance of so many bubble streams in one small area was impressive for us, the main flux of bubbles seem to be accounted by the scattered bubble streams estimated to 1000 – 1200 in the total area of C5 rather than the few tens of bubble streams in C5-central.

Towards the end of the dive the Niskin bottle was closed while flying at 2.8 m altitude with the ROV over C5-central.

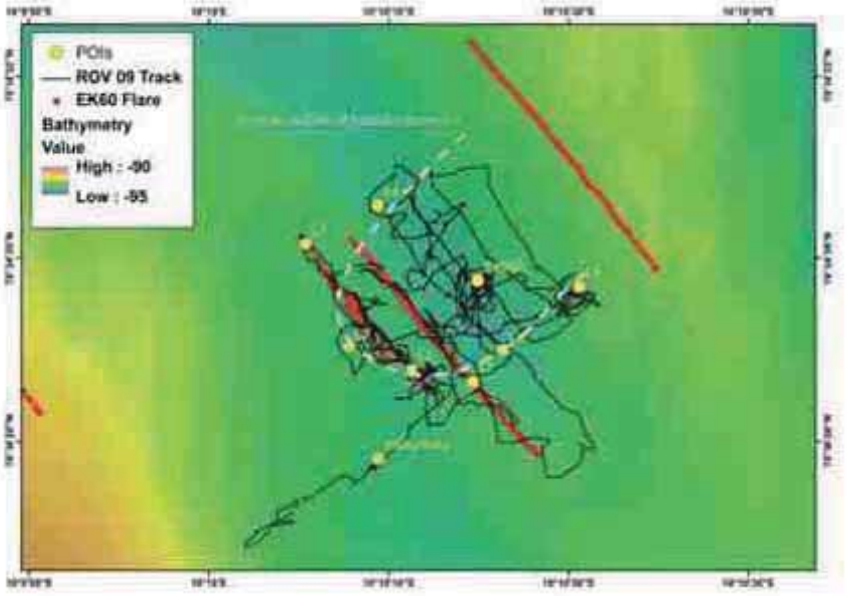

Fig. 4.8.24: Map of the Dive 09 area. Red dots represent flares mapped with EK60. Marker L1 to L7 were set during the dive in the navigation program Posiview and indicate the approximate extent of the bubble cluster C5; the SW sector, as the cluster very likely continuous to the NE.

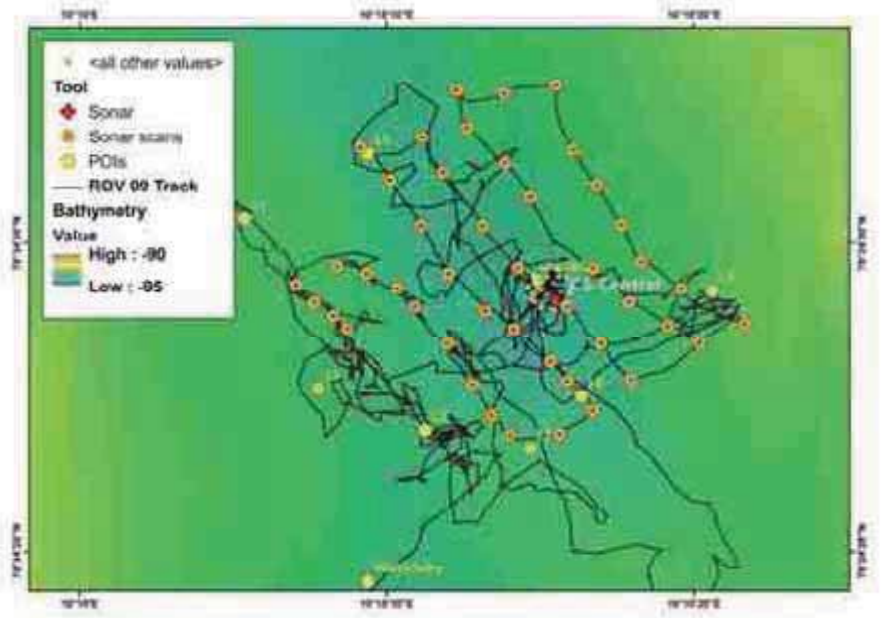

Fig. 4.8.25: Detailed map of the track of Dive 09 with the position of sonar scans. The positions of systematic scans within the larger area of C5 with more dispersed bubble streams are marked in orange, the central most dense cluster of bubble streams as shown in Fig. 4.8.26 is marked by a red cross and signified as C5-Central.

Table 4.8.5: Points of interest set during the ROV Dive 09 in the navigation program Posiview. Labels L1 to L7 were set approximately at the boundary between no bubble streams and bubble streams of cluster A1 C5.

Label	Lat / N	Long / E
L1	78.575044	10.168159
L2	78.574659	10.169795
L3	78.574732	10.168823
L4	78.574915	10.17239
L5	78.575159	10.169273
L6	78.57472	10.171205
L7	78.574626	10.170743
WalkyTalky	78.57439	10.169275
3xGBC	78.574933	10.170816

Table 4.8.6: Sonar scans conducted within the cluster A1 C5. Sonar settings were: scanning mode ultra, 675 kHz, contrast 22 dB, gain 19, range 2m, 180 °, 343° dirn.

Scan number	Time (UTC)	Latitude	Longitude	Number of bubble streams
1	08:45	78.574847	10.169085	
2	08:53:09	78.57487	10.168959	0
3	08:54:36	78.574894	10.168788	7
4	08:56:23	78.574925	10.168624	0
5	08:57:56	78.574959	10.168998	2
6	08:59:05	78.574946	10.169261	0
7	09:00:35	78.57492	10.169539	11
8	09:01:48	78.574887	10.169697	7
9	09:02:58	78.574812	10.169993	4
10	09:04:11	78.57474	10.170217	0
11	09:05:07	78.574684	10.170396	0
12	09:06:37	78.57465	10.170559	0
13	09:08:05	78.574652	10.171005	0
14	09:09:14	78.574693	10.171309	0
15	09:09:59	78.574747	10.17108	0
16	09:10:50	78.574781	10.170928	0
17	09:11:40	78.574846	10.170597	0
18	09:13:43	78.574879	10.170336	0
19	09:16:03	78.574945	10.170002	0
20	09:16:55	78.575031	10.169751	2
21	09:17:50	78.575112	10.169471	0
22	09:19:00	78.575169	10.169209	0
23	09:20:12	78.575187	10.169766	0
24	09:21:24	78.575126	10.169956	0
25	09:22:17	78.575031	10.170314	2
26	09:23:23	78.574956	10.170629	6
27	09:24:04	78.574887	10.171076	9
28	09:24:58	78.574812	10.17138	7
29	09:25:52	78.574749	10.171655	0
30	09:28:50	78.574814	10.172274	0
31	09:29:43	78.574852	10.17199	1
32	09:30:37	78.574894	10.171638	5
33	09:31:31	78.574955	10.171313	0
34	09:32:24	78.575002	78.575002	6
35	09:33:54	78.575081	10.170746	5
36	09:34:48	78.575142	10.170514	3
37	09:35:59	78.575204	10.170171	0
38	09:36:53	78.575271	10.170081	0
39	09:37:47	78.575265	10.170509	3
40	09:38:40	78.575281	10.170977	0
41	09:39:52	78.575165	10.171129	0

42	09:40:49	78.575102	10.171347	0
43	09:41:39	78.575033	10.171568	0
44	09:42:32	78.574966	10.171746	3
45	09:43:26	78.574919	10.172107	0
46	09:44:38	78.574857	10.172687	0

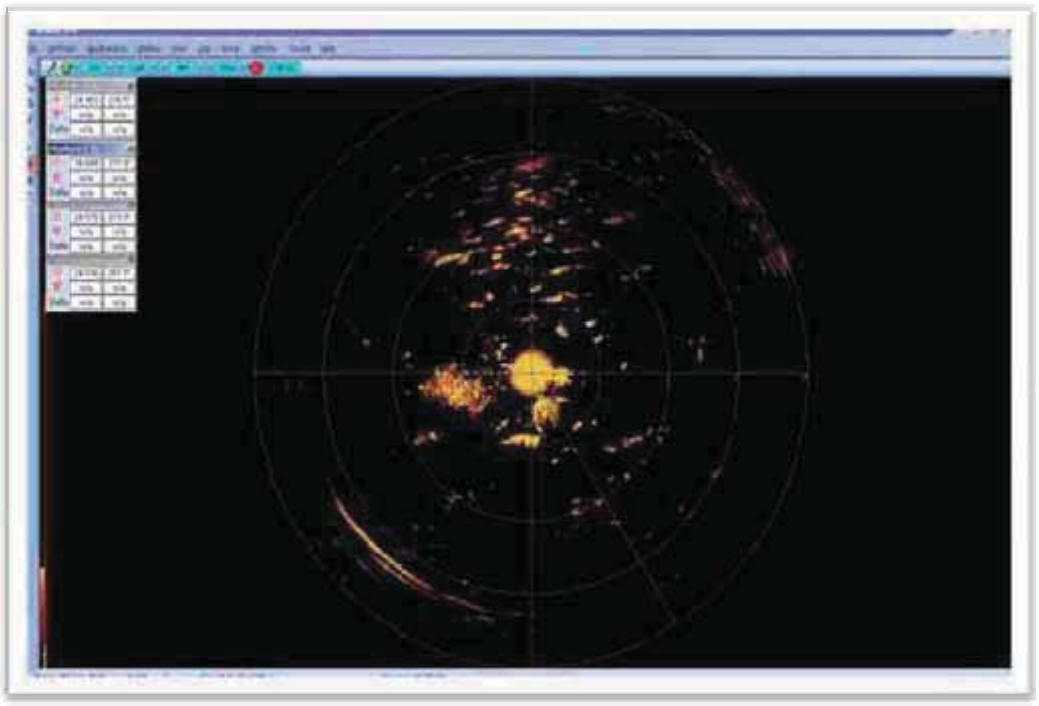

Fig. 4.8.26: Screen-shot from sonar control software shows high density of gas bubble plumes in the centre of selected area.

Fig 4.8.27: Seafloor image showing the quantification of one bubble stream using bubble catcher. White patches at the seafloor are bacterial mats. Course-grained material can be observed.

Table 4.8.7: Bubble catcher quantification.

	UTC time	Volume (mL)	Time period (s)	Flow rate (mL/s)
A1-C5-S2	09:57:45	10	-	
	09:58:25	20	40	0.25
	09:59:09	30	44	0.227
	09:59:54	40	45	0.222
	10:00:37	50	43	0.236
		40 ml in 172 s → 14 ml in 60 s	μ = 43	
A1-C5-S3	10:01:25	10	-	
	10:02:03	20	38	0.263
	10:02:35	30	32	0.313
	10:03:07	40	32	0.313
	10:03:39	50	32	0.313
		40 ml in 134 s → 17.9 ml in 60 s	μ = 33.5	
A1-C5S4	10:33:12	10	-	
	10:33:51	20	39	0.256
	10:34:55	30	64	0.156
	10:35:36	40	41	0.244
	10:36:01	50	25	0.4
		40 ml in 169 s → 14.2 ml in 60 s	μ = 42.25	
A1-C5-S5	10:40:51	10	-	
	10:41:38	20	47	0.213
	10:42:30	30	52	0.192
	10:43:00	40	30	0.333
	10:43:50	50	50	0.2
		40 ml in 179 s → 13.4 ml in 60 s	μ = 44.75	
A1-C5-S6+7	10:51:52	10	-	
	10:52:53	20	61	0.164
	10:54:26	30	93	0.108
	10:55:45	40	79	0.127
	10:57:10	50	85	0.118
		40 ml in 318 s → 7.5 ml in 60 s	μ = 79.5	
A1-C5-S8	11:26:00	10	-	
	11:27:14	20	74	0.135
	11:28:45	30	91	0.110
	11:29:53	40	68	0.147
	11:30:57	50	64	0.156
		40 ml in 297 s → 8.1 ml in 60 s	μ = 74.25	

4.9 Bubble Stream Analyses

(Miriam Römer)

This chapter aims at an integrated view on bubble streams in the different areas.

Area 1

Area 1 is the shallowest study area and located on the shelf at around 80-100 m water depth. Numerous flares were recorded during hydroacoustic surveys with EK60 and EM710. Most flares are located along the rim of the morphological high (Fig. 4.9.1). In some areas a high amount of flares in a small area cluster close together, forming highly intense anomalies in the echograms. One of these very intense flare areas was investigated during the first three ROV dives (Fig. 4.9.2). Several tens of flares were observed in EM710 within the selected dive area and at four of them, the source of gas emission could be found at the seafloor. The results obtained at the bubble streams are detailed below.

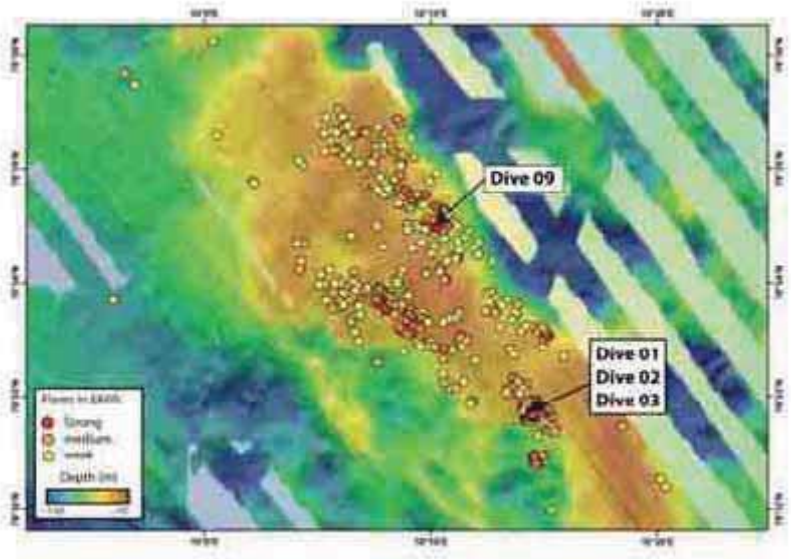

Fig. 4.9.1: Location of dives in Area 1 and flares detected by EK 60.

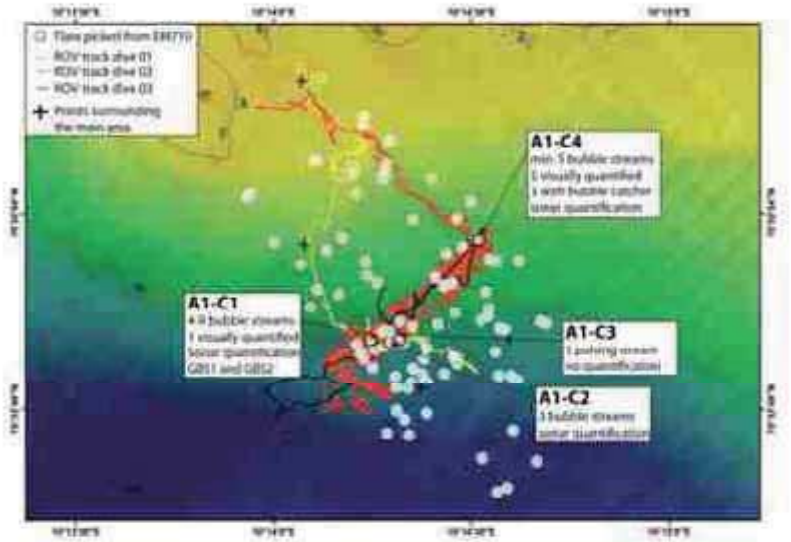

Fig. 4.9.2: Dive 01, 02, 03 and the location of cluster A1-C1 to A1-C4.

Table 4.9.1: Summary of observations and measurements at cluster A1-C1 to C4.

Cluster	Amount of streams	Stream	Variability	Visual quantification (ml/min)	Sonar quantification (ml/min)	Bubble catcher quantification (ml/min)	Sample
A1-C1	4-9	A1-C1-S1	stable		4.28		GBS1
		A1-C1-S2	stable	20.4	18.36		GBS2
		A1-C1-S3	stable		18.03		
		A1-C1-S4	stable		17.30		
	Total				**58**		
A1-C2	3	A1-C2-S1	stable		24.59		
		A1-C2-S2	stable		37.92		
		A1-C2-S3	stable		13.40		
	Total				**75.9**		
A1-C3	1		pulsing				
A1-C4	min. 5						
		A1-C4-S1	stable	21.6	21.81		
		A1-C4-S2	stable		43.71		
		A1-C4-S3	stable		54.68		
		A1-C4-S4	stable	18.3	36.74		
		A1-C4-S5	stable		39.52		
	Total				**196.4**		
A1-C4b	>7	A1-C4b-S1	stable		100.77		
		A1-C4b-S2	stable				
		A1-C4b-S3	stable				
		A1-C4b-S4	stable		73.72	70.0	
		A1-C4b-S5	stable				
		A1-C4b-S6	stable	21.4	33.09	20.0	
		A1-C4b-S7	stable		35.06	38.0	
		A1-C4b-S8	stable		7.47	10.0	
		A1-C4b-S9	pulsing		14.12		
	Total				**264.3**		

The cluster A1-C1 consisted of at least four bubble streams as revealed by sonar (Fig. 4.9.3). Quantification of the streams by sonar was possible (Tab. 4.9.1). Only two out of the four streams were visually documented in addition (Fig. 4.9.4). The cluster A1-C2 was only documented by sonar (Fig. 4.9.5). Only a transient bubble stream was visible in the sonar at cluster A1-C3 and no quantification was undertaken. Cluster A1-C4 again was documented and quantified using sonar (Fig. 4.9.6) and selected streams were quantified visually (Tab. 4.9.1). While these observations at A1-C4 were conducted during ROV dive 02 the same cluster was revisited during ROV dive 03. But the number of streams and the configuration were different from the dive before, therefore, we termed the cluster A1-C4b to stress that there are differences (Fig. 4.9.7).

Fig. 4.9.3: Cluster A1-C1. At least 4 bubble streams were observed with the sonar, sometimes few more transient streams appeared. All four bubble streams were quantified and emit between 4 and 18 ml/min. In total, all four streams emit ~58 ml/min.

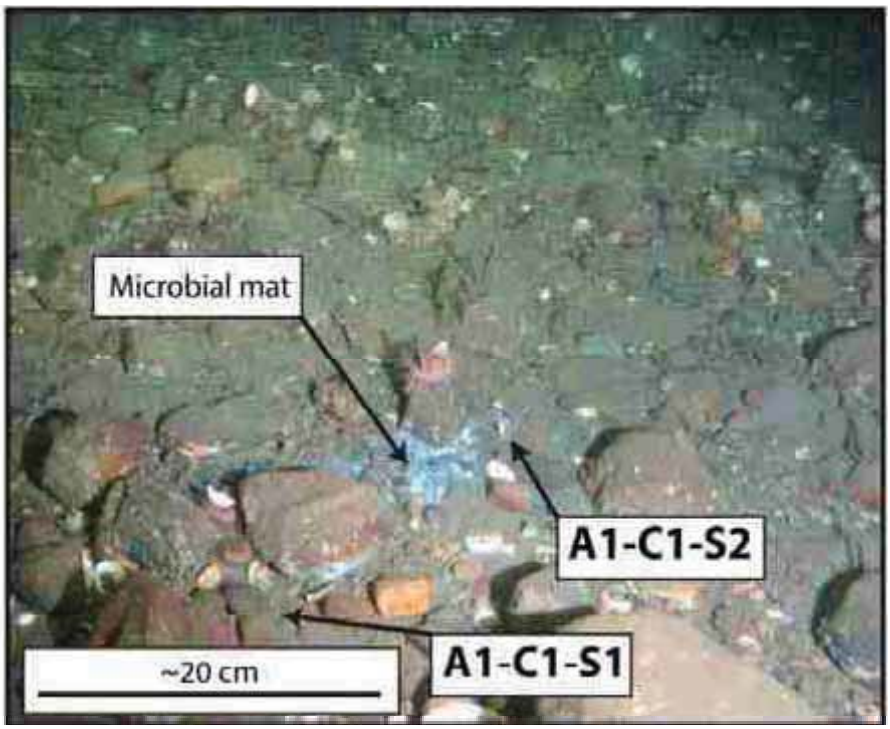

Fig. 4.9.4: A1-C1-S1 and A1-C1-S2 were documented visually. They are located at the rim of a microbial mat with a distance of about 20 cm to each other. A1-C-S2 was quantified visually and the result of 20.4 ml/min is very close to the result by sonar quantification (18.4 ml/min), confirming that the methods are reliable. The gas sample taken at A1-C1-S1 and A1-C1-S2 show both that methane is of biogenic (microbial sourced) methane.

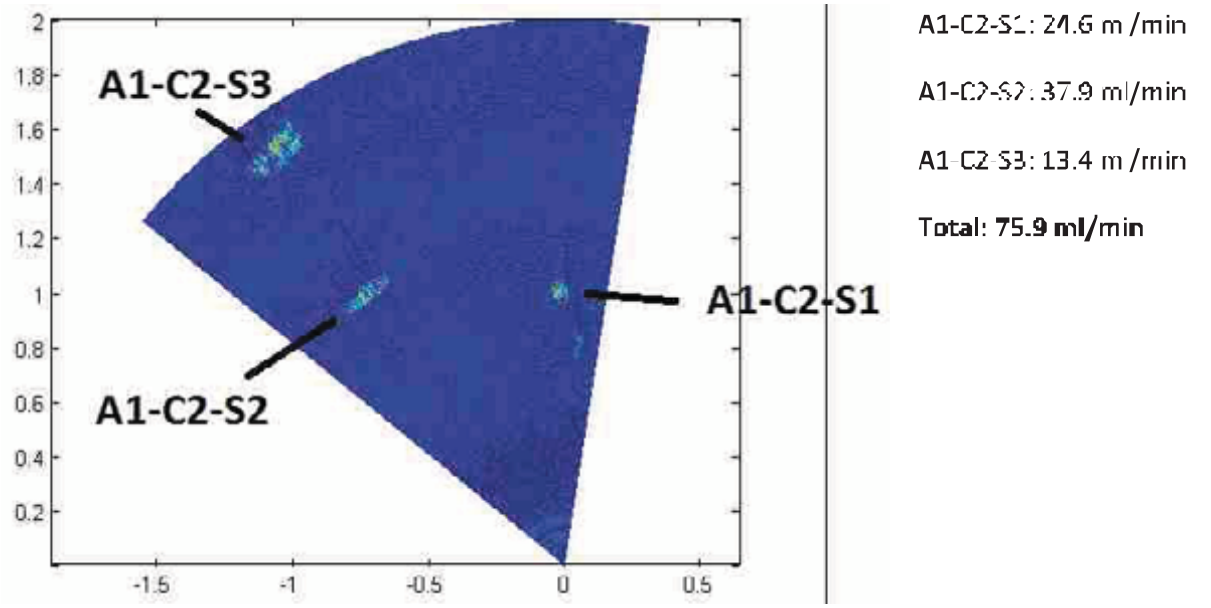

Fig. 4.9.5: Cluster A1-C2. Three bubble streams were detected and all three could be quantified using the sonar. Unfortunately the video recording failed when documenting this cluster and no visual quantification is possible.

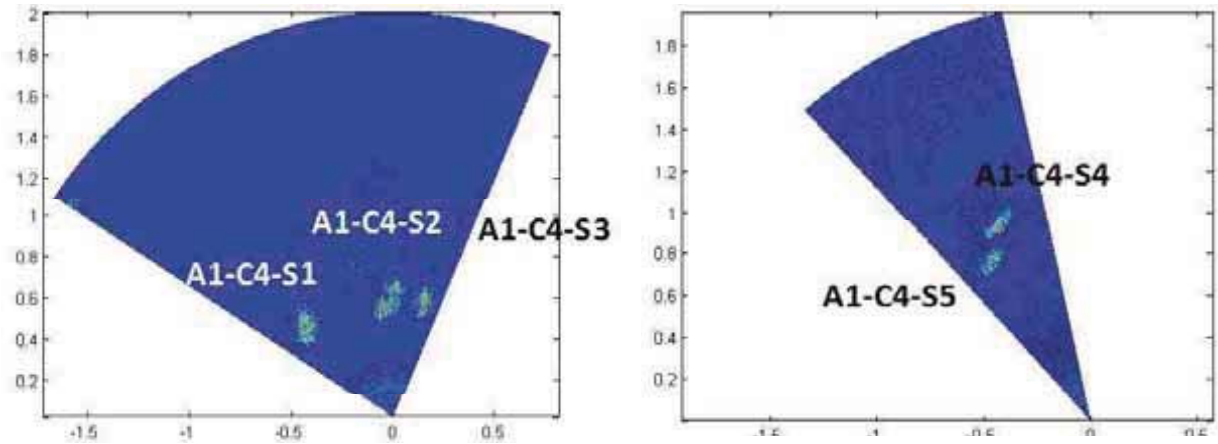

Fig. 4.9.6: Cluster A1-C4. At least 5 bubble streams were visible in the sonar during ROV dive 02. Three bubble streams close together became first visible and after turning the ROV a bit around two other were detected. All 5 were quantified with the sonar and A1-C4-S1, A1-C4-S4 and A1-C4-S5 also visually. All 5 together emit about 196.4 ml/min.

Fig. 4.9.7: During ROV Dive 03 the sonar scanning led to a slightly different amount of streams and at least 7 single streams were recorded and quantified. The total amount is 264.3 ml/min. 5 of the streams were additionally quantified using the bubble catcher resulting very similar amounts for single streams, which confirm again the reliability of the sonar quantification.
Either the cluster was not entirely mapped and bubble streams were missed for quantification or the amount of gas bubble streams and also the methane flux changed between the two dives with a difference of one day.

Summary A1-C1 to A1-C4

All together about 330 – 400 ml/min were emitted through the three quantified clusters. Each cluster emits between 58 and 265 ml/min, each corresponding to a flare visible in EM710. Assuming, over 100 flares emit each approximately the same amount of gas, ~33-40 L/min escape in an area of about 60000 m^2.

Systematic sonar mapping of bubble streams show that in an area of ~9000 m^2 a total amount of 227 streams escape (see Dive 3 and Chapter 4.11). If the streams emit all between 4 and 50 ml/min, in the mapped area an amount of 0.9-11 L/min escapes and for the entire area of intense flares (60000 m^2) the amount would be extrapolated to 6-76 L/min.

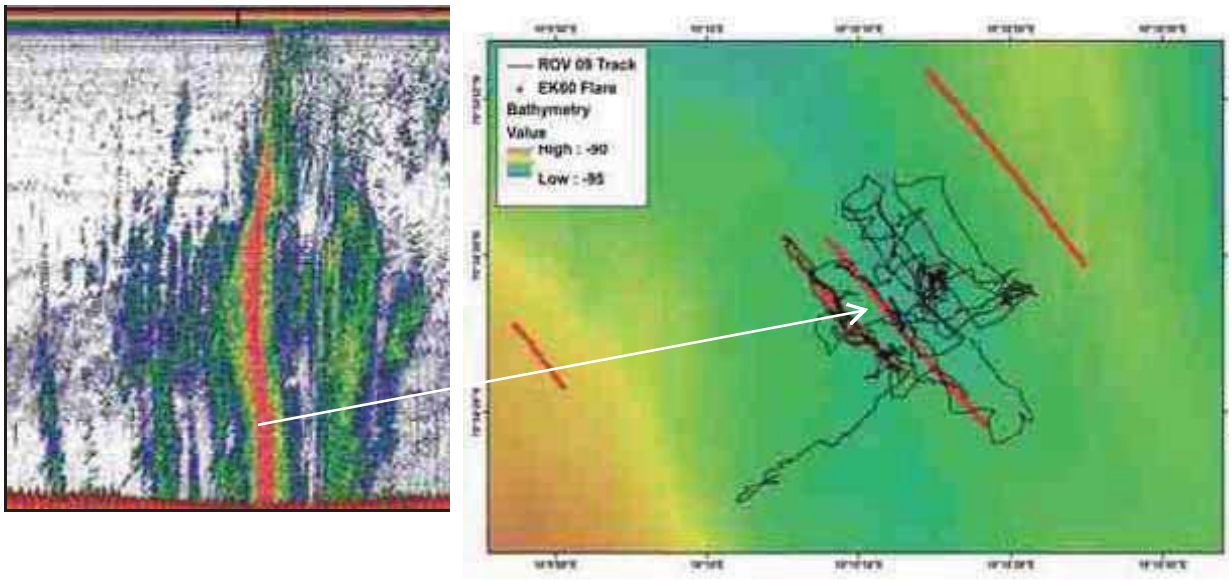

Fig. 4.9.8: Cluster A1-C5: Dive 09 was located in another very intense flare cluster in the northern part of Area 1 (Fig. 4.9.1). In the echogram of the EK60 the flare appears to be one of the most intensive ones detected in Area 1 and also reaching the sea surface (left). ROV Dive 09 was located exactly in the center of the strongest flare visible in the echogram (right).

Area 2

Numerous flares were detected in Area 2 (around 230 – 280 m water depth) using EK60 and EM710 and a specific region was chosen for ROV dives where a high amount of flares have been located close together. Two ROV dives have been performed in that area (Dive 04 and Dive 05, Fig. 4.9.9).

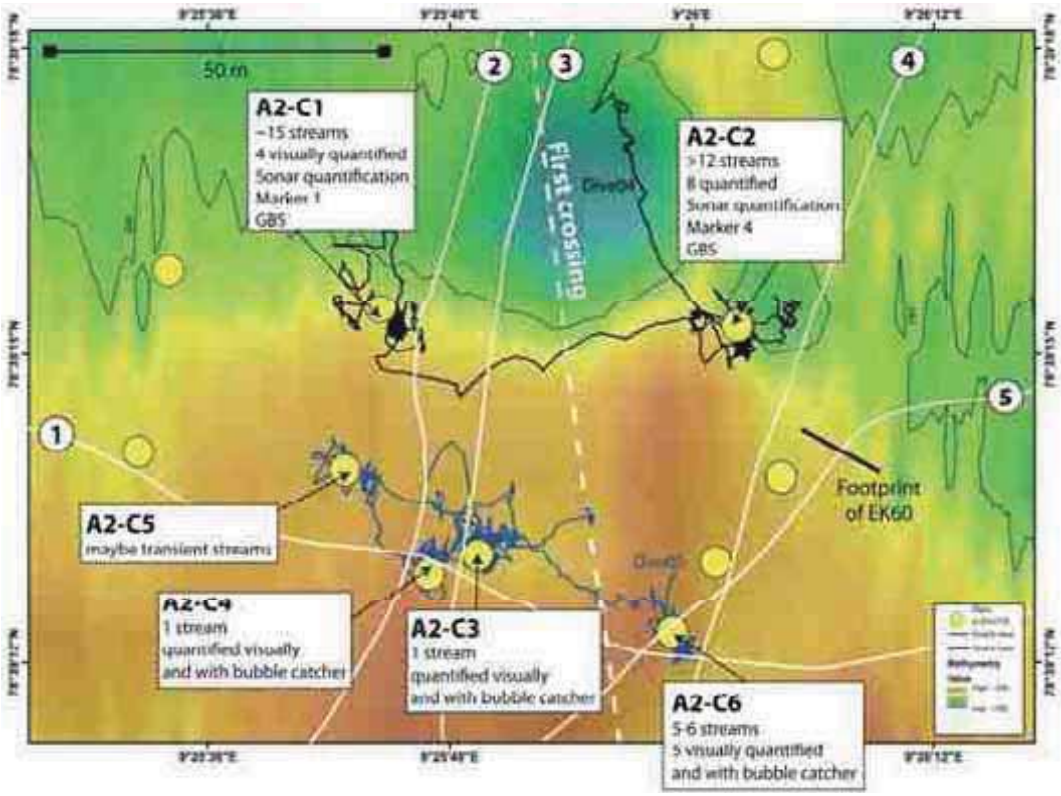

Fig. 4.9.9: Compilation map of the area investigated in Area 2.

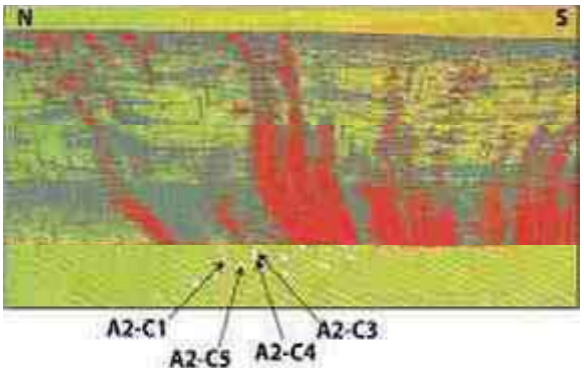

Fig. 4.9.10: The EK60 echogram shows intense flares, but those clusters found on the seafloor are not in the footprint range of the echosounder and are not visible.

As the flares are not close enough to the ship track, these flares where only very weak visible in the echogram of EK60 (footprint ~12% of the water depth = ~27m). South of the dive area, flares were crossed more exactly and appear much stronger in the echogramm (Fig. 4.9.10).

In order to be able to quantify the bubble stream clusters found during the ROV dives, a small survey was performed after Dive 05 and in total 5 lines cross the area in different directions (white lines numbered 1 – 5 in Fig. 4.9.9). The resulting echograms are shown in

Fig. 4.9.11, together with indications which flare is probably the corresponding cluster found at the seafloor.

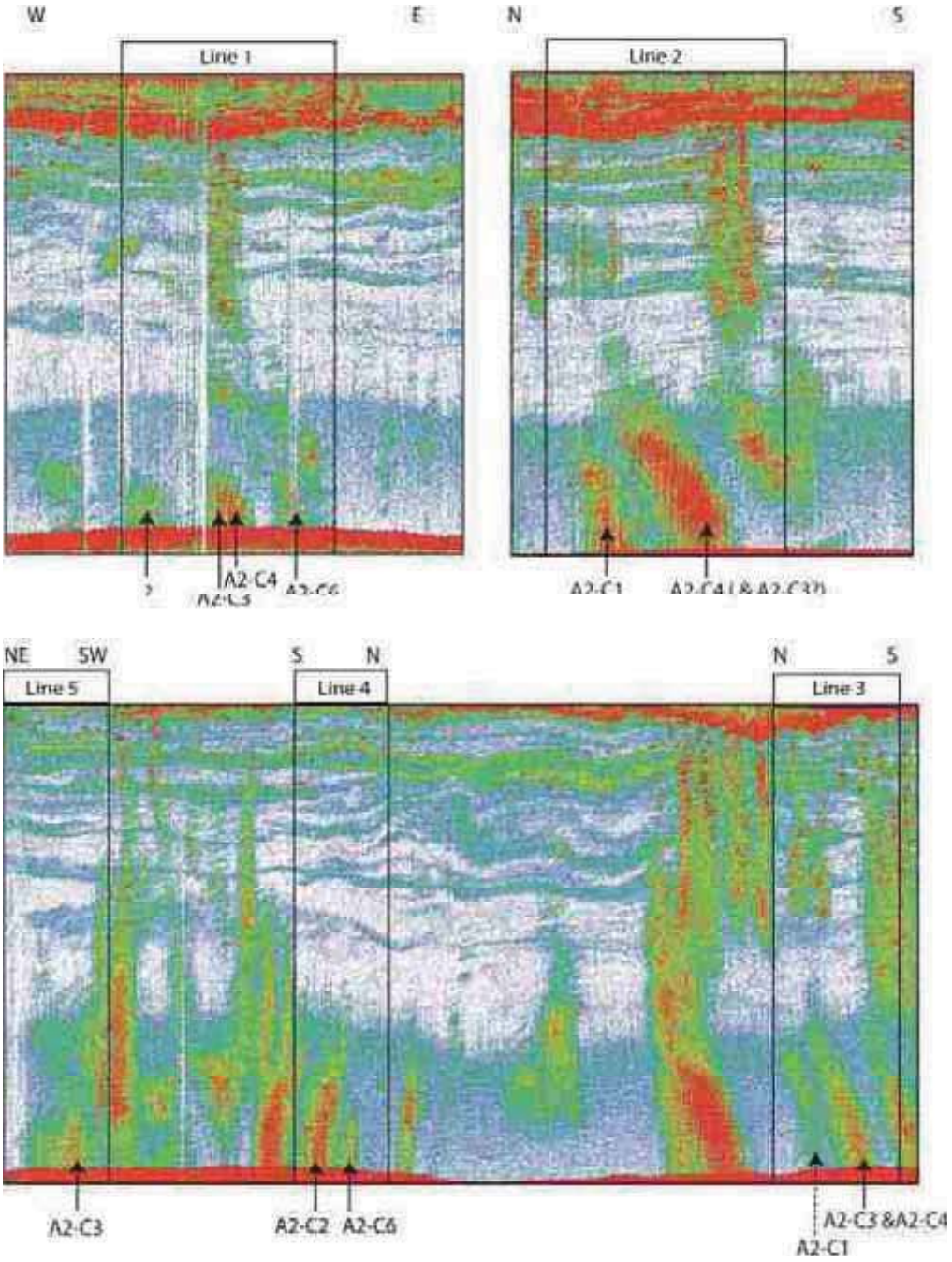

Fig. 4.9.11: All echograms of EK60 of the survey conducted after the dives to cross the clusters found at the seafloor. The corresponding clusters probably causing the flares are indicated with the arrows.

A very rough and preliminary classification of flares in EM710 in weak and strong was done and seafloor observations at each corresponding cluster indicates, that weak flares indeed are composed only of one bubble stream whereas strong flares are produced by more bubble streams.

Table 4.9.2: List of all clusters with the information of each bubble stream documented at the seafloor during ROV Dives 04 and 05.

Cluster	Number of bubble streams	Stream	Variability	Visual quantification	Sonar quantification	Bubble catcher quantification	EK60	EM710	Intensity
A2-C1							Line 2(&3)	Flare-A2-C1	strong
	~15	A2-C1-S1	stable	dive04: 17	dive04				
		A2-C1-S2	stable	dive04: 9.9	dive04				
		A2-C1-S3	stable	-	dive04				
		A2-C1-S4	stable	dive04: 23	dive04				
		Total		**49.9 * 5 = 250**					
A2-C2							Line 4	Flare -A2-C2, maybe only a part	strong
	>12	A2-C2-S1	stable	dive04: 21.7	dive04				
		A2-C2-S2	stable	dive04: 13	dive04				
		A2-C2-S3	stable	-	dive04				
		A2-C2-S4	stable	dive04: 8.5	dive04				
		A2-C2-S5	stable	dive04: 6.6	dive04				
		A2-C2-S6	stable	dive04: 20.5	dive04				
		A2-C2-S7	stable		dive04				
		A2-C2-S8	pulsing	dive04					
		Total		**70.3 * 2 = 140**					
A2-C3	1 (+1 transient seen in sonar)	A2-C3-S1		dive05: 26.5		dive05: 27.9	Lines 1,3 and 5	Flare-A2-C3	weak
A2-C4	1	A2-C4-S1		dive05: 5.2		dive05: 4.0	Lines 1,2 and 3	Flare-A2-C4	weak
A2-C5	0 (maybe transient)						Line 1	Flare-A2-C5	weak
A2-C6	5-6						Lines 1 and 4	Flare-A2-C6	strong
		A2-C6-S1	stable			dive05: 25.0			
		A2-C6-S2	stable			dive05: 19.4			
		A2-C6-S3	stable			dive05: 6.2			
		A2-C6-S4	pulsing			dive05: 8.2			
		A2-C6-S5	pulsing			dive05: 17.1			
		(A2-C6-S6)	transient in sonar						
		Total				**75.9**			

Cluster A2-C4 is characterized as a weak flare in EM710 and only one bubble stream could be found at the seafloor. This bubble stream (A2-C4-S1) was quantified using the bubble catcher, resulting a volume flux of 4 ml/min. In contrast, A2-C6 was characterized as a strong flare in EM710 and a cluster of 5 (maybe one more with transient character) bubble streams have been found and quantified with the bubble catcher. Each stream had a volume

flux between 6.2 and 25 ml/min and all together about 76 ml/min. All quantified clusters together emit ~500 ml/min (when extrapolating the streams quantified with the entire amount of streams visible in the sonar).

4.10 Visual Bubble Quantification

(Jan Boelmann)

All measured streams are listed in the following Table 4.10.1. Shown in the table are the stream names, starting time of recording in UTC, diameter distribution in mm, rising speed in mm/s, flux of each stream (ml/min) and the number of bubbles per minute. Also listed is the number of bubbles measured out for calculation. For the bubble count there were at least 400 frames counted.

Table 4.10.1 Results of visual quantification.

Stream	Time	Diameter distribution			Rising speed			Flux	Bubble Number	N
	[UTC]	[mm]	±	[mm]	[mm]	±	[mm]	[ml/min]	[B/min]	
A1-C1-S2	09:13	4.2	±	0.6	262	±	32	20.4	2965	753
A1-C4-S1	14:15	2.72	±	0.24	379	±	35	31.6	3000	25
A1-C4-S2		tbd								
A1-C4-S3		tbd								
A1-C4-S4	15:25	3.9	±	1.0	256	±	61	18.3	2410	1949
A1-C4-S5										
A1-C4b-S4/S5	08:13	3.6	±	0.9	317	±	81	25.8	3279	15302
A1-C4b-S1/S2/S3	09:05	2.27	±	0.34	387	±	34	23.7	4230	40
A1-C4b-S6	10:10	3.71	±	0.5	336	±	31	21.4	1785	30
A1-C4b-S7										
A2-C1-S1	10:08	2.4	±	0.4	261	±	26	17.1	2595	35
A2-C1-S2		1.8	±	0.3	253	±	28	9.9	2220	40
A2-C1-S4	10:20	3.1	±	0.6	285	±	44	23	1635	25
A2-C2-S1	12:00	2.2	±	0.4	395	±	53	21.7	3615	60
A2-C2-S2		2.1	±	0.3	404	±	61	13	2325	40
A2-C2-S4	12:24	2.6	±	0.3	372	±	37	8.5	930	20
A2-C2-S5	12:30	1.9	±	0.3	295	±	20	6.6	1515	30
A2-C2-S6	12:34	2.0	±	0.3	278	±	39	20.5	5085	70
A2-C2-S7										
A2-C3-S1	11:52	3.6	±	0.4	264	±	28	26.5	1185	25
A2-C4-S1	12:54	2.5	±	0.3	303	±	33	5.2	288	20
A3-C1-S1	07:29	3.8	±	0.9	263	±	53	9.4	208	40
A3-C3-S1	10:00	4.3	±	1.1	304	±	35	6.7	172	25
A1-C5-S3	10:07	tbd								
A1-C5-S2	10:19	tbd								
A1-C5-S8	11:14	tbd								

Except the streams A1-C1-S2, A1-C4-S5 and A1-C4b-S4/S5 were all streams manually counted and measured, these three were automatically counted and measured due to the good video and distribution conditions, which explains the higher number of bubbles counted. Also the number of frames used for counting is at least 7500 which correspond to five minutes.

Fig. 4.10.1 shows the rising speed over the diameter. Visible is that all streams are in a range from 1.5 mm to 4.5 mm diameter and between a rising speed of 253 mm/s and 404 mm/s. The different areas are divided into different colors for a better visibility. The area one and two are spread over the mentioned range in diameter and rising speed. The two data points of area three are close together in the upper diameter and in the lower rising speed scale. For a closer look of the distribution of area three the last streams need to be measured.

Fig. 4.10.2 shows the flux over diameter. As you can see the overall flux is spread over a rate between 5 and 35 ml/min. The first area is distributed in the upper half whereas the second area is spread over the complete scale. The area three lies in the lower quarter.

Fig. 4.10.3 shows the flux over the rising speed. The first area lies in the upper half whereas the second is spread over the whole scale. The third area lies in the lower quarter.

Fig. 4.10.4 shows the number of bubbles per minute over the rising speed. The areas one and two are spread over the complete scale whereas the number of bubbles is very low and also the rising speed lies at the lower edge at 250 -300 mm/s.

Fig. 4.10.5 shows the diameter distribution over all streams. The first area is spread from 2 mm up to 4.5 mm whereas the second area is spread a bit lower from 1.5 mm to 3.5 mm. The area three is at the upper scale at 4 mm to 4.5 mm.

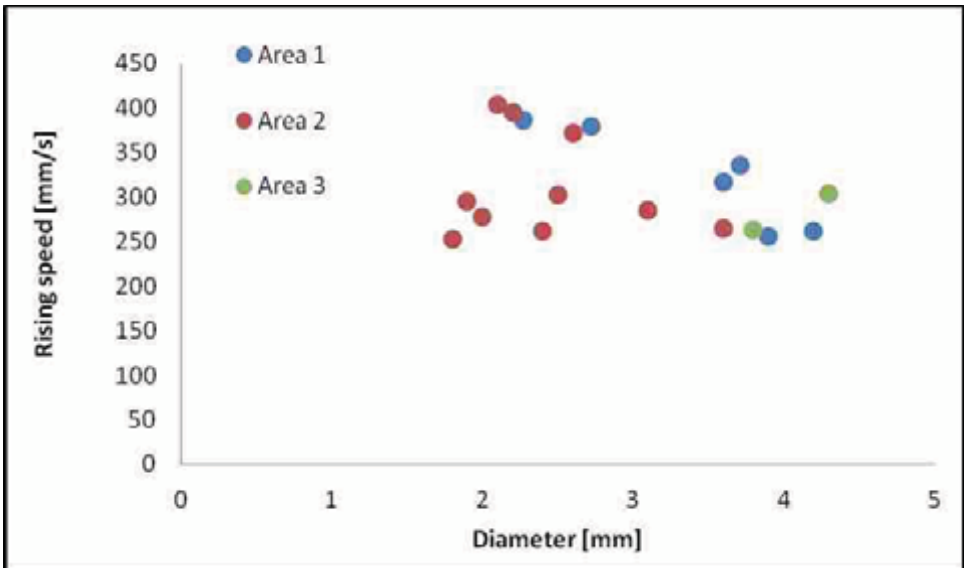

Fig. 4.10.1: Rising speed over diameter sorted by areas.

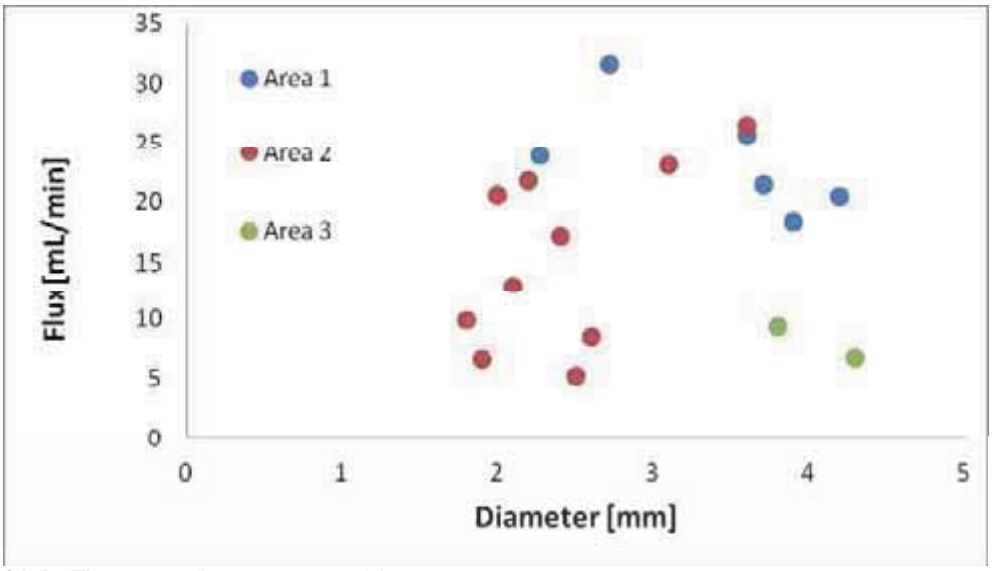

Figure 4.10.2: Flux over diameter sorted into areas.

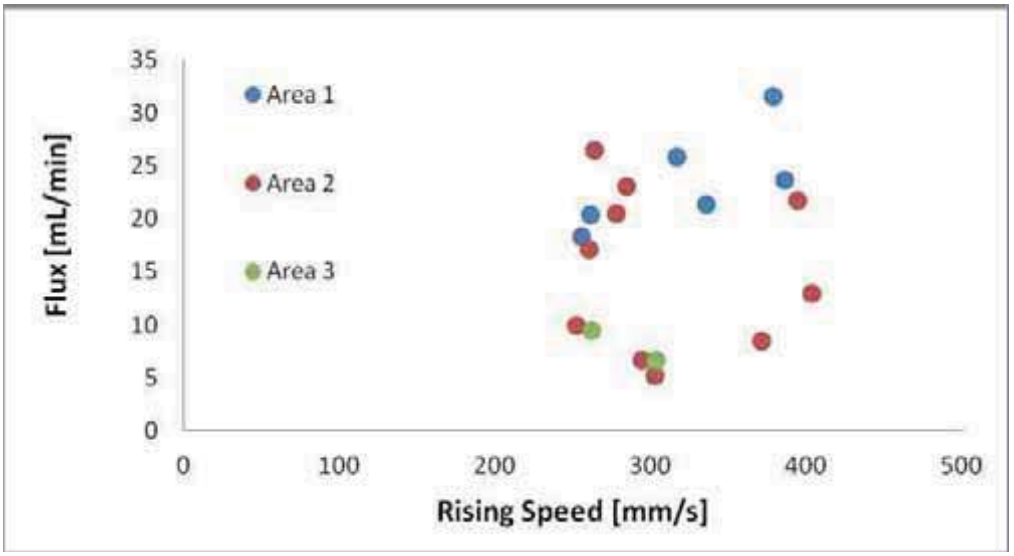

Fig. 4.10.3: Flux over rising speed sorted into areas.

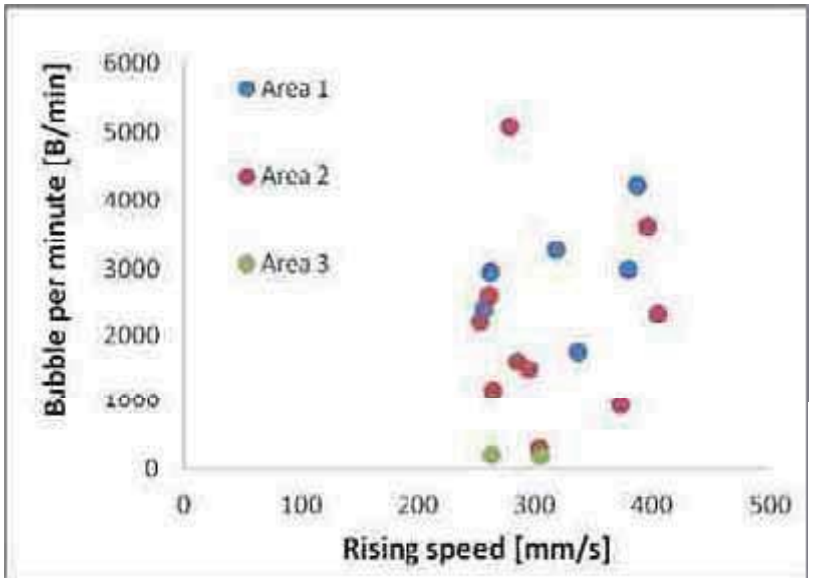

Fig. 4.10.4: Bubbles per minute over rising speed sorted by areas.

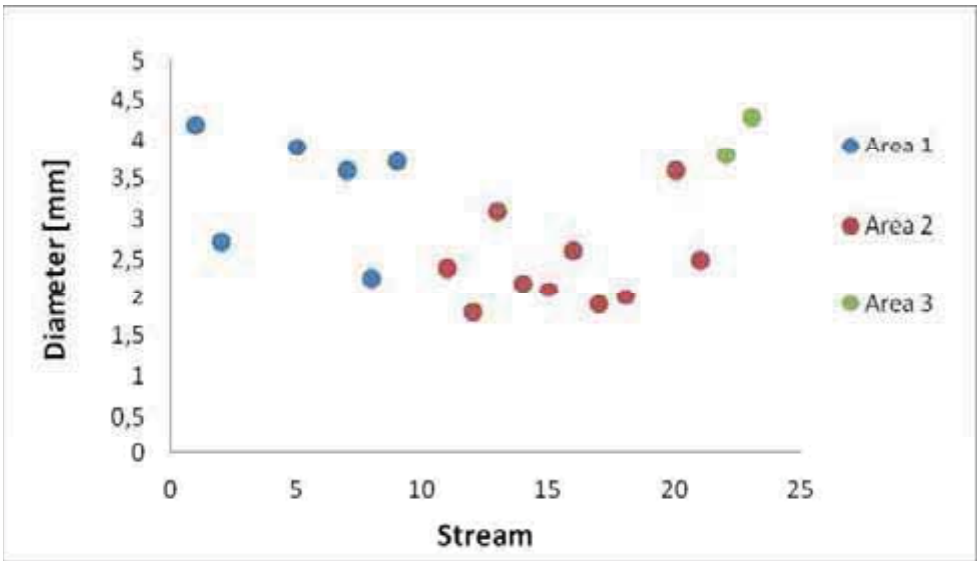

Fig. 4.10.5: Average diameter of streams.

4.11 Acoustic Gas Bubble Detection and Quantification (Sonex IMAGENEX)

(Michal Tomczyk)

Detailed acoustic investigation of bubble streams rising from the seafloor were conducted during HEINCKE HE-387 Cruise at the western Svalbard slope seep environment. During four ROV dives the data were collected by Imagenex sonar mounted on ROV in Area 1 at water depth ~90 meters. In order to conduct quantitative measurements with the Imagenex Imaging Sonar the ROV was positioned in front of the bubble streams situated at the seafloor. The position was adjusted such that the scanning sonar imaged the bubble streams as close as possible and such that the seafloor reflections just disappeared from the sonar images. Subsequently, the sonar performed a high resolution scan at 640 kHz for the purpose of the first described method, and at nine more frequencies to proceed the inversion model. For each seep site from 4 to 30 scans were performed for scan averaging. The time needed for scanning these areas is in the range of 2 minutes to 5 minutes, depending on the scanned angle. Fig. 4.11.1 shows a part of the sonar scan that was used for flux quantifications. Bubble streams show up as high backscatter of variable shape. From the video observation it is possible to distinguish two substreams that make one backscatter intensities cloud visible in the scanned sector (a bubble plume labeled as A1-C4-S2). For some of the bubble streams we also used the bubble catcher for further comparison of fluxes. The fluxes were in the range of 4 to 55 mL/min for individual bubble stream. Independent flux estimations using a funnel-shaped device show a good agreement with the results obtained using the acoustic model. All the flux measurements from Area 1 and Area 3 are summarized in Table 4.11.1.

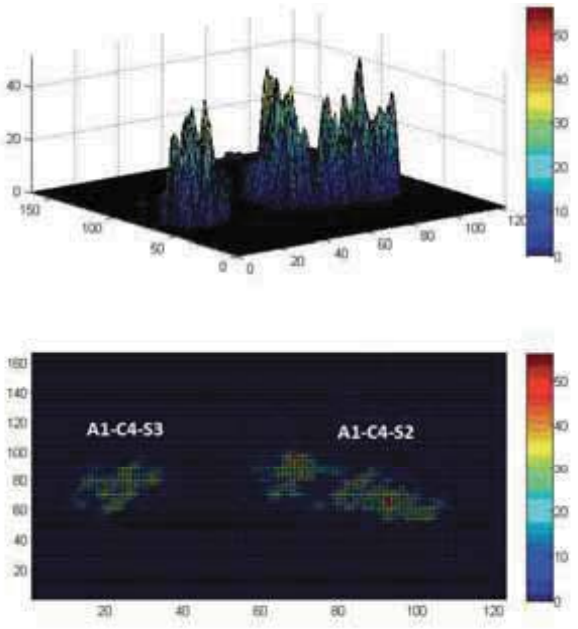

Fig. 4.11.1: The figure shows two high-backscatter areas labeled A1-C4-S3 and A1-C4-S2 (the second stream consists of two substreams). The same selected scanning sector with 3D projection (above) and 2D projection (below) show up as high backscatter of variable shape.

Flare mapping was conducted during the second ROV dive using the sonar. The ROV was maneuvered to the location of the flare mapped with one of the ship-borne echosounders (Kongsberg EM710 or SIMRAD fish-finder EK60) about 5 m above the bottom for scanning the water column for bubble reflections with the Imagenex 881A sonar. A height of up to 5 m above the seafloor was needed to avoid reflections from the seafloor as the vertical opening angle of the sonar is 20°. The scanning range was set to 10 meters. The frequency of emitted signal was 720 kHz, and pulse duration was 40 µsec. This procedure regularly resulted in successful detection of hydroacoustic anomalies in the water column and the localization of the bubble streams rising from the seafloor. Three transects were conducted over Area 1. The positions of gas bubble plumes are indicated on the map (Fig. 4.11.2). Due to sonar communication problems further investigation of gas emissions using the Imagenex 881A were not possible.

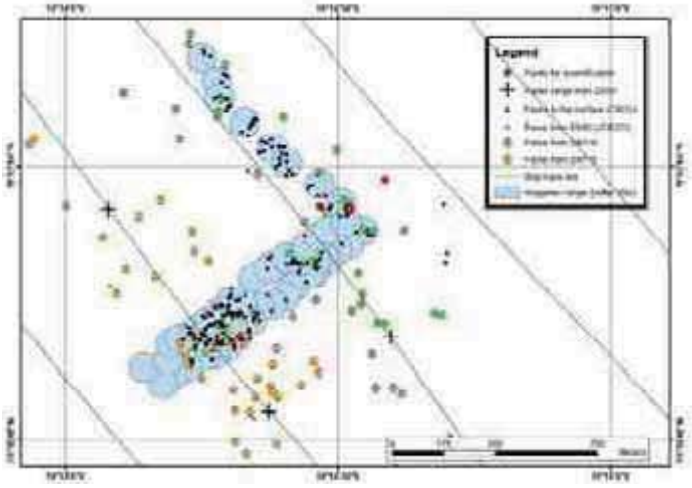

Fig. 4.11.2: The map shows the positions of flares mapped using different hydroacoustic tools in Area 1. More than 200 individual gas bubble streams were found while performing three individual transects using the Imagenex sonar.

Table 4.11.1: Result of the bubble quantification using sonar Imagenex

Dive No.	Bubble stream label	Scan 1	Scan 2	Scan 3	Scan 4	Scan 5	Scan 6	Scan 7	Scan 8	Scan 9	Scan 10	Scan 11	Scan 12	Scan 13	Scan 14	Scan 15	Scan 16	Scan 17	Scan 18	Scan 19
dive1	A1-C1-S1	3.9	4.7																	
	A1-C1-S2	16.6	20.1																	
	A1-C1-S3	13.7	22.4																	
	A1-C1-S4	13.5	21.1																	
dive2	A1-C2-S1	36.9	0.0	53.8	83.7	7.1	0.0	23.5	11.5	27.8	0.0	0.0	9.8	46.1	35.6	27.3	29.4			
	A1-C2-S2	39.3	49.6	36.0	35.1	24.2	79.2	38.8	3.2	46.6	26.4	4.9	62.9	27.9	26.3	34.8	71.6			
	A1-C2-S3	2.7	35.8	10.9	31.8	29.1	0.0	2.2	0.0	6.9	0.0	14.1	9.4	37.6	24.9	3.4	4.6			
	A1-C4-S3	17.0	19.9	27.0	26.5	18.7														
	A1-C4-S2	32.7	44.6	49.7	53.8	37.7														
	A1-C4-S1	47.1	62.9	53.7	56.2	43.5														
	A1-C4-S4	35.1	33.4	35.3	36.7	39.1	36.7	29.8	38.9	33.2	45.2	36.4	39.0							
	A1-C4-S5	40.3	38.7	36.3	44.9	39.5	34.1	39.9	42.5	27.6	43.0	49.3	38.1							
dive3	A1-C4b-S4, A1-C4b-S5	63.4	78.3	80.8	86.8	78.9	82.1	83.7	62.8	64.8	67.9	63.5	71.8							
	A1-C4b-S1, A1-C4b-S2, A1-C4b-S3	90.6	87.3	115.9	104.8	118.6	107.1	105.3	121.1	65.4	96.0	106.5	79.7							
	A1-C4b-S7	43.2	31.9	42.1	31.9	42.0	28.3	30.2	31.4	34.8	33.8									
	A1-C4b-S6	37.8	27.2	37.5	37.4	30.6	29.9	30.6	28.6	37.9	34.2									
	A1-C4b-S4, A1-C4b-S5	74.1	123.3	125.6	119.6	67.3	59.2	112.2	63.6	112.5	105.2	102.6	112.7	91.4	62.6					
	A1-C4b-S1, A1-C4b-S2, A1-C4b-S3	81.7	161.3	139.0	129.7	131.1	101.0	112.4	142.6	144.8	132.6	115.8	150.6	140.8	105.0					
	A1-C4b-S1, A1-C4b-S2, A1-C4b-S3	74.9	88.5	69.3	78.5	47.0	55.8	62.2	47.9	72.7	72.6	60.0	43.1	48.5	41.3	53.8	55.8	84.1	64.7	60.7
	A1-C4b-S1, A1-C4b-S2, A1-C4b-S3	23.5	24.5	21.4	22.5	23.9	23.7	23.6	21.7	22.2	22.9	25.3	22.9	24.0	21.1	22.5	22.3	23.3	22.3	21.1
	A1-C4b-S6, A1-C4b-S7	56.6	51.1	62.4	59.2	52.4	44.9	45.1	33.5	38.9	46.1	47.8	62.5	60.0	51.7	50.2	59.6	52.9	49.0	50.9
	A1-S4b-S9	14.4	12.8	10.0	11.5	11.5	4.7	10.1	8.7	12.2	19.4	16.1	12.5	26.3	21.0	16.4	14.6	17.9	19.1	6.5
	A1-S4b-S8	14.8	5.5	2.8	0.8	3.3	2.5	12.5	3.1	5.2	8.2	16.1	3.3	3.7	3.4	9.0	6.7	19.8	12.5	0.0
dive4	c1	48.9	48.5	71.3	59.8	62.2	45.8	53.1	48.8	62.0										
	c2	34.0	35.1	35.4	32.1	38.1	30.7	26.4	34.0	27.3										
	c3	45.8	50.7	48.8	65.3	66.1	47.0	59.1	54.5	42.4										
	c4	24.1	15.8																	
	c5	41.3	39.9																	
	c6	137.6	118.8																	
	c7	51.4	80.8																	

Table 4.11.1: continued.

Dive No.	Scan 20	Scan 21	Scan 22	Scan 23	Scan 24	Scan 25	Scan 26	Scan 27	Scan 28	Mean flux [mL/min]	Flux from bubbelcatcher [mL/min]
dive 1										4.3	
										18.4	
										18.0	
										17.3	
dive 2										24.6	
										37.9	
										13.4	
										21.8	
										43.7	
										54.7	
										36.7	
										39.5	
dive 3										73.7	70
										100.8	
										35.1	38
										33.1	30
										65.1	
										117.8	
	57.3	40.6	41.4	52.1	59.4	47.7	52.4	51.3	659	58.7	
	21.7	23.3	21.6	20.6	22.3	22.4	20.7	22.6	224	22.6	
	45.2	53.9	50.6	52.2	45.3	45.3	32.9	42.1	489	49.0	38
	9.6	23.8	16.4	19.0	24.4	14.0	11.0	5.9	35	14.1	
	7.0	7.0	9.7	8.0	14.5	13.2	0.0	7.1	100	7.5	10
dive 4										54.6	
										32.8	
										53.3	
										20.0	
										40.6	
										128.2	
										66.1	

4.12 Passive Acoustics (Hydrophone SM2M)

(Benoît Bergès)

The hydrophone unit was deployed two times:

- On 25 Aug 2012 attached to the ROV during Dive 03 (Area 1)
- On 04 Sept 2012 attached to a mooring (Area 1)

On both deployments, collected data were very noisy and estimates were very difficult to make as the inversion is extremely dependent on the noise floor.

Dive 03 deployment 25 Aug 2012. During this dive, the hydrophone was recording constantly and sequences where the ROV was kept silent were processed. It was hoped that the acoustic emissions from the bubble streams would overcome the noise floor. Two sequences with the ROV kept as silent as possible were performed next to bubble streams and away from any bubble streams. Power spectral densities together with sound pressure levels are presented in Fig. 4.12.1. Many signal processing techniques were employed in order to estimate flow rates but the noise floor was found to be too high for any proper estimate. This was due to the ambient noise but mainly from the noise of the ship.

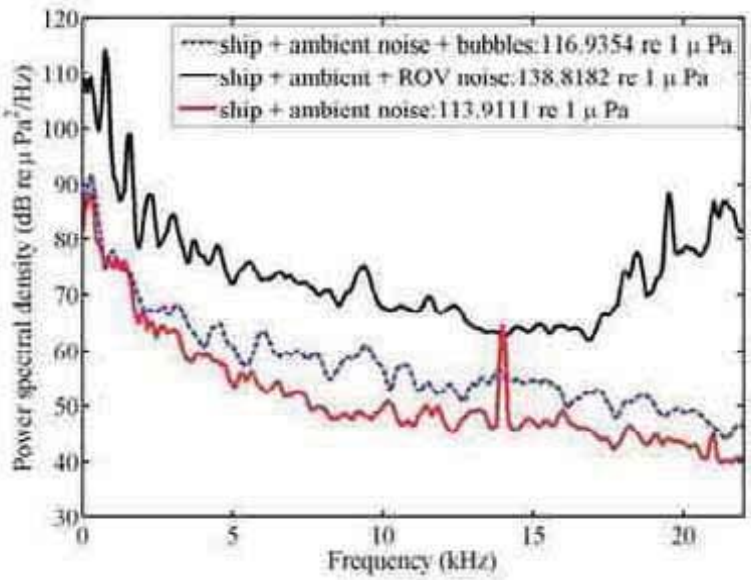

Fig. 4.12.1: Power spectral densities from hydrophone recording of Dive 03 during different sequences.

Mooring deployment 04 Sept 2012. After it was found that the solution of deploying the hydrophone on the ROV was not proper (too much noise), it was decided to deploy to ROV attached to a mooring (Fig. 4.12.2). This was deployed under good weather conditions and no problems appeared during the procedure on 04 Sept 2012. The selected area was the one that was studied during Dive 02 and 03.

The unit was recovered in the morning on 05 Sept 2012. The operation was performed without any noticeable problems.

Even if the background noise was found to be considerably diminished, the background noise was found to be still very important (Fig. 4.12.3). Some noise removal signal processing was applied and flow rates of order of magnitude of 117 mL/m^3 were found, compared to estimates of more than 250 mL/m^3 observed during Dive 02 and 03. The large error is most likely to be due to the important noise that makes the inversion technique difficult to apply.

No other try was given to deploy the mooring.

Fig. 4.12.2: Picture of the SM2M attached to the mooring line for deployment on 04 Sept 2012.

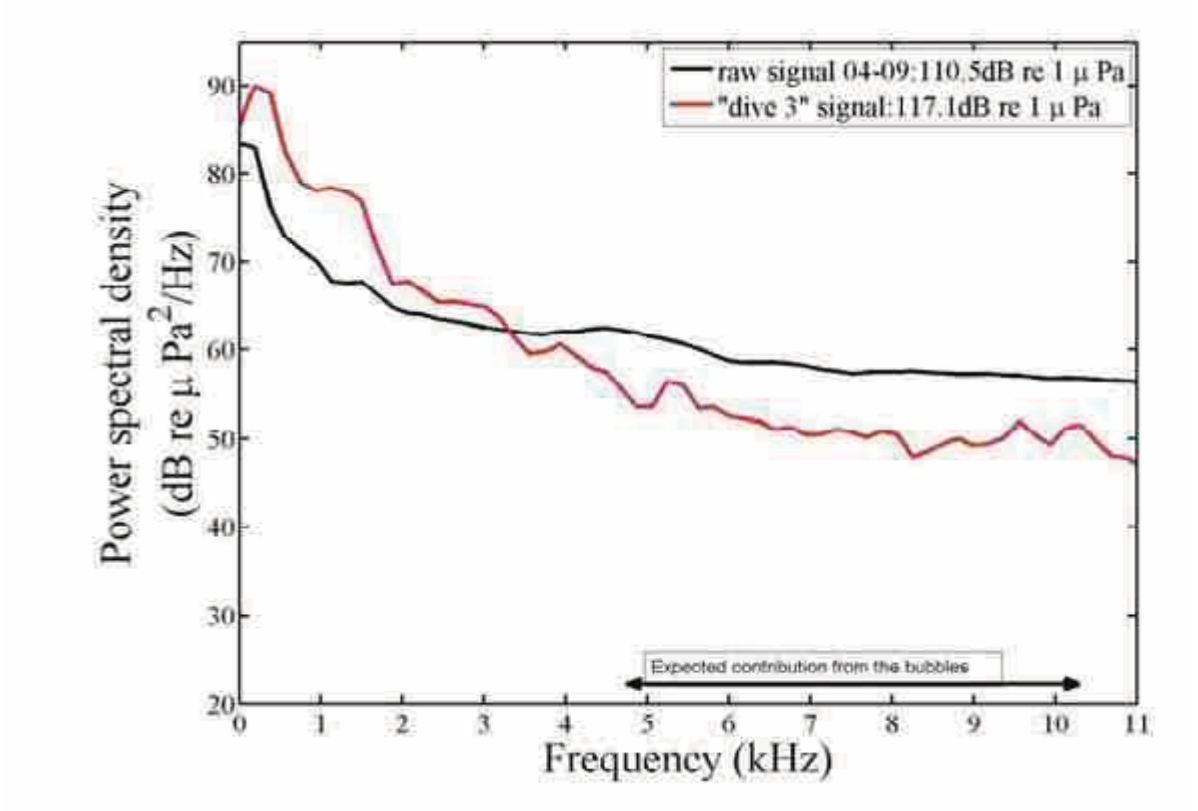

Fig. 4.12.3: Comparison of power spectral densities between deployment on 04 Sept 2012 and 25 Aug 2012.

4.13 Seafloor Sampling

(Heiko Sahling, Thomas Pape, Stefanie Kaboth)

Gravity cores. A gravity corer station (GeoB16808) was conducted at about 97 mbsl in Area 1 in order to check for the general accessibility of surface deposits in this region by gravity coring. On deck, only the core catcher was filled mostly with benthic animals, shell remnants, and rocks of pebble to gravel size.

Three gravity cores were taken in the 900 m pockmark area at selected sites characterized by low seafloor backscatter anomalies in order to check for sediment consistency and potential presence of gas hydrates. Core GeoB16830-1, which was recovered with a 3 m-cutting barrel, showed indications for sediment overpenetration. For cores GeoB16830-2 and -3, a 5 m-cutting barrel was installed and core recoveries were 351 cm and 424 cm, respectively. All these cores showed silty-clayey hemipelagic sediment in the core catcher and at the 1 m-segment cuts. Neither gas hydrates nor features related to gas expansion became apparent in these cores. The cores are left unopened for further analysis in the home lab.

Multi cores. Three multi corer have been taken on the transit back at water depth of about 1300 m water depth in order to collect living benthic foraminifera. In total, eleven cores were useful and stored in the fridge for keeping the foraminifera alive. These will be used by Jutta Wollenburg, AWI for mesocosm experiments.

4.14 Vent Gas Composition and Methane Distribution in the Water Column

(Thomas Pape, Patrizia Geprägs)

4.14.1 Non-Seep Sites

Concentrations of methane dissolved in the water column

Water samples collected during three other hydrocast stations (GeoB 16838-1, -39-1, -44-1) at the western border of the study area and at maximum water depths of 920 mbsl showed concentrations of dissolved methane < 5 nmol L^{-1}. Hence, these values might be considered as background concentrations of dissolved methane brought with the West Spitsbergen Current.

4.14.2 Seep Area 1 (ca. 90 m)

Molecular composition of vent gas

The molecular composition of vent gas sampled during ROV Dive 1 from the 80 m seepage area was strongly dominated by methane (98.992 mol.% of $\Sigma(C_1–C_3, CO_2)$), followed by carbon dioxide (0.989 mol.%), ethane (0.012), and much smaller amounts of higher homologues (Table 4.14.1). The respective C_1/C_2 ratio of 5,111 hints to microbial activity being the dominant formation process of light hydrocarbons present in vent gas in that area.

Table 4.14.1: Proportions of low-molecular-weight alkanes and CO_2 [in mol-% of $\Sigma(C_1–C_3, CO_2)$] in a vent gas samples collected at a seep at approx. 80 mbsl.

GeoB	ROV dive	GBS #	CH_4	C_2H_6	CO_2	C_3H_8	C_1/C_2
			[mol-%]	[mol-%]	[mol-%]	[mol-%]	
16807-2	1	1	98.977	0.013	1.009	tr.	7,852

tr.= < 0.001%

Concentrations of methane dissolved in the water column

Concentration profiles of dissolved methane were established for four CTD/RO stations and amended by data obtained for three near-bottom water samples collected during ROV dives (Fig. 4.14.1).

Highest concentrations of dissolved methane (1,489 nmol L^{-1}) were found for a water sample collected directly above a gas emission site during ROV Dive 1 (GeoB16807-4). For water samples taken with the rosette, elevated methane concentrations were generally found in deep water masses with highest concentrations observed for a station conducted within or close to gas flares (GeoB16814-1; 16855-2). With decreasing depth a strong depletion in methane with all samples containing less than 100 nmol L^{-1} in waters shallower than 40 mbsl was observed. In the 5 –to 20 mbsl depth interval relatively low methane concentrations approaching ≤11.3 nmol L^{-1} were found for all water samples except for two samples (34.4 and 63.8 nmol L^{-1}) taken at stations GeoB16810 and GeoB16855-2. These samples along with one near-surface sample collected at station GeoB16814 indicated a slight relative enrichment in dissolved methane in shallow waters.

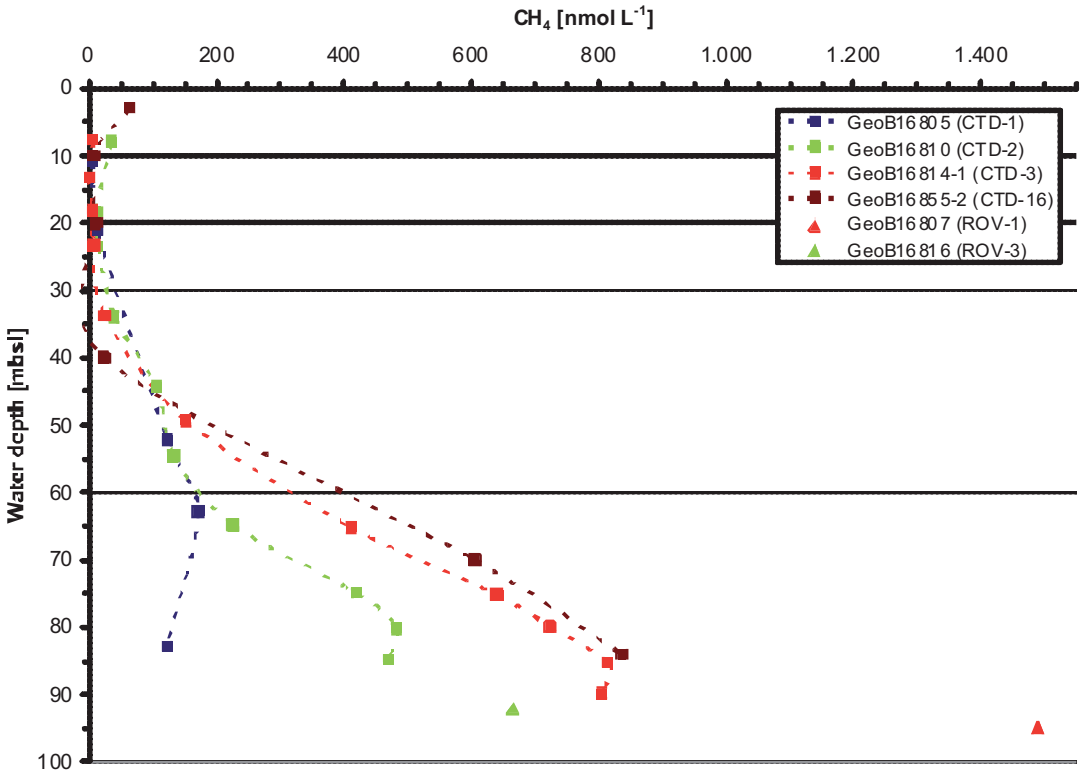

Fig. 4.14.1: Methane concentrations vs. water depth from water samples taken during hydrocasts and ROV dives directly above (CTD-3, ROV-1, CTD-16) and possibly remote from gas emission sites (CTD-1, -2, ROV-3). Identical color codes indicate that samples were taken at stations close to each other.

4.14.3 Seep Area 2 (ca. 240 m)

Molecular composition of vent gas

Light hydrocarbons in venting gas collected at two seep sites during dive GeoB16823 were predominantly composed of methane (>99.6 mol-%, Table 4.14.2). Carbon dioxide (> 0.2 mol-%) followed by ethane (0.007 mol-%) and traces of propane were less dominant ingredients of the gas samples. The resulting C_1/C_2 ratios exceeded 13,900 which suggests that hydrocarbons predominantly generated by microbial activity is fueling these seeps.

Table 4.14.2: Proportions of low-molecular-weight alkanes and CO_2 [in mol-% of $\Sigma(C_1–C_3, CO_2)$] in vent gas samples from seeps located at approx. 280 mbsl.

GeoB	ROV dive	GBS #	CH_4 [mol-%]	C_2H_6 [mol-%]	CO_2 [mol-%]	C_3H_8 [mol-%]	C_1/C_2
16823-2	4	1	99.689	0.007	0.303	tr.	15,161
16823-5	4	2	99.730	0.007	0.261	tr.	13,919

tr.= < 0.001%

Concentrations of methane dissolved in the water column

Concentration profiles of dissolved methane at sites positioned at about 240 mbsl were similar to those observed in waters above seeps at 80 mbsl (Fig. 4.14.2).

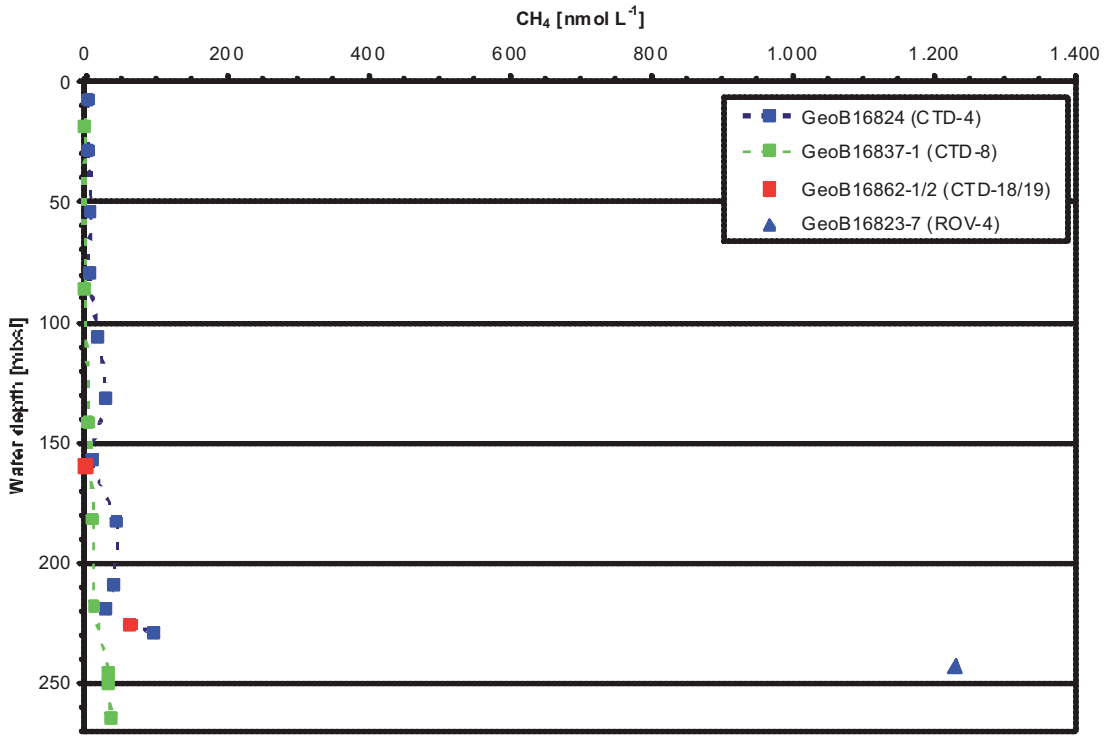

Fig. 4.14.2: Near-bottom water concentrations and vertical concentration profile of dissolved methane above seeps at about 240 m water depth.

Highest concentrations of dissolved methane were observed in deep waters with a near-bottom water sample taken during ROV Dive 4 (GeoB16823-7) containing 1,229.6 nmol L^{-1}. The deepest (229 mbsl) water sample taken during CTD/Ro station GeoB16824 close-by contained 96.0 nmol CH_4 L^{-1}. Elevated methane concentrations (up to 43.7 nmol L^{-1}) with regard to those found at reference stations were present in the 200-100 mbsl depth interval as well. However, in the uppermost 30 m of the water column dissolved methane concentrations were less than 5 nmol L^{-1}.

CTD/Ro station (GeoB16837) was carried out about 0.5 nm north of the seep area, i.e. in an area affected by the upstream of water masses. Highest concentrations of dissolved methane of 36.4 nmol L^{-1} were found about 7 m above the seafloor. In waters shallower than 110 mbsl dissolved methane concentrations were ≤ 4.1 nmol L^{-1}. These observations demonstrate that concentrations of dissolved methane fueled by seafloor seepage significantly decrease with increasing horizontal and vertical distance to the source.

4.14.4 Seep Area 3 (ca. 380 m)

Molecular composition of vent gas

The composition of hydrocarbons and carbon dioxide in vent gas from three seep sites was strongly dominated by methane (> 99.7 mol-%), amended by carbon dioxide and ethane (Table 4.14.3). The resulting C_1/C_2 values ≥ ca. 9,700 suggest that microbial activity is the dominant process of light hydrocarbon formation in the subsurface below these sites.

Table 4.14.3: Proportions of low-molecular-weight alkanes and CO_2 [in mol.% of $\Sigma(C_1–C_3, CO_2)$] in vent gas samples from seeps located at approx. 380 mbsl (GeoB16833) and 390 mbsl (GeoB16848), respectively.

GeoB	ROV dive	GBS #	CH_4	C_2H_6	CO_2	C_3H_8	C_1/C_2
			[mol-%]	[mol-%]	[mol-%]	[mol-%]	
16833-2	6	1	99.991	0.008	b.d.l.	tr.	12,213
16833-3	6	2	99.858	0.010	0.131	tr.	10,325
16848-2	8	2	99.703	0.010	0.286	tr.	9,697

tr. = < 0.001%

b.d.l. = below detection limit

Hydrate phase boundaries

Phase boundaries calculated for sI hydrates considering measured salinities and the slightly different compositions of the vent gas sampled during ROV dives 6 and 8 revealed very similar curves (Fig. 4.14.3).

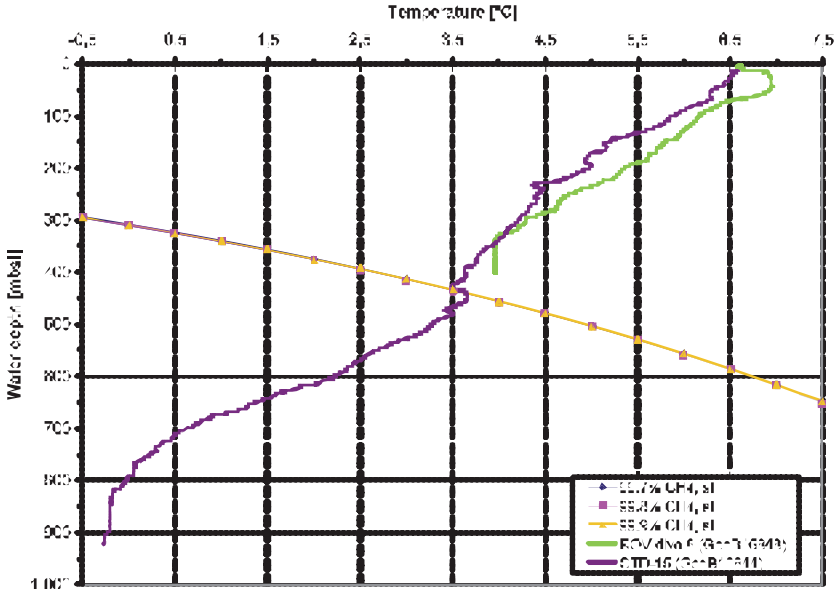

Fig. 4.14.3: Hydrate phase boundaries of submarine sI hydrates west off Spitsbergen calculated by use of molecular compositions of gas collected with the GBS during ROV dives from seeps located close to the GHSZ and water salinities determined during CTD casts. Note: Considering gas compositions, the presence of sII hydrates, which would be even less stable than sI hydrates, is unlikely. The crossing point of sI hydrate dissociation temperature and water column temperature is located at ca. 430 mbsl indicating the current position of the top of the GHSZ at that depth.

The hydrate dissociation temperature curves cross the actual water temperature profiles at ca. 434 mbsl, which is about 30 m deeper than the top of the GHSZ proposed by Westbrook et al. 2009. This difference might indicate that the seafloor section affected by current hydrate decomposition is broader than previously thought.

Concentrations of methane dissolved in the water column

Highest concentrations of dissolved methane (423 to 860 nmol CH_4 L^{-1}) in waters above seep sites situated at approx. 380 m water depth were observed for the three near-bottom water samples collected during ROV dives (GeoB16833-7, 16846-7, 16848-3; Fig. 4.14.4).

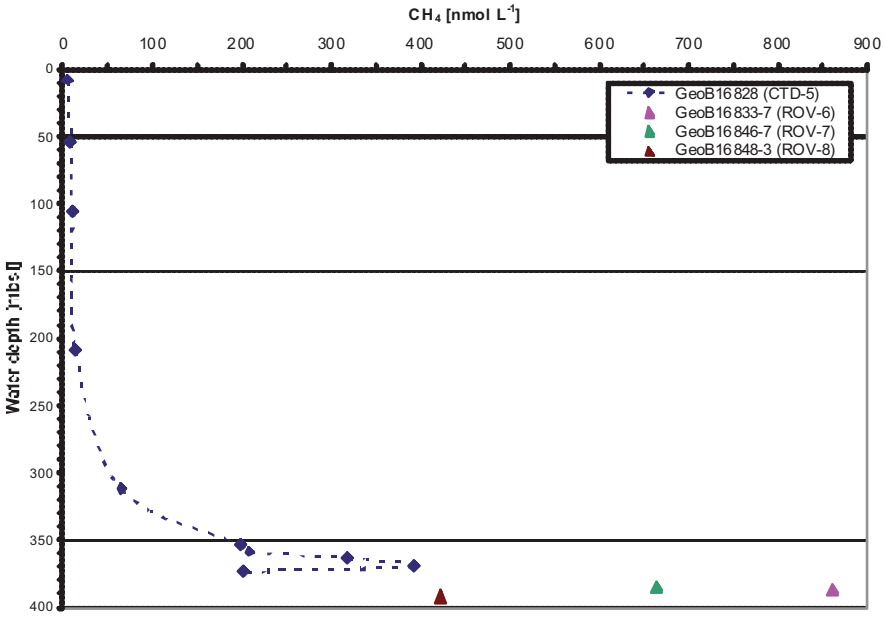

Fig. 4.14.4: Near-bottom water concentrations and vertical concentration profile of dissolved methane above seeps at about 380 m water depth.

For the only corresponding CTD/Rosette station (GeoB16828; CTD-5) maximum concentrations of 392 nmol CH_4 L^{-1} were found about 14 m above ground. With decreasing depth concentrations dropped significantly to 5.4 nmol CH_4 L^{-1} in the uppermost sample taken at approx. 8 mbsl.

4.14.5 'Pockmark' Area (866 mbsl)

Water samples were also taken in different water depths during GeoB16832 (CTD-6) in an area characterized by seafloor depressions formerly interpreted as pockmarks in the northwestern sector of the study area. All samples contained relatively low concentrations of dissolved methane (≤ 5.6 nmol L^{-1}), which are similar to concentrations measured at non-seep sites. These observations match the apparent lack of gas flares in the water column during hydroacoustic surveys (see Fig. 4.1.4).

4.14.6 Conclusions

- Seafloor gas seepage leads to elevated concentrations of dissolved methane in bottom waters. However, a significant methane reduction was observed with increasing distance to the emission site (tens to hundreds of meters) with steepest gradients close it
- Elevated concentrations of dissolved methane in surface waters were only found directly above seep sites
- C_1/C_2 ratios in venting gas hint to microbial activity as the major hydrocarbon production process in the subsurface of the west Spitsbergen continental shelf and slope
- The top of the gas hydrate stability zone might be positioned tens of meters deeper than previously thought

4.15 Methane and Carbon Dioxide Concentrations in Surface Waters

(Michael Glockzin, Heiko Sahling)

During the entire cruise, methane (and carbon dioxid) concentrations were continuously measured. Raw data of methane concentration as given by the analyzer are temperature sensitive, therefore a preliminary temperature-adjusted was applied on board. Fig. 4.15.1 to 4.15.6 show the values of temperature adjusted concentrations.

We used the data on board to look for any evidence of elevated methane concentration that could be attributed to the mapped gas emissions at the seafloor. Overall, we found no evidence for such a methane plume on scales of hundreds of meters to kilometers. As shown in Fig. 4.15.1 to 4.15.4, the surface methane concentrations appears to mainly be controlled by sea surface currents bringing water masses with different history to the area of interest. In general, the near-coast waters are methane-rich (and cold) whereas the open water masses are methane-depleted (and warm).

Only at the scale of tens of meters and only during relatively calm wind conditions, and only at water depth of ~ 90 m, elevated methane concentrations were found during ‘flare hunting experiments’ detailed in the Fig. 4.15.5 and 4.15.6 below.

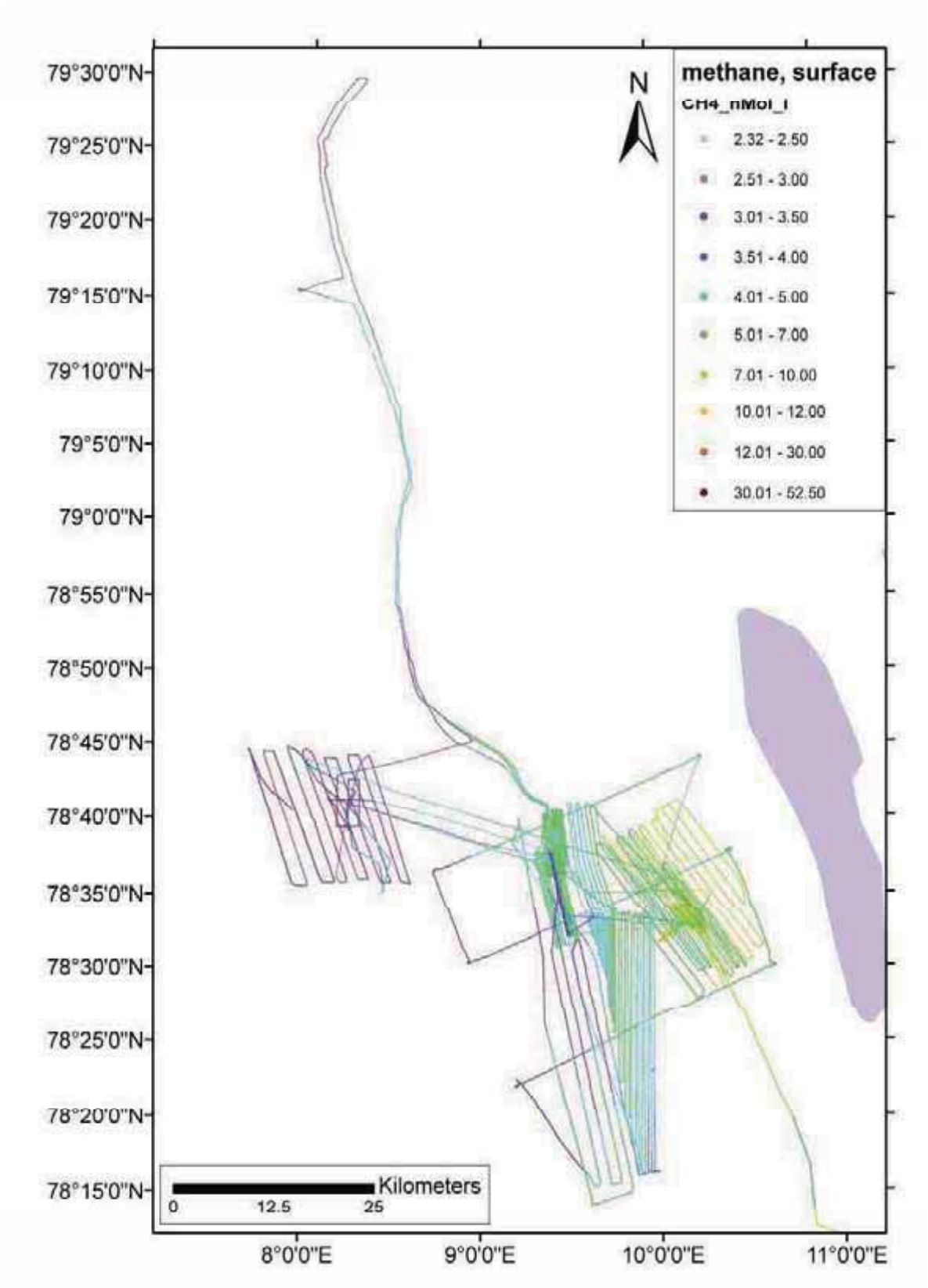

Fig. 4.15.1: Overview of methane surface concentrations continuously measured during Cruise HE-387. In general, the surface methane concentration seems to be controlled on large scales by currents bringing different water masses into the area of interest. Close to the coast where the coastal current flows, the methane concentrations are the highest. Offshore (and in the north), the lowest methane concentrations were measured indicating considerably warm and methane-poor water from the north Atlantic. In between these two systems is the West Spitsbergen Current with intermediate temperatures and methane concentrations.

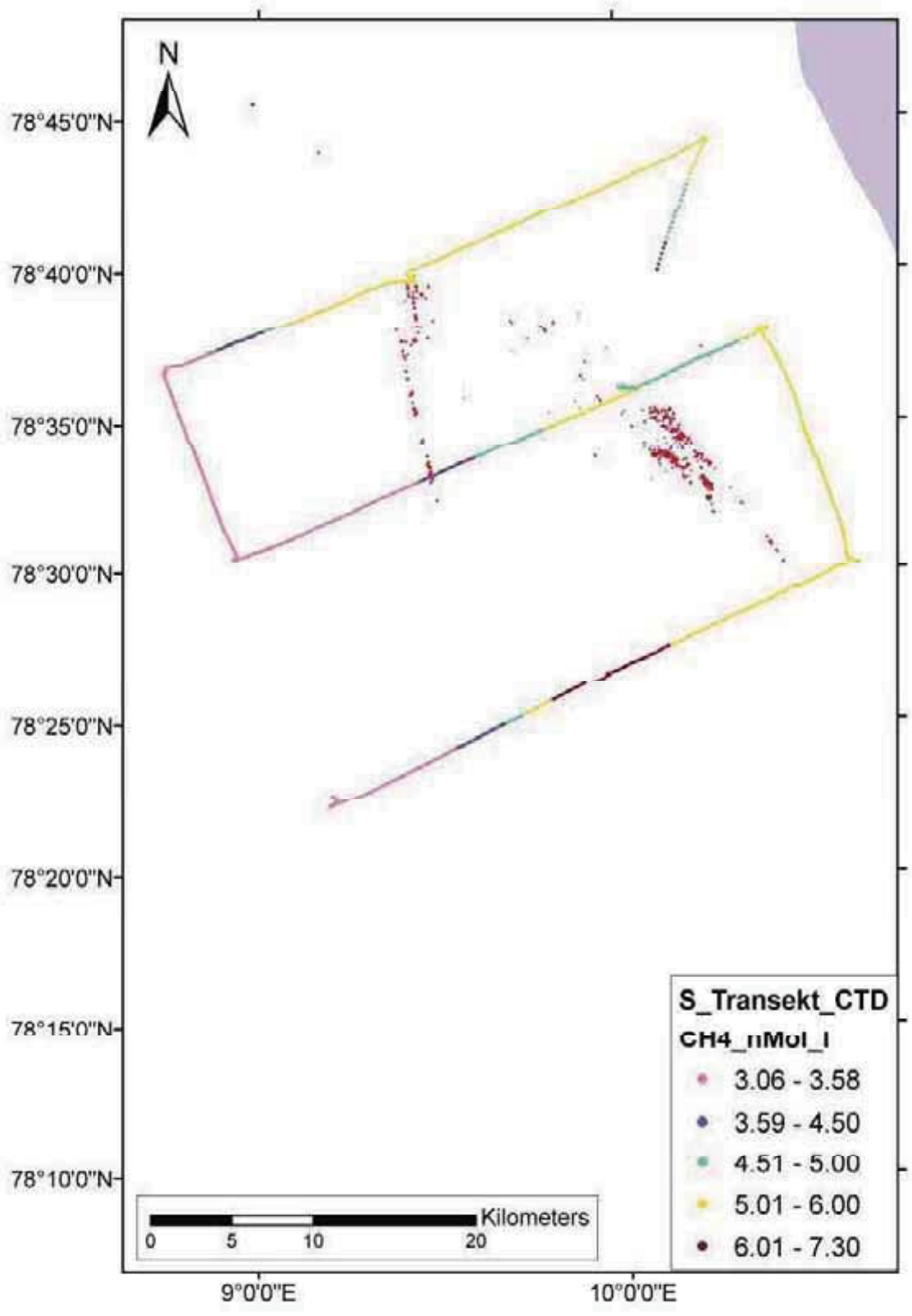

Fig. 4.15.2: The sea surface methane concentrations along the CTD/methane transects crossing the slope. At the time this survey was conducted S 5-6 winds dominated. High methane concentrations were measured close to the coast, where the coastal current flows in contrast to low methane concentrations offshore. Brown points indicate the position of flares mapped in the area at water depths of 80-90 m up to 380 m. The transects do not show any clear evidence of methane in surface waters to be measured down-stream (south) of the emissions.

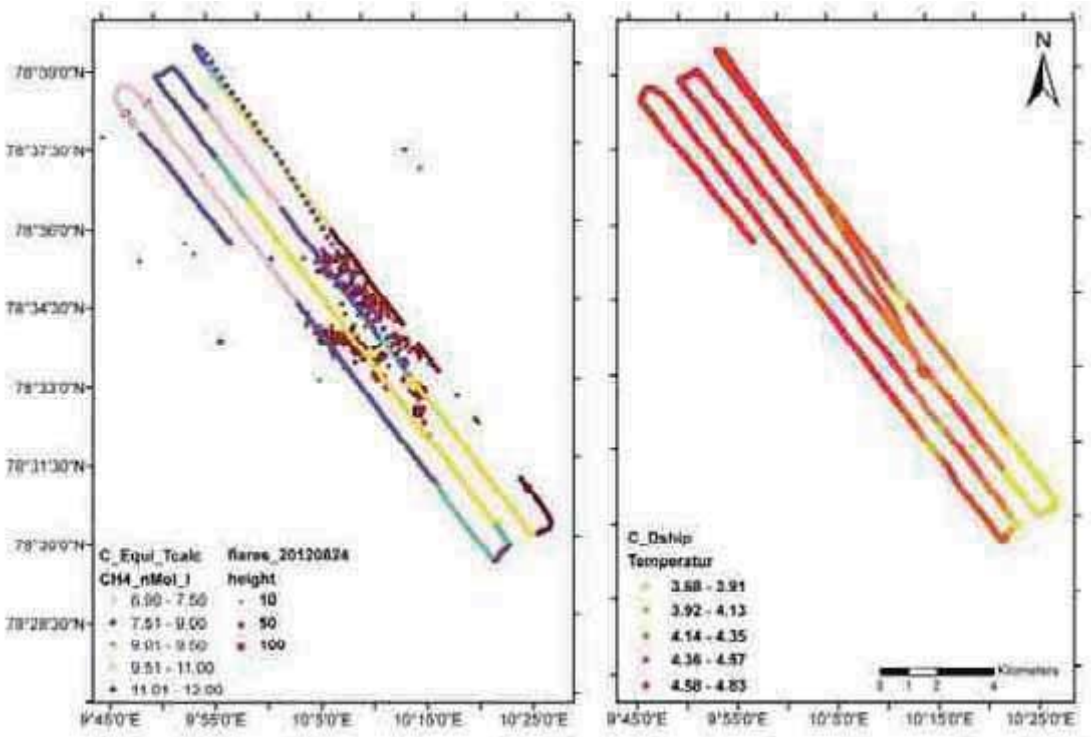

Fig. 4.15.3: Survey above the flares in 80-90 m water depths. Methane concentration (left) and surface temperatures (right) as measured by thermosalinograph from the ship. The methane concentrations show that on this scale the time lag of the measurement of the concentration is an issue (about ~ 20 min is the best guess). While there is no apparent pattern in methane concentration in this figure it looks better when the values are shifted back by 20 min. However, the resulting plot shows the general pattern of high methane towards the east and low methane toward the west, which is again the pattern caused by the surface currents. There is no apparent elevated methane surface plume above these sites on this scale.

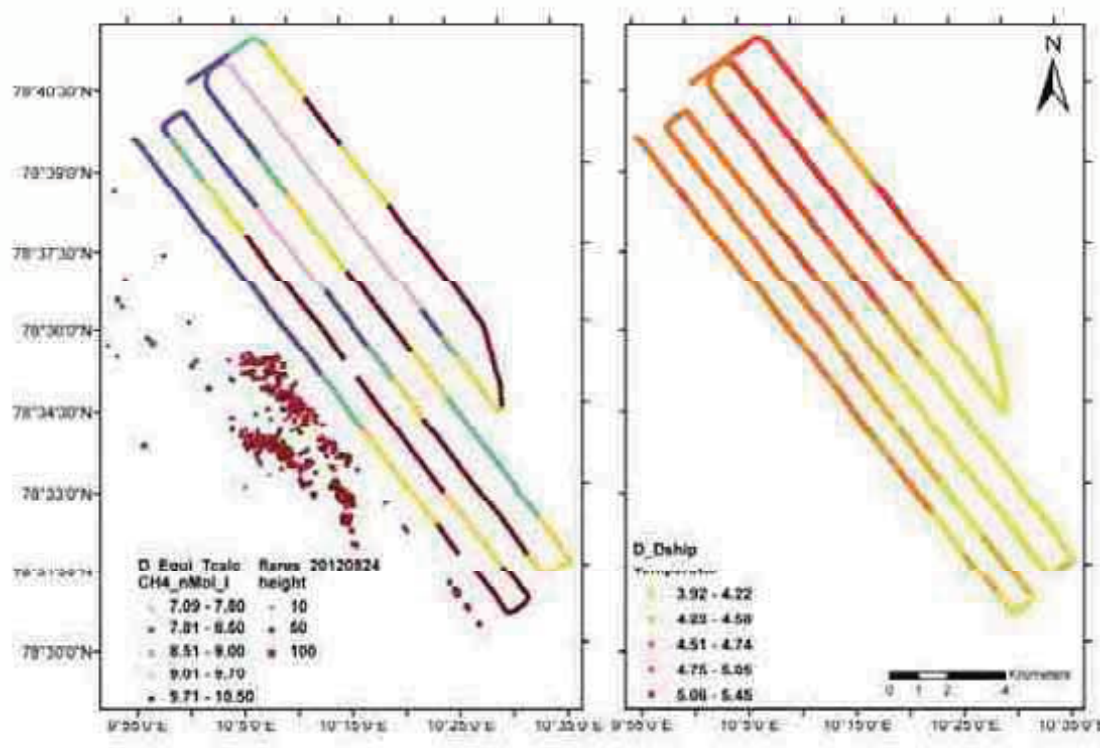

Fig. 4.15.4: Survey showing basically the same pattern as Fig. 4.15.3.

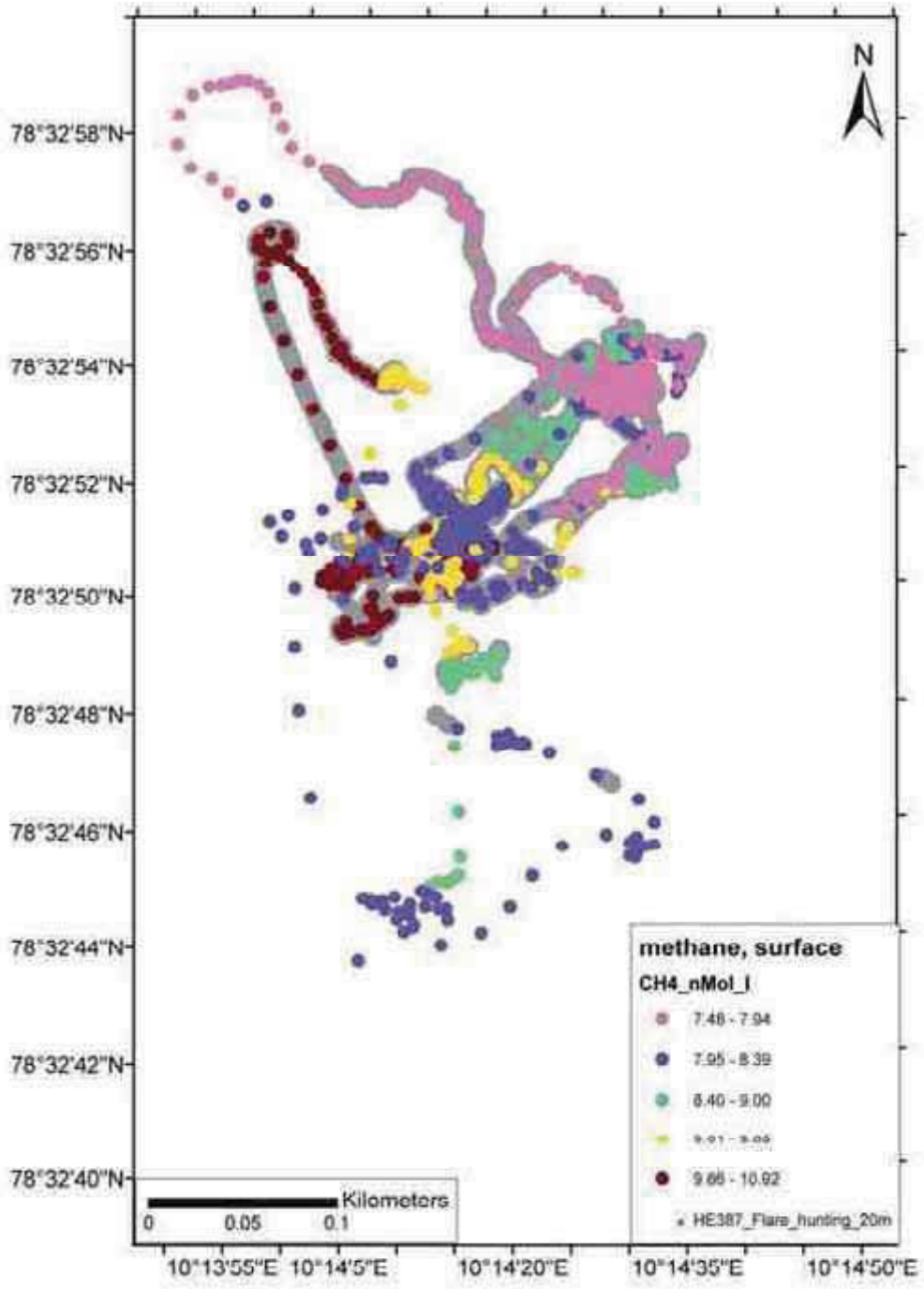

Fig. 4.15.5: Result of the 'plume hunting I'. During ROV Dive 2 high methane concentrations were measured in surface waters just above the emission located at 90 m water depth. The gas emission is well visible in EK 60 echosounder. Those sites along the ship track where the flare reached clearly to a depth of less than 20 m, which is about the depth of the mixed surface layer, are marked gray in the figure. In general, high methane concentrations were found above the acoustically determined flare. The ship slowly moved by alternating movement and stopping for the amount of time the equilibrator needs until stable methane concentrations were measured. A problem was, that the tool needed a long time to allow the methane concentration to decrease again after high values were measured. Therefore, basically elevated values were measured during this 'move-and-stop' experiment.
In order to really find out the limits of the plume, the ship moved out of the area towards the S and concentration decreased indeed (blue colors). Meanwhile, the wind speeds increased to S 5 about and suddenly, no surface methane anomaly was measured anymore (blue dots), therefore, the experiment was abandoned.

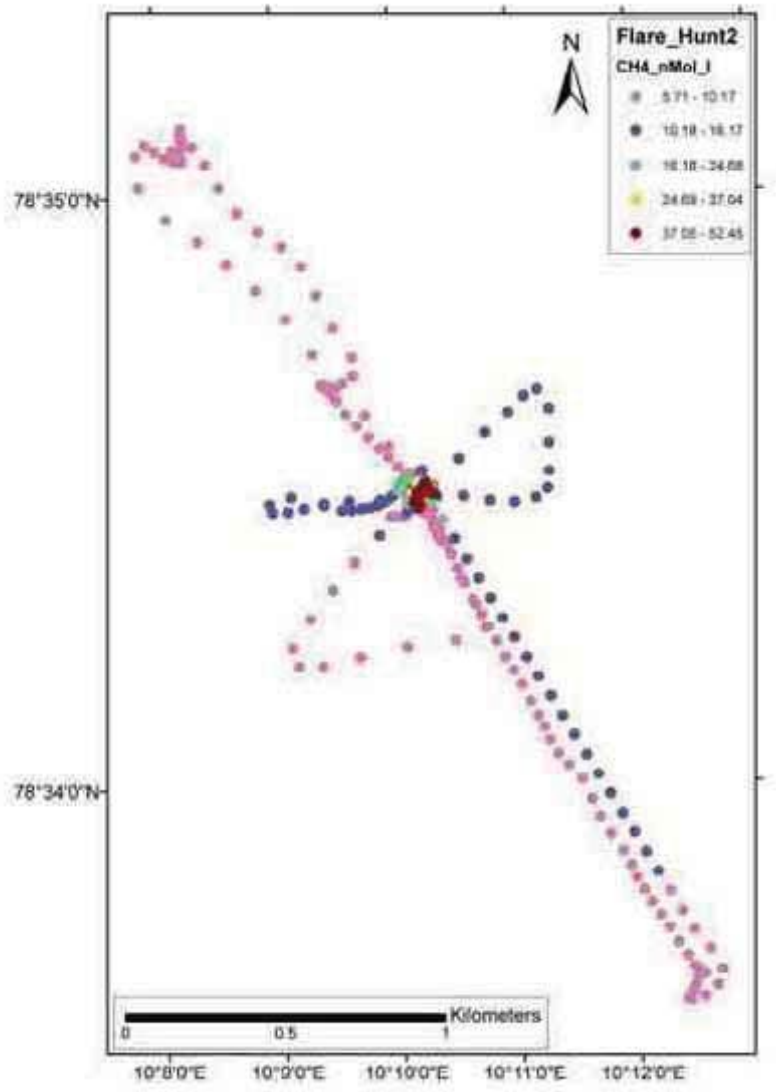

Fig. 4.15.6: Result of 'flare hunting II'. During ROV Dive 9 the ship was basically stationary and only moved at maximum a few tens of meters following the ROV. At one point, the ship was above a strong gas emission site also seen in EK 60. The bubbles could be traced from the seafloor at 90 m water depth to the sea surface. At that very moment the continuous measurement of methane in surface water measured the highest value of the entire survey, clearly indicating elevated methane concentration in surface waters due to the bubble plume. The wind was considerably slow while this observation was made.

Following this observation, we conducted another 'flare hunting' part II. We moved with the ship out of the plume after the ROV was on deck and crossed the area again three times W to E, NE to SW, and SE to NW in order to conduct EK 60 recordings. We crossed at slow ship speed of about 2-3 knots but this speed was too high to allow any elevated methane concentrations to be measured by the system. In order to study the extent of the methane plume at the surface, the ship slowly moved towards the gas emitting point from the NW, i.e. luv of the stream as the wind was blowing from the NW. Within about an hour we slowly moved towards the bubble stream but the concentrations of methane in the surface only increased when being right at the point above the stream, about 30-50 m NW of it was no signal at all. Within the plume CTD 55-2 was taken. In order to 'reset' the methane value in the 'machine', an air measurement was made while the ship moved out of the area.

The same exercise was repeated by coming from the SE in expectation that the methane plume may have drifted towards the SE with the winds. However, meanwhile wind speeds increased to about 5 Bft and, despite moving towards the point with gas emission, no anomalous methane concentration was found anymore! The wind has probably moved the plume away and water is too fast replaced to become methane charged from the bubble plume.

5. References

Caress, D.W., Chayes, D.N. (2001), Improved Management of Large Swath Mapping Datasets in MB-System Version 5, Abstract OS11B-0373. Eos Trans. Fall Meet. Suppl., 82(47).

Clay, C. S., and H. Medwin (1977), Acoustical Oceanography: Principles and Applications, John Wiley, New York.

Damm, E., Mackensen, A., Budeus, G., Faber, E., Hanfland, C. (2005) Pathways of methane in seawater: Plume spreading in an Arctic shelf environment (SW-Spitsbergen). Continental Shelf Research, 25(12-13), 1453-1472.

Dickens, G.R., Koelling, M., Smith, D.C., Schnieders, L., scientists, I.E., (2007) Rhizon sampling of pore waters on scientific drilling expeditions: An example from the IODP expedition 302, Arctic Coring Expedition (ACEX). Scientific Drilling, 4.

Gülzow, W., Rehder, G., Schneider, B., Schneider v. Deimling, J., Sadkowiak, B. (2011) A new method for continuous measurement of methane and carbon dioxide in surface waters of the Baltic Sea using off-axis integrated cavity output spectroscopy (ICOS), Limnology Oceanography Methods 9: 176-184

Hustoft, S., Bünz, S., Mienert, J. and Chand, S. (2009). Gas hydrate reservoir and active methane-venting province in sediments on <20 Ma young oceanic crust in the Fram Strait, offshore NW-Svalbard. Earth and Planetary Science Letters 284: 12-24.

Lammers, S., Suess, E. (1994) An improved head-space analysis method for methane in seawater. Marine Chemistry 47(2): 115-125.

Lebourges-Dhaussy, A. (1996), Caractérisation des populations planctoniques par acoustique multifréquence, Océnis, 22(1), 71-92.

Leighton, T. G., and P. R. White (2011) Quantification of undersea gas leaks from carbon capture and storage facilities, from pipelines and from methane seeps, by their acoustic emissions, P Roy Soc a-Math Phy, 468(2138), 485-510.

Nikolovska, A. and C. Waldmann (2006) Passive acoustic quantification of underwater gas seepage, Oceans-Ieee, 1403-1408.

Pape, T., Bahr, A., Rethemeyer, J., Kessler, J.D., Sahling, H., Hinrichs, K.U., Klapp, S.A., Reeburgh, W.S., Bohrmann, G. (2010) Molecular and isotopic partitioning of low-molecular weight hydrocarbons during migration and gas hydrate precipitation in deposits of a high-flux seepage site. Chemical Geology, 269(3-4), 350-363.

Rajan, A., Mienert, J. and Bünz, S. (2012) Acoustic evidence for a gas migration and release system in Arctic glaciated continental margins offshore NW-Svalbard. Marine and Petroleum Geology, 32(1): 36-49.

Rehder, G., Keir, R.S., Suess, E., Rhein, M. (1999) Methane in the northern Atlantic controlled by microbial oxidation and atmospheric history. Geophysical Research Letters, 26(5), 587-590.

Sarkar, S., Berndt, C., Minshull, T.A., Westbrook, G.K., Klaeschen, D., Masson, D.G., Chabert, A. and Thatcher, K.E. (2012) Seismic evidence for shallow gas-escape features associated with a retreating gas hydrate zone offshore west Svalbard. J. Geophys. Res. 117(B9): B09102.

Seeberg-Elverfeldt, J., Schlüter, M., Feseker, T., Kölling, M., (2005) Rhizon sampling of porewaters near the sediment-water interface of aquatic systems. Limnology and Oceanography: Methods, 3, 361-371.

Simmonds, E. J., and D. N. MacLennan (2005), Fisheries acoustics: theory and practice, 2nd ed., xvii, 437 p. pp., Blackwell Science, Oxford; Ames, Iowa.

Ślubowska-Woldengen, M., Rasmussen, T.L., Koç, N., Klitgaard-Kristensen, D., Solheim, A., (2007) Advection of Atlantic Water to the western and northern Svalbard shelf since 17,500 cal yr BP. Quarternary Science Reviews, 26, 463-478.

Thiede, J. & Myhre, .AM. (1996) Introduction of the North-Atlantic Gateways: Plate tectonic-paleoceanographic history and significance. *Proceedings of the Ocean Drilling Program* 151: 3-15 p.

Vagle, S., and D. M. Farmer (1992) The Measurement of Bubble-Size Distributions by Acoustical Backscatter, J Atmos Ocean Tech, 9(5), 630-644.

Vanneste, M., Guidard, S. and Mienert, J. (2005) Bottom-simulating reflections and geothermal gradients across the western Svalbard margin. Terra Nova, 17: 510-516.

Vogt, P.R., Gardner, J. and Crane, K., (1999) The Norwegian-Barents-Svalbard (NBS) continental margin: Introducing a natural laboratory of mass wasting, hydrates, and ascent of sediment, pore water, and methane. Geo-Marine Letters, 19: 2-21.

Vorren, T.O., Laberg, J.S., Blaume, F., Dowdeswell, J.A., Kanyon, N.H., Mienert, J., Rumohr, J. and Werner, F. (1998) The Norwegian-Greenland Sea continental margins: Morphology and late Quaternary sedimentary processes and environment. Quatenary Science Reviews, 17: 273-302.

Westbrook, G.K., Thatcher, K.E., Rohling, E.J., Piotrowski, A.M., Pälike, H., Osborne, A.H., Nisbet, E.G., Minshull, E.A., Lanoisellé, M., James, R.H., Hühnerbach, V., Green, D., Fisher, R.E., Crocker, A.J., Chabert, A., Bolton, C., Beszczynska-Möller, A., Berndt, C. and Aquilina, A. (2009) Escape of methane gas from the seabed along the west Spitsbergen continental margin. Geophysical Research Letters, 36: L15608.

Appendix 1: Station List

HE - 387															
				Time (UTC)				Begin / on seafloor		End / off seafloor					
Date 2012	St. No. He 387	GeoB No.	Instrument	Begin	Start Sci. Program	End Sci. Program	End	Latitude N°	Longitude W°	Latitude N°	Longitude W°	Water depth (m)	Area	Recovery Remarks
21.08.	1	16301	SVP	14:03		14:08	14:13			78°21.107'	10°40.830'	101	Area 1	
21.08.	2	16302	HS	14:50			09:49	78°21.87'	10°39.05'	78°34.39'	10°10.53'	88	Area 1	EK60, EM 710
22.08.	3	16303	SVP	10:18		10:22	10:25			78°32.330'	10°01.227'	149	Area 1	
22.08.	4	16304	HS	10:54			15:38	78°32.67'	9°59.51'	78°33.36'	10°9.98'	132	Area 1	EK60, EM 710
22.08.	5	16305	CTD	15:52		16:01	16:10			78°34.21'	10°6.05'	95.4	Area 1	7 of 11 bottles closed
22.08.	6	16306	HS	16:44			04:50	78°33.44'	10°14.33'	78°39.49'	9°54.16'	156	Area 1	EK60, EM 710
23.08.	7	16307	ROV Dive 01	07:23	07:43	12:18	12:28	78°32.366'	10°14.108'	78°32.840'	10°14.245'	91	Area 1	Imagenex sonar
23.08.	7-1	16307-1	Marker 2			10:05				78°32.839'	10°14.247'	94	Area 1	
23.08.	7-2	16307-2	GBS 1			10:19				78°32.838'	10°14.254'	94	Area 1	
23.08.	7-3	16307-3	GBS 2			10:35				78°32.839'	10°14.247'	94	Area 1	
23.08.	7-4	16307-4	Niskin			11:05				78°32.839'	10°14.246'	94	Area 1	
23.08.	8	16308	GC	12:48		13:00	13:09			78°32.840'	10°14.190'	97	Area 1	handful gravel & organisms
23.08.	9	16309	HS	13:14			16:01	78°32.80'	10°14.162'	78°32.815'	10°14.203'	96	Area 1	
23.08.	10	16310	CTD	16:02		16:13	16:29			78°32.82'	10°14.22'	96	Area 1	all bottles closed
23.08.	11	16311	HS	17:40			04:44	78°39.62'	9°55.38'	78°40.42'	9°59.98'	215	Area 1	EK60, EM 710
24.08.	12	16312	ROV Dive 02	06:03	06:13	15:50	16:02	78°32.36'	10°14.06'	78°32.837'	10°14.514'	93	Area 1	Imagenex sonar
24.08.	12-1	16312-1	Niskin			15:48				78°32.8664'	10°14.5177'	93	Area 1	
24.08.	13	16313	HS	16:13			17:55	78°32.38'	10°14.51'	78°32.84'	10°14.26'	93	Area 1	flare hunting !
24.08.	14-1	16314-1	CTD	17:58		18:09	18:20			78°32.85'	10°14.25'	93	Area 1	all bottles closed
24.08.	14-2	16314-2	HS	18:20			22:42	78°32.84'	10°14.27'	78°32.84'	10°14.04'	93	Area 1	continuation of flare hunting !
24.08.	15	16315	HS	33:41			04:55	78°29.09'	10°18.33'	78°33.05'	9°54.46'	135	Area 1	EK60, EM 710
25.08.	16	16316	ROV Dive 03	06:03	06:19	12:50	13:04	78°32.360'	10°14.390'	78°32.818'	10°14.093'	94	Area 1	Imagenex sonar
25.08.	16-1	16316-1	BC			06:55				78°32.88594'	10°14.52036'	92.7	Area 1	
25.08.	16-2	16316-2	Hydrophone			07:56				78°32.88524'	10°14.51904'	92.8	Area 1	
25.08.	16-3	16316-3	BC			08:53				78°32.88498'	10°14.51976'	92.6	Area 1	
25.08.	16-4	16316-4	BC			10:25				78°32.88564'	10°14.52072'	92.3	Area 1	
25.08.	16-5	16316-5	Hydrophone			10:48				78°32.88548'	10°14.5197'	91.6	Area 1	
25.08.	16-6	16316-6	Hydrophone			11:06				78°32.88444'	10°14.51904'	92	Area 1	
25.08.	16-7	16316-7	BC			11:46				78°32.83704'	10°14.25846'	94.3	Area 1	
25.08.	16-8	16316-8	Hydrophone			12:26				78°32.8371'	10°14.25832'	94.6	Area 1	

Appendix 1: Station List continued

HE - 387				Time (UTC)			Begin / on seafloor		End / off seafloor				
Date 2012	St. No. He 387	GeoB No.	Instrument	Begin	Start Sci. Program	End Sci. Program	End	Latitude N°	Longitude W°	Latitude N°	Longitude W°	Water depth (m)	Area	Recovery Remarks
25.08.	18-9	16818-9	Hydrophone			12:40				78°32.80878'	10°13.98006'	98.7	Area 1	
25.08.	16-10	16816-10	Niskin			12:45				78°32.80914'	10°13.98006'	97.2	Area 1	
25.08.	17	16817	HS	13:29			00:14	78°32.95'	10°13.72'	78°37.17'	9°23.31'	395	Area 1	EK60, EM 710
26.08.	18	16818	HS	00:26			04:42	78°36.64'	9°23.52'	78°37.82'	9°23.33'	390	Area 2	EK60, EM 710, notfares!
26.08.	19	16819	HS	04:42			08:39	78°37.82'	9°23.33'	78°37.80'	9°24.28'	372	Area 2	EK60, EM 710, notfares!
26.08.	20	16820	HS	09:56			13:06	78°41.43'	8°21.09'	78°42.68'	8°11.20'	897	Area 2	EK60, EM 710, notfares!
26.08.	21	16821	HS	14:22			07:12	78°45.65'	8°56.57'	78°39.86'	9°23.10'	272	Along 400 m contour	EK60, EM 710, notfares!
27.08.	22	16822	SVP	06:49		06:57	07:00			78°39.303'	9°25.632'	243	Area 2	
27.08.	23	16823	ROV Dive 04	08:08	08:27	14:36	14:55	78°39.25N'	9°25.737'	78°39.297'	9°25.952'	241	Area 2	magenex sonar
27.08.	23-1	16823-1	Marker 1			08:40				78°39.2534'	9°25.7603'	241	Area 2	
27.08.	23-2	16823-2	GBS 1			09:44				78°39.2542'	9°25.7554'	242	Area 2	
27.08.	23-3	16823-3	Rock sample			10:49				78°39.2562'	9°25.7543'	241	Area 2	
27.08.	23-4	16823-4	Marker 4			11:27				78°39.2524'	9°26.0438'	241	Area 2	
27.08.	23-5	16823-5	GBS 2			12:45				78°39.2518'	9°26.0407'	240	Area 2	
27.08.	23-6	16823-6	Rock sample			13:03				78°39.2514'	9°26.0443'	240	Area 2	
27.08.	23-7	16823-7	Niskin			14:04				78°39.1086'	9°26.0391'	240	Area 2	
27.08.	24	16824	CTD	15:50		16:12	16:28			78°39.251'	9°26.036'	242	Area 2	oxygen sensor out of order
27.08.	25	16825	HS	21:37			05:47	78°34.75'	9°30.32'	78°37.80'	9°18.58'	400	Area 3	EK 60, EM 710
28.08.	26	16826	ROV Dive 05	09:50	10:30	14:43	15:02	78°39.24'	9°25.96'	78°39.21'	9°26.12'	243	Area 2	Tritech sonar
28.08.	26-1	16826-1	BC			11:43				78°39.21606'	9°25.83406'	241.5	Area 2	
28.08.	26-2	16826-2	BC			12:32				78°39.21612'	9°25.78626'	241.1	Area 2	
28.08.	26-3	16826-3	BC			14:03				78°39.20076'	9°25.99512'	241	Area 2	
28.08.	26-4	16826-4	BC			14:07				78°39.20148'	9°25.99146'	241.5	Area 2	
28.08.	26-5	16826-5	BC			14:10				78°39.20172'	9°25.99722'	241.4	Area 2	
28.08.	26-6	16826-6	BC			14:27				78°39.201'	9°25.9968'	241.6	Area 2	
28.08.	26-7	16826-7	BC			14:37				78°39.20208'	9°25.98756'	239.3	Area 2	
28.08.	27	16827	HS	16:10			03:52	78°39.25'	9°26.53'	78°33.53'	9°45.48'	193	Area 2	EK 60, EM 710
29.08.	28	16828	CTD	04:38		04:55	05:14			78°37.224'	ca. 9°24.685'	383.5	Area 3	oxygen sensor out of order
29.08.	29	16829	HS	08:49			08:53	78°37.25'	9°22.73'	78°36.842'	9°27.056'	357	Area 3	EK 60, EM 710
29.08.	30-1	16830-1	GC - 3m	11:58		12:18	12:38			78°41.084'	8°16.553'	884.5	Pockmark Area	overpenetration

Appendix 1: Station List continued

HE - 387															
				Time (UTC)			Begin / on seafloor		End / off seafloor				Recovery	
Date 2012	St. No. He 387	GeoB No.	Instrument	Begin	Start Sci. Program	End Sci. Program	End	Latitude N°	Longitude W°	Latitude N°	Longitude W°	Water depth (m)	Area	Remarks
29.08.	30-2	16830-2	QC - 6m	13:16		15:31	13:50			78°41.114'	8°16.891'	884.2	Pockmark Area	361 cm recovery
29.08.	30-3	16830-3	QC - 6m	14:18		14:32	14:52			78°41.335'	8°15.780'	912	Pockmark Area	424 cm recovery
29.08.	31-1	16831-1	HS	16:29			16:04	78°44.37'	8°22.26'	78°41.28'	8°27.47'	797	Pockmark Area	
29.08.	31-2	16831-2	SVP	16:04		16:17	16:26			78°41.27'	8°27.40'	835.3	Pockmark Area	
29.08.	31-3	16831-3	HS	16:26			04:54	78°41.28'	8°27.35'	78°41.10'	8°16.58'	861	Pockmark Area	
30.08.	32	16832	CTD	04:12		04:33	04:56			78°41.075'	8°16.635'	886	Pockmark Area	
30.08.	33	16833	ROV Dive 06	06:57	07:14	12:30	13:00	78°37.233'	9°24.538'	78°37.091'	9°24.566'	382	Area 3	Tritech sonar
30.08.	33-1	16833-1	Marker 5			07:36				78°37.22022'	9°24.56883'	381	Area 3	
30.08.	33-2	16833-2	@BS 1			07:59				78°37.21648'	9°24.55922'	382	Area 3	
30.08.	33-3	16833-3	@BS 2			09:40				78°37.21032'	9°24.5697'	384	Area 3	
30.08.	33-4	16833-4	Marker 3			09:56				78°37.2093'	9°24.5652'	384	Area 3	
30.08.	33-5	16833-5	Clay sample			11:03				78°37.1657'	9°24.39245'	387	Area 3	
30.08.	33-6	16833-6	Clay sample			11:23				78°37.16918'	9°24.40842'	386	Area 3	
30.08.	33-7	16833-7	Riskin			12:23				78°37.209'	9°24.58304'	384	Area 3	
30.08.	34	16834	HS	13:10			10:20	78°37.977'	9°26.099'	78°33.304'	9°28.376'	253	Shelf	EK 60, EM 710, SES 2000
31.08.	35-1	16835-1	HS	10:16			19:29	78°32.85'	9°28.84'	78°37.78'	9°23.75'	386	Area 2	EK 60, EM 710
01.09.	35-2	16835-2	HS	20:01			07:19	78°36.90'	9°21.16'	78°33.43'	9°58.48'	283	Shelf	EK 60, EM 710
01.09.	36-1	16836-1	CTD	08:30		08:40	08:52			78°44.261'	10°15.377'	57	Cross section	
01.09.	36-2	16836-2	HS	08:54			10:36	78°44.94'	10°15.21'	78°40.08'	9°25.39'	ca.	Cross section	EK 60, EM 710, SES 2000
01.09.	37-1	16837-1	CTD	10:45		10:56	11:11			78°39.825'	9°25.812'	272	Cross section	
01.09.	37-2	16837-2	HS	11:14			12:42	78°39.71'	9°26.49'	78°36.87'	8°44.94'	582	Cross section	EK 60, EM 710, SES 2000
01.09.	38-1	16838-1	CTD	12:47		13:08	13:28			78°36.735'	8°44.431'	742	Cross section	
01.09.	38-2	16838-2	HS	14:04			15:11	78°36.518'	8°44.158'	78°30.62'	8°56.627'	792	Cross section	EK 60, EM 710, SES 2000
01.09.	39-1	16839-1	CTD	16:14		15:35	15:58			78°30.615'	8°56.064'	650	Cross section	
01.09.	39-2	16839-2	HS	16:34			19:00	78°30.60'	8°55.78'	78°36.05'	10°2.65'	600	Cross section	EK 60, EM 710, SES 2000
01.09.	40-1	16840-1	CTD	19:00		19:06	19:16			78°36.105'	10°03.207'	94	Cross section	
01.09.	40-2	16840-2	HS	20:04			20:45	78°36.16'	10°3.21'	78°37.92'	10°24.56'	86	Cross section	EK 60, EM 710, SES 2000

Appendix 1: Station List continued

HE - 387				Time (UTC)			Begin / on seafloor		End / off seafloor				Recovery Remarks
Date 2012	St. No He 387	GeoB No.	Gear (instrument)	Begin	Start Sci. Program	End Sci. Program	End	Latitude N°	Longitude W°	Latitude N°	Longitude W°	Water depth (m)	Area	
01.09.	41-1	16841-1	CTD	20:48		20:59	21:10			78°38.024'	10°25.336'	85	Cross section	
01.09.	41-2	16841-2	HS	21:45		23:07	78°38.01'	10°23.18'		78°30.39'	10°37.52'	110	Cross section	EK 60, EM 710, SES 2000
01.09.	42-1	16842-1	CTD	23:10		23:18	23:28			78°30.342'	10°38.252'	114,3	Cross section	
01.09.	42-2	16842-2	HS	23:55		01:38	78°30.245'	10°39.377'		78°26.681'	9°57.408'	160	Cross section	EK 60, EM 710, SES 2000
02.09.	43-1	16843-1	CTD	01:38		01:47	01:58			78°26.667'	9°57.535'	180	Cross section	
02.09.	43-2	16843-2	HS	02:29		04:18	78°25.712'	9°57.710'		78°22.334'	9°12.066'	550	Cross section	EK 60, EM 710, SES 2000
02.09.	44-1	16844-1	CTD	04:29		04:48	05:10			78°22.399'	9°12.420'	920	Cross section	
02.09.	45-1	16845-1	HS	05:01		06:32	78°22.176'	9°14.818'		78°15.748'	9°39.656'	550	South of Area 3	EK 60, EM 710
02.09.	45-2	16845-2	HS	08:32		11:08	78°15.748'	9°39.656'		78°31.076'	9°24.131'	390	South of Area 3	EK 60, EM 710
02.09.	45-3	16845-3	HS	11:08		11:54	78°31.076'	9°24.131'		78°35.373'	9°26.472'	430	South of Area 3	EK 60, EM 710
02.09.	46	16846	ROV Dive 07	12:10	12:29	15:17	15:45	78°35.402'	9°26.298'	78°35.381'	9°26.621'	386	Area 3	Tritech sonar
02.09.	46-1	16846-1	BC			13:30				78°35.38025'	9°26.62686'	385	Area 3	
02.09.	46-2	16846-2	BC			13:38				78°35.37948'	9°26.62344'	385	Area 3	
02.09.	46-3	16846-3	BC			13:40				78°35.37996'	9°26.62668'	385	Area 3	
02.09.	46-4	16846-4	BC			13:46				78°35.37965'	9°26.62584'	385	Area 3	
02.09.	46-5	16846-5	BC			14:03				78°35.38176'	9°26.60082'	385	Area 3	
02.09.	46-6	16846-6	BC			14:17				78°35.38122'	9°26.60442'	385	Area 3	
02.09.	46-7	16846-7	Niskin			15:14				78°35.38014'	9°26.8311'	384	Area 3	
02.09.	47-1	16847-1	HS	15:51		16:26	78°35.236'	9°26.611'		78°31.133'	9°27.486'	432	South of Area 3	EK 60, EM 710
02.09.	47-2	16847-2	HS	16:26		06:11	78°31.133'	9°27.486'		78°38.71'	9°11.23'	443	South of Area 3	EK 60, EM 710
03.09.	47-3	16847-3	HS	06:11		07:10	78°38.71'	9°11.23'		78°33.36'	9°28.55'	422	South of Area 3	EK 60, EM 710
03.09.	48	16848	ROV Dive 08	07:07	07:25	13:02	13:24	78°33.381'	9°28.497'	78°33.433'	9°28.250'	391	Area 3	Tritech sonar
03.09.	48-1	16848-1	Marker			07:42		28.50942		78°33.33365'	9°28.50942'	387,1	Area 3	
03.09.	48-2	16848-2	GBS			08:06		28.55626		78°33.32615'	9°28.55826'	386,7	Area 3	
03.09.	48-3	16848-3	Niskin			12:59		28.62408		78°33.43565'	9°28.62408'	389,7	Area 3	

Appendix 1: Station List continued

HE - 387				Time (UTC)			Begin / on seafloor		End / off seafloor				Recovery
Date 2012	St. No. He 387	GeoB No.	Instrument	Begin	Start Sci. Program	End Sci. Program	End	Latitude N°	Longitude W°	Latitude N°	Longitude W°	Water depth (m)	Area	Remarks
03.09	49-1	16849-1	HS	13:30			14:35			78°32.88'	10°11.74'	93	Shelf	EK 60, EM 710
03.09	49-2	16849-2	HS	14:35			14:59	78°32.88'	10°11.74'	78°32.85'	10°14.50'	95	Area 1	EK 60, EM 710
03.09	50	16850	Moor	15:46			16:02	78°32.88'	10°14.52'	78°32.88'	10°14.54'	92	Area 1	mooring deployed
03.09	51	16851	HS	17:11			23:05	78°32.45'	9°30.20'	78°32.56'	9°29.13'	397	Area 3	EK 60, EM 710
03.09	52-1	16852-1	HS	23:33			04:45	78°33.95'	9°37.53'	78°34.19'	9°41.90'	162	Shelf	EK 60, EM 710
04.09	52-2	16852-2	Moor	05:01			06:01	78°32.89'	10°14.48'	78°32.89'	10°14.48'	90.5	Area 1	hydrophone back on board
04.09	53	16853	ROV Dive 09	06:50	06:57	11:58	12:15	78°34.450'	10°10.040'	78°34.491'	10°10.252'	90	Area 1	Tritech sonar
04.09	53-1	16853-1	BC			09:50				78°34.4837'	10°10.2468'	90	Area 1	
04.09	53-2	16853-2	BC			09:55				78°34.4948'	10°10.2487'	90	Area 1	
04.09	53-3	16853-3	BC			10:01				78°34.4945'	10°10.2473'	90	Area 1	
04.09	53-4	16853-4	BC			10:31				78°34.4958'	10°10.2508'	90	Area 1	
04.09	53-5	16853-5	BC			10:40				78°34.4952'	10°10.2505'	90	Area 1	
04.09	53-6	16853-6	BC			10:50				78°34.4964'	10°10.2533'	90	Area 1	
04.09	53-7	16853-7	BC			11:25				78°34.4964'	10°10.2598'	90	Area 1	
04.09	54	16854	HS	12:20			13:11	78°34.47'	10°9.48'	78°34.91'	10°08.48'	85	Area 1	EK 60, EM 710
04.09	55-1	16855-1	HS	13:12			16:58	78°34.94'	10°08.23'	78°34.50'	10°10.20'	89	Area 1	flare hunting II'
04.09	55-2	16855-2	CTD	14:28		14:41	14:52			78°34.494'	10°10.234'	92	Area 1	in flare
04.09	56-1	16856-1	HS	17:06			14:45	78°34.74'	10°09.16'	78°35.75'	10°09.46'	92	Shelf	EK 60, EM 710
05.09	56-2	16856-2	HS	14:45			18:04	78°35.75'	10°09.46'	78°44.100'	9°00.689'	400	Shelf	EK 60, EM 710, SES 2000
05.09	57-1	16857-1	HS	18:05			22:24	78°44.029'	8°00.638'	78°41.90'	8°17.27'	961	Pockmark Area	EK 60, EM 710, SES 2000
05.09	57-2	16857-2	HS	22:24			10:01	78°41.90'	8°17.27'	78°41.705'	7°58.318'	1020	Pockmark Area	EK 60, EM 710, SES 2000
06.09	58	16858	HS	10:01			17:22	78°41.705'	7°58.318'	78°37.45'	9°39.94'	429	North of Area 3	EK 60, EM 710, SES 2000
06.09	59	16859	HS	17:23			09:42	78°37.37'	9°40.29'	78°30.73'	10°00.00'	148	North of Area 3	EK 60, EM 710
08.09	60	16860	CTD	10:32		10:32	10:42			78°28.429'	10°17.693'	150	Shelf	
08.09	61	16861	HS	11:18			13:49	78°28.631'	10°16.470'	78°39.105'	09°25.885'	195	Shelf	EK 60, EM 710
08.09	62-1	16862-1	CTD	13:51		14:00	14:08			78°39.112'	9°25.852'	240	Area 2	water samples

Appendix 1: Station List continued

HE - 387

Date 2012	St. No. He 387	GeoB No.	Instrument	Time (UTC) Begin	Start Sci. Program	End Sci. Program	End	Begin / on seafloor Latitude N°	Longitude W°	End / off seafloor Latitude N°	Longitude W°	Water depth (m)	Area	Recovery Remarks
08.09.	82-2	16882-2	CTD	14:31		14:38	14:44			78°39.115'	9°26.002'	240	Area 2	water samples
08.09.	82-3	16882-3	CTD	15:03		15:10	15:14			78°39.115'	9°25.958'	240	Area 2	water samples
08.09.	83	16883	HS	15:33			21:15	78°37.87'	9°24.14'	78°37.80'	9°23.45'	364	Area 3	EK 60, EM 710
09.09.				05:00			10:00	Portcall Longyearbyen						
09.09.	84-1	16884-1	MUC	17:46		18:07	18:40			77°31.409'	10°19.365'	1298	On transit south	4 good corers
09.09.	84-2	16884-2	MUC	18:57		19:17	20:00			77°31.850'	10°18.935'	1313	On transit south	4 good corers
09.09.	84-3	16884-3	MUC	20:07		20:28	22:11			77°32.195'	10°18.585'	1312	On transit south	3 good corers

Abbreviations:

CTD (Conductivity temperature depth)
MUC (Multicorer)
GC (Gravity Corer)
SVP (Sound Velocity Probe)
HS (Hydroacoustic Surveys)
Moor (Mooring)
ROV (Remotely Operated Vehicle CHEROKEE)
GBS (Gas Bubble Sampler)
BC (Bubble Catcher)
Niskin (Niskin water sample bottle on ROV)
Marker No. (Physical Marker on Seafloor)
Claw sample (Sampled by ROV manipulator)

Appendix 2: Hydroacoustic Surveys

GeoB - Nr.	Start / End	Date	Time (UTC)	Device	Objective	Observations
16802-1	start	21/08/2012	14:50	EM710, EK60 and partially also SES2000	calibating setlings during transit	lots of flares in EK60 and EM710
	end	21/08/2012	19:07	EM710, EK60 and partially also SES2001	calibating setlings during transit	lots of flares in EK60 and EM711
16802-2	start	21/08/2012	19:07	EM710 and EK60	Bathymetry and flare mapping	lots of flares in EK60 and EM710
	end	22/08/2012	6:39	EM710 and EK60	Bathymetry and flare mapping	ending line 69
16802-3	start	22/08/2012	6:39	EM710 and EK60	Transit	starting line 70
	end	22/08/2012	6:57	EM710 and EK60	Bathymetry and flare mapping	ending line 71
16802-4	start	22/08/2012	6:57	EM710 and EK60	Bathymetry and flare mapping	starting line 72
	end	22/08/2012	9:49	EM710 and EK60	Bathymetry and flare mapping	End due to time
16802-5	start	22/08/2012	9:49	EM710 and EK60	Transit	transit to SVP station
	end	22/08/2012	10:19	EM710 and EK60	Transit	
16804	start	22/08/2012	10:55	EM710 and EK60	multibeam calibration	
	end	22/08/2012		EM710 and EK60	multibeam calibration	
16806-1	start	22/08/2012	16:14	EM710 and EK60	Transit	
	end	22/08/2012	16:43	EM710 and EK60	Transit	
16806-2	start	22/08/2012	16:43	EM710 and EK60	Bathymetry and flare mapping	finish the last survey, which was stopped due to time
	end	22/08/2012	19:50	EM710 and EK60	Bathymetry and flare mapping	
16806-3	start	22/08/2012	19:50	EM710 and EK60	Transit	
	end	22/08/2012	20:20	EM710 and EK60	Transit	
16806-4	start	22/08/2012	20:20	EM710 and EK60	Bathymetry and flare mapping	
	end	23/08/2012	7:30	EM710 and EK60	Bathymetry and flare mapping	stop survey due to time
16809-1	start	23/08/2012	13:14	EM710 and EK60	Bathymetry and flare mapping	crossing the flare position of ROV dive01
	end	23/08/2012	15:01	EM710 and EK60	Bathymetry and flare mapping	
16809-2	start	23/08/2012	15:01	EM710 and EK60	Bathymetry and flare mapping	crossing active flare area further south than ROV dive 1 site
	end	23/08/2012	16:00	EM710 and EK60	Bathymetry and flare mapping	
16811-1	start	23/08/2012	16:35	EM710 and EK60	Transit	Transit to the point we stopped the survey GeoB16806-4

Appendix 2: Hydroacoustic Surveys, continued

GeoB - Nr.	Start / End	Date	Time (UTC)	Device	Objective	Observations
	end	23/08/2012	17:40	EM710 and EK60	Transit	
16811-2	start	23/08/2012	17:40	EM710 and EK60	Bathymetry and flare mapping	Finishing the survey GeoB16806-4
	end	24/08/2012	4:41	EM710 and EK60	Bathymetry and flare mapping	
16811-3	start	24/08/2012	4:41	EM710 and EK60	Transit	Transit to dive 01 location
	end	24/08/2012	6:00	EM710 and EK60	Transit	Reaching dive position
16813	start	24/08/2012	16:00	EM710 and EK60	Flare hunting	
	end	24/08/2012	17:55	EM710 and EK60	Flare hunting	
16814-2	start	24/08/2012	18:20	EM710 and EK60	Flare hunting	
	end	24/08/2012	22:42	EM710 and EK60	Flare hunting	
16815-1	start	24/08/2012	23:41	EM710 and EK60	Bathymetry and flare mapping	
	end	25/08/2012	4:55	EM710 and EK60	Bathymetry and flare mapping	
16817-1	start	25/08/2012	13:17	EM710 and EK60	Transit	Transit to fill in the gaps in the bathymetry
	end	25/08/2012	14:51	EM710 and EK60	Transit	
16817-2	start	25/08/2012	14:51	EM710 and EK60	Bathymetry and flare mapping	Survey in 280 m Flare Area
	end	26/08/2012	0:17	EM710 and EK60	Bathymetry and flare mapping	
16818	start	25/08/2012	0:29	EM710 and EK60	Bathymetry and flare mapping	Survey north along the 400 m isoline
	end	26/08/2012	4:42	EM710 and EK60	Bathymetry and flare mapping	
16819-1	start	25/08/2012	4:42	EM710 and EK60	Bathymetry and flare mapping	Survey in the 380m water depth
	end	26/08/2012	8:40	EM710 and EK60	Bathymetry and flare mapping	
16819-2	start	26/08/2012	8:20	EM710 and EK60	Transit	Steaming to 900m flare
	end	26/08/2012	9:58	EM710 and EK60	Transit	
16820-1	start	26/08/2012	9:58	EM710 and EK60	Bathymetry and flare mapping	Survey over 900m flare
	end	26/08/2012	13:05	EM710 and EK60	Bathymetry and flare mapping	
16820-2	start	26/08/2012	13:06	EM710 and EK60	Transit	Transit back to the 400m survey facing north
	end	26/08/2012	14:23	EM710 and EK60	Transit	
16821-1	start	26/08/2012	14:23	EM710 and EK60	Bathymetry and flare mapping	Survey continuation of the 400m isoline to the north and crossing of a possible flare in 750m water depth

Appendix 2: Hydroacoustic Surveys, continued

GeoB - Nr.	Start / End	Date	Time (UTC)	Device	Objective	Observations
	end	27/08/2012	9:30	EM710 and EK60	Bathymetry and flare mapping	
16825-1	start	27/08/2012	16:34	EM710 and EK60	Bathymetry and flare mapping	Survey continuation in the 380m flare area of station #19
	end	27/08/2012	20:48	EM710 and EK60	Bathymetry and flare mapping	
16825-2	start	27/08/2012	20:57	EM710 and EK60	Bathymetry and flare mapping	survey in the 380m flare area, east of 16825-1
	end	28/08/2012	5:47	EM710 and EK60	Bathymetry and flare mapping	
16827-1	start	28/08/2012	15:17	EM710 and EK60	Bathymetry and flare mapping	crossing cluster locations found during ROV dive for quantification with EK60
	end	28/08/2012	16:11	EM710 and EK60	Bathymetry and flare mapping	
16827-2	start	28/08/2012	16:11	EM710 and EK60	Bathymetry and flare mapping	Transit to Bathymetric survey - first part
	end	29/08/2012	3:52	EM710 and EK60	Bathymetry and flare mapping	
16828	start	29/08/2012	3:52	EM710 and EK60	Transit	transit to CTD station
	end	29/08/2012	4:33	EM710 and EK60	Transit	
16829-1	start	29/08/2012	6:49	EM710, EK60 and SES2000	Bathymetry and flare mapping	Bathymetric survey - flares at 250 m depth
	end	29/08/2012	9:35	EM710, EK60 and SES2000	Bathymetry and flare mapping	
16829-2	start	29/08/2012	9:35	EM710, EK60 and SES2000	Transit	Transit to 900m flare
	end	29/08/2012	11:23	EM710, EK60 and SES2000	Transit	
16831-1	start	29/08/2012	15:13	EM710, EK60 and SES2000	Bathymetry and flare mapping	Survey in 900m flare area
	end	30/08/2012	3:21	EM710, EK60 and SES2000	Bathymetry and flare mapping	
16831-2	start	30/08/2012	3:21	EM710, EK60 and SES2000	Transit	steaming to CTD station
	end	30/08/2012	4:12	EM710, EK60 and SES2000	Transit	
16832-2	start	30/08/2012	4:58	EM710, EK60 and SES2000	Transit	steaming to ROV station
	end	30/08/2012	6:50	EM710, EK60 and SES2000	Transit	
16834-1	start	30/08/2012	13:08	EM710 and EK60	Bathymetry and flare mapping	Bathymetric survey at the shelf - continuation of Station
	end	31/08/2012	8:09	EM710 and EK60	Bathymetry and flare mapping	
16834-2	start	31/08/2012	8:09	EM710 and EK60	Transit	
	end	31/08/2012	10:23	EM710 and EK60	Transit	
16835-1	start	31/08/2012	10:24	EM710 and EK60	Bathymetry and flare mapping	Repitition of St 19-1 to analyse the variability of the flares in 380m water depth

Appendix 2: Hydroacoustic Surveys, continued

GeoB - Nr.	Start / End	Date	Time (UTC)	Device	Objective	Observations
	end	31/08/2012	19:30	EM710 and EK60	Bathymetry and flare mapping	
16835-2	start	31/08/2012	19:45	EM710 and EK60	Bathymetry and flare mapping	line for mapping 400m flares
	end	31/08/2012		EM710 and EK60	Bathymetry and flare mapping	
16835-3	start	31/08/2012		EM710 and EK60	Bathymetry and flare mapping	
	end	01/09/2012	7:19	EM710 and EK60	Bathymetry and flare mapping	
16835-4	start	01/09/2012	7:19	EM710, EK60 and SES2010	Transit	transit to shallow site for CTD
	end	01/09/2012	8:28	EM710, EK60 and SES2010	Transit	
16836-2	start	01/09/2012	8:55	EM710, EK60 and SES2010	Subbottom survey	
	end	01/09/2012	10:36	EM710, EK60 and SES2010	Subbottom survey	
16837-2	start	01/09/2012	11:14	EM710, EK60 and SES2010	Subbottom survey	
	end	01/09/2012	12:43	EM710, EK60 and SES2010	Subbottom survey	
16838-2	start	01/09/2012	14:03	EM710, EK60 and SES2010	Subbottom survey	
	end	01/09/2012	15:10	EM710, EK60 and SES2010	Subbottom survey	
16839-2	start	01/09/2012	16:34	EM710, EK60 and SES2010	Subbottom survey	
	end	01/09/2012	19:00	EM710, EK60 and SES2010	Subbottom survey	
16840-2	start	01/09/2012	20:00	EM710, EK60 and SES2010	Subbottom survey	
	end	01/09/2012	20:46	EM710, EK60 and SES2010	Subbottom survey	
16841-2	start	01/09/2012	21:44	EM710, EK60 and SES2010	Subbottom survey	
	end	01/09/2012	23:09	EM710, EK60 and SES2010	Subbottom survey	
16842-2	start	01/09/2012	23:55	EM710, EK60 and SES2010	Subbottom survey	
	end	02/09/2012	1:36	EM710, EK60 and SES2010	Subbottom survey	
16843-2	start	02/09/2012	2:29	EM710, EK60 and SES2010	Subbottom survey	
	end	02/09/2012	4:18	EM710, EK60 and SES2010	Subbottom survey	
16845-1	start	02/09/2012	5:46	EM710, EK60 and SES2010	Transit	transit to upper slope south HS
	end	02/09/2012	8:32	EM710, EK60 and SES2010	Transit	
16845-2	start	02/09/2012	8:32	EM710 and EK60	Bathymetry and flare mapping	Survey south of AREA 3
	end	02/09/2012	11:07	EM710 and EK60	Bathymetry and flare mapping	

Appendix 2: Hydroacoustic Surveys, continued

GeoB - Nr.	Start / End	Date	Time (UTC)	Device	Objective	Observations
16845-3	start	02/09/2012	11:07	EM710 and EK60	Transit	transit to AREA 3 dive 07location
	end	02/09/2012	11:54	EM710 and EK60	Transit	
16847-1	start	02/09/2012	15:51	EM710 and EK60	Transit	Transit from ROV dive07 position to survey start
	end	02/09/2012	16:26	EM710 and EK60	Transit	
16847-2	start	02/09/2012	16:26	EM710 and EK60	Bathymetry and flare mapping	Continuation of survey south of AREA 3 (station 45)
	end	03/09/2012	6:12	EM710 and EK60	Bathymetry and flare mapping	
16847-3	start	03/09/2012	6:12	EM710 and EK60	Transit	transit to AREA 3 dive 08 location
	end	03/09/2012	7:02	EM710 and EK60	Transit	
16849-1	start	03/09/2012	13:30	EM710 and EK60	Transit	transit to mooring location
	end	03/09/2012	14:37	EM710 and EK60	Transit	
16849-2	start	03/09/2012	14:37	EM710 and EK60	Bathymetry and flare mapping	Survey over the morring location
	end	03/09/2012		EM710 and EK60	Bathymetry and flare mapping	
16851-1	start	03/09/2012	16:15	EM710 and EK60	Transit	transit to temporal flare 380 m study
	end	03/09/2012	17:11	EM710 and EK60	Transit	
16851-2	start	03/09/2012	17:11	EM710 and EK60	Bathymetry and flare mapping	Repetition of the 4 Lines in AREA3 for temporal study of flare variability
	end	03/09/2012	23:05	EM710 and EK60	Bathymetry and flare mapping	
16852-1	start	03/09/2012	23:33	EM710 and EK60	Bathymetry and flare mapping	
	end	04/09/2012	4:45	EM710 and EK60	Bathymetry and flare mapping	
16852-2	start	04/09/2012	4:46	EM710 and EK60	Transit	transit to mooring location
	end	04/09/2012	5:48	EM710 and EK60	Transit	
16852-4	start	04/09/2012	6:01	EM710 and EK60	Transit	transit to ROV dive 09 position
	end	04/09/2012	6:58	EM710 and EK60	Transit	
16854	start	04/09/2012	12:13	EM710 and EK60	Flare mapping	Crossing flare at dive09 position for EK60 quantification in different directions - 3 times
	end	04/09/2012	13:11	EM710 and EK60	Flare mapping	
16855	start	04/09/2012	13:12	EM710 and EK60	Bathymetry and flare mapping	
	end	04/09/2012	16:58	EM710 and EK60	Bathymetry and flare mapping	

Appendix 2: Hydroacoustic Surveys, continued

GeoB - Nr.	Start / End	Date	Time (UTC)	Device	Objective	Observations
16856-1	start	04/09/2012	17:06	EM710 and EK60	Bathymetry and flare mapping	
	end	05/09/2012	14:47	EM710 and EK60	Bathymetry and flare mapping	
16856-2	start	05/09/2012	14:47	EM710, EK60 and also SES2000 from 15:50	Transit	Transit to 900m area
	end	05/09/2012	18:04	EM710, EK60 and SES2000	Transit	
16857-1	start	05/09/2012	18:04	EM710, EK60 and SES2000	Subbottom survey	Survey in the 900 m flare area to search for seep indications
	end	06/09/2012	22:24	EM710, EK60 and SES2000	Subbottom survey	Survey in the 900 m flare area to search for seep indications
16857-2	start	06/09/2012	22:24	EM710, EK60 and SES2000	Subbottom survey	Survey in the 900 m flare area to search for seep indications
	end	06/09/2012	23:36	EM710, EK60 and SES2000	Subbottom survey	Survey in the 900 m flare area to search for seep indications
16857-3	start	06/09/2012	23:36	EM710, EK60 and SES2000	Subbottom survey	Survey in the 900 m flare area to search for seep indications
	end	06/09/2012	10:01	EM710, EK60 and SES2000	Subbottom survey	Survey in the 900 m flare area to search for seep indications
16858	start	06/09/2012	10:01	EM710, EK60 and SES2000 until 11:05	Bathymetry and flare mapping	Bathymetric survey Outer shelf north
	end	06/09/2012	17:22	EM710 and EK60	Bathymetry and flare mapping	
16859-1	start	06/09/2012	17:22	EM710 and EK60	Bathymetry and flare mapping	bathymetric survey filling gaps and to southern flares
	end	08/09/2012	9:42	EM710 and EK60	Bathymetry and flare mapping	
16859-2	start	08/09/2012	9:42	EM710 and EK60	Transit	transit to CTD station
	end	08/09/2012	10:17	EM710 and EK60	Transit	
16861	start	08/09/2012	11:31	EM710 and EK60	Bathymetry and flare mapping during transit	During transit between CTD stations filling a gap in the bathymetry
	end	08/09/2012	13:49	EM710 and EK60	Bathymetry and flare mapping during transit	
16863	start	08/09/2012	15:14	EM710 and EK60	Bathymetry and flare mapping	Repetition of the variability survey: 4 lines in AREA3
	end	08/09/2012	21:15	EM710 and EK60	Bathymetry and flare mapping	

Appendix 3:CTD Profiles

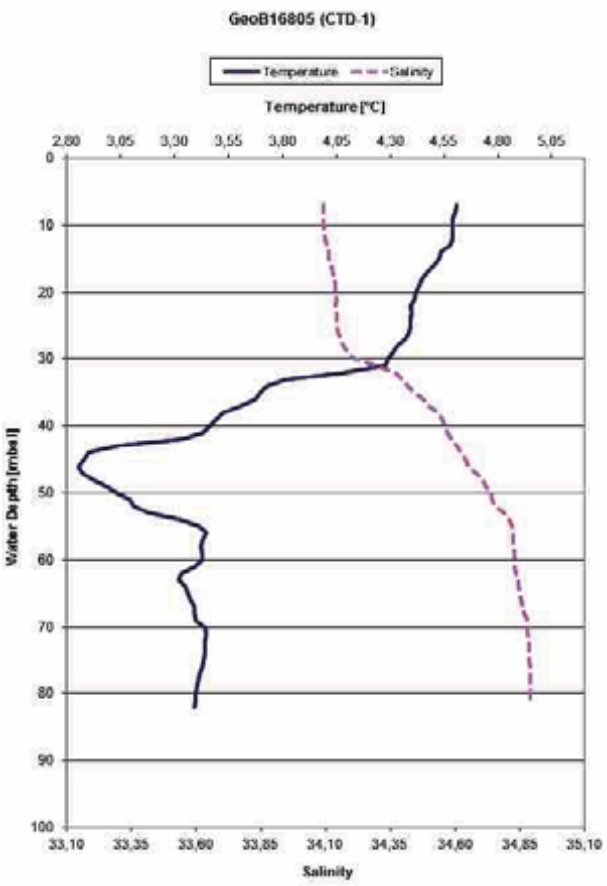

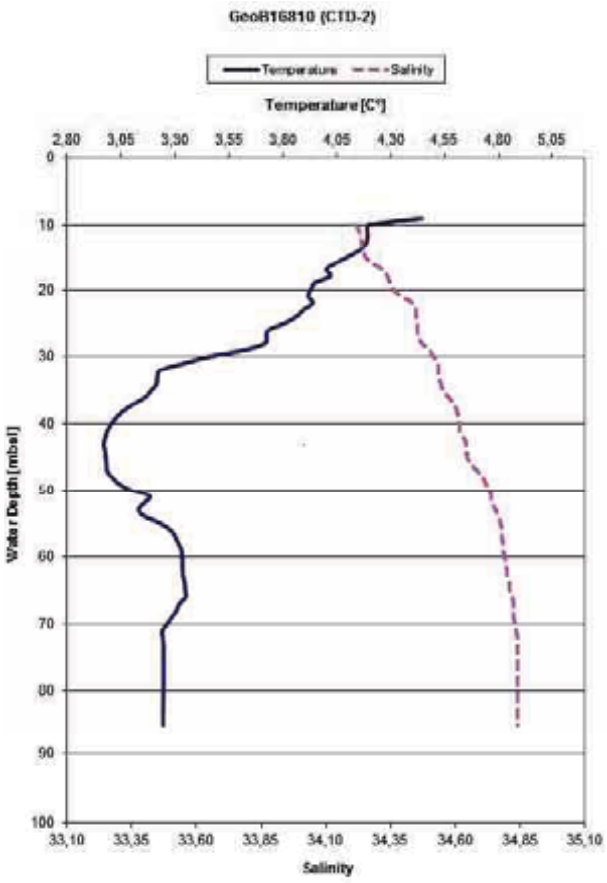

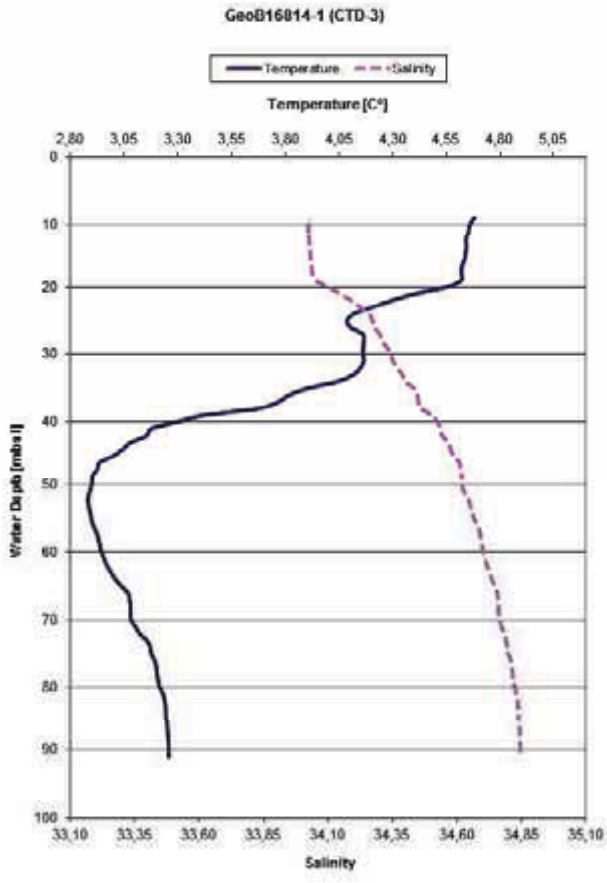

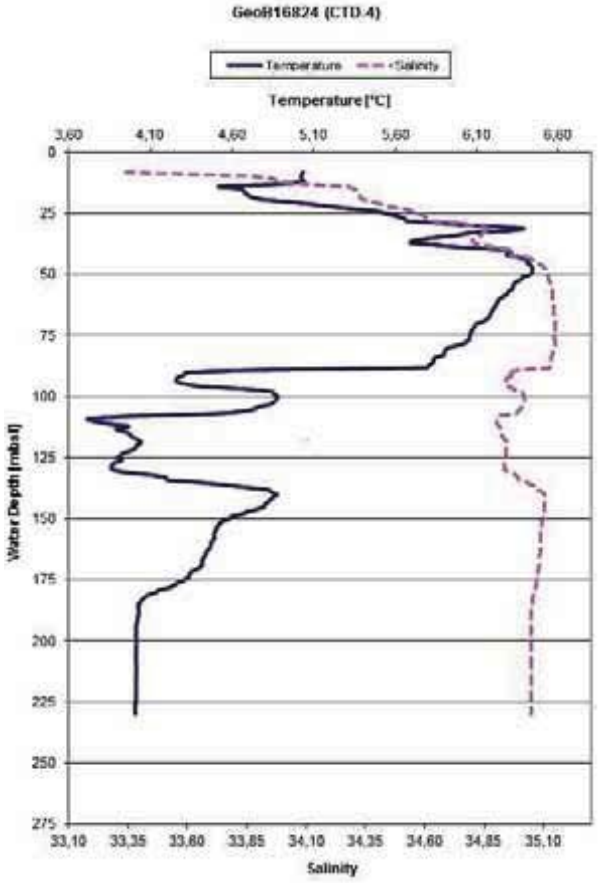

Appendix 3:CTD Profiles, continued

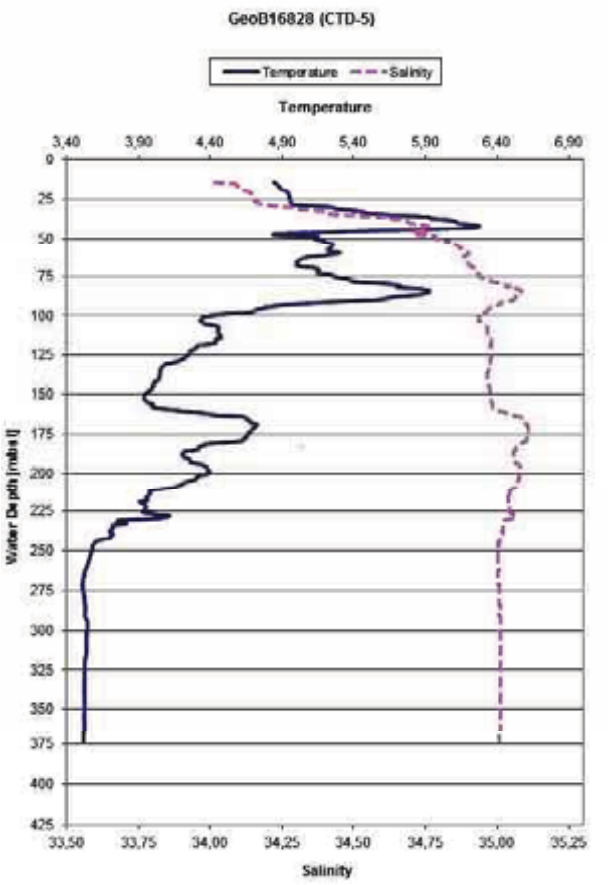

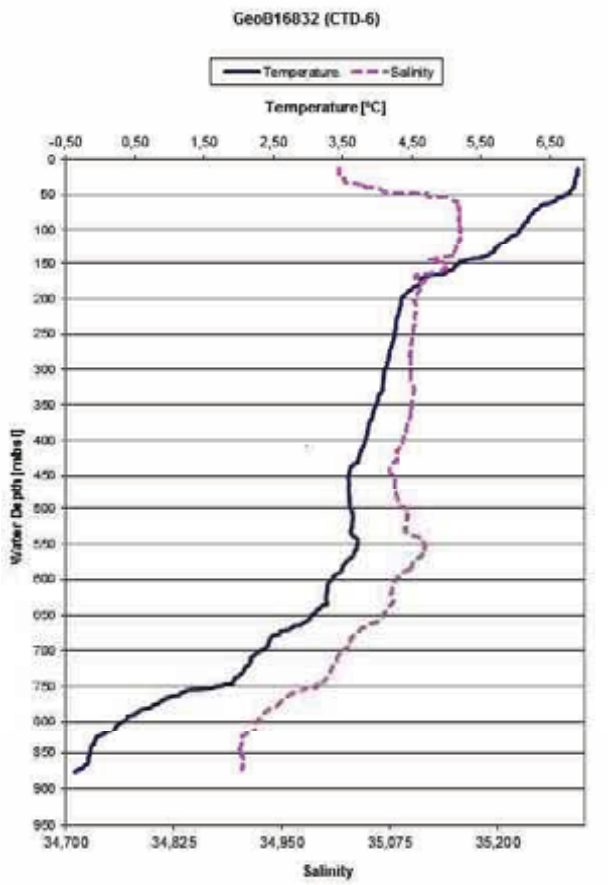

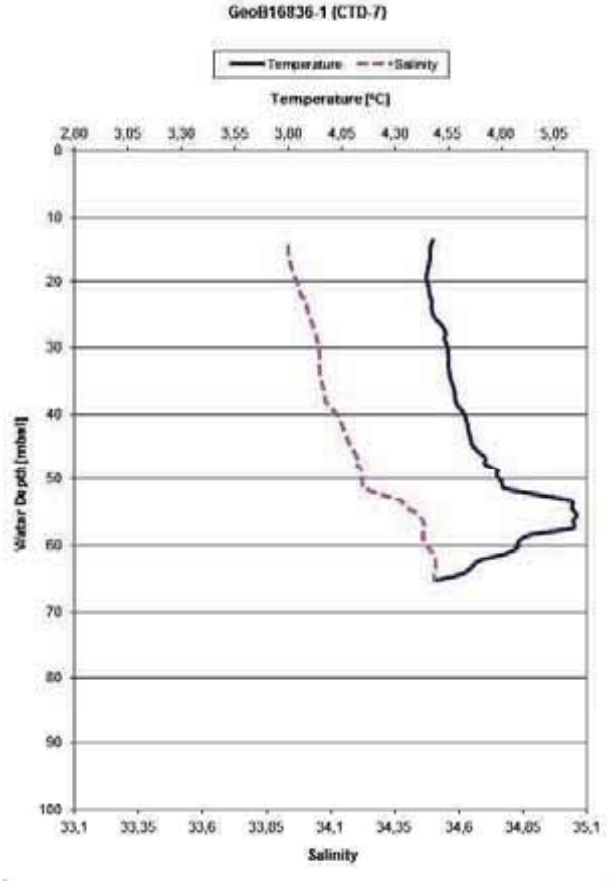

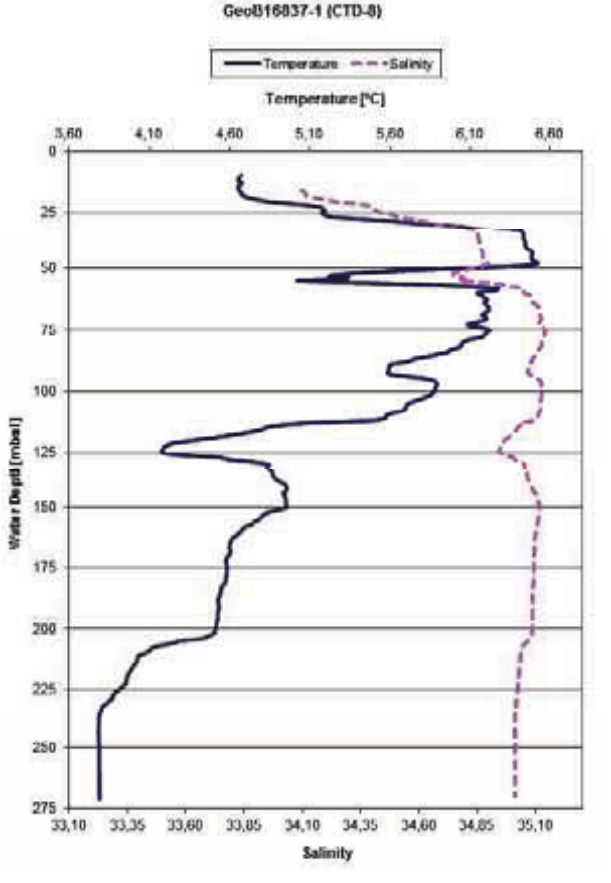

Appendix 3:CTD Profiles, continued

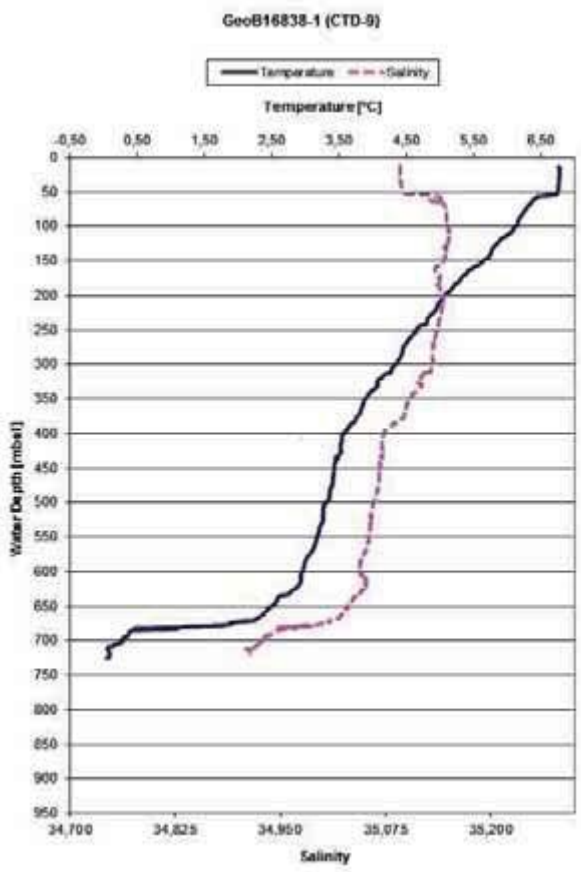

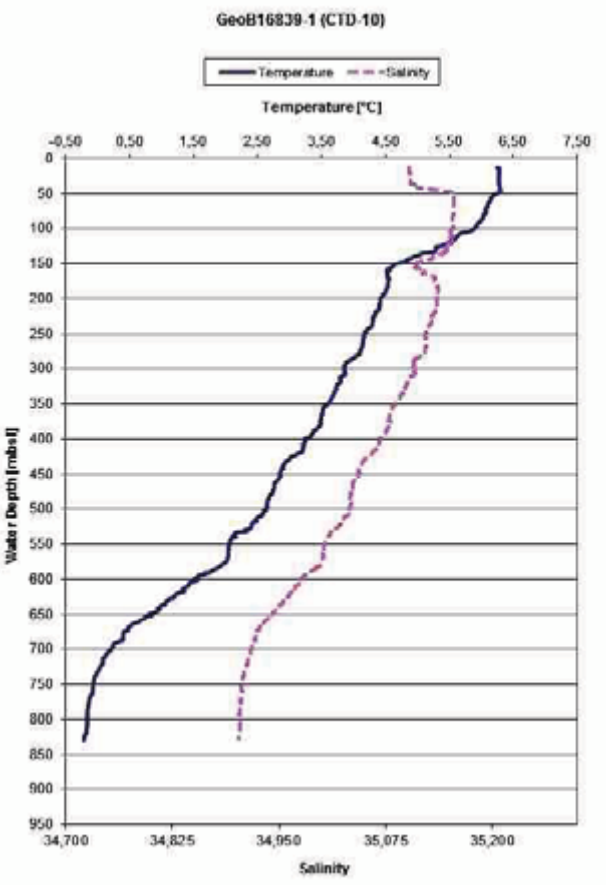

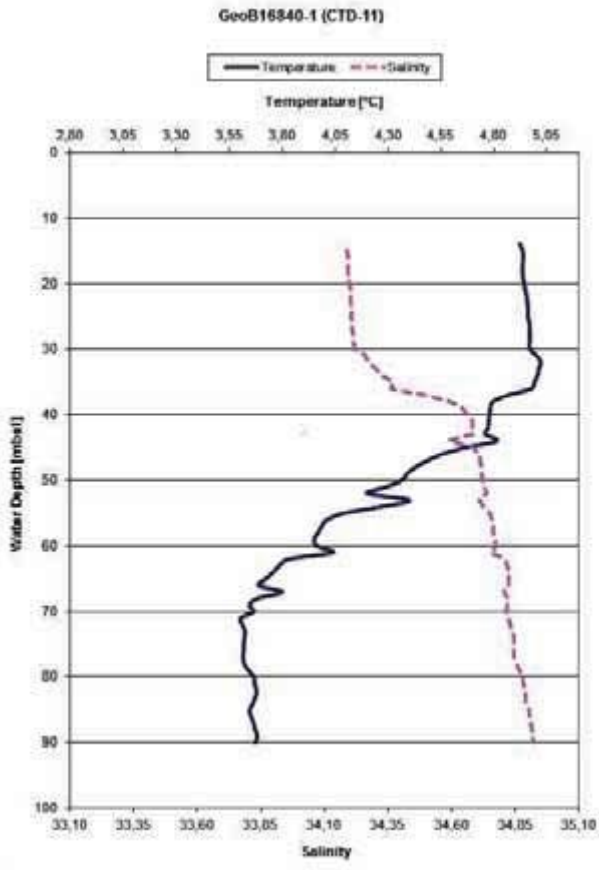

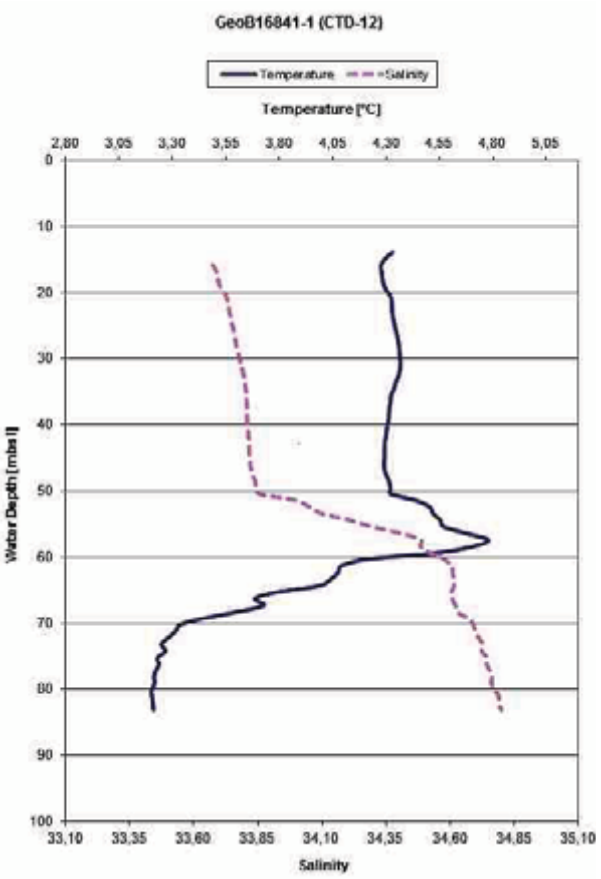

Appendix 3:CTD Profiles, continued

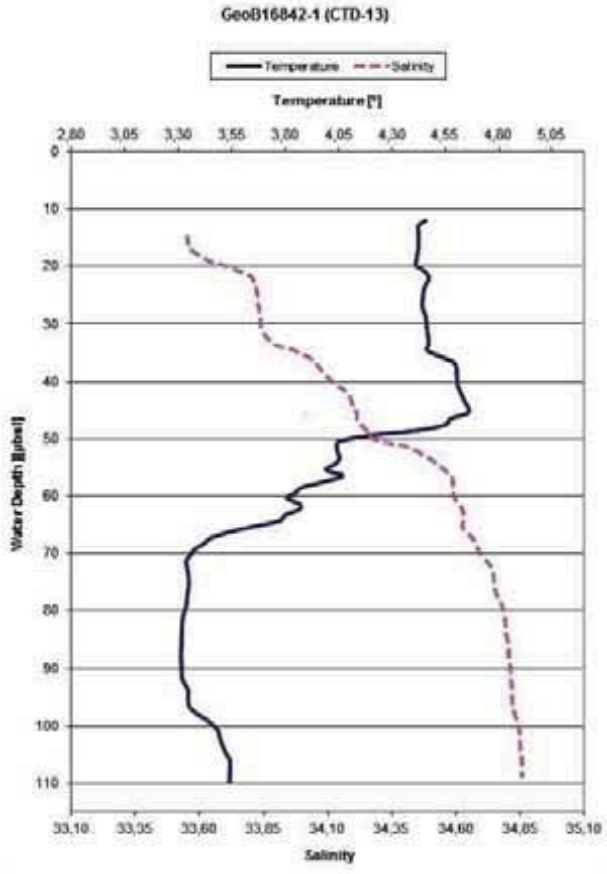

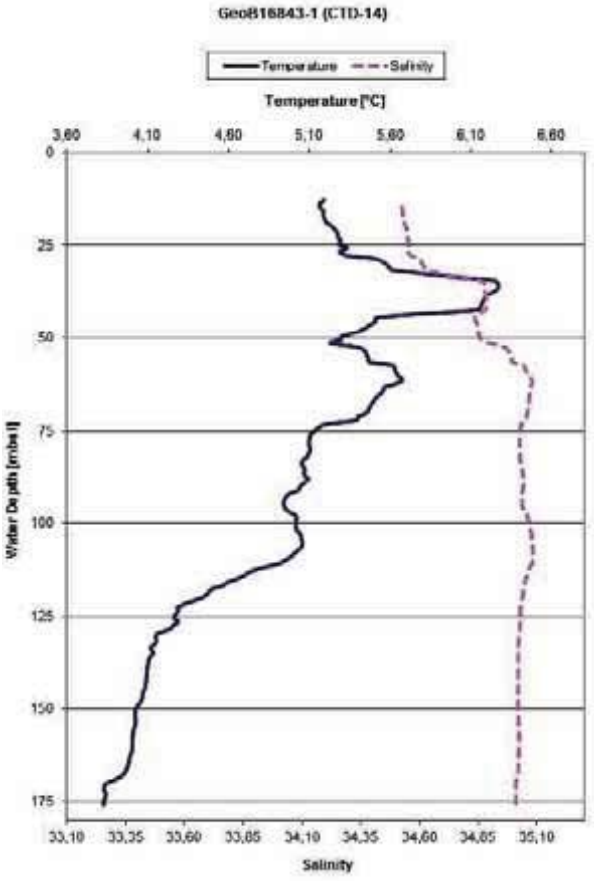

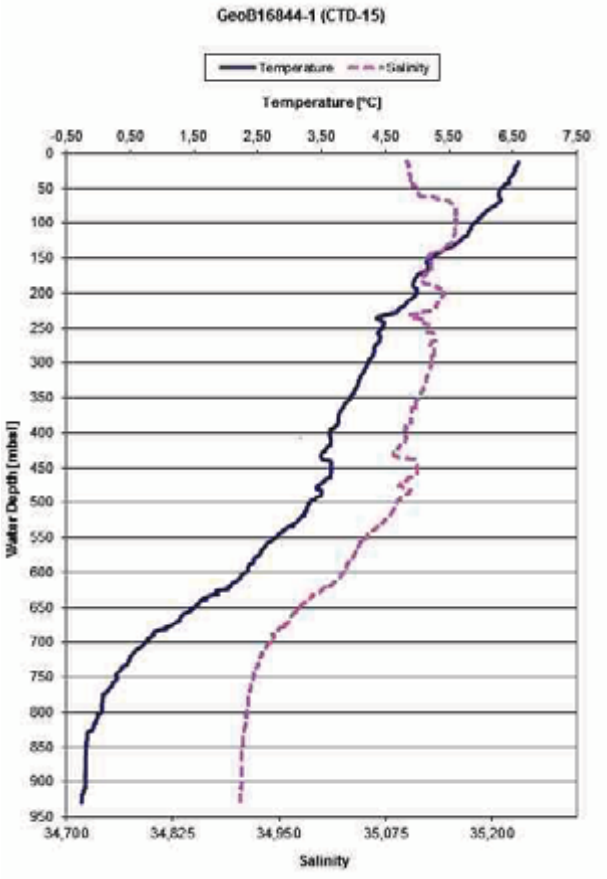

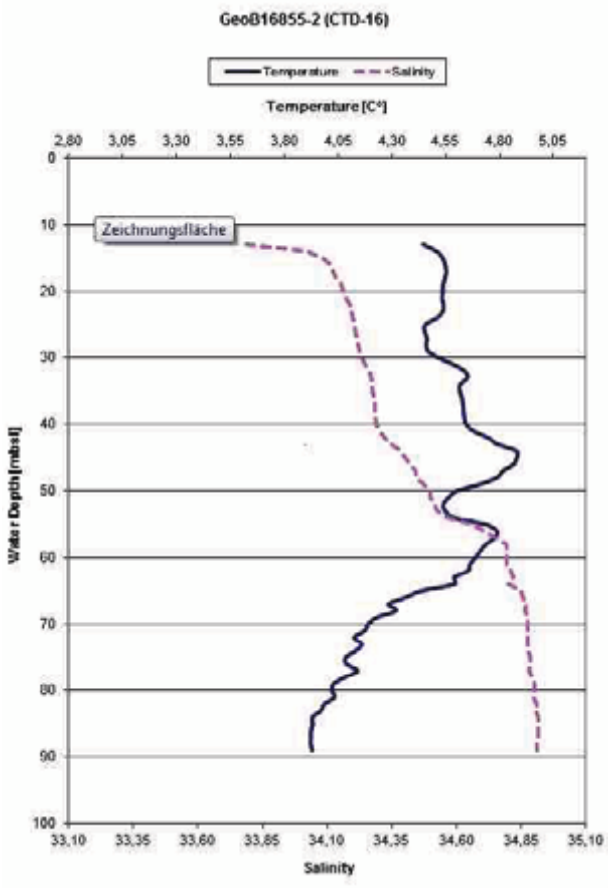

Appendix 3:CTD Profiles, continued

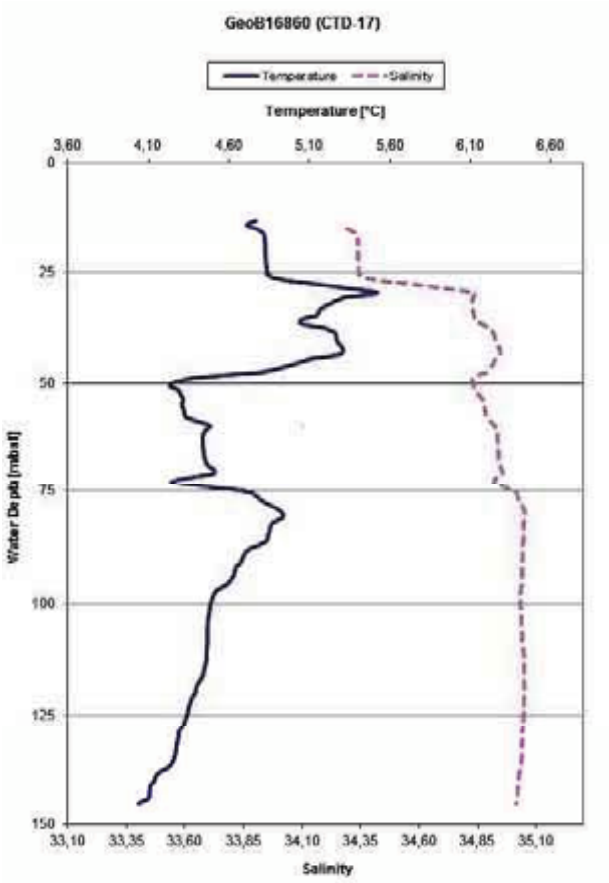

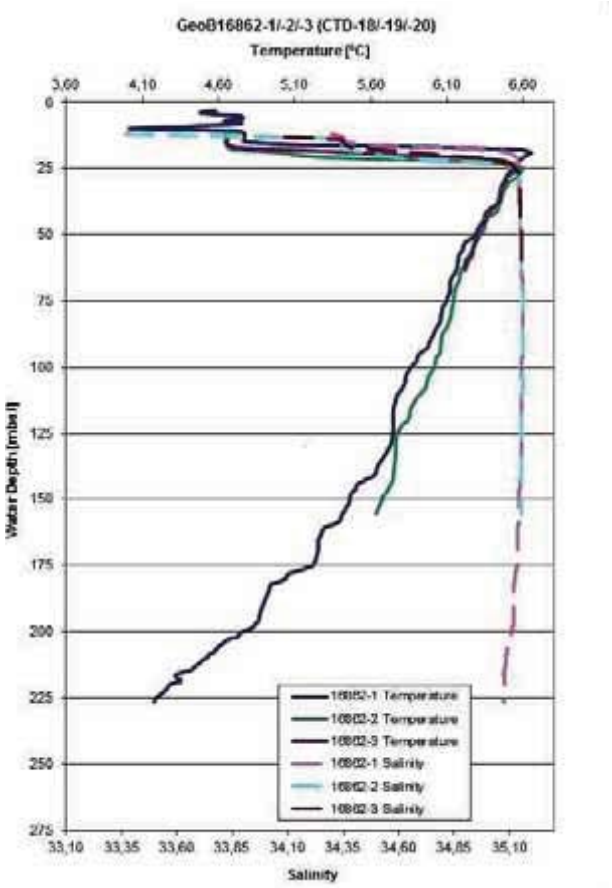

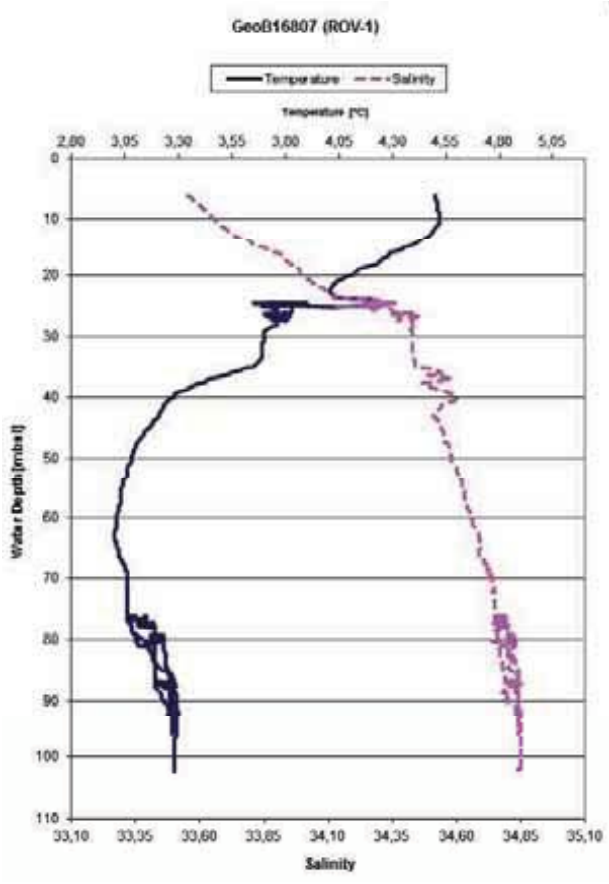

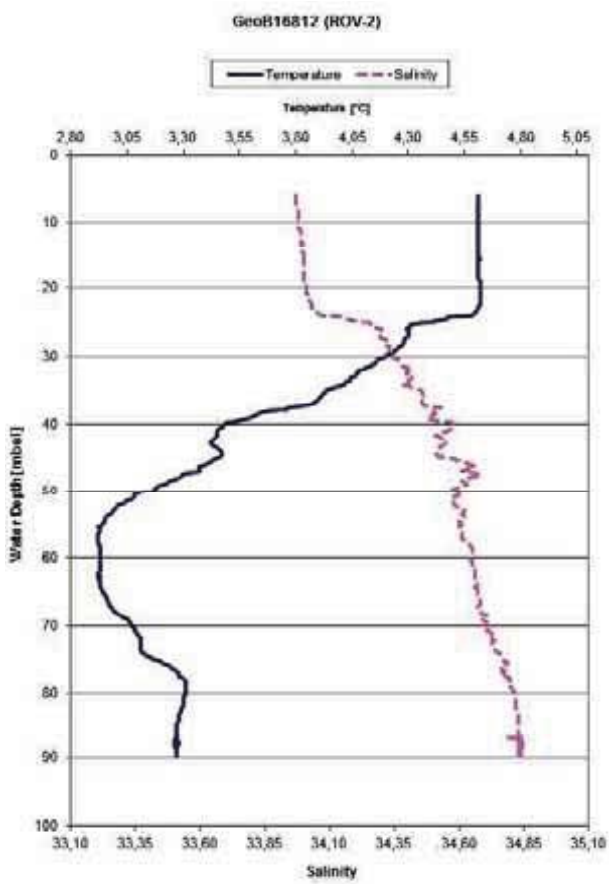

Appendix 3:CTD Profiles, continued

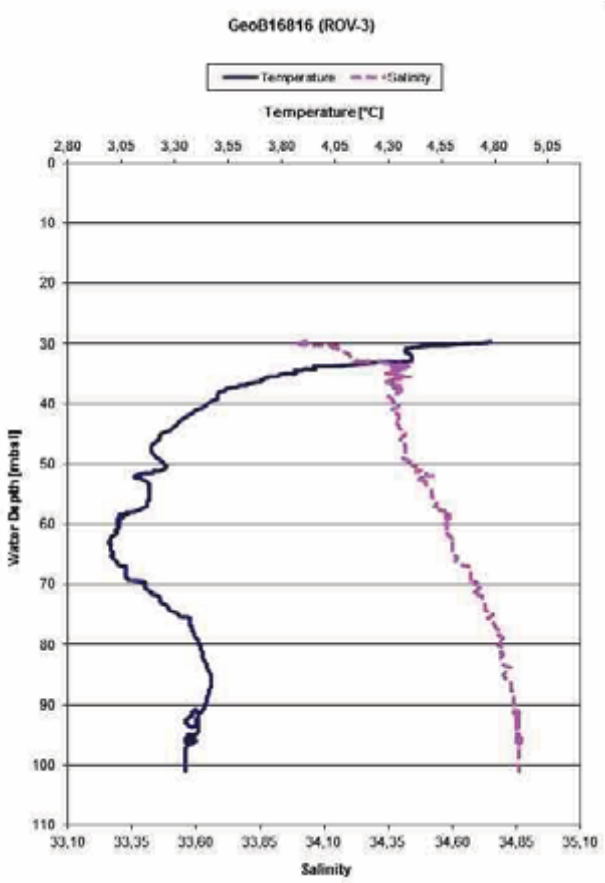

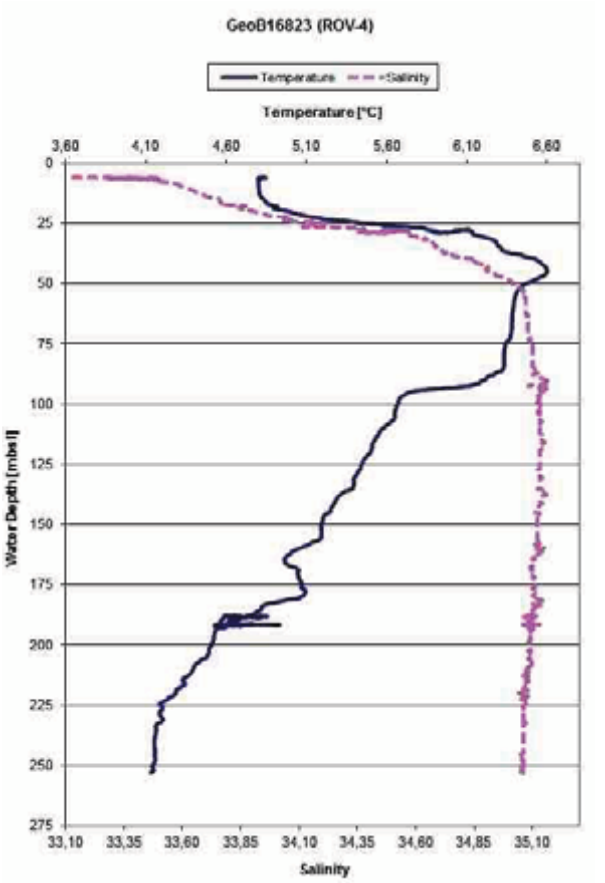

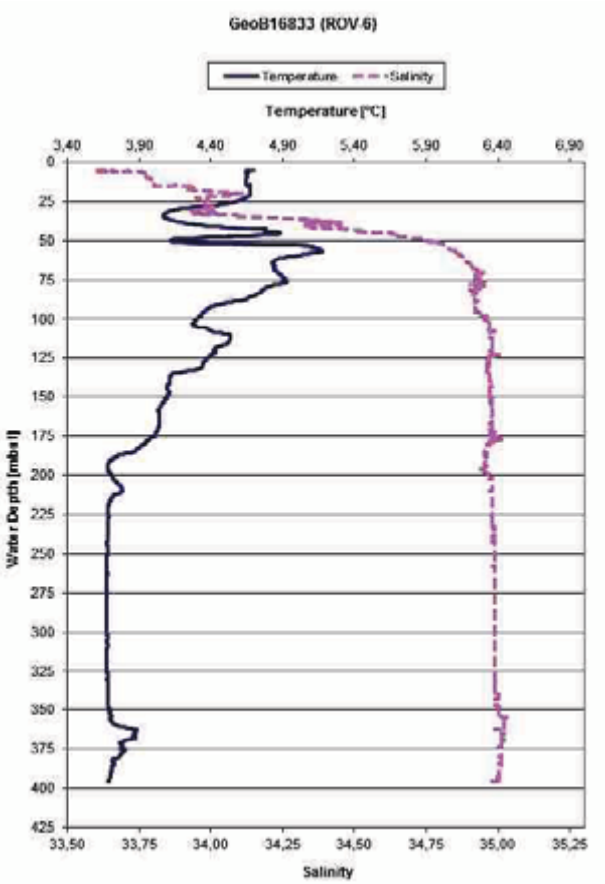

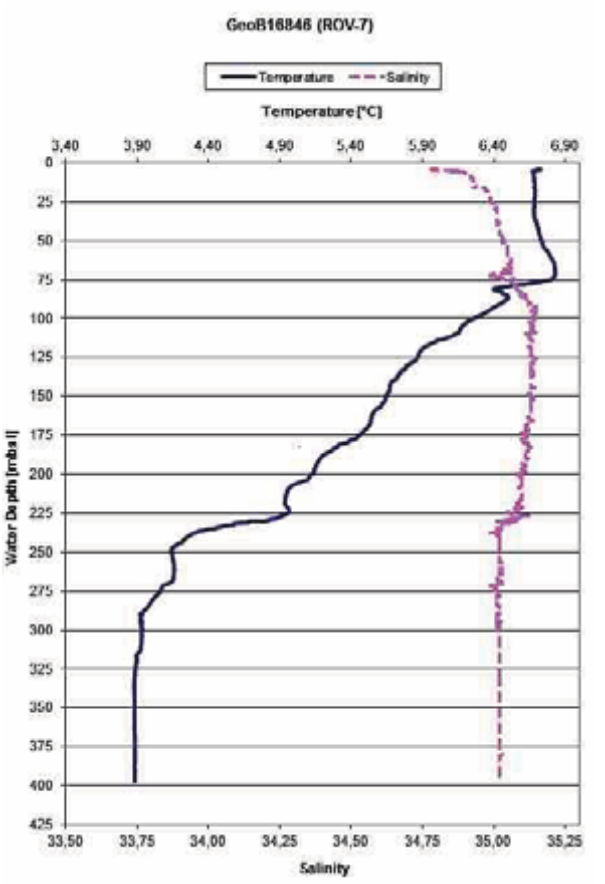

Appendix 3:CTD Profiles, continued

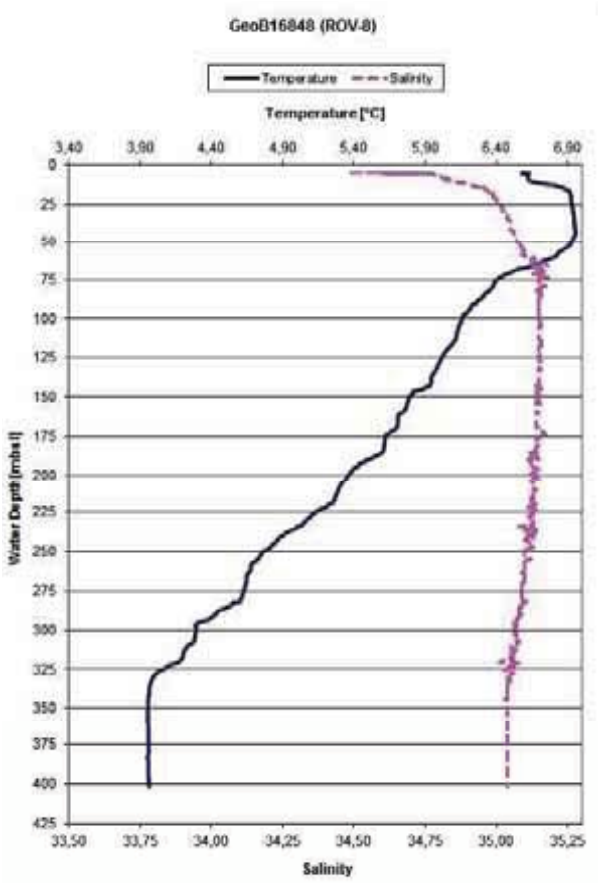

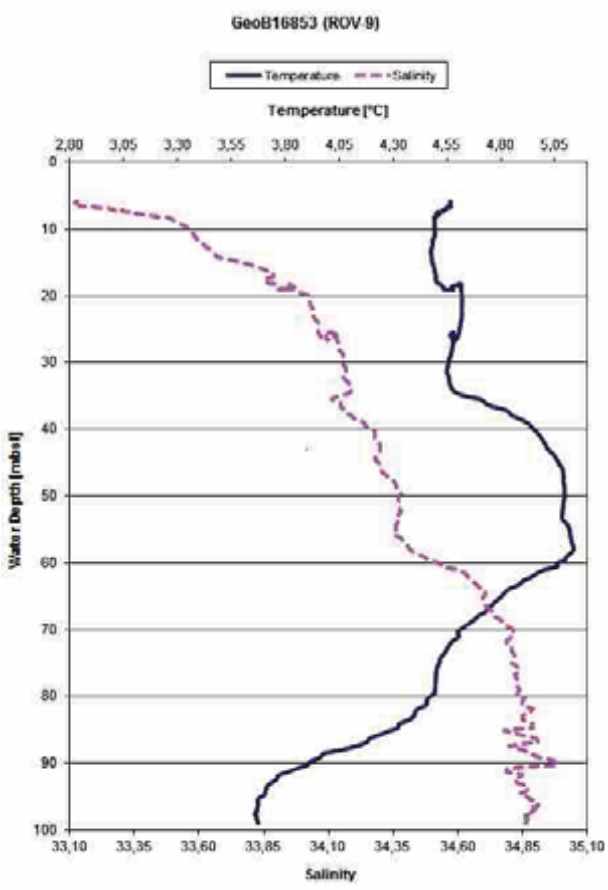

Appendix 4: List of Water and Gas Samples

Date	Tool	GeoB No.	Sample # (Bottle # / [ROV station #])	Water depth [mbsl]	Sample type	On board analytics Gas composition & concentration MARUM	Onshore analytics Pore water ingredients MARUM	Onshore analytics Gas purge & trap IOW
22.08.2012	CTD-1	16805	2	82,89	Dissolved gas	x		
			5	62,77	Dissolved gas	x		
			6	52,27	Dissolved gas	x		
			7	52,42	Dissolved gas	x		
			11	21,22	Dissolved gas	x		
			12	10,79	Dissolved gas	x		
23.08.2012	ROV-1	16807	[4]	94,00	Dissolved gas	x		
			[2]	94,00	Vent gas	x		
			[3]	94,00	Vent gas	x		
23.08.2012	CTD-2	16810	1	84,76	Dissolved gas	x		
			2	80,17	Dissolved gas	x		
			4	75,01	Dissolved gas	x		
			5	64,82	Dissolved gas	x		
			6	54,54	Dissolved gas	x		
			7	44,33	Dissolved gas	x		
			8	33,94	Dissolved gas	x		
			9	23,52	Dissolved gas	x		
			10	18,27	Dissolved gas	x		
			12	7,97	Dissolved gas	x		
24.08.2012	CTD-3	16814	1	89,80	Dissolved gas	x		
			2	85,24	Dissolved gas	x		
			4	79,97	Dissolved gas	x		
			5	75,14	Dissolved gas	x		
			6	65,11	Dissolved gas	x		
			7	49,36	Dissolved gas	x		
			8	33,75	Dissolved gas	x		
			9	23,36	Dissolved gas	x		
			10	18,23	Dissolved gas	x		
			11	13,19	Dissolved gas	x		
			12	7,70	Dissolved gas	x		
25.08.2012	ROV-3	16816	[10]	97,20	Dissolved gas	x		
27.08.2012	ROV-4	16823	[7]	240,00	Dissolved gas	x		
			[2]	242,00	Vent gas	x		

Appendix 4: List of Water and Gas Samples, continued

Date	Tool	GeoB No.	Sample # (Bottle # / [ROV station #])	Water depth [mbsl]	Sample type	On board analytics Gas composition & concentration MARUM	Onshore analytics Pore water ingredients MARUM	Onshore analytics Gas purge & trap IOW
			[5]	240,00	Vent gas	x		
27.08.2012	CTD-4	16824	1	229,39	Dissolved gas	x		x
			2	219,29	Dissolved gas	x		x
			4	209,29	Dissolved gas	x		x
			5	183,10	Dissolved gas	x		x
			6	157,48	Dissolved gas	x		x
			7	131,33	Dissolved gas	x		x
			8	105,75	Dissolved gas	x		x
			9	79,84	Dissolved gas	x		x
			10	54,41	Dissolved gas	x		x
			11	28,44	Dissolved gas	x		x
			12	7,79	Dissolved gas	x		x
29.08.2012	CTD-5	16828	1	373,66	Dissolved gas	x		
			2	369,60	Dissolved gas	x		
			4	363,81	Dissolved gas	x		
			5	358,61	Dissolved gas	x		
			6	353,35	Dissolved gas	x		
			7	312,26	Dissolved gas	x		
			8	209,26	Dissolved gas	x		
			9	105,88	Dissolved gas	x		
			10	54,48	Dissolved gas	x		
			12	7,90	Dissolved gas	x		
	GC	16830-3	1	15 cmbsf	Pore water		x	
			2	49 cmbsf	Pore water		x	
			3	99 cmbsf	Pore water		x	
			4	149 cmbsf	Pore water		x	
			5	199 cmbsf	Pore water		x	
			6	249 cmbsf	Pore water		x	
			7	299 cmbsf	Pore water		x	
			8	349 cmbsf	Pore water		x	
			9	399 cmbsf	Pore water		x	
30.08.2012	CTD-6	16832	1	877,08	Dissolved gas	x		
			2	859,68	Dissolved gas	x		

Appendix 4: List of Water and Gas Samples, continued

Date	Tool	GeoB No.	Sample #	Water depth	Sample type	On board analytics	Onshore analytics	Onshore analytics
			(Bottle # / [ROV station #])	[mbsl]		Gas composition & concentration	Pore water ingredients	Gas purge & trap
						MARUM	MARUM	IOW
			4	829,61	Dissolved gas	x		
			5	778,28	Dissolved gas	x		
			6	621,96	Dissolved gas	x		
			7	415,08	Dissolved gas	x		
			8	260,47	Dissolved gas	x		
			9	106,04	Dissolved gas	x		
			10	54,01	Dissolved gas	x		
			11	12,96	Dissolved gas	x		
			12	4,81	Dissolved gas	x		
30.08.2012	ROV-6	16833	[7]	384,00	Dissolved gas	x		
			[2]	382,00	Vent gas	x		
			[3]	384,00	Vent gas	x		
01.09.2012	CTD-7	16836-1	1	64,14	Dissolved gas	x		x
			2	62,03	Dissolved gas	x		x
			4	57,27	Water			x
			5	54,77	Water			x
			6	49,78	Dissolved gas	x		x
			7	34,08	Water			x
			8	28,24	Water			x
			9	23,29	Dissolved gas	x		x
			10	17,87	Water			x
			11	12,68	Dissolved gas	x		x
			12	6,13	Dissolved gas	x		x
01.09.2012	CTD-8	16837-1	1	265,16	Dissolved gas	x		x
			2	250,48	Dissolved gas	x		x
			4	246,05	Dissolved gas	x		x
			5	217,83	Dissolved gas	x		x
			6	182,08	Dissolved gas	x		x
			7	141,93	Dissolved gas	x		x
			8	85,71	Dissolved gas	x		x
			9	44,53	Dissolved gas	x		x
			10	18,59	Dissolved gas	x		x
			11	13,56	Dissolved gas	x		x

Appendix 4: List of Water and Gas Samples, continued

Date	Tool	GeoB No.	Sample #	Water depth	Sample type	On board analytics	Onshore analytics	Onshore analytics
			(Bottle # / [ROV station #])	[mbsl]		Gas composition & concentration	Pore water ingredients	Gas purge & trap
						MARUM	MARUM	IOW
			12	6,39	Dissolved gas	x		x
01.09.2012	CTD-9	16838-1	1	722,75	Water			x
			2	714,02	Dissolved gas	x		x
			4	667,14	Water			x
			5	559,72	Water			x
			6	459,32	Water			x
			7	205,54	Water			x
			8	152,84	Dissolved gas	x		x
			9	101,33	Dissolved gas	x		x
			10	22,21	Water			x
			11	13,26	Dissolved gas	x		x
			12	5,16	Dissolved gas	x		x
01.09.2012	CTD-10	16839-1	1	829,44	Water			x
			2	792,57	Water			x
			4	704,73	Dissolved gas	x		x
			5	557,21	Dissolved gas	x		x
			6	403,96	Water			x
			7	302,86	Water			x
			8	198,77	Dissolved gas	x		x
			9	101,31	Dissolved gas	x		x
			10	26,08	Water			x
			11	12,35	Dissolved gas	x		x
			12	5,32	Dissolved gas	x		x
01.09.2012	CTD-11	16840-1	1	87,35	Water			x
			2	85,17	Dissolved gas	x		x
			4	75,06	Water			x
			5	34,13	Dissolved gas	x		x
			6	28,11	Water			x
			7	24,17	Water			x
			8	18,88	Water			x
			9	13,63	Dissolved gas	x		x
			10	7,69	Water			x
			11	5,66	Dissolved gas	x		x

Appendix 4: List of Water and Gas Samples, continued

Date	Tool	GeoB No.	Sample # (Bottle # / [ROV station #])	Water depth [mbsl]	Sample type	On board analytics Gas composition & concentration MARUM	Onshore analytics Pore water ingredients MARUM	Onshore analytics Gas purge & trap IOW
			12	5,92	Water			x
01.09.2012	CTD-12	16841-1	1	82,95	Dissolved gas	x		x
			2	75,35	Dissolved gas	x		x
			4	69,28	Water			x
			5	60,62	Dissolved gas	x		x
			6	54,79	Water			x
			7	44,98	Water			x
			8	34,73	Dissolved gas	x		x
			9	23,94	Water			x
			10	18,47	Dissolved gas	x		x
			11	13,81	Water			x
			12	6,71	Dissolved gas	x		x
01.09.2012	CTD-13	16842-1	1	109,48	Water			x
			2	106,66	Dissolved gas	x		x
			4	95,24	Water			x
			5	84,60	Dissolved gas	x		x
			6	68,49	Water			x
			7	59,51	Dissolved gas	x		x
			8	42,89	Water			x
			9	32,74	Water			x
			10	17,30	Dissolved gas	x		x
			11	11,73	Water			x
			12	4,69	Dissolved gas	x		x
02.09.2012	CTD-14	16843-1	1	176,43	Water			x
			2	167,81	Dissolved gas	x		x
			4	146,68	Dissolved gas	x		x
			5	136,98	Water			x
			6	105,39	Dissolved gas	x		x
			7	84,05	Water			x
			8	63,72	Dissolved gas	x		x
			9	37,38	Water			x
			10	22,12	Water			x
			11	12,47	Dissolved gas	x		x

Appendix 4: List of Water and Gas Samples, continued

Date	Tool	GeoB No.	Sample #	Water depth	Sample type	On board analytics	Onshore analytics	Onshore analytics
			[Bottle # / [ROV station #]]	[mbsl]		Gas composition & concentration	Pore water ingredients	Gas purge & trap
						MARUM	MARUM	IOW
			12	4,30	Water			x
02.09.2012	CTD-15	16844-1	1	933,00	Water			x
			2	910,85	Dissolved gas	x		x
			4	858,05	Water			x
			5	652,57	Dissolved gas	x		x
			6	444,02	Water			x
			7	309,60	Dissolved gas	x		x
			8	208,12	Water			x
			9	105,27	Dissolved gas	x		x
			10	54,16	Water			x
			11	22,92	Dissolved gas	x		x
			12	6,13	Water			x
02.09.2012	ROV-7	16846	[7]	384,00	Dissolved gas	x		
03.09.2012	ROV-8	16848	[3]	389,70	Dissolved gas	x		
			[2]	386,70	Vent gas	x		
	ROV-9	16853	[9]	92,20	Dissolved gas	x		
04.09.2012	CTD-16	16855-2	1	87,77	Dissolved gas	x		x
			2	84,58	Dissolved gas	x		x
			4	78,84	Water			x
			5	74,34	Dissolved gas	x		x
			6	64,01	Water			x
			7	42,70	Dissolved gas	x		x
			8	32,33	Water			x
			9	22,82	Dissolved gas	x		x
			10	12,09	Dissolved gas	x		x
			11	7,15	Water			x
			12	5,01	Dissolved gas	x		x

Appendix 5: Table Summarizing Studied Bubble Streams

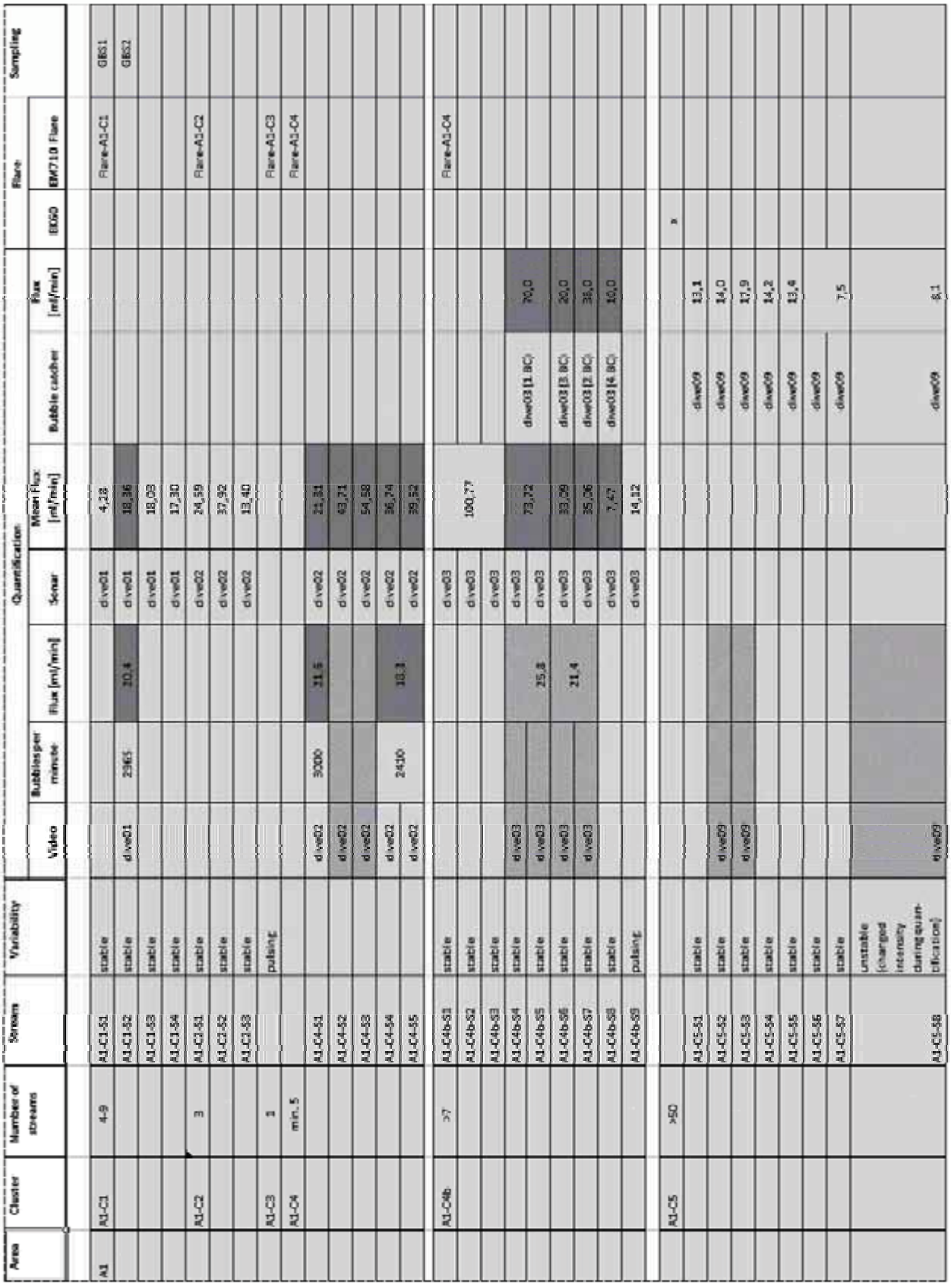

Area	Cluster	Number of streams	Streams	Variability	Quantification: Video	Quantification: Bubbles per minute	Quantification: Flux [ml/min]	Quantification: Sonar	Quantification: Mean Flux [ml/min]	Quantification: Bubble catcher	Quantification: Flux [ml/min]	Flare: EK60	Flare: EM710 Flare	Sampling
A1	A1-C1	4-9	A1-C1-S1	stable				dive01	4,28				Flare-A1-C1	GB31
			A1-C1-S2	stable	dive01	2365	10,4	dive01	18,36					GB32
			A1-C1-S3	stable				dive01	18,03					
			A1-C1-S4	stable				dive01	17,30					
	A1-C2	3	A1-C2-S1	stable				dive02	24,59				Flare-A1-C2	
			A1-C2-S2	stable				dive02	37,92					
			A1-C2-S3	stable				dive02	13,40					
	A1-C3	1		pulsing									Flare-A1-C3	
	A1-C4	min. 5											Flare-A1-C4	
			A1-C4-S1		dive02	3000	31,5	dive02	21,31					
			A1-C4-S2		dive02			dive02	63,71					
			A1-C4-S3		dive02			dive02	54,58					
			A1-C4-S4		dive02	2430	18,3	dive02	36,74					
			A1-C4-S5		dive02			dive02	39,52					
	A1-C4b	37	A1-C4b-S1	stable				dive03					Flare-A1-C4	
			A1-C4b-S2	stable				dive03	100,77					
			A1-C4b-S3	stable				dive03						
			A1-C4b-S4	stable	dive03		25,8	dive03	73,72	dive03 (1 BC)	70,0			
			A1-C4b-S5	stable	dive03			dive03						
			A1-C4b-S6	stable	dive03		21,4	dive03	33,09	dive03 (3 BC)	20,0			
			A1-C4b-S7	stable	dive03			dive03	35,06	dive03 (2 BC)	38,0			
			A1-C4b-S8	stable				dive03	7,47	dive03 (4 BC)	10,0			
			A1-C4b-S9	pulsing				dive03	14,82					
	A1-C5	>50												
			A1-C5-S1	stable						dive09	13,1			
			A1-C5-S2	stable	dive09					dive09	14,0			
			A1-C5-S3	stable	dive09					dive09	17,9			
			A1-C5-S4	stable						dive09	14,2			
			A1-C5-S5	stable						dive09	13,4			
			A1-C5-S6	stable						dive09				
			A1-C5-S7	stable						dive09	7,5			
			A1-C5-S8	unstable (changed intensity during quantification)	dive09					dive09	8,1			

Appendix 5: Table Summarizing Studied Bubble Streams, continued

Area	Cluster	Number of streams	Stream	Variability	Quantification							Flare		Sampling
					Video	Bubbles per minute	Flux [ml/min]	Sonar	Mean flux [ml/min]	Bubble catcher	Flux [ml/min]	EK60	EM710 Flare	
A2	A2-C1	~15										x	Flare-A2-C1	GB51
								dive04: ~7 streams together	140,71					
			A2-C1-S1	stable	dive04	2595	17,1							
			A2-C1-S2	stable	dive04	2220	9,9							
			A2-C1-S3	stable	-									
			A2-C1-S4	stable	dive04	1635	23							
	A2-C2	>12										x	Flare-A2-C2, maybe only a part	Water sample
								dive04: ~10 streams together	254,84					
			A2-C2-S1	stable	dive04	3615	21,7							
			A2-C2-S2	stable	dive04	2325	13							
			A2-C2-S3	stable	-									
			A2-C2-S4	stable	dive04	930	8,5							
			A2-C2-S5	stable	dive04	1515	6,6							
			A2-C2-S6	stable	dive04	5085	20,5							GB52
			A2-C2-S7	stable	dive04									
			A2-C2-S8	pulsing	x (dive04)									
	A2-C3	1 (+1 transient seen in sonar)	A2-C3-S1		dive05	1185	26,5			dive05	27,9	x	Flare-A2-C3	
	A2-C4	1	A2-C4-S1		dive05	288	5,2			dive05	4,0	x	Flare-A2-C4	
	A2-C5	0 (maybe transient)										x	Flare-A2-C5	
	A2-C6	5-6										x	Flare-A2-C6	
			A2-C6-S1	stable						dive05	25,0			
			A2-C6-S2	stable						dive05	19,4			
			A2-C6-S3	stable						dive05	6,2			
			A2-C6-S4	pulsing						dive05	8,2			
			A2-C6-S5	pulsing						dive05	17,1			
			(A2-C6-S6)	present in sonar										

Appendix 5: Table Summarizing Studied Bubble Streams, continued

Area	Cluster	Number of streams	Stream	Variability	Quantification						Flare		Sampling
					Video	Bubbles per minute	Flux [ml/min]	Sonar	Mean Flux [ml/min]	Bubble catcher	Flux [ml/min]	EK60	EM710 Flare	
A3														
	A3-C1	3-10 transient											Flare-A3-C1	
			A3-C1-S1	stable	dive06	208	9,4							GS51
	A3-C2	>5 transient											Flare-A3-C2	
	A3-C3	~3 transient											Flare-A3-C3	Watersample
			A3-C3-S1	periodic pulsing	dive06	172	6,7							GS52
	A3-C4	No, but pogonophora field											Flare-A3-C4	
	A3-C5	~5-8												
			A3-C5-S1	pulsing						dive07	6,3			
			A3-C5-S2	pulsing						dive07	31			
			A3-C5-S3	pulsing						dive07	37,5			
			A3-C5-S4	pulsing						dive07	41			
	A3-C6	~5-8												
			A3-C6-S1	pulsing						dive07	3			
			A3-C6-S2	pulsing						dive07	32			
	A3-C7	3-4		unstable										Watersample
	A3-C8	~5		transient										
	A3-C9	~6		transient										GS52
	A3-C10	2-3		transient										
	A3-C11	5-6	A3-C11-S1	transient	dive08									
			A3-C11-S2	transient	dive08									
	A3-C12	reactive streams												
	A3-C13													
	A3-C14	reactive streams												
	A3-C15	~3		transient										
	A3-C16	>3		transient										Watersample

Appendix 6: List of Flare Locations picked from EK60

flare_id	time	lat	lon	sum	sum_area	area	height
2108001	18:07:25	78,38355317	10,12618313	6,7846	0,561005	18,5	30,7
2108002	18:11:18	78,38347731	10,13837500	8,1775	0,297460	22,1	41,3
2108003	18.17.40	78,37541667	10,15665735	20,6601	0,272521	75,3	52,0
2108004	18:19:54	78,37533900	10,15717400	25,3230	0,537457	48,5	57,4
2108005	18:20:38	78,37157100	10,11950935	35,1477	1,100158	51,1	81,5
2108006	18:21:04	78,37380100	10,17258017	3,3050	0,192942	17,1	37,0
2108007	18:26:58	78,37024817	10,15716400	5,8677	0,217505	27,1	54,8
2108008	18:39:11	78,36311100	10,21570367	2,0608	0,107825	19,3	47,9
2108009	18.43.12	78,36415253	10,22255535	3,7597	0,117263	52,1	44,4
2108010	18:55:35	78,37774253	10,14636567	4,3583	0,260456	16,7	37,8
2108011	19:00:72	78,37407917	10,11879500	15,3971	0,337071	53,1	60,5
2108012	19:02:46	78,37485067	10,15917200	8,4547	0,480922	17,5	38,7
2108013	19:03:52	78,37510400	10,15601183	4,3946	0,315455	13,1	47,0
2108014	19:04:75	78,37310937	10,14977750	3,1772	0,308763	8,5	33,7
2108015	19:25:59	78,35160017	10,25624635	2,9153	0,524905	5,5	24,2
2108016	19:28:08	78,34535717	10,24516100	3,7123	0,205195	18,0	57,5
2108017	19:75:16	78,34515517	10,25011567	7,7303	0,435005	10,1	31,0
2108018	19:29:54	78,34752150	10,25245786	12,5117	0,405475	25,4	53,9
2108019	19:40:25	78,34572257	10,25521567	10,3106	0,498150	26,0	51,9
2108020	19:43:17	78,34737367	10,24905367	3,0798	0,512343	5,0	27,3
2108021	19:43:51	78,34798067	10,24637535	7,2578	0,535172	21,5	56,2
2108022	19:45:0	78,34505537	10,24172950	67,2761	1,259597	51,1	71,7
2108023	19:46:04	78,35013550	10,23714517	2,9778	0.134378	19.3	56.5
2108024	19:46:43	78,35086600	10,25421150	2,8252	0,121987	23,2	55,5
2108025	19:47:32	78,35159517	10,23152117	2,0520	0,401197	7,9	33,4
2108026	19:48:13	78,35309583	10,23973117	7,7994	0,245098	52,0	56,7
2108027	19:48:55	78,35265500	10,22787377	4,9454	0,922154	5,4	31,4
2108028	19:59:54	78,36208621	10,18710417	5,7419	0,250597	21,9	43,7
2108029	20.06.40	78,36791600	10,16330350	1,7081	0,438851	3,9	20,6
2108030	20:27:28	78,36133953	10,18457417	1,4602	0,291726	5,0	19,4
2108031	20:37:21	78,35121100	10,23616450	27,8105	0,379095	77,1	71,0
2108032	20.38.18	78,35038733	10,23079367	2,2611	0,137993	16,4	37,3
2108033	20:39:34	78,34105937	10,23615750	11,5623	0,484540	23,3	51,5
2108034	20:40:38	78,34747850	10,24075316	92,1110	1,305122	70,5	66,1
2108035	20.41.20	78,34725700	10,24345450	44,0775	0,984144	44,3	71,3
2108036	20:42:26	78,34581150	10,24758735	2,7070	0,118275	22,2	51,5
2108037	20:41:17	78,34527457	10,24156967	2,9179	0,176187	17,0	45,1
2108038	20.43.51	78,34470167	10,25408950	5,3163	0,453930	11,6	27,5
2108039	20:54:40	78,34553253	10,24013517	24,0461	0,475224	50,5	58,7
2108040	20:56:15	78,34817751	10,23127785	180,7551	1,444494	125,9	77,7
2108041	21.00.02	78,35098867	10,22279085	13,2213	0,395204	46,5	54,3
2108042	21:07:48	78,35527457	10,19151267	13,5582	1,041190	13,0	40,5
2108043	21:08:35	78,35890400	10,18877050	11,0967	0,577811	19,1	44,1
2108044	21.11.10	78,36123833	10,15030400	0,7736	0,204934	3,9	28,5
2108045	21:26:27	78,37491317	10,13740050	2,2989	0,195179	11,7	55,8
2108046	21:30:34	78,37197331	10,13157785	1,4910	0,200691	7,4	30,0
2108047	21:34:02	78,36537817	10,14560717	1,8365	0,221454	3,5	30,2
2108048	21:37:14	78,36080757	10,17610967	1,5868	0,185115	10,7	46,8
2108049	21:44:36	78,35501250	10,18734985	21,8379	0,394171	53,4	61,5
2108050	21.45.14	78,35741267	10,18937617	4,3092	0,280275	14,9	35,5
2108051	21:47:47	78,35514658	10,19515183	1,4559	0,102180	14,4	35,5
2108052	21:56:18	78,34143333	10,23591717	0,6319	0,144913	4,4	21,9
2108053	21:58:29	78,34416353	10,24548036	3,7876	0,216803	17,5	43,2
2108054	22:05:37	78,34127750	10,25290100	10,5512	0,415547	90,6	71,4
2108055	22:30:35	78,36759717	10,14358467	1,5798	0.196470	8.0	40.3
2108056	22:56:47	78,36702300	10,14057200	2,0427	0,375423	5,4	24,4
2108057	22:57:08	78,36364050	10,14213517	1,1605	0,130775	8,9	36,0
2108058	22:58:39	78,36475057	10,17019535	1,7437	0,155487	11,3	33,5
2108059	23:01:20	78,36231117	10,18015717	5,7606	0,189690	60,5	46,5

flare_id	time	lat	lon	sum	sum_area	area	height
2108060	23:03:47	78,55675183	10,18263183	7,7357	0,245346	30,7	50,0
2108061	23:22:34	78,54117217	10,24809083	8,1756	0,206674	27,6	52,5
2108062	23:24:41	78,54084483	10,24464957	128,5435	1,051341	121,3	75,5
2108063	23:29:39	78,54117150	10,24178130	14,0115	0,601483	53,5	81,2
2108064	23:42:42	78,55801000	10,17656730	22,7765	0,624425	36,5	55,0
2108065	23:45:07	78,56106067	10,15811130	13,4920	0,140878	21,1	51,5
2108066	23:49:08	78,56194050	10,15327930	6,1574	0,201380	25,6	50,0
2108067	23:50:15	78,56280467	10,15168587	17,1084	0,456133	37,6	60,6
2208001	00:01:41	78,57455083	10,10810133	1,4141	0,110157	8,1	19,7
2208002	00:10:53	78,56527067	10,15699933	22,8975	0,287503	75,5	73,5
2208003	00:17:41	78,56454767	10,15080823	5,3720	0,326372	16,6	45,0
2208004	00:18:17	78,56294150	10,14780130	12,2925	0,635300	17,6	41,4
2208005	00:20:12	78,56206033	10,14950483	30,1501	0,752329	43,6	53,1
2208006	00:21:06	78,56121567	10,15820700	22,8872	0,561575	40,8	51,5
2208007	00:22:54	78,55809017	10,15874917	20,2097	0,412208	42,1	63,4
2208008	00:24:50	78,55794717	10,16084417	1,9079	0,230149	8,4	41,5
2208009	00:28:21	78,55715817	10,17054333	3,7158	0,229087	15,5	44,8
2208010	00:50:38	78,55209653	10,19065217	1,3182	0,130531	27,8	50,0
2208011	00:48:43	78,54008367	10,24359817	39,3168	1,057597	54,5	70,4
2208012	00:57:17	78,54925100	10,20797933	3,2821	0,851545	5,8	15,0
2208013	01:01:27	78,55719453	10,15560817	10,7221	0,422715	24,9	46,1
2208014	01:08:02	78,55882600	10,15958730	18,6608	0,630023	25,3	63,1
2208015	01:09:30	78,56068450	10,15321330	102,1055	0,811445	114,5	75,8
2208016	01:10:31	78,56119017	10,14958817	9,1298	0,549163	17,5	75,6
2208017	01:11:49	78,56244300	10,14348500	83,1501	1,012060	82,1	73,3
2208018	01:12:43	78,56538167	10,15870933	28,4515	0,551055	51,7	70,9
2208019	01:13:27	78,56410753	10,15072430	17,1195	0,525787	19,6	64,0
2208020	01:15:14	78,56595367	10,12903130	20,6526	0,451324	53,9	43,0
2208021	01:32:20	78,56518067	10,12658530	9,6544	0,494355	22,4	52,5
2208022	01:34:20	78,56329250	10,13456217	31,1476	0,479965	73,7	68,4
2208023	01:36:13	78,56183683	10,14017900	34,1575	0,595790	57,3	60,5
2208024	01:36:46	78,55968417	10,14930333	11,2273	0,826511	15,5	34,7
2208025	01:38:21	78,55918783	10,15154817	11,9300	0,712101	11,7	31,9
2208026	01:41:20	78,55745500	10,15891387	3,9863	0,215561	13,5	50,4
2208027	01:43:43	78,55780450	10,15670883	1,0117	0,256108	5,4	15,2
2208028	01:43:51	78,55528000	10,17384917	1,9734	0,112787	13,1	36,8
2208029	01:47:16	78,55105250	10,18122287	9,0160	0,137403	45,7	48,2
2208030	01:48:07	78,55125050	10,18434383	1,5530	0,222265	8,8	36,7
2208031	01:50:50	78,54579317	10,19373543	10,7739	0,271393	19,0	61,0
2208032	02:11:00	78,55114000	10,13056030	7,0637	0,300007	20,4	47,1
2208033	02:11:58	78,55105083	10,17678100	6,4725	0,408615	17,6	36,4
2208034	02:20:47	78,55958317	10,14319209	3,0217	0,180323	20,1	43,5
2208035	02:24:29	78,56284617	10,16228523	53,0132	0,858586	95,4	65,5
2208036	02:24:44	78,56407617	10,15164953	12,8306	1,156155	10,6	50,0
2208037	02:25:37	78,56382000	10,12850933	40,0032	0,945370	43,3	67,0
2208038	02:26:17	78,56444167	10,12398617	16,0739	0,461963	34,9	61,6
2208039	02:27:56	78,56492167	10,11994933	4,7758	0,254100	16,6	56,5
2208040	02:30:47	78,56525850	10,11040109	1,9749	0,374575	5,3	25,5
2208041	02:43:54	78,56676650	10,11016153	6,4063	0,312496	20,5	45,7
2208042	02:44:21	78,56607067	10,11360417	4,2792	0,221586	15,5	47,3
2208043	02:47:11	78,56528867	10,11643617	6,3430	0,345513	13,4	43,0
2208044	02:48:51	78,56676367	10,12306023	16,5345	0,216596	55,0	72,7
2208045	02:49:55	78,56225167	10,19867933	7,5963	0,281121	27,5	41,9
2208046	03:29:03	78,55653067	10,14683200	1,0871	0,142925	11,8	41,4
2208047	03:35:50	78,56444167	10,11480550	47,6140	0,616185	65,3	67,2
2208048	03:36:06	78,56450633	10,11277230	5,7811	0,451025	11,7	29,1
2208049	03:39:54	78,56551117	10,11109833	4,3938	0,271783	16,2	63,0
2208050	03:53:04	78,56854050	10,09260817	0,4154	0,152452	2,7	11,8
2208051	03:54:29	78,56704467	10,09011130	1,2418	0,280151	11,7	43,8
2208052	03:54:53	78,56657500	10,09936083	3,0231	0,217763	15,9	49,0
2208053	03:55:24	78,56505083	10,10600830	3,7214	0,358715	16,1	35,7

flare_id	time	lat	lon	sum	sum_area	area	height
2208054	03:57:10	78,36421053	10,10935695	1,3026	0,266085	4,9	23,5
2208055	03:58:19	78,36210100	10,11303350	5,7808	0,537020	17,2	40,1
2208056	04:29:25	78,36182957	10,11171084	3,5901	0,307037	11,5	39,0
2208057	04:44:02	78,36193751	10,10654707	4,7037	0,337024	14,1	27,0
2208058	04:46:06	78,36301683	10,10206136	1,4071	0,161154	5,7	30,6
2208059	04:47:10	78,36360900	10,08601517	1,6004	0,211093	7,5	30,8
2208060	04:54:30	78,37339217	10,07377235	2,3539	0,572197	4,4	17,5
2208061	05:02:53	78,36645167	10,05736100	2,1812	0,275821	8,0	37,3
2208062	05:04:54	78,36460050	10,08532711	6,7722	0,300074	10,7	47,9
2208063	05:05:12	78,36433153	10,09690417	3,4197	0,749428	4,6	28,5
2208064	05:05:43	78,36285283	10,01877367	5,2440	0,580547	13,5	47,5
2208065	05:06:22	78,36324401	10,10162117	1,3750	0,179013	10,7	37,9
2208066	05:08:34	78,36145750	10,10911735	2,8270	0,449050	5,5	45,5
2208067	05:31:55	78,36085283	10,10734550	2,1984	0,670083	5,9	34,3
2208068	05:34:01	78,36314017	10,10080000	4,1770	0,477574	8,6	29,5
2208069	05:35:04	78,36404400	10,09455400	9,0090	0,436190	19,7	43,5
2208070	05:55:58	78,36475000	10,07150500	6,4768	0,554351	11,7	41,8
2208071	05:57:38	78,36510017	10,08670367	2,1996	0,287949	8,5	36,7
2208072	06:01:19	78,36963953	10,07110785	0,4726	0,237253	3,0	17,4
2208073	06:12:51	78,36655000	10,07056567	2,2656	0,419281	5,5	30,2
2208074	06:17:18	78,36191983	10,08966300	1,1649	0,161154	7,9	30,1
2208075	06:18:28	78,36373350	10,09489117	7,3183	0,398023	18,4	38,1
2208076	06:21:24	78,35510757	10,11403167	0,9773	0,175875	5,5	20,5
2208077	06:36:52	78,35482200	10,13738450	0,6717	0,348410	1,8	11,0
2208078	07.07.01	78,36716517	10,17768785	2,4937	0,239638	10,4	41,6
2208079	07:22:57	78,38125553	10,11913517	8,1046	0,450221	18,0	46,7
2208080	07:26:11	78,38425651	10,19616750	2,1080	0,121755	18,0	47,3
2208081	07.27.14	78,38826567	10,10252335	7,2084	0,425653	17,0	46,5
2208082	07:28:09	78,38651017	10,10824100	3,8751	0,205447	18,1	48,5
2208083	07:30:34	78,38960400	10,08830300	8,6172	0,307199	28,1	59,3
2208084	07.34.18	78,38504850	10,09418367	6,7527	0,239658	26,1	59,3
2208085	07:36:13	78,38565117	10,10425583	2,0517	0,157085	13,2	35,2
2208086	07:37:01	78,38417081	10,16611313	1,8178	0,218451	7,4	37,3
2208087	07.38.35	78,38411817	10,11398017	1,7141	0,148353	11,6	42,6
2208088	07:48:25	78,37754000	10,13259000	2,4758	0,275807	8,8	30,4
2208089	07:50:17	78,37363100	10,11019500	0,9290	0,155371	6,1	34,7
2208090	07.52.05	78,37085467	10,16754517	1,1411	0,219248	5,2	27,2
2208091	07:53:59	78,36897157	10,17526118	1,6765	0,726692	2,3	17,1
2208092	08:06:10	78,35584457	10,23496900	4,8374	0,135757	31,9	51,7
2208093	08.06.55	78,35604017	10,22795325	4,1422	0,246301	16,3	50,3
2208094	08:16:19	78,36079083	10,21711000	1,4807	0,173868	8,5	30,5
2208095	08:19:16	78,36349700	10,20751517	6,8564	0,281911	24,1	59,9
2208096	08:27:07	78,36972100	10,17855650	1,5198	0,134777	11,3	46,0
2208097	08:29:24	78,37197400	10,13957584	1,1003	0,191974	5,7	31,7
2208098	08:32:05	78,37463037	10,10890193	1,9280	0,172173	10,5	42,1
2208099	08:35:57	78,37516150	10,14418185	6,5407	0,264293	24,7	57,7
2208100	08:37:17	78,37594257	10,13709084	5,1774	0,700084	14,7	44,9
2208101	08:38:30	78,38115750	10,15291107	2,4090	0,290179	8,5	20,5
2208102	08:40:53	78,38205617	10,12066667	2,0583	0,269064	7,7	36,2
2208103	08:47:19	78,38007217	10,10491484	14,8455	0,550197	24,6	55,7
2208104	08:46:35	78,38554853	10,10303685	19,7099	0,545709	36,3	49,0
2208105	08:51:10	78,38848800	10,10906436	17,7056	0,420423	41,2	58,5
2208106	08:54:14	78,38467457	10,12731150	8,6795	0,718190	11,6	51,3
2208107	09.00.10	78,37507700	10,14505035	1,3740	0,365367	4,5	23,5
2208108	09:01:13	78,37505317	10,14050050	37,1441	0,574023	64,6	80,8
2208109	09:01:15	78,37757050	10,11108400	1,7817	0,517870	3,5	22,1
2208110	09:04:32	78,37480800	10,10295095	58,3474	1,363439	59,1	60,5
2208111	09:04:57	78,37431350	10,13455750	9,4411	0,488810	19,3	56,4
2208112	09:17:08	78,36251217	10,21211015	10,3921	0,473550	21,9	51,5
2208113	09.17.39	78,36310117	10,21440750	7,1236	0,342621	20,3	64,0
2208114	09:30:52	78,36501383	10,20759785	4,2201	0,212481	19,7	57,7

flare_id	time	lat	lon	sum	sum_area	area	height
2208115	09:43:57	78,57040067	10,18707583	7,3491	0,670559	11,6	45,2
2208116	09:45:23	78,57079082	10,18367617	13,3217	0,582590	22,9	50,1
2208117	09:46:50	78,57117617	10,18475855	4,0117	0,351373	14,2	55,1
2208118	09:47:10	78,57144417	10,18112700	7,1502	0,247080	13,7	57,2
2208119	09:49:09	78,57621252	10,17670855	2,0870	0,272717	11,0	32,0
2208120	09:51:15	78,57787050	10,17815917	125,9004	4,165927	35,0	80,0
2208121	09:51:02	78,57534000	10,15654783	27,8190	1,212044	23,9	53,7
2208122	09:53:27	78,57447700	10,16285028	2,6873	0,251797	11,0	43,6
2208123	09:55:20	78,57716000	10,15290617	0,7871	0,175251	4,8	23,1
2208124	09:58:57	78,56465367	10,15007430	10,2578	0,474343	21,6	60,9
2208125	09:59:56	78,56555650	10,12542283	13,8048	0,615027	11,9	54,1
2208126	10:31:47	78,55919817	10,11107757	1,7911	0,241041	7,4	46,6
2208127	11:10:13	78,50411267	9,93395350	2,3932	0,058424	25,3	63,7
2208128	13:30:09	78,35733800	10,15805057	3,2410	0,252505	12,4	42,1
2208129	13:40:24	78,35917767	10,14857900	2,1611	0,527061	4,1	31,3
2208130	13:40:43	78,35975183	10,14391037	3,2537	0,379359	5,9	33,7
2208131	13:41:05	78,36057083	10,14386183	3,1578	0,676287	6,3	50,0
2208132	13:41:53	78,36249053	10,13740517	42,7916	1,651470	27,7	55,6
2208133	13:41:43	78,36258417	10,15153830	13,5814	1,185501	11,6	63,4
2208134	13:43:05	78,36555567	10,12894700	19,9141	1,672775	11,9	65,9
2208135	13:44:53	78,36413000	10,13072413	6,5294	0,621373	10,5	62,0
2208136	16:20:04	78,36574383	10,12953033	7,8051	0,449830	17,5	53,8
2208137	16:20:40	78,36531567	10,15190700	5,4578	0,410675	12,4	52,7
2208138	16:21:05	78,36507783	10,15171143	22,7181	0,772911	29,1	69,0
2208139	16:21:26	78,36485000	10,15323200	6,0054	0,377010	13,9	56,2
2208140	16:21:45	78,36465800	10,15667457	3,2373	0,279425	15,7	50,6
2208141	16:21:59	78,36445083	10,15758180	5,1910	0,526171	10,8	52,7
2208142	16:25:08	78,36249833	10,15158633	3,6812	0,437014	9,1	45,7
2208143	16:25:54	78,36141783	10,15088457	8,1741	0,754077	10,8	33,5
2208144	16:27:55	78,36078100	10,13479733	1,1898	0,291885	5,9	37,6
2208145	16:31:57	78,35381217	10,13894100	11,2532	0,457655	25,1	59,9
2208146	16:37:50	78,35824000	10,10841117	8,1751	0,361845	26,5	55,7
2208147	16:58:52	78,37078167	10,18560883	15,6705	0,613865	27,0	51,4
2208148	17:04:09	78,37406183	10,16844583	79,2065	2,272565	34,9	83,7
2208149	17:05:27	78,37503800	10,15406300	51,3004	0,911156	65,5	77,2
2208150	17:08:39	78,37659257	10,15091717	2,7051	1,111807	2,4	13,0
2208151	17:08:53	78,37520700	10,15309183	5,0431	0,932982	5,6	40,7
2208152	17:09:53	78,37260050	10,15027753	34,9125	0,925017	37,7	53,9
2208153	17:10:40	78,38024150	10,14791977	34,2956	1,376769	24,9	44,0
2208154	17:12:56	78,38175300	10,14152417	2,7455	0,229106	12,0	34,9
2208155	17:13:55	78,38197000	10,14051653	1,4008	0,250411	5,6	25,1
2208156	17:17:07	78,38537883	10,12684283	1,8919	0,443547	4,3	25,4
2208157	17:22:19	78,38980782	10,11749023	4,9406	0,399051	12,4	40,5
2208158	17:24:40	78,38671083	10,11914758	6,0217	0,536202	11,9	41,6
2208159	17:25:07	78,38667067	10,12829430	5,3000	0,431161	13,1	35,3
2208160	17:28:11	78,38521467	10,15162437	8,8350	0,501334	17,6	54,1
2208161	17:30:11	78,38246867	10,14425867	24,8095	0,759033	31,0	56,1
2208162	17:33:52	78,37930117	10,15650957	39,8731	0,719799	55,4	54,6
2208163	17:35:22	78,37795067	10,16147628	1,1365	0,160715	7,1	32,6
2208164	17:37:40	78,37592417	10,17294800	30,6478	0,818711	37,7	60,9
2208165	17:38:49	78,37494217	10,17367493	119,6183	1,509383	79,2	77,7
2208166	17:39:51	78,37432052	10,17609528	28,9661	0,775424	30,0	51,2
2208167	17:47:51	78,37115050	10,18771417	2,3769	0,218497	9,6	52,9
2208168	17:49:47	78,36537900	10,21121293	7,4296	0,439001	17,3	51,2
2208169	17:50:56	78,36435600	10,21506833	2,0076	0,332635	6,7	55,6
2208170	17:51:41	78,36309133	10,21750530	4,4068	0,374121	13,1	67,8
2208171	17:53:09	78,36527353	10,21920733	3,3708	0,213073	13,4	45,3
2208172	17:54:22	78,36126082	10,22710150	4,6793	0,188539	25,5	47,9
2208173	17:55:10	78,35962150	10,23351917	1,1346	0,140807	8,1	36,5
2208174	18:08:43	78,35730617	10,24887800	1,4077	0,133133	11,9	33,9
2208175	18:10:04	78,36025750	10,25708080	4,2903	0,252162	15,2	42,6

flare_id	time	lat	lon	sum	sum_area	area	height
2208176	18:11:35	78.36195517	10,23097317	1,7181	0,262779	5,5	45,1
2208177	18.12.14	78.36223717	10,22918317	1,3032	0,235000	5,5	36,3
2208178	18:26:18	78.37511357	10,18011400	87,5372	0,997797	88,2	76,0
2208179	18:27:15	78.37387117	10,17772317	8,3172	0,525470	17,7	79,3
2208180	18:28:42	78.37563233	10,17445550	61,4302	1,362093	45,1	70,5
2208181	18:28:54	78.37381200	10,17331481	9,2805	0,729468	11,6	53,9
2208182	18:29:35	78.37785700	10,17014595	49,7013	1,079427	46,1	73,0
2208183	18:31:47	78.37155083	10,16322536	27,1484	1,140642	23,8	75,5
2208184	18:36:14	78.38402217	10,14572050	14,1025	0,711101	19,7	54,1
2208185	18:37:10	78.38451353	10,14133585	4,2942	0,603871	7,1	43,4
2208186	18:37:37	78.38342017	10,14142417	4,5268	0,634394	7,1	42,6
2208187	18:38:11	78.38321481	10,14832915	1,7867	0,303641	5,8	37,5
2208188	18.40.11	78.38755853	10,15150517	2,1461	0,437013	4,9	32,0
2208189	18:50:07	78.38562683	10,16652367	2,7940	0,368837	7,6	35,0
2208190	18:41:55	78.38606157	10,15171400	4,4243	0,440921	10,1	40,2
2208191	18:44:48	78.38769717	10,16670067	3,6815	0,440484	8,2	39,5
2208192	18:47:20	78.38337150	10,14628077	7,9438	0,469156	16,7	54,1
2208193	18:55:10	78.37711951	10,17569300	52,1040	1,073489	50,2	74,1
2208194	18.35.34	78.37708400	10,17747450	6,1489	0,392011	13,7	46,3
2208195	18:56:02	78.37561053	10,17920785	4,5647	0,329614	13,6	48,9
2208196	18:57:10	78.37557050	10,18018500	10,2473	0,608950	16,9	50,0
2208197	18.37.33	78.37489853	10,18035307	4,0024	0,238948	13,5	48,3
2208198	18:58:27	78.37136117	10,19215767	7,5618	0,293025	25,2	56,1
2208199	19:01:17	78.37164031	10,19869686	2,4742	0,223074	11,0	41,3
2208200	19.02.12	78.37074017	10,20208000	2,3806	0,316390	7,5	37,3
2208201	19:08:43	78.36375117	10,22900050	5,8129	0,257125	23,0	53,5
2208202	19:08:45	78.36169917	10,23016310	6,1577	0,705111	11,3	41,3
2208203	19.13.18	78.36005300	10,24331967	50,1653	0,475063	105,6	82,1
2208204	19:13:54	78.35726457	10,24548750	8,6150	0,567727	15,2	50,2
2208205	19:15:05	78.35825891	10,21103950	57,0345	0,995814	57,3	80,1
2208206	19.20.22	78.35375200	10,26510650	2,0984	0,323273	6,4	40,3
2208207	19:18:43	78.35482251	10,25358050	17,5905	1,521987	10,5	35,0
2208208	19:34:11	78.35627561	10,21189513	57,1109	1,945921	27,5	79,1
2208209	19.24.58	78.35363933	10,25042100	3,9944	0,407052	9,8	62,2
2208210	19:25:00	78.35607963	10,24907017	2,3041	0,367187	5,9	33,5
2208211	19:35:14	78.36973130	10,21201050	1,9020	0,137308	13,3	47,7
2208212	19.37.52	78.37264750	10,20212685	2,2429	0,265995	8,4	34,5
2208213	19:39:54	78.37422300	10,19176567	21,0672	0,398775	52,2	76,1
2208214	19:48:37	78.38151717	10,11585413	2,8174	0,171301	16,4	51,1
2208215	19.51.59	78.38406250	10,13415750	16,2433	0,444133	36,6	61,6
2208216	19:56:57	78.38351400	10,11191700	8,2177	0,325501	25,2	56,2
2208217	19:56:30	78.38059117	10,13039917	12,5141	0,506903	24,6	61,0
2208218	19:50:59	78.38600267	10,06700300	2,0456	0,240294	8,5	32,7
2208219	19:59:57	78.38595717	10,10506617	2,4729	0,317031	5,7	44,5
2208220	20:00:31	78.38579950	10,08850567	1,4304	0,190068	7,5	53,0
2208221	20:21:03	78.39575217	9,94014217	5,3087	0,256498	21,0	68,0
2208222	20:29:12	78.39712890	9,97152713	3,7017	0,349501	10,9	54,1
2208223	20:39:16	79.00095717	9,90283517	4,1138	0,475069	8,7	51,0
2208224	20:30:20	78.60896350	9,89548083	2,2102	0,250397	8,8	53,4
2208225	20:38:17	78.43193560	9,80070000	11,7611	0,421984	27,6	77,3
2208226	20:49:40	79.03439183	9,79399417	14,2103	0,542713	26,3	72,3
2208227	20:51:26	78.03375283	9,78147500	110,6610	1,664298	66,5	124,2
2208228	21:04:06	78.03556481	9,88210757	47,3126	0,487501	97,0	97,3
2208229	21.21.12	78.01045183	9,90708083	1,6091	0,232038	7,2	44,0
2208230	21:41:53	78.38532663	10,06960000	1,0701	0,124510	8,6	50,8
2208231	21:43:17	78.38160017	10,06576713	2,4922	0,163320	15,0	55,2
2208232	21:46:37	78.38123483	10,09081550	1,8995	0,333858	5,6	52,9
2208233	21:48:44	78.37249617	10,09871085	1,9828	0,262962	7,5	52,0
2208234	21:52:18	78.36707300	10,06571950	1,2540	0,205500	6,1	52,5
2208235	21.39.19	78.36323233	10,09585685	6,3664	0,330243	18,7	56,4
2208236	22:00:06	78.35612817	10,08908250	8,2228	0,421200	19,5	56,7

flare_id	time	lat	lon	sum	sum_area	area	height
2208237	23:00:29	78,56585367	10,10047693	6,9132	0,493439	14,0	50,4
2208238	23:00:47	78,56620750	10,10260530	2,5161	0,216055	11,6	48,6
2208239	23:27:37	[illegible]	10,25580917	[illegible]	[illegible]	14,7	[illegible]
2208240	23:44:52	78,55518367	10,17002900	4,5376	0,397485	11,5	37,4
2208241	23:46:10	78,55725050	10,16072023	6,0977	0,420632	14,0	45,6
2208242	23:50:05	[illegible]	[illegible]	[illegible]	[illegible]	17,5	[illegible]
2208243	23:50:54	78,56194350	10,15114733	19,0991	1,330537	14,3	47,5
2208244	23:51:52	78,56623850	10,14596257	6,8854	0,468606	14,7	53,7
2308001	00:07:27	[illegible]	10,07295117	[illegible]	0,067485	10,0	[illegible]
2308002	00:07:52	78,58446217	10,07000017	0,7156	0,109517	4,2	21,1
2308003	00:21:19	78,60190562	10,00652483	0,0029	0,156154	5,8	25,0
2308004	[illegible]	78,54384150	[illegible]	[illegible]	[illegible]	7,3	35,7
2308005	01.21.23	78.52577867	9.96850653	0.8656	0.177727	4,9	25.9
2308006	01.46:20	78,39081017	10,09084437	8,4457	0,225525	37,4	60,6
2308007	01:47:40	78,38875017	10,09744930	1,7819	0,271715	13,0	41,1
2308008	01:51:56	78,38149850	10,12380000	6,8308	0,290339	23,1	53,9
2308009	01:54:16	78,38102117	10,12554133	5,1974	0,559065	8,7	41,1
2308010	01:55:44	78,38017083	10,13794683	2,3477	0,210148	9,2	25,7
2308011	01.57.52	78,37445100	10,14963137	0,4259	0,159475	2,3	17,1
2308012	02:05:06	78,36707888	10,17697808	0,5359	0,410412	1,3	11,4
2308013	02:11:43	78,35607167	10,23177808	2,9219	0,132794	19,2	50,7
2308014	02.14.44	78,35072883	10,25608017	1,3034	0,231943	6,8	23,0
2308015	02:16:17	78,34871254	10,27448950	29,5568	0,718825	55,6	75,1
2308016	02:17:52	78,34825050	10,27608498	[illegible]	0,238171	13,3	51,5
2308017	02.18.53	78,34771283	10,24803217	5,9728	0,351206	13,7	51,9
2308018	02:19:05	78,34507354	10,25386853	2,7244	0,210894	9,4	30,4
2308019	02:19:38	78,34529951	10,25671498	1,3275	0,340183	4,5	28,5
2308020	02.55.43	78,30560517	10,44057683	3,1418	0,331250	9,5	33,7
2308021	02:57:09	78,30510067	10,44845250	1,6058	0,252224	6,4	53,1
2308022	03:00:59	78,31115151	10,45240833	1,1242	0,291419	13,7	51,9
2308023	03.01.04	78,31179853	10,45051217	26,1749	2,040293	12,9	53,9
2308024	03:01:44	78,31565417	10,41604457	29,0725	0,452537	62,9	117,6
2308025	03:04:14	78,31574867	10,41141908	17,6945	0,551310	31,0	85,6
2308026	03.04.58	78,31684900	10,41149737	5,3410	0,426962	12,5	33,2
2308027	03:05:08	78,31884067	10,40476853	1,7530	0,243847	7,2	45,9
2308028	03:19:04	78,33364383	10,35977650	1,7858	0,279309	6,6	26,5
2308029	03.19.50	78,33775767	10,35573623	5,5518	0,316037	17,6	41,1
2308030	03:25:36	78,34543000	10,30770983	2,7530	0,411491	6,7	37,0
2308031	03:53:51	78,38568800	10,17090883	1,4575	0,172901	7,8	33,4
2308032	03.57.03	78,38795267	10,15223117	4,1750	0,138755	30,1	73,1
2308033	03:58:53	78,39007117	10,14404417	11,0308	0,361256	30,4	65,3
2308034	03:59:20	78,39007389	10,14201083	12,4645	0.712789	17.5	60.2
2308035	05.18:17	78,38047782	10,12806717	8,5358	0,208401	25,6	58,2
2308036	05:20:25	78,38375467	10,14476457	3,5711	0,242561	13,9	63,4
2308037	05:21:58	78,37957317	10,15063807	11,5827	0.554409	20.9	65.0
2308038	05:22:47	78,37465717	10,17110623	64,3330	1,251084	51,4	73,1
2308039	05:23:30	78,37005917	10,18501917	8,2059	0,262281	31,5	61,2
2308040	05:33:29	78,35215350	10,25110707	10,8102	0.542330	19.9	54.1
2308041	05:50:21	78,34906750	10,25640750	9,2052	0,350465	25,8	54,0
2308042	05:51:50	78,34904767	10,24606908	26,2904	1,141181	23,0	55,1
2308043	13:19:04	78,34740267	10,25890833	147,3701	1,970011	73,8	83,7
2308044	13:20:00	78,34797667	10,24111917	20,8277	0,918028	31,0	82,1
2308045	13:20:23	78,34825767	10,24219617	26,1715	1,010637	25,9	75,3
2308046	13.20.49	78.34854750	10,24327983	37,7080	1,307155	26.8	73.5
2308047	13:21:23	78,34804563	10,24464083	17,7806	0,732535	25,3	67,5
2308048	13:21:45	78,34925100	10,24490517	18,0904	0,862963	21,7	64,6
2308049	13:24:24	78,34915317	10,25899217	38,8531	0,825304	45,9	77,5
2308050	13:25:56	78,34850452	10,26045737	70,4546	1,504056	46,8	71,9
2308051	13:26:50	78,34829017	10,25814617	12,0310	0,846257	14,5	55,0
2308052	13.27.50	78,34735967	10,25699333	43,2160	1,177451	36,7	41,6
2308053	13:34:54	78,34545052	10,25698480	8,0421	0,649590	12,5	43,4

flare_id	time	lat	lon	sum	sum_area	area	height
2308054	13:36:00	78,34733650	10,23711017	24,9106	1,160461	21,5	58,5
2308055	13.36.43	78,34790283	10,23760635	79,1332	1,060362	40,2	90,2
2308056	13:37:18	78,34[illegible]	10,23728167	15,6700	0,745597	[illegible]	56,1
2308057	13:39:11	78,34907850	10,23877150	16,1056	0,726321	37,9	60,1
2308058	13:43:50	78,35114017	10,23353217	2,7708	0,260042	10,3	30,0
2308059	13:44:12	78,35[illegible]700	10,23211517	1,9796	0,275110	6,7	[illegible]
2308060	13:47:06	78,34573850	10,23490500	35,6140	1,473811	22,7	73,0
2308061	13:47:54	78,34533817	10,23550167	6,0914	0,600653	5,7	42,5
2308062	13:48:04	78,34[illegible]	10,23621717	22,7[illegible]	1,025[illegible]	[illegible]	71,1
2308063	13:48:37	78,34773467	10,23652685	30,0385	1,730824	17,5	62,3
2308064	13:49:01	78,34730067	10,23758450	52,9765	1,004632	26,5	74,5
2308065	13:49:14	78,34574200	10,23879510	56,1821	1,540[illegible]	37,7	79,[illegible]
2308066	13.50.19	78,34320700	10,23955385	15,3345	0.422104	36,3	78,5
2308067	13:50:01	78,34706467	10,23954517	101,5282	2,028783	50,1	84,0
2308068	13:52:10	78,347[illegible]457	10,23772711	75,[illegible]	1,6[illegible]	[illegible]	76,[illegible]
2308069	14:00:08	78,34773750	10,23654850	40,2558	1,691888	23,5	53,6
2308070	14:00:58	78,34405650	10,23576535	31,1225	1,004405	51,0	58,5
2308071	14:05:17	78,34754800	10,23557617	69,[illegible]	1,142[illegible]	60,6	79,6
2308072	14.10.42	78,34690500	10,24030350	175,5609	1,894874	97,9	93,5
2308073	14:12:00	78,34[illegible]267	10,24454785	15,5595	0,545475	26,[illegible]	77,1
2308074	14:14:01	78,34[illegible]517	10,24817250	5,7548	0,351124	10,1	45,[illegible]
2308075	14.15.31	78,34473867	10,23830350	5,9916	0,545293	17,4	34,5
2308076	14:21:52	78,34[illegible]857	10,24919567	4,4549	0,178185	25,2	45,4
2308077	14:24:56	78,34[illegible]	10,24251517	41,8373	1,780183	34,1	54,3
2308078	14.24.35	78,34705750	10,24115417	32,4220	1,615687	20,1	69,4
2308079	14:25:27	78,34714858	10,24975550	84,0012	2,545505	53,5	84,5
2308080	14:26:07	78,34711550	10,23712950	74,1111	1,525749	48,7	72,7
2308081	14.27.07	78,34754050	10,23438100	13,5181	0,501743	26,9	54,4
2308082	14:36:05	78,34713763	10,23830[illegible]	131,7506	1,015604	84,5	82,0
2308083	14:36:49	78,34718050	10,24096783	77,5890	1,589024	43,6	71,1
2308084	14.37.37	78,34714650	10,24357233	39,1713	1,623313	24,1	44,4
2308085	14:38:27	78,34701717	10,24513888	12,0022	0,317027	27,[illegible]	51,5
2308086	14:39:11	78,34704957	10,24896767	4,9527	0,525491	19,0	51,3
2308087	14.41.46	78,34686850	10,23650400	25,6248	0,304098	26,5	56,4
2308088	14:47:56	78,3478[illegible]317	10,24403550	10,1827	0,307541	33,[illegible]	54,2
2308089	14:48:01	78,34783757	10,27230500	6,8645	0,375225	18,1	40,9
2308090	14.48.36	78,34772550	10,24034733	5,5620	0,428344	13,0	43,0
2308091	14:49:12	78,34761253	10,24757281	6,2166	0,475654	11,0	55,1
2308092	14:50:08	78,34748450	10,24459067	50,7973	0,920679	53,1	81,7
2308093	14.51.00	78,34739453	10,24203567	35,3361	0,669902	49,9	67,5
2308094	14:51:10	78,34722717	10,23975450	87,4787	1,411171	61,9	84,1
2308095	14:52:14	78,34709600	10,23784950	32,0981	0.781179	41,0	61,3
2308096	15:06:04	78,340[illegible]3567	10,24[illegible]33533	101,0512	0,969620	116,2	95,0
2308097	15:06:07	78,34044200	10,24751084	37,2017	0,714124	47,0	97,3
2308098	15:10:39	78,34041867	10,24941017	17,0827	0.335757	52,1	93,5
2308099	15:14:20	78,34063067	10,24650067	95,3211	1,640262	56,6	101,7
2308100	15:14:52	78,34075[illegible]	10,24500767	41,1317	1,70[illegible]	28,[illegible]	91,[illegible]
2308101	15:15:33	78,34090417	10,24209135	41,3744	0.806191	47.7	93,5
2308102	15:30:12	78,34031400	10,24200517	23,0580	0,307834	64,7	90,1
2308103	15:31:29	78,34085417	10,24615614	121,8074	1,121380	108,[illegible]	97,[illegible]
2308104	15:52:10	78,34114600	10,24837500	13,5335	0,462904	29,3	57,7
2308105	15:30:07	78,34108117	10,24342300	16,7724	0,304781	42,5	82,1
2308106	15:[illegible]	78,34011617	10,24100767	60,5485	0,649014	71,1	97,9
2308107	15.40.31	78,34003833	10,24404535	17,7907	0.795331	22,4	50,3
2308108	15:41:02	78,33162250	10,24378836	4,5940	0,184743	24,3	80,8
2308109	15:45:56	78,34018817	10,24[illegible]	15,1180	0,271612	21,1	73,[illegible]
2308110	15:51:07	78,34099053	10,24306267	153,3473	1,254390	134,6	92,0
2308111	16:40:58	78,35015400	10,22444567	1,2270	0,445724	2,7	15,7
2308112	16:[illegible]	78,35060[illegible]	10,22292367	0,9645	0,179474	1,8	37,1
2308113	16.30.39	78,36520067	10,17304335	1,7907	0,277193	6,5	42,3
2308114	16:55:57	78,37524300	10,14277085	1,1959	0,115[illegible]	10,5	78,4

flare_id	time	lat	lon	sum	sum_area	area	height
2308115	16:57:07	78,58052750	10,15367917	2,9878	0,245041	13,2	43,9
2308116	16:58:58	78,58419883	10,12254050	2,7850	0,265571	10,5	41,5
2308117	17:00:10	78,58858000	[illegible]	[illegible]	[illegible]	15,5	40,8
2308118	17:01:41	78,58968167	10,17002517	4,1038	0,330491	14,6	44,7
2308119	17:02:21	78,59006017	10,10201400	3,2274	0,324354	9,9	44,6
2308120	[illegible]	[illegible]	[illegible]	[illegible]	[illegible]	7,2	[illegible]
2408001	00:40:28	78,51757753	10,25619837	11,3707	0,901791	13,6	23,9
2408002	00:45:42	78,52574267	10,25261823	22,6322	1,472342	15,4	35,8
2408003	[illegible]	[illegible]	[illegible]	[illegible]	[illegible]	[illegible]	[illegible]
2408004	23:51:24	78,53705200	10,25363530	2,1212	0,033373	35,6	63,1
2408005	23:54:57	78,53260800	10,25021423	2,1640	0,034304	62,4	65,4
2508001	[illegible]	[illegible]	[illegible]	[illegible]	[illegible]	4,9	11,9
2508002	01.01.22	78.59531850	9.87853283	0.4337	0.037847	7,5	20,4
2508003	01.28:00	78,62036352	9.74142300	0,3442	0,030585	11,1	25,1
2508004	[illegible]	[illegible]	[illegible]	[illegible]	[illegible]	20,0	[illegible]
2508005	01:37:11	78,64070483	9.70343483	0,3132	0,018143	17,2	43,4
2508006	01:57:11	[illegible]	[illegible]	0,4754	0,052561	9,1	17,6
2508007	[illegible]	[illegible]	[illegible]	[illegible]	[illegible]	2,6	15,1
2508008	03.29.21	78,34845017	10,19650683	1,9777	0,034104	36,5	75,8
2508009	[illegible]	78,35137183	[illegible]	0,5072	[illegible]	24,4	62,6
2508010	[illegible]	[illegible]	[illegible]	[illegible]	[illegible]	[illegible]	57,4
2508011	13.31.23	78,36051217	10,25826430	0,4534	0,033384	13,5	43,5
2508012	[illegible]	[illegible]	[illegible]	[illegible]	[illegible]	35,2	70,0
2508013	[illegible]	[illegible]	[illegible]	1,4775	[illegible]	[illegible]	[illegible]
2508014	14.03.57	78,38979383	10,12728400	1,9430	0,175123	11,1	70,0
2508015	[illegible]	[illegible]	[illegible]	[illegible]	[illegible]	[illegible]	60,5
2508016	[illegible]	[illegible]	[illegible]	[illegible]	[illegible]	9,4	48,9
2508017	14.05.19	78,38975753	10,10064683	0,6130	0,041984	13,5	43,4
2508018	[illegible]	[illegible]	[illegible]	[illegible]	[illegible]	[illegible]	[illegible]
2508019	[illegible]	[illegible]	[illegible]	[illegible]	[illegible]	27,5	44,0
2508020	14.32.28	78,38965883	9,80879080	0,3032	0,047237	12,1	13,0
2508021	14:55:44	[illegible]	[illegible]	[illegible]	[illegible]	[illegible]	12,8
2508022	[illegible]	[illegible]	[illegible]	0,7692	[illegible]	5,0	13,7
2508023	15.27.51	78,64108050	9,48828183	0,8675	0,031293	27,7	55,2
2508024	[illegible]	[illegible]	[illegible]	[illegible]	[illegible]	21,6	55,9
2508025	[illegible]	78,56047217	9,47791900	0,4930	0,048373	10,5	25,8
2508026	16.25.22	78,65564750	9,46851480	0,7937	0,035607	22,3	52,7
2508027	[illegible]	[illegible]	[illegible]	[illegible]	[illegible]	[illegible]	53,1
2508028	17:54:39	78,55565317	9,45447017	[illegible]	0,015907	71,0	151,4
2508029	18.12.48	78,66543862	9,43880380	0,9060	0,025274	35,0	42,4
2508030	[illegible]	[illegible]	[illegible]	[illegible]	[illegible]	[illegible]	[illegible]
2508031	18:18:54	78,55950083	9,43571457	10,1790	0,041737	243,5	140,2
2508032	18:20:51	78,66738462	9,44095183	4,5442	0,023783	187,5	75,6
2508033	[illegible]	[illegible]	[illegible]	[illegible]	[illegible]	[illegible]	[illegible]
2508034	18:38:59	78,55736789	9,45346030	1,0474	0,034083	30,5	44,1
2508035	18:50:52	78,63862017	9,45280867	3,0633	0,026514	114,3	115,2
2508036	[illegible]	[illegible]	[illegible]	[illegible]	[illegible]	[illegible]	[illegible]
2508037	19:17:57	78,53787383	9,44325617	3,3834	0,040011	83,1	83,7
2508038	19:19:40	78,64281400	9,45431683	12,5840	0,063104	199,4	106,2
2508039	[illegible]	[illegible]	[illegible]	[illegible]	[illegible]	[illegible]	[illegible]
2508040	19:21:11	78,64504753	9,43723283	4,0364	0,109195	36,9	60,1
2508041	19:25:18	78,64846100	9,43452967	14,6062	0,083650	175,7	81,6
2508042	[illegible]	[illegible]	[illegible]	[illegible]	[illegible]	[illegible]	74,6
2508043	19.30.00	78,65555750	9,43303983	24,2132	0,105393	250,0	128,2
2508044	19:30:51	78,65447850	[illegible]	1,2846	0,055565	25,0	54,4
2508045	[illegible]	[illegible]	[illegible]	[illegible]	[illegible]	57,2	67,0
2508046	20:11:49	78,66105700	9,41493617	5,3874	0,044093	120,3	73,5
2508047	20:14:50	[illegible]	[illegible]	15,4715	[illegible]	259,7	146,2
2508048	20:17:17	[illegible]	[illegible]	[illegible]	[illegible]	[illegible]	54,7
2508049	20.18.57	78,65459100	9,41303667	2,7856	0,034005	81,9	73,5
2508050	[illegible]	[illegible]	[illegible]	5,2979	[illegible]	[illegible]	80,1

flare_id	time	lat	lon	sum	sum_area	area	height
2508051	20:41:35	78.52580650	9,45477483	12,4105	0,026129	475,2	204,2
2508052	20:54:03	78.52550083	9,42475083	0,5578	0,025122	22,2	45,4
2508053	21:16:32	[illegible]	9,40867650	1,6711	0,047474	[illegible]	[illegible]
2508054	22:12:14	78.52503700	9,40693907	4,6015	0,027701	156,1	79,5
2508055	22:28:55	78,52006167	9,41410623	2,3919	0,024394	97,6	62,1
2508056	22:41:10	78,51877450	9,40862700	3,6106	0,030521	118,3	76,5
2508057	22:54:32	78.52045817	9,40397870	3,3503	0,027415	131,7	81,4
2508058	22:56:10	78.52295353	9,40142523	2,4573	0,028155	87,3	90,2
2508059	22:59:25	[illegible]	9,40800683	[illegible]	0,058190	250,0	126,0
2608001	03:01:35	78.75947050	8,98293583	4,6245	0,050451	91,7	115,3
2608002	03:27:12	78,73861457	9,16752417	2,2524	0,048952	45,5	73,5
2608003	04:38:08	[illegible]	9,10411183	1,7793	0,031857	56,7	51,0
2608004	04:53:17	78.51304083	9,40988617	5,8540	0,039087	147,0	79,9
2608005	04:56:55	78.50515450	9,41414050	3,8205	0,026111	146,3	97,3
2608006	05:00:38	78,59297117	9,42104417	7,9908	0,029121	137,4	135,1
2608007	05:03:39	78.59347117	9,42804837	1,6733	0,025744	63,1	68,5
2608008	05:05:54	78,59204353	9,45181700	2,7705	0,017533	158,0	120,8
2608009	[illegible]	78,58612457	9,43759330	6,1742	0,040590	171,5	100,1
2608010	05:17:16	78,57330050	9,45215183	1,9203	0,017318	100,6	102,2
2608011	05:25:44	78,56017817	9,45692017	2,8106	0,025191	101,6	90,5
2608012	05:29:11	[illegible]	9,47294883	7,3942	0,012471	208,3	100,3
2608013	05:31:25	78.55003617	9,47714083	3,6837	0,026921	190,9	94,0
2608014	05:43:55	78,54114353	9,49190817	1,1376	0,027889	90,7	58,2
2608015	05:50:50	78,55286750	9,48057583	15,7323	0,011495	396,4	144,7
2608016	05:52:30	78.55611400	9,47673967	12,0773	0,031688	253,7	136,1
2608017	05:54:28	[illegible]	9,47391583	7,7162	0,045577	150,5	145,5
2608018	05:56:05	[illegible]	9,47108583	3,0970	0,014224	[illegible]	80,0
2608019	05:59:04	78.56475350	9,46755800	1,9070	0,029101	65,5	77,5
2608020	06:04:26	78,57514850	9,45572550	1,8011	0,016164	96,6	102,2
2608021	06:14:14	78,59074700	9,43812283	1,8958	0,017451	179,9	138,1
2608022	06:20:54	78,60085567	9,42728797	2,0069	0,027349	72,9	93,0
2608023	06:28:08	78,62071457	9,40672617	1,1613	0,049075	25,0	56,4
2608024	[illegible]	[illegible]	9,40480500	2,4658	0,046348	53,5	79,0
2608025	06:35:01	78.62841200	9,40279917	5,6587	0,056199	100,7	96,3
2608026	06:37:55	78,62776100	9,40754800	9,8007	0,050145	197,7	201,4
2608027	06:39:31	78.63087550	9,39990417	8,9003	0,050801	176,5	[illegible]
2608028	06:42:53	78.63357453	9,39392797	3,4929	0,039239	92,5	41,7
2608029	06:48:56	78,62437750	9,40406600	21,7455	0,015691	635,1	117,1
2608030	[illegible]	78,61573850	9,41071830	25,6857	0,049127	541,0	212,1
2608031	06:53:22	78.61740083	9,41304133	2,1711	0,051411	42,2	59,1
2608032	06:55:58	78,61170500	9,41756907	18,2405	0,041955	435,7	156,1
2608033	06:59:37	78.60755817	9,42451017	11,1149	0,047373	293,6	93,4
2608034	07:01:21	[illegible]	9,42782517	2,0494	0,030812	66,5	55,5
2608035	07:08:57	78,59801450	9,43387150	6,7416	0,024075	270,5	152,7
2608036	07:11:31	78.58595667	9,44437930	12,4193	0,020013	630,0	201,7
2608037	07:17:59	78.57571933	9,45546100	2,5720	0,019297	133,2	115,6
2608038	07:27:50	78,56195600	9,47196600	6,5143	0,032465	201,1	101,4
2608039	07:29:36	78.56165133	9,47459717	1,9585	0,019643	99,7	97,9
2608040	07:33:47	78.55202453	9,48375500	3,9570	0,055392	71,1	81,4
2608041	07:35:19	[illegible]	9,48601783	7,1906	0,032150	292,4	124,5
2608042	07:39:14	78.54449800	9,49279597	10,7750	0,039179	275,0	137,6
2608043	07:41:21	78.54081350	9,49722600	6,8552	0,023790	287,4	125,4
2608044	07:46:36	[illegible]	9,49597450	4,1575	0,028037	148,1	102,7
2608045	07:51:17	78.55075800	9,49141167	2,8415	0,045128	63,0	101,2
2608046	07:53:57	78.55465600	9,48750883	20,1265	0,036035	558,5	259,2
2608047	07:55:06	78,55710950	9,48426583	3,0247	0,027027	138,5	111,9
2608048	07:56:16	78.56397033	9,47744700	1,7549	0,020850	83,3	108,3
2608049	08:07:52	78,56632600	9,47273083	6,5766	0,037421	175,7	156,2
2608050	08:05:18	78,57412961	9,45578780	4,8104	0,015741	[illegible]	151,9
2608051	08:08:06	78.57501100	9,46076917	5,0549	0,034117	147,5	136,1
2608052	08:12:56	78,58583257	9,45262657	6,8234	0,036083	175,6	178,6

flare_id	time	lat	lon	sum	sum_area	area	height
2608053	05:14:40	78,58978750	9,41289150	4,4693	0,033349	139,5	157,5
2608054	05:16:22	78,59265250	9,41369033	2,2757	0,022275	102,2	120,6
2608055	05:19:57	78,59571433	9,41122950	9,9237	0,031281	291,5	136,8
2608056	05:28:41	78,51291867	9,42113617	14,9517	0,136055	221,1	157,0
2608057	05:29:49	78,61465417	9,42137750	9,2051	0,140443	65,3	102,2
2608058	05:37:36	[illegible]	[illegible]	12,4801	0,041705	299,1	217,4
2608059	05:57:23	78,52739459	9,40770293	1,4551	0,032721	64,7	56,1
2608060	05:59:27	78,53087717	9,40261867	3,3327	0,022627	160,5	153,9
2608061	[illegible]	[illegible]	[illegible]	[illegible]	0,040400	27,5	62,2
2608062	14:51:42	78,70965250	8,27411517	1,3913	0,031003	41,7	57,6
2708001	05:36:52	78,55555850	9,42062433	7,9753	0,020102	265,0	113,4
2708002	15:47:57	[illegible]	9,41970667	2,1859	0,028766	75,1	65,1
2708003	15:51:18	78,52255489	9,41714033	1,1656	0,032134	53,3	86,0
2708004	15:54:27	78,51720553	9,42286853	4,0733	0,045581	100,1	97,1
2708005	15:57:40	[illegible]	9,42989117	2,0181	0,045771	44,1	57,8
2708006	17:11:49	78,38796700	9,45477550	0,9232	0,032073	40,7	56,4
2708007	17:15:56	78,38681100	9,45182953	1,7536	0,026605	67,4	65,1
2708008	17:19:35	78,37869967	9,46491000	2,3111	0,030021	76,0	62,1
2708009	17:23:50	78,36671967	9,47797400	2,3495	0,033193	73,3	73,3
2708010	17:31:47	78,35702700	9,48547200	2,4323	0,020107	121,0	104,2
2708011	17:34:55	78,35965717	9,49456083	5,7212	0,021751	261,3	116,6
2708012	17:38:16	78,34682633	9,49939867	7,1237	0,041311	171,7	105,3
2708013	17:54:51	78,35161117	9,49595317	3,0019	0,026552	115,5	158,3
2708014	17:59:40	78,35392167	9,49410000	1,4378	0,024349	130,1	84,7
2708015	18:04:39	78,36784967	9,48307317	3,6005	0,018931	190,2	128,2
2708016	18:05:21	78,37040850	9,47195753	7,1018	0,037530	190,2	125,7
2708017	18:51:41	78,61469281	9,45606031	1,1501	0,012568	11,7	47,5
2708018	18:37:23	78,62045000	9,42414217	2,3035	0,035049	65,3	73,3
2708019	18:51:56	78,59271767	9,41515717	0,4451	0,014481	25,0	50,9
2708020	18:54:31	78,59554067	9,42405451	1,4016	0,012364	20,9	38,1
2708021	19:01:53	78,61515050	9,43623133	0,6020	0,038635	17,2	40,2
2708022	19:32:50	78,56305050	9,48541957	1,1149	0,025187	82,5	85,0
2708023	20:10:37	78,76977750	9,49059057	0,9451	0,010455	13,7	51,4
2708024	20:55:11	78,63329483	9,43375100	3,4513	0,057303	59,9	55,5
2708025	20:55:17	78,53754550	9,44011950	2,1817	0,051303	42,5	55,0
2708026	21:01:54	78,53065267	9,41821717	1,4015	0,032713	63,5	68,6
2708027	23:03:04	78,62906553	9,43251253	3,7371	0,078974	47,3	84,4
2708028	23:06:50	78,58186283	9,43317953	1,2979	0,114023	17,7	47,5
2808001	01:54:06	78,78706950	9,19991417	1,9746	0,050493	39,1	58,6
2808002	03:06:03	78,38675350	9,28983050	2,0060	0,032030	90,9	123,6
2808003	15:20:57	78,55755433	9,45087717	19,9055	0,308780	64,5	106,7
2808004	15:24:26	78,55287467	9,45364917	20,6572	0,490725	43,1	51,0
2808005	15:25:52	78,55509850	9,43448753	15,5679	0,422489	36,9	44,1
2808006	15:27:10	78,55567283	9,43795657	5,0601	0,296001	17,0	40,2
2808007	15:34:43	78,55525253	9,43163757	57,6018	0,730785	78,9	53,7
2808008	15:37:43	78,55535217	9,43000280	9,4612	0,240074	35,3	45,7
2808009	15:39:41	78,55400517	9,42586717	8,4741	0,305877	27,7	43,5
2808010	15:42:40	78,55254300	9,41730317	2,0856	0,095294	21,9	63,4
2808011	15:49:57	78,55584382	9,42587317	1,5860	0,128010	12,4	25,0
2808012	15:51:05	78,55534117	9,41652741	4,0138	0,271121	17,0	25,6
2808013	15:53:26	78,56018750	9,43290400	6,2896	0,134396	44,6	69,6
2808014	16:02:00	78,55324382	9,43241200	9,2601	0,159102	59,5	58,2
2808015	16:07:11	78,55542000	9,45083091	51,6516	0,280497	179,6	84,0
2808016	16:10:52	78,55555067	9,42934153	23,7606	0,301987	65,7	59,2
2808017	16:30:00	78,55535050	9,41831853	14,1509	0,125134	113,1	87,5
2808018	16:36:11	78,54887050	9,43112107	11,0845	0,115043	66,0	67,4
2808019	16:40:09	78,54636059	9,43321853	16,0841	0,138250	101,3	80,9
2808020	16:44:50	78,53422017	9,46410350	0,5674	0,054472	10,3	24,8
2808021	17:48:07	78,74191081	9,62461117	0,2757	0,065113	4,2	19,7
2808022	17:58:47	78,34562867	9,62303617	0,3038	0,051273	5,7	13,6
2808023	18:00:54	78,54047400	9,63241117	0,4354	0,050783	8,6	30,0

flare_id	time	lat	lon	sum	sum_area	area	height
2908024	18:06:39	78.51720667	9,65143433	0,4700	0,042087	11,3	27,9
2908025	20:07:24	78.50580150	9,68468017	2,4093	0,057284	42,1	53,7
2908026	20:12:11	78.50786900	9,68562137	0,6294	0,043715	14,1	56,0
2908027	21:11:14	78.49070717	9,70372817	0,4781	0,076744	5,2	19,0
2908028	21:15:59	78.49096650	9,70750517	2,3406	0,096520	24,3	56,0
2908029	22:44:19	78.49550917	9,71300530	0,7747	0,041655	18,5	44,4
2908030	23:40:59	78.35144753	9,75151257	2,1593	0,072229	29,5	49,0
2908031	23:42:13	78.34525850	9,75073733	3,1871	0,077782	41,0	66,4
2908001	00:17:34	78.47364017	9,72958290	7,1447	0,074453	96,4	122,4
2908002	00:18:16	78.47433317	9,72649283	5,8206	0,094347	61,6	77,0
2908003	00:49:57	78.46615800	9,75805100	1,1515	0,048817	23,6	84,3
2908004	01:24:21	78.37812121	9,73571943	0,9314	0,045103	19,1	47,8
2908005	01:27:49	78.34030400	9,74027483	0,7509	0,045779	16,4	53,3
2908006	01:28:51	78.34545753	9,74040083	1,7549	0,067792	25,6	62,3
2908007	01:29:30	78.34274117	9,74057917	2,9199	0,091711	40,7	90,6
2908008	01:30:37	78.35389917	9,74062593	2,1016	0,036053	59,3	54,6
2908009	01:31:52	78.35405457	9,74057250	2,0869	0,089581	23,5	63,3
2908010	01:35:54	78.35752617	9,74557717	0,2566	0,036179	7,1	21,0
2908011	01:32:30	78.33401417	9,74773600	2,5910	0,137133	18,9	49,3
2908012	01:52:59	78.33275050	9,74752733	1,1651	0,050182	23,2	56,7
2908013	02:21:11	78.47411183	9,74719545	1,7615	0,029658	59,1	54,5
2908014	02:30:37	78.45363317	9,74694433	0,6726	0,029204	23,0	37,5
2908015	02:45:00	78.43737200	9,75641743	0,8508	0,035375	24,5	64,1
2908016	03:12:11	78.48111957	9,75682100	0,1858	0,032417	5,7	21,0
2908017	03:36:11	78.32554383	9,75751600	0,2646	0,030449	3,2	19,6
2908018	03:48:14	78.35175400	9,75800967	4,1787	0,095421	44,0	80,5
2908019	04:00:15	78.37285731	9,70692593	0,1001	0,065747	1,5	11,5
2908020	04:25:46	78.61580017	9,41260067	6,0775	0,149663	40,9	51,5
2908021	06:55:06	78.62224583	9,40772463	13,6155	0,077567	174,6	138,0
2908022	07:18:32	78.62041500	9,40721700	15,1947	0,197183	91,1	74,5
2908023	07:38:12	78.61343733	9,42559283	7,4261	0,092830	90,0	96,7
2908024	07:58:06	78.61744657	9,41752443	15,4524	0,119970	137,1	97,7
2908025	08:17:15	78.61155617	9,41524513	8,9294	0,086181	102,9	111,4
2908026	08:40:07	78.61371233	9,41942100	19,9287	0,211228	94,6	98,5
2908027	08:57:28	78.61155583	9,41536550	12,1587	0,141585	84,2	87,5
2908028	09:09:04	78.61194250	9,42782717	36,5163	0,285390	136,0	171,7
2908029	09:23:53	78.60963750	9,41352523	25,9406	0,216044	120,1	90,4
2908030	09:24:56	78.61135717	9,40787613	8,5570	0,112275	76,2	107,4
2908031	09:39:38	78.50810257	9,47920500	16,2487	0,115027	140,4	59,5
2908032	10:03:03	78.61645767	9,41090050	5,5744	0,062025	89,9	100,7
3008001	13:58:00	78.51817717	9,77600700	0,1962	0,014790	13,4	36,1
3008002	14:39:31	78.47929059	9,77479993	0,7815	0,094987	16,9	52,7
3008003	14:51:57	78.46336063	9,77460723	1,4415	0,059002	24,5	54,0
3008004	15:51:49	78.45111257	9,79155743	0,2247	0,024690	9,2	35,4
3008005	15:56:40	78.45505950	9,79110917	0,2079	0,015769	13,3	32,3
3008006	15:59:52	78.46485117	9,79092200	0,5580	0,019025	28,3	40,3
3008007	16:45:17	78.35509961	9,79171563	0,2247	0,009095	24,7	45,8
3008008	17:32:46	78.47347300	9,80889993	0,1636	0,009961	16,9	29,1
3008009	17:43:20	78.45144500	9,80799050	0,4583	0,009778	46,9	78,5
3008010	17:51:38	78.42737650	9,80772683	0,3427	0,017180	19,1	47,0
3008011	19:53:50	78.43529967	9,82091733	0,4401	0,015303	52,6	90,1
3008012	20:27:33	78.55201317	9,82877523	1,0533	0,040885	25,8	45,3
3008013	20:29:14	78.55351521	9,83006167	0,4422	0,013877	31,9	49,1
3008014	20:40:01	78.35374500	9,84918093	0,5778	0,017104	53,5	68,5
3008015	20:41:02	78.35181000	9,84805583	3,7745	0,060625	62,3	67,0
3008016	21:31:38	78.44487017	9,84172603	0,1022	0,018456	5,6	16,7
3008017	21:57:44	78.43093767	9,84307067	0,1734	0,014681	11,5	33,1
3008018	21:50:59	78.42529153	9,84207623	0,8967	0,021715	41,9	60,6
3008019	21:48:00	78.44179157	9,85744157	0,0046	0,000019	248,5	54,1
3008020	23:48:08	78.44338867	9,86344167	0,0067	0,000003	2360,5	73,0
3108001	00:57:41	78.55426553	9,85656163	2,2755	0,065734	64,1	95,5

flare_id	time	lat	lon	sum	sum_area	area	height
3108002	01:28:59	78,46794167	9,28037853	0,4913	0,034573	20,0	50,9
3108003	01:29:42	78,46521750	9,28005753	0,4725	0,028152	16,8	36,0
3108004	04:31:51	78,[illegible]	[illegible]	0,47[illegible]	0,010807	43,7	73,0
3108005	04:34:13	78,46517083	9,29829857	0,5211	0,030793	23,5	41,7
3108006	04:36:22	78,46061300	9,29567853	0,7477	0,024200	30,9	42,4
3108007	05:18:56	[illegible]	[illegible]	0,4508	0,016551	16,9	65,7
3108008	07:24:40	78,55950453	9,51963253	0,9893	0,037511	37,2	73,0
3108009	08:15:40	78,47065717	9,51501017	1,7550	0,025765	65,2	80,1
3108010	10:18:40	78,55[illegible]483	9,477[illegible]	4,8209	0,027[illegible]	[illegible]	89,6
3108011	10:21:18	78,55787317	9,47129267	6,1302	0,045351	134,7	103,3
3108012	10:42:12	78,59118750	9,43210267	4,2970	0,028672	149,6	106,0
3108013	10:47:57	78,59859417	9,42454000	0,[illegible]	0,028[illegible]	22,2	47,7
3108014	10:49:52	78,50534167	9,42043957	2,1731	0,045384	48,0	68,2
3108015	10:52:20	78,50819000	9,41461767	2,4640	0,029215	84,3	101,0
3108016	10:57:24	[illegible]	9,48700[illegible]	[illegible]	0,026[illegible]	[illegible]	[illegible],4
3108017	11:20:57	78,62552453	9,39963200	12,2885	0,048313	254,3	116,9
3108018	11:25:24	78,52185400	9,40[illegible]	7,5134	0,042465	176,[illegible]	85,0
3108019	11:[illegible]	[illegible]	9,41[illegible]	4,0[illegible]	0,029437	[illegible]	75,3
3108020	11:33:42	78,60964850	9,41816583	5,7598	0,037016	83,9	69,7
3108021	11:3[illegible]	78,50725[illegible]	9,426[illegible]	6,[illegible]	0,054[illegible]	122,1	85,4
3108022	[illegible]	[illegible]	[illegible]	7,[illegible]	0,046138	170,[illegible]	90,8
3108023	12:18:00	78,35707083	9,47384583	5,7336	0,037777	151,3	106,2
3108024	12:20:24	78,55[illegible]	9,477[illegible]	9,3[illegible]	0,050565	153,[illegible]	127,[illegible]
3108025	12:2[illegible]	[illegible]	9,4757[illegible]	5,7817	0,071374	81,0	83,8
3108026	12:24:56	78,34969083	9,48814433	14,9629	0,049837	300,2	111,2
3108027	12:[illegible]	[illegible]	9,49477517	5,2051	0,032[illegible]	156,[illegible]	95,[illegible]
3108028	[illegible]	[illegible]	9,49421657	4,2[illegible]	0,0[illegible]	[illegible],7	106,1
3108029	12:45:51	78,35193317	9,48873017	4,6387	0,040440	119,3	90,9
3108030	12:[illegible]:54	[illegible]	9,4836[illegible]	[illegible]	0,041295	71,6	71,[illegible]
3108031	[illegible]	[illegible]	9,47098[illegible]	[illegible]	0,03[illegible]	[illegible]	[illegible],9
3108032	13:09:50	78,39130617	9,44201583	8,7918	0,030720	296,2	157,7
3108033	13:12:30	[illegible]	9,43572650	6,4765	0,025[illegible]	254,1	117,[illegible]
3108034	13:21:44	78,51163917	9,420[illegible]	9,1[illegible]	0,047390	194,0	97,3
3108035	13:25:09	78,61731383	9,41374817	11,7939	0,038833	303,7	162,1
3108036	14:01:50	[illegible]	9,4207[illegible]	47,2705	0,061[illegible]	768,1	[illegible]4,1
3108037	14:13:12	78,51017850	9,42010117	110,8101	0,118029	939,7	138,8
3108038	15:19:24	78,36526517	9,47920780	16,1540	0,043222	373,3	87,2
3108039	15:3[illegible]	78,55067417	9,49[illegible]	38,5765	0,039525	554,1	10[illegible]
3108040	[illegible]	78,75420100	9,48521117	4,8011	0,046871	102,5	95,7
3108041	16:09:50	78,36313367	9,47206067	7,2700	0,050675	143,3	98,9
3108042	[illegible]	[illegible]	9,46[illegible]	4,6[illegible]	0,039174	118,7	81,7
3108043	16:15:47	78,37912383	9,46084100	6,0751	0,048735	124,7	99,2
3108044	16:21:54	78,38569082	9,45275850	5,8045	0,051775	112,1	104,7
3108045	16:25:[illegible]	[illegible]	9,4[illegible]8817	6,[illegible]	0,035[illegible]	195,[illegible]	108,[illegible]
3108046	16:37:23	78,61081117	9,42023017	6,0051	0,084854	77,9	70,2
3108047	16:38:52	78,61292362	9,42412983	20,2011	0,230836	121,0	105,3
3108048	16:4[illegible]	[illegible]	9,411[illegible]	17,[illegible]	0,057[illegible]	301,[illegible]	170,1
3108049	16:51:59	78,58079100	9,49367630	4,9955	0,072535	95,5	70,8
3108050	17:05:49	78,62535367	9,40255183	23,2536	0,054409	515,5	122,4
3108051	17:11:[illegible]	[illegible]	9,4817[illegible]	[illegible]	0,068[illegible]	497,[illegible]	[illegible]
3108052	17:23:40	78,60524700	9,41781630	31,1795	0,036937	463,7	127,7
3108053	17:27:52	78,50898367	9,42204683	14,6718	0,052226	280,0	98,7
3108054	[illegible]	[illegible]	9,4770[illegible]	16,0[illegible]	0,07[illegible]	217,[illegible]	107,[illegible]
3108055	18:12:52	78,35416353	9,47883017	11,8930	0,084141	141,4	95,9
3108056	18:16:47	78,34061583	9,48214067	17,8514	0,072222	247,2	84,6
3108057	[illegible]	78,[illegible]4147117	9,4942[illegible]	2,7[illegible]48	0,032423	[illegible]	[illegible],7
3108058	18:38:50	78,35289783	9,47903130	18,8013	0,048271	384,7	144,2
3108059	18:42:15	78,[illegible]5772117	9,47294517	14,0445	0,056363	247,0	140,4
3108060	19:0[illegible]	[illegible]	9,4762[illegible]	[illegible]	0,031567	84,5	102,8
3108061	19:13:53	78,60637067	9,42146753	9,7817	0,049421	197,9	87,1
3108062	19:1[illegible]	78,[illegible]	9,41[illegible]	21,1517	0,05[illegible]	325,5	156,2

flare_id	time	lat	lon	sum	sum_area	area	height
2108063	19:24:36	78.52917459	9,40299500	8,6992	0,060624	143,4	104,1
2108064	19.27.37	78.52759767	9,39792600	9,5100	0,074282	127,9	101,1
2108065	20:12:36	[illegible]	[illegible]	7,3944	0,049059	157,5	154,6
2108065	20:15:09	78.38711717	9,79959200	6,8515	0,030158	136,0	135,0
109001	01:27:56	78.44561150	9,96308050	7,1127	0,026211	213,5	106,4
109002	01:40:27	[illegible]	[illegible]	1,1064	[illegible]	46,0	56,5
109003	03:54:41	78.44454567	9,95003700	4,9737	0,028440	174,9	64,0
109004	06:56:24	78.45530000	9,97042067	1,0170	0,025732	39,5	62,2
109005	09:45:17	[illegible]	[illegible]	[illegible]	[illegible]	71,0	56,0
109006	09:52:13	78.39720800	9,77451983	0,6032	0,035883	16,9	23,5
109007	11:16:09	78.36202800	9,45408417	4,2599	0,060722	69,5	62,5
109008	17:45:57	[illegible]	9,46710900	10,7956	[illegible]	217,0	154,9
109009	18.13.08	78.37375800	9,71192783	1,0531	0,038943	27,5	48,4
109010	20:42:40	78.53032653	10,35871686	0,4571	0,102172	4,5	3,2
209001	00:16:16	[illegible]	[illegible]	3,4108	0,032077	106,4	89,5
209002	01:51:30	78.44715567	9,98754767	0,7921	0,035878	138,9	73,7
209003	01:47:56	78.44444700	9,95720400	15,4555	0,040043	386,2	55,7
209004	02:22:11	[illegible]	[illegible]	5,2934	[illegible]	175,9	79,2
209005	02.26.09	78.44321353	9,96108567	7,8711	0,038123	206,3	63,1
209006	02:52:42	78.42172600	9,80606583	0,3647	0,045375	8,4	19,4
209007	22:10:09	[illegible]	[illegible]	0,9934	[illegible]	64,7	45,8
209008	22.15.02	78.50713767	9,58041900	1,2546	0,017831	70,4	71,7
209009	22:16:58	[illegible]	9,58885067	1,7977	[illegible]	110,6	97,4
209010	22:20:54	[illegible]	[illegible]	3,4701	[illegible]	138,2	112,7
209011	22.23.19	78.49424000	9,59675783	13,0179	0,049690	262,0	130,8
209012	22:25:43	[illegible]	9,60081783	1,2641	0,025055	53,5	54,5
209013	22:35:02	[illegible]	[illegible]	6,1521	0,029181	216,2	94,1
309001	17.56.10	78.38576050	9,45004267	7,4502	0,079773	93,4	100,8
309002	18:03:58	[illegible]	9,44050883	15,4404	0,035179	438,9	149,1
309003	18:18:38	[illegible]	[illegible]	49,4119	[illegible]	391,3	119,3
309004	18.19.39	78.31417550	9,42220517	10,4077	0,113810	96,9	96,2
309005	18:24:46	78.31114950	[illegible]	[illegible]	[illegible]	214,0	80,4
309006	18:39:10	[illegible]	9,41237517	5,9724	[illegible]	197,0	84,3
309007	18.36.20	78.33102250	9,40322900	5,8080	0,037490	154,9	62,1
309008	18:48:19	[illegible]	[illegible]	[illegible]	[illegible]	832,0	132,7
309009	18:52:39	78.31573967	9,41090870	32,0775	0,095329	346,9	117,2
309010	18.58.02	78.31377350	9,41775133	20,5242	0,041943	450,3	134,6
309011	19:04:08	[illegible]	[illegible]	20,9621	0,047517	[illegible]	114,1
309012	19:17:31	[illegible]	[illegible]	10,6467	[illegible]	430,2	110,9
309013	19.06.42	78.30445200	9,42806067	1,4667	0,034403	42,6	36,3
309014	[illegible]	[illegible]	[illegible]	4,7025	[illegible]	224,0	100,6
309015	19:44:37	78.36950067	9,47200493	6,7261	0,032196	208,9	115,9
309016	19:46:44	78.36181400	9,47462717	4,5749	0,024762	191,5	122,0
309017	19:55:54	[illegible]	[illegible]	5,7977	[illegible]	155,9	77,1
309018	19:58:15	78.34954030	9 45757107	6 9134	0,038979	177,3	100,8
309019	20:02:42	78.34443833	9,48340700	6,4120	0,056027	114,4	73,6
309020	[illegible]	[illegible]	[illegible]	[illegible]	[illegible]	169,2	94,4
309021	20:12:36	78.35330217	9,48061483	20,9173	0,046083	453,9	132,7
309022	20:25:43	78.35575200	9,47680630	15,9891	0,060098	260,7	120,1
309023	20:48:14	[illegible]	[illegible]	[illegible]	0,050484	215,5	125,0
309024	20:51:24	78.36148617	9,47148883	7,4183	0,035389	230,9	137,9
309025	20:54:04	78.36421817	9,46795183	3,0786	0,026492	181,0	130,8
309026	[illegible]	[illegible]	[illegible]	2,6147	[illegible]	101,5	94,0
309027	21.08.52	78.30123753	9,42073283	4,0174	0,027010	148,7	111,4
309028	21:13:51	78.30530417	9,42096117	10,9553	0,046827	250,7	96,8
309029	21:17:37	[illegible]	[illegible]	25,4049	[illegible]	[illegible]	146,3
309030	21:27:48	78.32108500	9,40318593	6,4577	0,041738	134,7	84,1
309031	21:29:43	78.32279163	9,40806737	8,0597	0,055824	141,1	110,2
309032	[illegible]	[illegible]	[illegible]	[illegible]	[illegible]	375,9	154,0
309033	21.36.30	78.32394167	9,39472100	10,7434	0,039431	130,3	110,4
309034	21:42:42	[illegible]	[illegible]	8,3646	[illegible]	237,1	156,5

flare_id	time	lat	lon	sum	sum_area	area	height
309025	21:59:58	78,51262167	9,41110917	8,1117	0,035781	228,0	91,1
309026	22:05:12	78,50632300	9,41374367	9,0144	0,028754	255,5	82,6
309027	22:10:14	78,50725183	9,42781217	4,6361	0,031429	146,5	72,5
309028	22:21:18	78,58916787	9,45493767	7,1830	0,064101	112,1	96,8
309029	22:52:42	78,55615650	9,47112383	11,4006	0,056473	202,4	158,3
309030	22:57:55	78,55107400	9,47701163	4,6469	0,028647	163,6	87,7
409001	03:03:12	78,55654867	9,86013050	0,3578	0,032595	25,5	27,6
409002	05,58:54	78,54800382	10,26817800	21,7111	0,137765	157,6	40,5
409003	05:59:20	78,54813083	10,27045745	36,0286	0,237403	151,7	57,1
409004	06:01:10	78,54511153	10,24190200	32,1470	0,256001	125,6	51,0
409005	06:07:27	78,54854262	10,24180628	5,7956	0,062063	93,3	51,1
409006	06:08:19	78,55001900	10,24302817	2,9115	0,037711	74,4	45,0
409007	06:11:50	78,55276383	10,22703833	2,7334	0,030177	90,5	47,8
409008	06:20:41	78,57077217	10,19194083	1,0457	0,042230	46,1	34,7
409009	[illegible]	78,57727167	10,17608717	0,6609	0,013470	27,0	25,0
409010	13:30:50	78,37481753	10,17370217	33,0141	0,339329	136,9	81,5
409011	12:54:52	78,57474452	10,19688167	44,4562	0,157145	286,0	87,6
409012	[illegible]	78,57744708	10,18957730	30,1029	0,151841	254,5	80,7
409013	13.04.28	78,37613383	10,16382933	32,1707	0,191364	272,6	79,5
409014	13:02:14	78,38245450	10,17850333	7,6729	0,058760	114,1	75,0
409015	13:31:30	78,38451167	10,13091830	1,4821	0,025631	57,4	23,6
409016	13.38.27	78,38510667	10,15720183	3,9157	0,035337	153,8	61,4
409017	13:45:56	78,38473054	10,13690750	24,8654	0,019555	75,4	55,5
409018	13:48:44	78,38221017	10,14897430	2,0181	0,027159	77,5	47,3
409019	13.00.23	78,36969053	10,13427867	1,4909	0,021089	70,7	35,0
409020	15:00:22	78,56137083	10,20874630	2,2904	0,028085	81,5	57,1
409021	17:07:14	78,57961281	10,14513430	10,5115	0,077551	134,8	75,1
409022	17.13.12	78,58808617	10,03813437	1,9514	0,044951	43,4	63,2
409023	17:15:05	78,59134400	10,07696817	0,5744	0,041810	25,4	27,2
409024	17:59:54	78,52168917	9,99784667	1,0758	0,019459	57,8	41,9
409025	18.01.47	78,65453900	9,70147580	2,4057	0,027252	83,6	73,9
409026	19:54:56	78,54053467	9,62460653	0,2109	0,024577	8,2	18,6
409027	19:59:57	78,56517217	9,74911617	1,3137	0,019463	11,4	51,7
409028	20.57.40	78,67234253	9,60125330	0,3057	0,015171	20,2	24,2
509001	00:45:54	78,51205817	9,75565650	2,7814	0,047512	46,2	57,8
509002	03:58:10	78,06217117	10,08154117	0,9216	0,042313	21,8	33,7
509003	03.59.24	78,56541783	10,07759483	1,4617	0,048082	30,4	45,0
509004	04:01:34	78,56556033	10,03976250	0,4063	0,021123	15,5	35,5
509005	04:04:04	78,56760967	10,03171700	0,4979	0,019073	13,7	31,8
509006	05.22.51	78,63825900	9,79784250	1,0435	0,039702	26,3	46,5
509007	05:27:57	78,64317250	9,78429010	1,0345	0,031457	30,0	37,5
509008	05:29:42	78,64552950	9,78057307	2,8357	0,035309	80,4	73,0
509009	05:58:02	78,60580217	9,97085133	0,7557	0,019611	35,7	44,6
509010	06:11:37	78,58925083	10,05266757	0,4232	0,029216	14,1	36,4
509011	00:24:29	78,16008900	10,13489607	12,0787	0,084140	143,5	75,6
509012	07:38:58	78,34154717	10,25282433	1,1851	0,020654	57,5	53,9
509013	07:50:27	78,15911161	10,18051900	1,6371	0,027629	56,6	49,1
509014	08:08:15	78,38444067	10,09977900	0,3244	0,042051	5,3	14.5
509015	08:27:09	78,51086450	9,99794467	0,2808	0,023915	11,7	22,1
509016	08:29:41	78,48042017	10,04180117	0,1102	0,012163	10,7	37,7
509017	09:30:57	78,60641367	10,05374830	0,3232	0,018500	23,7	37,5
509018	01:38:51	78,39256850	10,10868833	1,0858	0,041033	25,0	41,0
509019	06:41:50	78,18709750	10,11950195	1,4122	0,019812	15,6	57,9
509020	09.43.01	78,38542083	10,12890800	1,3749	0,038891	41,0	53,0
509021	09:45:07	78,38192817	10,14186357	4,0808	0,106563	35,2	63,4
509022	09:47:19	78,37804100	10,15516417	11,7201	0,141671	86,0	66,6
509023	09:49:56	78,37446067	10,16913693	9,3531	0,149894	63,4	81,6
509024	10:03:04	78,34888817	10,25390817	0,8979	0,027512	32,6	41,0
509025	10:22:53	78,31913017	10,17010851	0,4132	0,021491	19,5	49,4
509026	10.23.08	78,31481750	10,33357983	0,9138	0,039909	30,5	43,6
509027	11:04:14	78,33394083	10,32758333	1,2515	0,054021	30,7	31,8

flare_id	time	lat	lon	sum	sum_area	area	height
509028	11:08:59	78.73779100	10,33284917	25,4951	0.161837	145,2	69.3
509029	11.11.43	78.84061133	10,31064636	28,1136	0,184518	152,4	63,4
509030	11:16:01	78.34551857	10,26878167	9,2561	0,127617	74,1	54,1
509031	11:19:07	78.35027951	10,27458915	4,5179	0.060753	74.3	69.5
509032	11:29:28	78.36466017	10,22152100	1,4079	0,024602	57,2	52,1
509033	11:38:27	78.37327450	10,18271781	5,4561	0,064561	84,9	84,8
509034	11:40:47	78.37523650	10,17152100	12,2304	0.171003	71.5	70.5
509035	11:50:29	78.39012000	10,12803350	8,5912	0,097612	88,0	57,6
509036	12:11:21	78.31400281	10,04106450	1,1124	0,027470	40,5	55,4
509037	13:22:17	78.31585500	10,43002417	0,5540	0.015603	35.1	27.1
509038	13:55:49	78.30533853	10,46647517	0,3268	0,018858	17,3	37,0
509039	17:42:22	78.54267781	9,43804500	1,1702	0,063441	18,3	51,0
609001	17.00.17	78.54143100	9,44123533	0,4130	0.030171	13.7	34.3
609002	21:26:52	78.57218067	9,82198650	1,4162	0,011464	123,5	80,7
609003	22:48:17	78.45102750	9,89477917	1,9772	0,014457	137,1	57,4
609004	23:45:31	78.43003617	10,20455385	0,0100	0,000003	3571,8	86,1
609005	23:45:57	78.43002617	10,20455285	0,0092	0,000003	453,7	56,5
709001	02:09:31	78.45118431	10,22916185	0,6491	0,011480	56,9	27,5
709002	02.10.14	78.35300733	10,23971900	0,4275	0,035051	12,9	21,3
709003	02:26:57	78.36602450	10,22913485	0,6202	0,017515	35,7	36,3
709004	02:38:12	78.46344917	10,22884919	0,7886	0,021158	37,5	37,5
709005	02.45.46	78.38364600	10,23639407	1,3244	0,025023	57,5	43,3
709006	05:05:06	78.37134253	10,24775400	0,4872	0,010594	45,1	23,5
709007	06:27:36	78.44911800	10,27052550	2,1679	0,024751	84,1	44,0
709008	06.38.46	78.36029217	10,26895785	0,6420	0,025351	27,3	39,3
709009	06:44:52	78.46565457	10,25865135	1,7984	0,017185	104,4	52,3
709010	06:56:31	78.47845351	10,21771900	0,9080	0,018115	50,9	29,1
709011	07.00.01	78.38339150	10,26819417	0,9531	0,011403	83,7	62,4
709012	07:35:56	78.41455600	10,25577850	0,5112	0,015757	33,5	43,1
709013	10:31:38	78.46753617	10,17912550	0,7160	0,049004	14,9	30,3
709014	10.23.27	78.30441133	10,17938717	0,4441	0,018399	23,9	36,1
709015	10:30:22	78.45332553	10,17848850	0,8044	0,024406	33,0	47,5
709016	12:41:10	78.45762550	10,11591485	6,9375	0,064117	108,4	70,7
709017	12.46.17	78.35377867	10,13612350	2,9636	0,048393	61,0	72,7
709018	12:54:25	78.36404453	10,15400050	1,8640	0,045417	40,7	43,5
709019	12:56:04	78.76481050	10.17595000	2.7004	0.035411	73.1	70.1
709020	13.42.25	78.46683100	10,13179367	0,1966	0,009067	20,6	19,5
709021	16:15:00	78.40178817	10,14056050	0,1954	0,011575	16,2	24,5
709022	19:11:40	78.47791831	10,14630885	1,6790	0,016924	99,7	79,7
709023	19.26.40	78.37317467	10,10472900	1,2184	0,017769	68,6	78,0
709024	20:50:16	78.43570800	10,07895515	4,7095	0,000745	6371,4	146,1
709025	23:50:16	78.43570800	10,07895595	4,7949	0.001499	3197,9	148.7
709026	23:50:46	78.43570800	10,07865585	3,9582	0,000773	5099,7	79,1
809001	00:06:25	78.49729517	10,04956150	2,7505	0,022670	122,0	56,5
809002	00:10:00	78.39983837	10.04970000	0.9587	0.022363	42.9	61.1
809003	02:51:12	78.41403467	10,05041685	6,0220	0,022044	273,2	56,0
809004	03:40:16	78.42586757	10,01207767	35,1640	0,076054	460,1	134,1
809005	09:54:10	78.43179600	10,07132517	24,7375	0.060398	409,4	137.7
809006	06:25:07	78.43186517	10,02226386	3,1651	0,020098	157,5	97,2

Publications of this series:

No. 1 **Wefer, G., E. Suess and cruise participants**
Bericht über die POLARSTERN-Fahrt ANT IV/2, Rio de Janeiro - Punta Arenas, 6.11. - 1.12.1985.
60 pages, Bremen, 1986.

No. 2 **Hoffmann, G.**
Holozänstratigraphie und Küstenlinienverlagerung an der andalusischen Mittelmeerküste.
173 pages, Bremen, 1988. (out of print)

No. 3 **Wefer, G. and cruise participants**
Bericht über die METEOR-Fahrt M 6/6, Libreville - Las Palmas, 18.2. - 23.3.1988.
97 pages, Bremen, 1988.

No. 4 **Wefer, G., G.F. Lutze, T.J. Müller, O. Pfannkuche, W. Schenke, G. Siedler, W. Zenk**
Kurzbericht über die METEOR-Expedition No. 6, Hamburg - Hamburg, 28.10.1987 - 19.5.1988.
29 pages, Bremen, 1988. (out of print)

No. 5 **Fischer, G.**
Stabile Kohlenstoff-Isotope in partikulärer organischer Substanz aus dem Südpolarmeer (Atlantischer Sektor). 161 pages, Bremen, 1989.

No. 6 **Berger, W.H. and G. Wefer**
Partikelfluß und Kohlenstoffkreislauf im Ozean.
Bericht und Kurzfassungen über den Workshop vom 3.-4. Juli 1989 in Bremen.
57 pages, Bremen, 1989.

No. 7 **Wefer, G. and cruise participants**
Bericht über die METEOR - Fahrt M 9/4, Dakar - Santa Cruz, 19.2. - 16.3.1989.
103 pages, Bremen, 1989.

No. 8 **Kölling, M.**
Modellierung geochemischer Prozesse im Sickerwasser und Grundwasser.
135 pages, Bremen, 1990.

No. 9 **Heinze, P.-M.**
Das Auftriebsgeschehen vor Peru im Spätquartär. 204 pages, Bremen, 1990. (out of print)

No. 10 **Willems, H., G. Wefer, M. Rinski, B. Donner, H.-J. Bellmann, L. Eißmann, A. Müller, B.W. Flemming, H.-C. Höfle, J. Merkt, H. Streif, G. Hertweck, H. Kuntze, J. Schwaar, W. Schäfer, M.-G. Schulz, F. Grube, B. Menke**
Beiträge zur Geologie und Paläontologie Norddeutschlands: Exkursionsführer.
202 pages, Bremen, 1990.

No. 11 **Wefer, G. and cruise participants**
Bericht über die METEOR-Fahrt M 12/1, Kapstadt - Funchal, 13.3.1990 - 14.4.1990.
66 pages, Bremen, 1990.

No. 12 **Dahmke, A., H.D. Schulz, A. Kölling, F. Kracht, A. Lücke**
Schwermetallspuren und geochemische Gleichgewichte zwischen Porenlösung und Sediment im Wesermündungsgebiet. BMFT-Projekt MFU 0562, Abschlußbericht. 121 pages, Bremen, 1991.

No. 13 **Rostek, F.**
Physikalische Strukturen von Tiefseesedimenten des Südatlantiks und ihre Erfassung in Echolotregistrierungen. 209 pages, Bremen, 1991.

No. 14 **Baumann, M.**
Die Ablagerung von Tschernobyl-Radiocäsium in der Norwegischen See und in der Nordsee.
133 pages, Bremen, 1991. (out of print)

No. 15 **Kölling, A.**
Frühdiagenetische Prozesse und Stoff-Flüsse in marinen und ästuarinen Sedimenten.
140 pages, Bremen, 1991.

No. 16 **SFB 261 (ed.)**
1. Kolloquium des Sonderforschungsbereichs 261 der Universität Bremen (14.Juni 1991):
Der Südatlantik im Spätquartär: Rekonstruktion von Stoffhaushalt und Stromsystemen.
Kurzfassungen der Vorträge und Poster. 66 pages, Bremen, 1991.

No. 17 **Pätzold, J. and cruise participants**
Bericht und erste Ergebnisse über die METEOR-Fahrt M 15/2, Rio de Janeiro - Vitoria,
18.1. - 7.2.1991. 46 pages, Bremen, 1993.

No. 18 **Wefer, G. and cruise participants**
Bericht und erste Ergebnisse über die METEOR-Fahrt M 16/1, Pointe Noire - Recife,
27.3. - 25.4.1991. 120 pages, Bremen, 1991.

No. 19 **Schulz, H.D. and cruise participants**
Bericht und erste Ergebnisse über die METEOR-Fahrt M 16/2, Recife - Belem, 28.4. - 20.5.1991.
149 pages, Bremen, 1991.

No. 20 **Berner, H.**
Mechanismen der Sedimentbildung in der Fram-Straße, im Arktischen Ozean und in der Norwegischen See. 167 pages, Bremen, 1991.

No. 21 **Schneider, R.**
Spätquartäre Produktivitätsänderungen im östlichen Angola-Becken: Reaktion auf Variationen im Passat-Monsun-Windsystem und in der Advektion des Benguela-Küstenstroms.
198 pages, Bremen, 1991. (out of print)

No. 22 **Hebbeln, D.**
Spätquartäre Stratigraphie und Paläozeanographie in der Fram-Straße. 174 pages, Bremen, 1991.

No. 23 **Lücke, A.**
Umsetzungsprozesse organischer Substanz während der Frühdiagenese in ästuarinen Sedimenten.
137 pages, Bremen, 1991.

No. 24 **Wefer, G. and cruise participants**
Bericht und erste Ergebnisse der METEOR-Fahrt M 20/1, Bremen - Abidjan, 18.11.- 22.12.1991.
74 pages, Bremen, 1992.

No. 25 **Schulz, H.D. and cruise participants**
Bericht und erste Ergebnisse der METEOR-Fahrt M 20/2, Abidjan - Dakar, 27.12.1991 - 3.2.1992.
173 pages, Bremen, 1992.

No. 26 **Gingele, F.**
Zur klimaabhängigen Bildung biogener und terrigener Sedimente und ihrer Veränderung durch die Frühdiagenese im zentralen und östlichen Südatlantik. 202 pages, Bremen, 1992.

No. 27 **Bickert, T.**
Rekonstruktion der spätquartären Bodenwasserzirkulation im östlichen Südatlantik über stabile Isotope benthischer Foraminiferen. 205 pages, Bremen, 1992. (out of print)

No. 28 **Schmidt, H.**
Der Benguela-Strom im Bereich des Walfisch-Rückens im Spätquartär. 172 pages, Bremen, 1992.

No. 29 **Meinecke, G.**
Spätquartäre Oberflächenwassertemperaturen im östlichen äquatorialen Atlantik.
181 pages, Bremen, 1992.

No. 30 **Bathmann, U., U. Bleil, A. Dahmke, P. Müller, A. Nehrkorn, E.-M. Nöthig, M. Olesch, J. Pätzold, H.D. Schulz, V. Smetacek, V. Spieß, G. Wefer, H. Willems**
Bericht des Graduierten Kollegs. Stoff-Flüsse in marinen Geosystemen.
Berichtszeitraum Oktober 1990 - Dezember 1992. 396 pages, Bremen, 1992.

No. 31 **Damm, E.**
Frühdiagenetische Verteilung von Schwermetallen in Schlicksedimenten der westlichen Ostsee.
115 pages, Bremen, 1992.

No. 32 **Antia, E.E.**
Sedimentology, Morphodynamics and Facies Association of a mesotidal Barrier Island Shoreface (Spiekeroog, Southern North Sea). 370 pages, Bremen, 1993.

No. 33 **Duinker, J. and G. Wefer (ed.)**
Bericht über den 1. JGOFS-Workshop. 1./2. Dezember 1992 in Bremen. 83 pages, Bremen, 1993.

No. 34 **Kasten, S.**
Die Verteilung von Schwermetallen in den Sedimenten eines stadtbremischen Hafenbeckens.
103 pages, Bremen, 1993.

No. 35 **Spieß, V.**
Digitale Sedimentographie. Neue Wege zu einer hochauflösenden Akustostratigraphie.
199 pages, Bremen, 1993.

No. 36 **Schinzel, U.**
Laborversuche zu frühdiagenetischen Reaktionen von Eisen (III) - Oxidhydraten in marinen Sedimenten.189 pages, Bremen, 1993.

No. 37 **Sieger, R.**
CoTAM - ein Modell zur Modellierung des Schwermetalltransports in Grundwasserleitern.
56 pages, Bremen, 1993. (out of print)

No. 38 **Willems, H. (ed.)**
Geoscientific Investigations in the Tethyan Himalayas. 183 pages, Bremen, 1993.

No. 39 **Hamer, K.**
Entwicklung von Laborversuchen als Grundlage für die Modellierung des Transportverhaltens von Arsenat, Blei, Cadmium und Kupfer in wassergesättigten Säulen. 147 pages, Bremen, 1993.

No. 40 **Sieger, R.**
Modellierung des Stofftransports in porösen Medien unter Ankopplung kinetisch gesteuerter Sorptions- und Redoxprozesse sowie thermischer Gleichgewichte. 158 pages, Bremen, 1993.

No. 41 **Thießen, W.**
Magnetische Eigenschaften von Sedimenten des östlichen Südatlantiks und ihre paläozeanographische Relevanz. 170 pages, Bremen, 1993.

No. 42 **Spieß, V. and cruise participants**
Report and preliminary results of METEOR-Cruise M 23/1, Kapstadt - Rio de Janeiro, 4.-25.2.1993. 139 pages, Bremen, 1994.

No. 43 **Bleil, U. and cruise participants**
Report and preliminary results of METEOR-Cruise M 23/2, Rio de Janeiro - Recife, 27.2.-19.3.1993 133 pages, Bremen, 1994.

No. 44 **Wefer, G. and cruise participants**
Report and preliminary results of METEOR-Cruise M 23/3, Recife - Las Palmas, 21.3. - 12.4.1993 71 pages, Bremen, 1994.

No. 45 **Giese, M. and G. Wefer (ed.)**
Bericht über den 2. JGOFS-Workshop. 18./19. November 1993 in Bremen. 93 pages, Bremen, 1994.

No. 46 **Balzer, W. and cruise participants**
Report and preliminary results of METEOR-Cruise M 22/1, Hamburg - Recife, 22.9. - 21.10.1992. 24 pages, Bremen, 1994.

No. 47 **Stax, R.**
Zyklische Sedimentation von organischem Kohlenstoff in der Japan See: Anzeiger für Änderungen von Paläoozeanographie und Paläoklima im Spätkänozoikum. 150 pages, Bremen, 1994.

No. 48 **Skowronek, F.**
Frühdiagenetische Stoff-Flüsse gelöster Schwermetalle an der Oberfläche von Sedimenten des Weser Ästuares. 107 pages, Bremen, 1994.

No. 49 **Dersch-Hansmann, M.**
Zur Klimaentwicklung in Ostasien während der letzten 5 Millionen Jahre: Terrigener Sedimenteintrag in die Japan See (ODP Ausfahrt 128). 149 pages, Bremen, 1994.

No. 50 **Zabel, M.**
Frühdiagenetische Stoff-Flüsse in Oberflächen-Sedimenten des äquatorialen und östlichen Südatlantik. 129 pages, Bremen, 1994.

No. 51 **Bleil, U. and cruise participants**
Report and preliminary results of SONNE-Cruise SO 86, Buenos Aires - Capetown, 22.4. - 31.5.93 116 pages, Bremen, 1994.

No. 52 **Symposium: The South Atlantic: Present and Past Circulation.**
Bremen, Germany, 15 - 19 August 1994. Abstracts. 167 pages, Bremen, 1994.

No. 53 **Kretzmann, U.B.**
57Fe-Mössbauer-Spektroskopie an Sedimenten - Möglichkeiten und Grenzen. 183 pages, Bremen, 1994.

No. 54 **Bachmann, M.**
Die Karbonatrampe von Organyà im oberen Oberapt und unteren Unteralb (NE-Spanien, Prov. Lerida): Fazies, Zyklo- und Sequenzstratigraphie. 147 pages, Bremen, 1994. (out of print)

No. 55 **Kemle-von Mücke, S.**
Oberflächenwasserstruktur und -zirkulation des Südostatlantiks im Spätquartär. 151 pages, Bremen, 1994.

No. 56 **Petermann, H.**
Magnetotaktische Bakterien und ihre Magnetosome in Oberflächensedimenten des Südatlantiks. 134 pages, Bremen, 1994.

No. 57 **Mulitza, S.**
Spätquartäre Variationen der oberflächennahen Hydrographie im westlichen äquatorialen Atlantik. 97 pages, Bremen, 1994.

No. 58 **Segl, M. and cruise participants**
Report and preliminary results of METEOR-Cruise M 29/1, Buenos-Aires - Montevideo, 17.6. - 13.7.1994
94 pages, Bremen, 1994.

No. 59 **Bleil, U. and cruise participants**
Report and preliminary results of METEOR-Cruise M 29/2, Montevideo - Rio de Janiero 15.7. - 8.8.1994. 153 pages, Bremen, 1994.

No. 60 **Henrich, R. and cruise participants**
Report and preliminary results of METEOR-Cruise M 29/3, Rio de Janeiro - Las Palmas 11.8. - 5.9.1994. Bremen, 1994. (out of print)

No. 61 **Sagemann, J.**
Saisonale Variationen von Porenwasserprofilen, Nährstoff-Flüssen und Reaktionen in intertidalen Sedimenten des Weser-Ästuars. 110 pages, Bremen, 1994. (out of print)

No. 62 **Giese, M. and G. Wefer**
Bericht über den 3. JGOFS-Workshop. 5./6. Dezember 1994 in Bremen.
84 pages, Bremen, 1995.

No. 63 **Mann, U.**
Genese kretazischer Schwarzschiefer in Kolumbien: Globale vs. regionale/lokale Prozesse.
153 pages, Bremen, 1995. (out of print)

No. 64 **Willems, H., Wan X., Yin J., Dongdui L., Liu G., S. Dürr, K.-U. Gräfe**
The Mesozoic development of the N-Indian passive margin and of the Xigaze Forearc Basin in southern Tibet, China. – Excursion Guide to IGCP 362 Working-Group Meeting "Integrated Stratigraphy". 113 pages, Bremen, 1995. (out of print)

No. 65 **Hünken, U.**
Liefergebiets - Charakterisierung proterozoischer Goldseifen in Ghana anhand von Fluideinschluß - Untersuchungen. 270 pages, Bremen, 1995.

No. 66 **Nyandwi, N.**
The Nature of the Sediment Distribution Patterns in ther Spiekeroog Backbarrier Area, the East Frisian Islands. 162 pages, Bremen, 1995.

No. 67 **Isenbeck-Schröter, M.**
Transportverhalten von Schwermetallkationen und Oxoanionen in wassergesättigten Sanden. - Laborversuche in Säulen und ihre Modellierung -. 182 pages, Bremen, 1995.

No. 68 **Hebbeln, D. and cruise participants**
Report and preliminary results of SONNE-Cruise SO 102, Valparaiso - Valparaiso, 95.
134 pages, Bremen, 1995.

No. 69 **Willems, H. (Sprecher), U.Bathmann, U. Bleil, T. v. Dobeneck, K. Herterich, B.B. Jorgensen, E.-M. Nöthig, M. Olesch, J. Pätzold, H.D. Schulz, V. Smetacek, V. Speiß. G. Wefer**
Bericht des Graduierten-Kollegs Stoff-Flüsse in marine Geosystemen.
Berichtszeitraum Januar 1993 - Dezember 1995. 45 & 468 pages, Bremen, 1995.

No. 70 **Giese, M. and G. Wefer**
Bericht über den 4. JGOFS-Workshop. 20./21. November 1995 in Bremen. 60 pages, Bremen, 1996. (out of print)

No. 71 **Meggers, H.**
Pliozän-quartäre Karbonatsedimentation und Paläozeanographie des Nordatlantiks und des Europäischen Nordmeeres - Hinweise aus planktischen Foraminiferengemeinschaften.
143 pages, Bremen, 1996. (out of print)

No. 72 **Teske, A.**
Phylogenetische und ökologische Untersuchungen an Bakterien des oxidativen und reduktiven marinen Schwefelkreislaufs mittels ribosomaler RNA. 220 pages, Bremen, 1996. (out of print)

No. 73 **Andersen, N.**
Biogeochemische Charakterisierung von Sinkstoffen und Sedimenten aus ostatlantischen Produktions-Systemen mit Hilfe von Biomarkern. 215 pages, Bremen, 1996.

No. 74 **Treppke, U.**
Saisonalität im Diatomeen- und Silikoflagellatenfluß im östlichen tropischen und subtropischen Atlantik. 200 pages, Bremen, 1996.

No. 75 **Schüring, J.**
Die Verwendung von Steinkohlebergematerialien im Deponiebau im Hinblick auf die Pyritverwitterung und die Eignung als geochemische Barriere. 110 pages, Bremen, 1996.

No. 76 **Pätzold, J. and cruise participants**
Report and preliminary results of VICTOR HENSEN cruise JOPS II, Leg 6, Fortaleza - Recife, 10.3. - 26.3. 1995 and Leg 8, Vítoria - Vítoria, 10.4. - 23.4.1995.
87 pages, Bremen, 1996.

No. 77 **Bleil, U. and cruise participants**
Report and preliminary results of METEOR-Cruise M 34/1, Cape Town - Walvis Bay, 3.-26.1.1996.
129 pages, Bremen, 1996.

No. 78 **Schulz, H.D. and cruise participants**
Report and preliminary results of METEOR-Cruise M 34/2, Walvis Bay - Walvis Bay, 29.1.-18.2.96
133 pages, Bremen, 1996.

No. 79 **Wefer, G. and cruise participants**
Report and preliminary results of METEOR-Cruise M 34/3, Walvis Bay - Recife, 21.2.-17.3.1996.
168 pages, Bremen, 1996.

No. 80 **Fischer, G. and cruise participants**
Report and preliminary results of METEOR-Cruise M 34/4, Recife - Bridgetown, 19.3.-15.4.1996. 105 pages, Bremen, 1996.

No. 81 **Kulbrok, F.**
Biostratigraphie, Fazies und Sequenzstratigraphie einer Karbonatrampe in den Schichten der Oberkreide und des Alttertiärs Nordost-Ägyptens (Eastern Desert, N'Golf von Suez, Sinai). 153 pages, Bremen, 1996.

No. 82 **Kasten, S.**
Early Diagenetic Metal Enrichments in Marine Sediments as Documents of Nonsteady-State Depositional Conditions. Bremen, 1996.

No. 83 **Holmes, M.E.**
Reconstruction of Surface Ocean Nitrate Utilization in the Southeast Atlantic Ocean Based on Stable Nitrogen Isotopes. 113 pages, Bremen, 1996.

No. 84 **Rühlemann, C.**
Akkumulation von Carbonat und organischem Kohlenstoff im tropischen Atlantik: Spätquartäre Produktivitäts-Variationen und ihre Steuerungsmechanismen. 139 pages, Bremen, 1996.

No. 85 **Ratmeyer, V.**
Untersuchungen zum Eintrag und Transport lithogener und organischer partikulärer Substanz im östlichen subtropischen Nordatlantik. 154 pages, Bremen, 1996.

No. 86 **Cepek, M.**
Zeitliche und räumliche Variationen von Coccolithophoriden-Gemeinschaften im subtropischen Ost-Atlantik: Untersuchungen an Plankton, Sinkstoffen und Sedimenten. 156 pages, Bremen, 1996.

No. 87 **Otto, S.**
Die Bedeutung von gelöstem organischen Kohlenstoff (DOC) für den Kohlenstoffffluß im Ozean. 150 pages, Bremen, 1996.

No. 88 **Hensen, C.**
Frühdiagenetische Prozesse und Quantifizierung benthischer Stoff-Flüsse in Oberflächensedimenten des Südatlantiks. 132 pages, Bremen, 1996.

No. 89 **Giese, M. and G. Wefer**
Bericht über den 5. JGOFS-Workshop. 27./28. November 1996 in Bremen. 73 pages, Bremen, 1997.

No. 90 **Wefer, G. and cruise participants**
Report and preliminary results of METEOR-Cruise M 37/1, Lisbon - Las Palmas, 4.-23.12.1996. 79 pages, Bremen, 1997.

No. 91 **Isenbeck-Schröter, M., E. Bedbur, M. Kofod, B. König, T. Schramm & G. Mattheß**
Occurrence of Pesticide Residues in Water - Assessment of the Current Situation in Selected EU Countries. 65 pages, Bremen 1997.

No. 92 **Kühn, M.**
Geochemische Folgereaktionen bei der hydrogeothermalen Energiegewinnung. 129 pages, Bremen 1997.

No. 93 **Determann, S. & K. Herterich**
JGOFS-A6 "Daten und Modelle": Sammlung JGOFS-relevanter Modelle in Deutschland. 26 pages, Bremen, 1997.

No. 94 **Fischer, G. and cruise participants**
Report and preliminary results of METEOR-Cruise M 38/1, Las Palmas - Recife, 25.1.-1.3.1997, with Appendix: Core Descriptions from METEOR Cruise M 37/1. Bremen, 1997.

No. 95 **Bleil, U. and cruise participants**
Report and preliminary results of METEOR-Cruise M 38/2, Recife - Las Palmas, 4.3.-14.4.1997. 126 pages, Bremen, 1997.

No. 96 **Neuer, S. and cruise participants**
Report and preliminary results of VICTOR HENSEN-Cruise 96/1. Bremen, 1997.

No. 97 **Villinger, H. and cruise participants**
Fahrtbericht SO 111, 20.8. - 16.9.1996. 115 pages, Bremen, 1997.

No. 98 **Lüning, S.**
Late Cretaceous - Early Tertiary sequence stratigraphy, paleoecology and geodynamics of Eastern Sinai, Egypt. 218 pages, Bremen, 1997.

No. 99 **Haese, R.R.**
Beschreibung und Quantifizierung frühdiagenetischer Reaktionen des Eisens in Sedimenten des Südatlantiks. 118 pages, Bremen, 1997.

No. 100 **Lührte, R. von**
Verwertung von Bremer Baggergut als Material zur Oberflächenabdichtung von Deponien - Geochemisches Langzeitverhalten und Schwermetall-Mobilität (Cd, Cu, Ni, Pb, Zn). Bremen, 1997.

No. 101 **Ebert, M.**
Der Einfluß des Redoxmilieus auf die Mobilität von Chrom im durchströmten Aquifer. 135 pages, Bremen, 1997.

No. 102 **Krögel, F.**
Einfluß von Viskosität und Dichte des Seewassers auf Transport und Ablagerung von Wattsedimenten (Langeooger Rückseitenwatt, südliche Nordsee). 168 pages, Bremen, 1997.

No. 103 **Kerntopf, B.**
Dinoflagellate Distribution Patterns and Preservation in the Equatorial Atlantic and Offshore North-West Africa. 137 pages, Bremen, 1997.

No. 104 **Breitzke, M.**
Elastische Wellenausbreitung in marinen Sedimenten - Neue Entwicklungen der Ultraschall Sedimentphysik und Sedimentechographie. 298 pages, Bremen, 1997.

No. 105 **Marchant, M.**
Rezente und spätquartäre Sedimentation planktischer Foraminiferen im Peru-Chile Strom. 115 pages, Bremen, 1997.

No. 106 **Habicht, K.S.**
Sulfur isotope fractionation in marine sediments and bacterial cultures. 125 pages, Bremen, 1997.

No. 107 **Hamer, K., R.v. Lührte, G. Becker, T. Felis, S. Keffel, B. Strotmann, C. Waschkowitz, M. Kölling, M. Isenbeck-Schröter, H.D. Schulz**
Endbericht zum Forschungsvorhaben 060 des Landes Bremen: Baggergut der Hafengruppe Bremen-Stadt: Modelluntersuchungen zur Schwermetallmobilität und Möglichkeiten der Verwertung von Hafenschlick aus Bremischen Häfen. 98 pages, Bremen, 1997.

No. 108 **Greeff, O.W.**
Entwicklung und Erprobung eines benthischen Landersystemes zur in situ-Bestimmung von Sulfatreduktionsraten mariner Sedimente. 121 pages, Bremen, 1997.

No. 109 **Pätzold, M. und G. Wefer**
Bericht über den 6. JGOFS-Workshop am 4./5.12.1997 in Bremen. Im Anhang: Publikationen zum deutschen Beitrag zur Joint Global Ocean Flux Study (JGOFS), Stand 1/1998. 122 pages, Bremen, 1998.

No. 110 **Landenberger, H.**
CoTReM, ein Multi-Komponenten Transport- und Reaktions-Modell. 142 pages, Bremen, 1998.

No. 111 **Villinger, H. und Fahrtteilnehmer**
Fahrtbericht SO 124, 4.10. - 16.10.199. 90 pages, Bremen, 1997.

No. 112 **Gietl, R.**
Biostratigraphie und Sedimentationsmuster einer nordostägyptischen Karbonatrampe unter Berücksichtigung der Alveolinen-Faunen. 142 pages, Bremen, 1998.

No. 113 **Ziebis, W.**
The Impact of the Thalassinidean Shrimp Callianassa truncata on the Geochemistry of permeable, coastal Sediments. 158 pages, Bremen 1998.

No. 114 **Schulz, H.D. and cruise participants**
Report and preliminary results of METEOR-Cruise M 41/1, Málaga - Libreville, 13.2.-15.3.1998. Bremen, 1998.

No. 115 **Völker, D.J.**
Untersuchungen an strömungsbeeinflußten Sedimentationsmustern im Südozean. Interpretation sedimentechographischer Daten und numerische Modellierung. 152 pages, Bremen, 1998.

No. 116 **Schlünz, B.**
Riverine Organic Carbon Input into the Ocean in Relation to Late Quaternary Climate Change. 136 pages, Bremen, 1998.

No. 117 **Kuhnert, H.**
Aufzeichnug des Klimas vor Westaustralien in stabilen Isotopen in Korallenskeletten. 109 pages, Bremen, 1998.

No. 118 **Kirst, G.**
Rekonstruktion von Oberflächenwassertemperaturen im östlichen Südatlantik anhand von Alkenonen. 130 pages, Bremen, 1998.

No. 119 **Dürkoop, A.**
Der Brasil-Strom im Spätquartär: Rekonstruktion der oberflächennahen Hydrographie während der letzten 400 000 Jahre. 121 pages, Bremen, 1998.

No. 120 **Lamy, F.**
Spätquartäre Variationen des terrigenen Sedimenteintrags entlang des chilenischen Kontinentalhangs als Abbild von Klimavariabilität im Milankovič- und Sub-Milankovič-Zeitbereich. 141 pages, Bremen, 1998.

No. 121 **Neuer, S. and cruise participants**
Report and preliminary results of POSEIDON-Cruise Pos 237/2, Vigo – Las Palmas, 18.3.-31.3.1998. 39 pages, Bremen, 1998

No. 122 **Romero, O.E.**
Marine planktonic diatoms from the tropical and equatorial Atlantic: temporal flux patterns and the sediment record. 205 pages, Bremen, 1998.

No. 123 **Spiess, V. und Fahrtteilnehmer**
Report and preliminary results of RV SONNE Cruise 125, Cochin – Chittagong, 17.10.-17.11.1997. 128 pages, Bremen, 1998.

No. 124 **Arz, H.W.**
Dokumentation von kurzfristigen Klimaschwankungen des Spätquartärs in Sedimenten des westlichen äquatorialen Atlantiks. 96 pages, Bremen, 1998.

No. 125 **Wolff, T.**
Mixed layer characteristics in the equatorial Atlantic during the late Quaternary as deduced from planktonic foraminifera. 132 pages, Bremen, 1998.

No. 126 **Dittert, N.**
Late Quaternary Planktic Foraminifera Assemblages in the South Atlantic Ocean: Quantitative Determination and Preservational Aspects. 165 pages, Bremen, 1998.

No. 127 **Höll, C.**
Kalkige und organisch-wandige Dinoflagellaten-Zysten in Spätquartären Sedimenten des tropischen Atlantiks und ihre palökologische Auswertbarkeit. 121 pages, Bremen, 1998.

No. 128 **Hencke, J.**
Redoxreaktionen im Grundwasser: Etablierung und Verlagerung von Reaktionsfronten und ihre Bedeutung für die Spurenelement-Mobilität. 122 pages, Bremen 1998.

No. 129 **Pätzold, J. and cruise participants**
Report and preliminary results of METEOR-Cruise M 41/3, Vítoria, Brasil – Salvador de Bahia, Brasil, 18.4. - 15.5.1998. Bremen, 1999.

No. 130 **Fischer, G. and cruise participants**
Report and preliminary results of METEOR-Cruise M 41/4, Salvador de Bahia, Brasil – Las Palmas, Spain, 18.5. – 13.6.1998. Bremen, 1999.

No. 131 **Schlünz, B. und G. Wefer**
Bericht über den 7. JGOFS-Workshop am 3. und 4.12.1998 in Bremen. Im Anhang: Publikationen zum deutschen Beitrag zur Joint Global Ocean Flux Study (JGOFS), Stand 1/ 1999. 100 pages, Bremen, 1999.

No. 132 **Wefer, G. and cruise participants**
Report and preliminary results of METEOR-Cruise M 42/4, Las Palmas - Las Palmas - Viena do Castelo; 26.09.1998 - 26.10.1998. 104 pages, Bremen, 1999.

No. 133 **Felis, T.**
Climate and ocean variability reconstructed from stable isotope records of modern subtropical corals (Northern Red Sea). 111 pages, Bremen, 1999.

No. 134 **Draschba , S.**
North Atlantic climate variability recorded in reef corals from Bermuda. 108 pages, Bremen, 1999.

No. 135 **Schmieder, F.**
Magnetic Cyclostratigraphy of South Atlantic Sediments. 82 pages, Bremen, 1999.

No. 136 **Rieß, W.**
In situ measurements of respiration and mineralisation processes – Interaction between fauna and geochemical fluxes at active interfaces. 68 pages, Bremen, 1999.

No. 137 **Devey, C.W. and cruise participants**
Report and shipboard results from METEOR-cruise M 41/2, Libreville – Vitoria, 18.3. – 15.4.98. 59 pages, Bremen, 1999.

No. 138 **Wenzhöfer, F.**
Biogeochemical processes at the sediment water interface and quantification of metabolically driven calcite dissolution in deep sea sediments. 103 pages, Bremen, 1999.

No. 139 **Klump, J.**
Biogenic barite as a proxy of paleoproductivity variations in the Southern Peru-Chile Current. 107 pages, Bremen, 1999.

No. 140 **Huber, R.**
Carbonate sedimentation in the northern Northatlantic since the late pliocene. 103 pages, Bremen, 1999.

No. 141 **Schulz, H.**
Nitrate-storing sulfur bacteria in sediments of coastal upwelling. 94 pages, Bremen, 1999.

No. 142 **Mai, S.**
Die Sedimentverteilung im Wattenmeer: ein Simulationsmodell. 114 pages, Bremen, 1999.

No. 143 **Neuer, S. and cruise participants**
Report and preliminary results of Poseidon Cruise 248, Las Palmas - Las Palmas, 15.2.-26.2.1999. 45 pages, Bremen, 1999.

No. 144 **Weber, A.**
Schwefelkreislauf in marinen Sedimenten und Messung von in situ Sulfatreduktionsraten. 122 pages, Bremen, 1999.

No. 145 **Hadeler, A.**
Sorptionsreaktionen im Grundwasser: Unterschiedliche Aspekte bei der Modellierung des Transportverhaltens von Zink. 122 pages, 1999.

No. 146 **Dierßen, H.**
Zum Kreislauf ausgewählter Spurenmetalle im Südatlantik: Vertikaltransport und Wechselwirkung zwischen Partikeln und Lösung. 167 pages, Bremen, 1999.

No. 147 **Zühlsdorff, L.**
High resolution multi-frequency seismic surveys at the Eastern Juan de Fuca Ridge Flank and the Cascadia Margin – Evidence for thermally and tectonically driven fluid upflow in marine sediments. 118 pages, Bremen 1999.

No. 148 **Kinkel, H.**
Living and late Quaternary Coccolithophores in the equatorial Atlantic Ocean: response of distribution and productivity patterns to changing surface water circulation. 183 pages, Bremen, 2000.

No. 149 **Pätzold, J. and cruise participants**
Report and preliminary results of METEOR Cruise M 44/3, Aqaba (Jordan) - Safaga (Egypt) – Dubá (Saudi Arabia) – Suez (Egypt) - Haifa (Israel), 12.3.-26.3.-2.4.-4.4.1999. 135 pages, Bremen, 2000.

No. 150 **Schlünz, B. and G. Wefer**
Bericht über den 8. JGOFS-Workshop am 2. und 3.12.1999 in Bremen. Im Anhang: Publikationen zum deutschen Beitrag zur Joint Global Ocean Flux Study (JGOFS), Stand 1/ 2000. 95 pages, Bremen, 2000.

No. 151 **Schnack, K.**
Biostratigraphie und fazielle Entwicklung in der Oberkreide und im Alttertiär im Bereich der Kharga Schwelle, Westliche Wüste, SW-Ägypten. 142 pages, Bremen, 2000.

No. 152 **Karwath, B.**
Ecological studies on living and fossil calcareous dinoflagellates of the equatorial and tropical Atlantic Ocean. 175 pages, Bremen, 2000.

No. 153 **Moustafa, Y.**
Paleoclimatic reconstructions of the Northern Red Sea during the Holocene inferred from stable isotope records of modern and fossil corals and molluscs. 102 pages, Bremen, 2000.

No. 154 **Villinger, H. and cruise participants**
Report and preliminary results of SONNE-cruise 145-1 Balboa – Talcahuana, 21.12.1999 – 28.01.2000. 147 pages, Bremen, 2000.

No. 155 **Rusch, A.**
Dynamik der Feinfraktion im Oberflächenhorizont permeabler Schelfsedimente. 102 pages, Bremen, 2000.

No. 156 **Moos, C.**
Reconstruction of upwelling intensity and paleo-nutrient gradients in the northwest Arabian Sea derived from stable carbon and oxygen isotopes of planktic foraminifera. 103 pages, Bremen, 2000.

No. 157 **Xu, W.**
Mass physical sediment properties and trends in a Wadden Sea tidal basin. 127 pages, Bremen, 2000.

No. 158 **Meinecke, G. and cruise participants**
Report and preliminary results of METEOR Cruise M 45/1, Malaga (Spain) - Lissabon (Portugal), 19.05. - 08.06.1999. 39 pages, Bremen, 2000.

No. 159 **Vink, A.**
Reconstruction of recent and late Quaternary surface water masses of the western subtropical Atlantic Ocean based on calcareous and organic-walled dinoflagellate cysts. 160 pages, Bremen, 2000.

No. 160 **Willems, H. (Sprecher), U. Bleil, R. Henrich, K. Herterich, B.B. Jørgensen, H.-J. Kuß, M. Olesch, H.D. Schulz, V. Spieß, G. Wefer**
Abschlußbericht des Graduierten-Kollegs Stoff-Flüsse in marine Geosystemen. Zusammenfassung und Berichtszeitraum Januar 1996 - Dezember 2000. 340 pages, Bremen, 2000.

No. 161 **Sprengel, C.**
Untersuchungen zur Sedimentation und Ökologie von Coccolithophoriden im Bereich der Kanarischen Inseln: Saisonale Flussmuster und Karbonatexport. 165 pages, Bremen, 2000.

No. 162 **Donner, B. and G. Wefer**
Bericht über den JGOFS-Workshop am 18.-21.9.2000 in Bremen: Biogeochemical Cycles: German Contributions to the International Joint Global Ocean Flux Study. 87 pages, Bremen, 2000.

No. 163 **Neuer, S. and cruise participants**
Report and preliminary results of Meteor Cruise M 45/5, Bremen – Las Palmas, October 1 – November 3, 1999. 93 pages, Bremen, 2000.

No. 164 **Devey, C. and cruise participants**
Report and preliminary results of Sonne Cruise SO 145/2, Talcahuano (Chile) - Arica (Chile), February 4 – February 29, 2000. 63 pages, Bremen, 2000.

No. 165 **Freudenthal, T.**
Reconstruction of productivity gradients in the Canary Islands region off Morocco by means of sinking particles and sediments. 147 pages, Bremen, 2000.

No. 166 **Adler, M.**
Modeling of one-dimensional transport in porous media with respect to simultaneous geochemical reactions in CoTReM. 147 pages, Bremen, 2000.

No. 167 **Santamarina Cuneo, P.**
Fluxes of suspended particulate matter through a tidal inlet of the East Frisian Wadden Sea (southern North Sea). 91 pages, Bremen, 2000.

No. 168 **Benthien, A.**
Effects of CO2 and nutrient concentration on the stable carbon isotope composition of C37:2 alkenones in sediments of the South Atlantic Ocean. 104 pages, Bremen, 2001.

No. 169 **Lavik, G.**
Nitrogen isotopes of sinking matter and sediments in the South Atlantic. 140 pages, Bremen, 2001.

No. 170 **Budziak, D.**
Late Quaternary monsoonal climate and related variations in paleoproductivity and alkenone-derived sea-surface temperatures in the western Arabian Sea. 114 pages, Bremen, 2001.

No. 171 **Gerhardt, S.**
Late Quaternary water mass variability derived from the pteropod preservation state in sediments of the western South Atlantic Ocean and the Caribbean Sea. 109 pages, Bremen, 2001.

No. 172 **Bleil, U. and cruise participants**
Report and preliminary results of Meteor Cruise M 46/3, Montevideo (Uruguay) – Mar del Plata (Argentina), January 4 – February 7, 2000. Bremen, 2001.

No. 173 **Wefer, G. and cruise participants**
Report and preliminary results of Meteor Cruise M 46/4, Mar del Plata (Argentina) – Salvador da Bahia (Brazil), February 10 – March 13, 2000. With partial results of METEOR cruise M 46/2. 136 pages, Bremen, 2001.

No. 174 **Schulz, H.D. and cruise participants**
Report and preliminary results of Meteor Cruise M 46/2, Recife (Brazil) – Montevideo (Uruguay), December 2 – December 29, 1999. 107 pages, Bremen, 2001.

No. 175 **Schmidt, A.**
Magnetic mineral fluxes in the Quaternary South Atlantic: Implications for the paleoenvironment. 97 pages, Bremen, 2001.

No. 176 **Bruhns, P.**
Crystal chemical characterization of heavy metal incorporation in brick burning processes. 93 pages, Bremen, 2001.

No. 177 **Karius, V.**
Baggergut der Hafengruppe Bremen-Stadt in der Ziegelherstellung. 131 pages, Bremen, 2001.

No. 178 **Adegbie, A. T.**
Reconstruction of paleoenvironmental conditions in Equatorial Atlantic and the Gulf of Guinea Basins for the last 245,000 years. 113 pages, Bremen, 2001.

No. 179 **Spieß, V. and cruise participants**
Report and preliminary results of R/V Sonne Cruise SO 149, Victoria - Victoria, 16.8. - 16.9.2000. 100 pages, Bremen, 2001.

No. 180 **Kim, J.-H.**
Reconstruction of past sea-surface temperatures in the eastern South Atlantic and the eastern South Pacific across Termination I based on the Alkenone Method. 114 pages, Bremen, 2001.

No. 181 **von Lom-Keil, H.**
Sedimentary waves on the Namibian continental margin and in the Argentine Basin – Bottom flow reconstructions based on high resolution echosounder data. 126 pages, Bremen, 2001.

No. 182 **Hebbeln, D. and cruise participants**
PUCK: Report and preliminary results of R/V Sonne Cruise SO 156, Valparaiso (Chile) - Talcahuano (Chile), March 29 - May 14, 2001. 195 pages, Bremen, 2001.

No. 183 **Wendler, J.**
Reconstruction of astronomically-forced cyclic and abrupt paleoecological changes in the Upper Cretaceous Boreal Realm based on calcareous dinoflagellate cysts. 149 pages, Bremen, 2001.

No. 184 **Volbers, A.**
Planktic foraminifera as paleoceanographic indicators: production, preservation, and reconstruction of upwelling intensity. Implications from late Quaternary South Atlantic sediments. 122 pages, Bremen, 2001.

No. 185 **Bleil, U. and cruise participants**
Report and preliminary results of R/V METEOR Cruise M 49/3, Montevideo (Uruguay) - Salvador (Brasil), March 9 - April 1, 2001. 99 pages, Bremen, 2001.

No. 186 **Scheibner, C.**
Architecture of a carbonate platform-to-basin transition on a structural high (Campanian-early Eocene, Eastern Desert, Egypt) – classical and modelling approaches combined. 173 pages, Bremen, 2001.

No. 187 **Schneider, S.**
Quartäre Schwankungen in Strömungsintensität und Produktivität als Abbild der Wassermassen-Variabilität im äquatorialen Atlantik (ODP Sites 959 und 663): Ergebnisse aus Siltkorn-Analysen. 134 pages, Bremen, 2001.

No. 188 **Uliana, E.**
Late Quaternary biogenic opal sedimentation in diatom assemblages in Kongo Fan sediments. 96 pages, Bremen, 2002.

No. 189 **Esper, O.**
Reconstruction of Recent and Late Quaternary oceanographic conditions in the eastern South Atlantic Ocean based on calcareous- and organic-walled dinoflagellate cysts. 130 pages, Bremen, 2001.

No. 190 **Wendler, I.**
Production and preservation of calcareous dinoflagellate cysts in the modern Arabian Sea. 117 pages, Bremen, 2002.

No. 191 **Bauer, J.**
Late Cenomanian – Santonian carbonate platform evolution of Sinai (Egypt): stratigraphy, facies, and sequence architecture. 178 pages, Bremen, 2002.

No. 192 **Hildebrand-Habel, T.**
Die Entwicklung kalkiger Dinoflagellaten im Südatlantik seit der höheren Oberkreide. 152 pages, Bremen, 2002.

No. 193 **Hecht, H.**
Sauerstoff-Optopoden zur Quantifizierung von Pyritverwitterungsprozessen im Labor- und Langzeit-in-situ-Einsatz. Entwicklung - Anwendung – Modellierung. 130 pages, Bremen, 2002.

No. 194 **Fischer, G. and cruise participants**
Report and Preliminary Results of RV METEOR-Cruise M49/4, Salvador da Bahia – Halifax, 4.4.-5.5.2001. 84 pages, Bremen, 2002.

No. 195 **Gröger, M.**
Deep-water circulation in the western equatorial Atlantic: inferences from carbonate preservation studies and silt grain-size analysis. 95 pages, Bremen, 2002.

No. 196 **Meinecke,G. and cruise participants**
Report of RV POSEIDON Cruise POS 271, Las Palmas - Las Palmas, 19.3.-29.3.2001. 19 pages, Bremen, 2002.

No. 197 **Meggers, H. and cruise participants**
Report of RV POSEIDON Cruise POS 272, Las Palmas - Las Palmas, 1.4.-14.4.2001. 19 pages, Bremen, 2002. (out of print)

No. 198 **Gräfe, K.-U.**
Stratigraphische Korrelation und Steuerungsfaktoren Sedimentärer Zyklen in ausgewählten Borealen und Tethyalen Becken des Cenoman/Turon (Oberkreide) Europas und Nordwestafrikas. 197 pages, Bremen, 2002.

No. 199 **Jahn, B.**
Mid to Late Pleistocene Variations of Marine Productivity in and Terrigenous Input to the Southeast Atlantic. 97 pages, Bremen, 2002.

No. 200 **Al-Rousan, S.**
Ocean and climate history recorded in stable isotopes of coral and foraminifers from the northern Gulf of Aqaba. 116 pages, Bremen, 2002.

No. 201 **Azouzi, B.**
Regionalisierung hydraulischer und hydrogeochemischer Daten mit geostatistischen Methoden. 108 pages, Bremen, 2002.

No. 202 **Spieß, V. and cruise participants**
Report and preliminary results of METEOR Cruise M 47/3, Libreville (Gabun) - Walvis Bay (Namibia), 01.06 - 03.07.2000. 70 pages, Bremen 2002.

No. 203 **Spieß, V. and cruise participants**
Report and preliminary results of METEOR Cruise M 49/2, Montevideo (Uruguay) - Montevideo, 13.02 - 07.03.2001. 84 pages, Bremen 2002.

No. 204 **Mollenhauer, G.**
Organic carbon accumulation in the South Atlantic Ocean: Sedimentary processes and glacial/interglacial Budgets. 139 pages, Bremen 2002.

No. 205 **Spieß, V. and cruise participants**
Report and preliminary results of METEOR Cruise M49/1, Cape Town (South Africa) - Montevideo (Uruguay), 04.01.2001 - 10.02.2001. 57 pages, Bremen, 2003.

No. 206 **Meier, K.J.S.**
Calcareous dinoflagellates from the Mediterranean Sea: taxonomy, ecology and palaeoenvironmental application. 126 pages, Bremen, 2003.

No. 207 **Rakic, S.**
Untersuchungen zur Polymorphie und Kristallchemie von Silikaten der Zusammensetzung Me2Si2O5 (Me:Na, K). 139 pages, Bremen, 2003.

No. 208 **Pfeifer, K.**
Auswirkungen frühdiagenetischer Prozesse auf Calcit- und Barytgehalte in marinen Oberflächen-sedimenten. 110 pages, Bremen, 2003.

No. 209 **Heuer, V.**
Spurenelemente in Sedimenten des Südatlantik. Primärer Eintrag und frühdiagenetische Überprägung. 136 pages, Bremen, 2003.

No. 210 **Streng, M.**
Phylogenetic Aspects and Taxonomy of Calcareous Dinoflagellates. 157 pages, Bremen 2003.

No. 211 **Boeckel, B.**
Present and past coccolith assemblages in the South Atlantic: implications for species ecology, carbonate contribution and palaeoceanographic applicability. 157 pages, Bremen, 2003.

No. 212 **Precht, E.**
Advective interfacial exchange in permeable sediments driven by surface gravity waves and its ecological consequences. 131 pages, Bremen, 2003.

No. 213 **Frenz, M.**
Grain-size composition of Quaternary South Atlantic sediments and its paleoceanographic significance. 123 pages, Bremen, 2003.

No. 214 **Meggers, H. and cruise participants**
Report and preliminary results of METEOR Cruise M 53/1, Limassol - Las Palmas – Mindelo, 30.03.2002 - 03.05.2002. 81 pages, Bremen, 2003.

No. 215 **Schulz, H.D. and cruise participants**
Report and preliminary results of METEOR Cruise M 58/1, Dakar – Las Palmas, 15.04..2003 – 12.05.2003. Bremen, 2003.

No. 216 **Schneider, R. and cruise participants**
Report and preliminary results of METEOR Cruise M 57/1, Cape Town – Walvis Bay, 20.01. – 08.02.2003. 123 pages, Bremen, 2003.

No. 217 **Kallmeyer, J.**
Sulfate reduction in the deep Biosphere. 157 pages, Bremen, 2003.

No. 218 **Røy, H.**
Dynamic Structure and Function of the Diffusive Boundary Layer at the Seafloor. 149 pages, Bremen, 2003.

No. 219 **Pätzold, J., C. Hübscher and cruise participants**
Report and preliminary results of METEOR Cruise M 52/2&3, Istanbul – Limassol – Limassol, 04.02. – 27.03.2002. Bremen, 2003.

No. 220 **Zabel, M. and cruise participants**
Report and preliminary results of METEOR Cruise M 57/2, Walvis Bay – Walvis Bay, 11.02. – 12.03.2003. 136 pages, Bremen 2003.

No. 221 **Salem, M.**
Geophysical investigations of submarine prolongations of alluvial fans on the western side of the Gulf of Aqaba-Red Sea. 100 pages, Bremen, 2003.

No. 222 **Tilch, E.**
Oszillation von Wattflächen und deren fossiles Erhaltungspotential (Spiekerooger Rückseitenwatt, südliche Nordsee). 137 pages, Bremen, 2003.

No. 223 **Frisch, U. and F. Kockel**
Der Bremen-Knoten im Strukturnetz Nordwest-Deutschlands. Stratigraphie, Paläogeographie, Strukturgeologie. 379 pages, Bremen, 2004.

No. 224 **Kolonic, S.**
Mechanisms and biogeochemical implications of Cenomanian/Turonian black shale formation in North Africa: An integrated geochemical, millennial-scale study from the Tarfaya-LaAyoune Basin in SW Morocco. 174 pages, Bremen, 2004. Report online available only.

No. 225 **Panteleit, B.**
Geochemische Prozesse in der Salz- Süßwasser Übergangszone. 106 pages, Bremen, 2004.

No. 226 **Seiter, K.**
Regionalisierung und Quantifizierung benthischer Mineralisationsprozesse. 135 pages, Bremen, 2004.

No. 227 **Bleil, U. and cruise participants**
Report and preliminary results of METEOR Cruise M 58/2, Las Palmas – Las Palmas (Canary Islands, Spain), 15.05. – 08.06.2003. 123 pages, Bremen, 2004.

No. 228 **Kopf, A. and cruise participants**
Report and preliminary results of SONNE Cruise SO175, Miami - Bremerhaven, 12.11 - 30.12.2003. 218 pages, Bremen, 2004.

No. 229 **Fabian, M.**
Near Surface Tilt and Pore Pressure Changes Induced by Pumping in Multi-Layered Poroelastic Half-Spaces. 121 pages, Bremen, 2004.

No. 230 **Segl, M. , and cruise participants**
Report and preliminary results of POSEIDON cruise 304 Galway – Lisbon, 5. – 22. Oct. 2004. 27 pages, Bremen 2004

No. 231 **Meinecke, G. and cruise participants**
Report and preliminary results of POSEIDON Cruise 296, Las Palmas – Las Palmas, 04.04 – 14.04.2003. 42 pages, Bremen 2005.

No. 232 **Meinecke, G. and cruise participants**
Report and preliminary results of POSEIDON Cruise 310, Las Palmas – Las Palmas, 12.04 – 26.04.2004. 49 pages, Bremen 2005.

No. 233 **Meinecke, G. and cruise participants**
Report and preliminary results of METEOR Cruise 58/3, Las Palmas - Ponta Delgada, 11.06 - 24.06.2003. 50 pages, Bremen 2005.

No. 234 **Feseker, T.**
Numerical Studies on Groundwater Flow in Coastal Aquifers. 219 pages. Bremen 2004.

No. 235 **Sahling, H. and cruise participants**
Report and preliminary results of R/V POSEIDON Cruise P317/4, Istanbul-Istanbul , 16 October - 4 November
2004. 92 pages, Bremen 2004.

No. 236 **Meinecke, G. und Fahrtteilnehmer**
Report and preliminary results of POSEIDON Cruise 305, Las Palmas (Spain) - Lisbon (Portugal), October 28th – November 6th, 2004. 43 pages, Bremen 2005.

No. 237 **Ruhland, G. and cruise participants**
Report and preliminary results of POSEIDON Cruise 319, Las Palmas (Spain) - Las Palmas (Spain), December 6th – December 17th, 2004. 50 pages, Bremen 2005.

No. 238 **Chang, T.S.**
Dynamics of fine-grained sediments and stratigraphic evolution of a back-barrier tidal basin of the German Wadden Sea (southern North Sea). 102 pages, Bremen 2005.

No. 239 **Lager, T.**
Predicting the source strength of recycling materials within the scope of a seepage water prognosis by means of standardized laboratory methods. 141 pages, Bremen 2005.

No. 240 **Meinecke, G.**
DOLAN - Operationelle Datenübertragung im Ozean und Laterales Akustisches Netzwerk in der Tiefsee. Abschlußbericht. 42 pages, Bremen 2005.

No. 241 **Guasti, E.**
Early Paleogene environmental turnover in the southern Tethys as recorded by foraminiferal and organic-walled dinoflagellate cysts assemblages. 203 pages, Bremen 2005.

No. 242 **Riedinger, N.**
Preservation and diagenetic overprint of geochemical and geophysical signals in ocean margin sediments related to depositional dynamics. 91 pages, Bremen 2005.

No. 243 **Ruhland, G. and cruise participants**
Report and preliminary results of POSEIDON cruise 320, Las Palmas (Spain) - Las Palmas (Spain), March 08th - March 18th, 2005. 57 pages, Bremen 2005.

No. 244 **Inthorn, M.**
Lateral particle transport in nepheloid layers – a key factor for organic matter distribution and quality in the Benguela high-productivity area. 127 pages, Bremen, 2006.

No. 245 **Aspetsberger, F.**
Benthic carbon turnover in continental slope and deep sea sediments: importance of organic matter quality at different time scales. 136 pages, Bremen, 2006.

No. 246 **Hebbeln, D. and cruise participants**
Report and preliminary results of RV SONNE Cruise SO-184, PABESIA, Durban (South Africa) – Cilacap (Indonesia) – Darwin (Australia), July 08th - September 13th, 2005. 142 pages, Bremen 2006.

No. 247 **Ratmeyer, V. and cruise participants**
Report and preliminary results of RV METEOR Cruise M61/3. Development of Carbonate Mounds on the Celtic Continental Margin, Northeast Atlantic. Cork (Ireland) – Ponta Delgada (Portugal), 04.06. – 21.06.2004. 64 pages, Bremen 2006.

No. 248 **Wien, K.**
Element Stratigraphy and Age Models for Pelagites and Gravity Mass Flow Deposits based on Shipboard XRF Analysis. 100 pages, Bremen 2006.

No. 249 **Krastel, S. and cruise participants**
Report and preliminary results of RV METEOR Cruise M65/2, Dakar - Las Palmas, 04.07. – 26.07.2005. 185 pages, Bremen 2006.

No. 250 **Heil, G.M.N.**
Abrupt Climate Shifts in the Western Tropical to Subtropical Atlantic Region during the Last Glacial. 121 pages, Bremen 2006.

No. 251 **Ruhland, G. and cruise participants**
Report and preliminary results of POSEIDON Cruise 330, Las Palmas – Las Palmas, November 21th – December 03rd, 2005. 48 pages, Bremen 2006.

No. 252 **Mulitza , S. and cruise participants**
Report and preliminary results of METEOR Cruise M65/1, Dakar – Dakar, 11.06.- 1.07.2005. 149 pages, Bremen 2006.

No. 253 **Kopf, A. and cruise participants**
Report and preliminary results of POSEIDON Cruise P336, Heraklion - Heraklion, 28.04. – 17.05.2006. 127 pages, Bremen, 2006.

No. 254 **Wefer, G. and cruise participants**
Report and preliminary results of R/V METEOR Cruise M65/3, Las Palmas - Las Palmas (Spain), July 31st - August 10th, 2005. 24 pages, Bremen 2006.

No. 255 **Hanebuth, T.J.J. and cruise participants**
Report and first results of the POSEIDON Cruise P342 GALIOMAR, Vigo – Lisboa (Portugal), August 19th – September 06th, 2006. Distribution Pattern, Residence Times and Export of Sediments on the Pleistocene/Holocene Galician Shelf (NW Iberian Peninsula). 203 pages, Bremen, 2007.

No. 256 **Ahke, A.**
Composition of molecular organic matter pools, pigments and proteins, in Benguela upwelling and Arctic Sediments. 192 pages, Bremen 2007.

No. 257 **Becker, V.**
Seeper - Ein Modell für die Praxis der Sickerwasserprognose. 170 pages, Bremen 2007.

No. 258 **Ruhland, G. and cruise participants**
Report and preliminary results of Poseidon cruise 333, Las Palmas (Spain) – Las Palmas (Spain), March 1st – March 10th, 2006. 32 pages, Bremen 2007.

No. 259 **Fischer, G., G. Ruhland and cruise participants**
Report and preliminary results of Poseidon cruise 344, leg 1 and leg 2, Las Palmas (Spain) – Las Palmas (Spain),
Oct. 20th –Nov 2nd & Nov. 4th – Nov 13th, 2006. 46 pages, Bremen 2007.

No. 260 **Westphal, H. and cruise participants**
Report and preliminary results of Poseidon cruise 346, MACUMA. Las Palmas (Spain) – Las Palmas (Spain), 28.12.2006 – 15.1.2007. 49 pages, Bremen 2007.

No. 261 **Bohrmann, G., T. Pape, and cruise participants**
Report and preliminary results of R/V METEOR Cruise M72/3, Istanbul – Trabzon – Istanbul, March 17th – April 23rd, 2007. Marine gas hydrates of the Eastern Black Sea. 130 pages, Bremen 2007.

No. 262 **Bohrmann, G., and cruise participants**
Report and preliminary results of R/V METEOR Cruise M70/3, Iraklion – Iraklion, 21 November – 8 December 2006. Cold Seeps of the Anaximander Mountains / Eastern Mediterranean. 75 pages, Bremen 2008.

No. 263 **Bohrmann, G., Spiess, V., and cruise participants**
Report and preliminary results of R/V Meteor Cruise M67/2a and 2b, Balboa -- Tampico -- Bridgetown, 15 March -- 24 April, 2006. Fluid seepage in the Gulf of Mexico. Bremen 2008.

No. 264 **Kopf, A., and cruise participants**
Report and preliminary results of Meteor Cruise M73/1: LIMA-LAMO (Ligurian Margin Landslide Measurements & Observatory), Cadiz, 22.07.2007 – Genoa, 11.08.2007. 170 pages, Bremen 2008.

No. 265 **Hebbeln, D., and cruise participants**
Report and preliminary results of RV Pelagia Cruise 64PE284. Cold-water Corals in the Gulf of Cádiz and on Coral Patch Seamount (NE Atlantic). Portimão - Portimão, 18.02. - 09.03.2008. 90 pages, Bremen 2008.

No. 266 **Bohrmann, G. and cruise participants**
Report and preliminary results of R/V Meteor Cruise M74/3, Fujairah – Male, 30 October - 28 November, 2007. Cold Seeps of the Makran subduction zone (Continental margin of Pakistan). 161 pages, Bremen 2008.

No. 267 **Sachs, O.**
Benthic organic carbon fluxes in the Southern Ocean: Regional differences and links to surface primary production and carbon export. 143 pages, Bremen, 2008.

No. 268 **Zonneveld, K. and cruise participants**
Report and preliminary results of R/V POSEIDON Cruise P339, Piräus - Messina, 16 June - 2 July 2006. CAPPUCCINO - Calabrian and Adriatic palaeoproductivity and climatic variability in the last two millenia. 61 pages, Bremen, 2008.

No. 269 **Ruhland, G. and cruise participants**
Report and preliminary results of R/V POSEIDON Cruise P360, Las Palmas (Spain) - Las Palmas (Spain), Oct. 29th - Nov. 6th, 2007. 27 pages, Bremen, 2008.

No. 270 **Ruhland, G., G. Fischer and cruise participants**
Report and preliminary results of R/V POSEIDON Cruise 365 (Leg 1+2). Leg 1: Las Palmas - Las Palmas, 13.4. - 16.4.2008. Leg 2: Las Palmas - Las Palmas, 18.4. - 29.4.2008. 40 pages, Bremen, 2009.

No. 271 **Kopf, A. and cruise participants**
Report and preliminary results of R/V POSEIDON Cruise P386: NAIL (Nice Airport Landslide), La Seyne sur Mer, 20.06.2009 – La Seyne sur Mer, 06.07.2009. 161 pages, Bremen, 2009.

No. 272 **Freudenthal, T., G. Fischer and cruise participants**
Report and preliminary results of Maria S. Merian Cruise MSM04/4 a & b, Las Palmas (Spain) – Las Palmas (Spain), Feb 27th – Mar 16th & Mar 19th – Apr 1st, 2007. 117 pages, Bremen 2009.

No. 273 **Hebbeln, D., C. Wienberg, L. Beuck, A. Freiwald, P. Wintersteller and cruise participants**
Report and preliminary results of R/V POSEIDON Cruise POS 385 "Cold-Water Corals of the Alboran Sea (western Mediterranean Sea)", Faro - Toulon, May 29 - June 16, 2009. 79 pages, Bremen 2009.

No. 274 **Zonneveld, K. and cruise participants**
Report and preliminary results of R/V Poseidon Cruises P 366-1 and P 366-2, Las Palmas - Las Palmas - Vigo, 03 -19 May 2008 and 22 -30 May 2008. PERGAMOM Proxy Education and Research cruise off Galicai, Morocco and Mauretania. 47 pages, Bremen 2010.

No. 275 **Wienberg, C. and cruise participants**
Report and preliminary results of RV POSEIDON cruise POS400 "CORICON - Cold-water corals along the Irish continental margin", Vigo - Cork, June 29 - July 15 2010. 46 pages, Bremen 2010.

No. 276 **Villinger, H. and cruise participants**
Report and preliminary results of R/V Sonne Cruise SO 207, Caldera-Caldera, 21 June - 13 July, 2010. SeamountFlux: Efficient cooling in young oceanic crust caused by circulation of seawater through seamounts (Guatemala Basin, East Pacific Ocean). 161 pages, Bremen 2010.

No. 277 **Fischer, G. and cruise participants**
Report and preliminary results of RV POSEIDON Cruise POS 396, Las Palmas - Las Palmas (Spain), 24 February - 8 March 2010. 22 pages, Bremen 2011.

No. 278 **Bohrmann, G. and cruise participants**
Report and preliminary results of RV MARIA S. MERIAN Cruise MSM 15/2, Istanbul (Turkey) – Piraeus (Greece), 10 May - 2 June 2010. Origin and structure of methane, gas hydrates and fluid flows in the Black Sea. 130 pages, Bremen 2011.

No. 279 **Hebbeln, D. and cruise participants**
Report and preliminary results of RV SONNE Cruise SO-211, Valparaíso - Valparaíso, 2 November – 29 November 2010. ChiMeBo. Bremen 2011.

No. 280 **Bach, W. and cruise participants**
Report and preliminary results of RV SONNE Cruise SO 216, Townsville (Australia) - Makassar (Indonesia), June 14 – July 23, 2011. BAMBUS, Back-Arc Manus Basin Underwater Solfataras. 87 pages, Bremen 2011.

No. 281 **Bohrmann, G. and cruise participants**
Report and preliminary results of RV METEOR Cruise M84/2, Istanbul – Istanbul, 26 February – 02 April, 2011. Origin and Distribution of Methane and Methane Hydrates in the Black Sea. 164 pages, Bremen 2011.

No. 282 **Zonneveld, K. and cruise participants**
Report and preliminary results of R/V POSEIDON Cruise P398, Las Palmas – Lissabon, 1 – 16 April 2010. PAPOCA, Production and preservation of organic carbon in relationship to dust input and nepheloid layers in the upwelling area off NW Africa. 33 pages, Bremen 2011.

No. 283 **Hanebuth, T. J. J. and cruise participants**
Report and preliminary results of RV METEOR Cruise M84/4, GALIOMAR III, Vigo – Vigo, 1st – 28th May, 2011. 139 pages, Bremen 2012.

No. 284 **Kopf, A. and cruise participants**
Report and preliminary results of RV POSEIDON Cruise P410: MUDFLOW (Mud volcanism, Faulting and Fluid Flow on the Mediterranean Ridge Accretionary Complex), Heraklion / Greece, 12.03.2011 – Taranto / Italy, 01.04.2011. 128 pages, Bremen 2012.

No. 285 **Krastel, S., G. Wefer and cruise participants**
Report and preliminary results of RV METEOR Cruise M78/3. Sediment transport off Uruguay and Argentina: From the shelf to the deep sea. 19.05.2009 – 06.07.2009, Montevideo (Uruguay) – Montevideo (Uruguay). 79 pages, Bremen 2012.

No. 286 **Kopf, A. and cruise participants**
Report and preliminary results of RV POSEIDON Cruise P429. MEDFLUIDS: Slope Stability, Mud volcanism, Faulting and Fluid Flow in the Eastern Mediterranean Sea (Cretan Sea, Mediterranean Ridge) and Ligurian Margin (Nice slope), Heraklion / Greece, 22.03.2012 – La Seyne sur Mer / France, 06.04.2012. 80 pages, Bremen 2012.

No. 287 **Fischer, G. and cruise participants**
Report and preliminary results of RV POSEIDON Cruise P425. Las Palmas – Las Palmas, 16.01.2012 – 30.01.2012. 32 pages, Bremen 2012.

No. 288 **Mohtadi, M. and cruise participants**
Report and preliminary results of RV SONNE Cruise SO 221. INVERS. Hong Kong – Hong Kong, 17.05.2012 – 07.06.2012. 168 pages, Bremen 2012.

No. 289 **Mohtadi, M. and cruise participants**
Report and preliminary results of RV SONNE Cruise SO 223T. TransGeoBiOc. Pusan – Suva, 09.09.2012 – 08.10.2012. 47 pages, Bremen 2012.

No. 290 **Hebbeln, D., Wienberg, C. and cruise participants**
Report and preliminary results of R/V Maria S. Merian cruise MSM20-4. WACOM – West-Atlantic Cold-water Corals Ecosystems: The West Side Story. Bridgetown – Freeport, 14 March – 7 April 2012. 120 pages, Bremen 2012.

No. 291 **Sahling, H. and cruise participants**
R/V Heincke Cruise Report HE-387. Gas emissions at the Svalbard continental margin. Longyearbyen – Bremerhaven, 20 August – 16 September 2012. 170 pages. Bremen, 2012.